Contents

Figures

INTRODUCTION

OBJECTIFS

PART I

PART II

PART III

CONCLUSIONS AND PERSPECTIVES

ANNEXES

Tables

INTRODUCTION

Implications du parasitisme dans l'écologie et l'évolution du phytoplancton

Le phytoplancton représente les organismes autotrophes vis-à-vis du carbone et qui utilisent la lumière comme source d'énergie. Ces micro-organismes photosynthétiques vivant en suspension dans l'eau regroupent ainsi les cyanobactéries (procaryotes) et les microalgues (eucaryotes). Le phytoplancton constitue la base de la chaîne alimentaire aquatique et joue un rôle critique dans le fonctionnement des cycles biogéochimiques majeurs en étant responsable de la fixation de près de la moitié du carbone sur la planète. Traditionnellement l'étude de l'écologie du phytoplancton s'est focalisée sur l'implication des facteurs abiotiques sur sa croissance et sa mortalité. Or, le phytoplancton est en interaction permanente avec les organismes qui l'entourent. Ces interactions biotiques peuvent être transitoires, à l'instar des interactions proie-prédateur (broutage), ou alors elles peuvent être durables et impliquer des échanges complexes (comme par exemple de matériel génétique) qui s'établissent dans le temps, on parle alors de symbioses (en grec « vivre ensemble ») (Combes, 2000). Les symbioses engageant des organismes phytoplanctoniques peuvent être de différente nature (Annexe- 1). Parmi celles-ci, le parasitisme est probablement l'une des plus anciennes interactions durables décrites dans la nature. Dans ce type d'association l'un des partenaires, le parasite, va se développer aux dépends de l'autre, l'hôte. L'hôte représente un habitat, une source d'énergie, une couveuse voire même un moyen de transport (Combes, 2001). La finalité du parasitisme n'est pas nécessairement d'induire la mortalité de l'hôte dans tous les cas d'infections. Cependant, un parasite tuant son hôte afin de réaliser son cycle est appelé un parasitoïde (Combes, 2001). Ce terme n'est néanmoins pas communément utilisé dans les publications scientifiques, souvent remplacé par « parasite » ou « pathogène ». Toutes les classes phytoplanctoniques sont susceptibles d'être infectées par de multiples parasites. Ceux-ci peuvent se développer à l'extérieur de leur hôte (ectoparasite), ou peuvent s'installer à l'intérieur de la cellule hôte (endoparasite). Ces parasites incluent des virus, des bactéries et des eucaryotes représentés dans les principales lignées phylogénétiques (Fungi, Cercozoa, Amoebozoa, Syndiniales, Oomycetes, etc.) (Gachon *et al.*, 2010; Jacquet *et al.*, 2011; Salomon and Imai, 2006). Bien que cette interaction soit l'une des plus répandues sur terre, l'étude des parasites de phytoplancton, et plus généralement des parasites aquatiques, a longtemps été négligée du fait des méthodes d'écologie non adaptées, des morphologies microscopiques compliquées à identifier et des quantifications souvent limitées (Chambouvet *et al.*, 2015). Au cours des dernières décennies, les études sur les associations phytoplancton-parasites ont pourtant souligné l'énorme diversité de ces interactions et leur importance écologique dans le fonctionnement et l'évolution des écosystèmes.

- **Parasites : moteurs dans l'évolution**

Les parasites sont reconnus comme des moteurs d'évolution et d'innovation génétique des populations d'hôte. Par exemple, l'implication de virus dans les échanges de matériel génétique par transfert horizontal (i.e., partage d'informations génétiques entre organismes sans relation parent-descendance) est connue depuis longtemps. Il existe deux mécanismes principaux d'échanges génétiques impliquant les virus : la transformation et la transduction. Dans le premier cas, la cellule hôte lysée va libérer du matériel génétique qui devient utilisable pour d'autres organismes. Le virus induit donc indirectement du transfert génétique. Le processus de transduction correspond à l'échange d'ADN entre différents micro-organismes via des entités virales lorsque du matériel de l'hôte est encapsidé durant l'assemblage viral. Le virus alors infectieux possède un fragment d'ADN de son hôte, qui sera transféré lors de la prochaine infection (Fuhrman, 1999). La contribution des virus aux transferts horizontaux de gènes par transduction est clairement établie chez les bactéries hétérotrophes mais elle est moins étudiée chez le phytoplancton. Les analyses génomiques semblent toutefois indiquer que les virus de phytoplancton ont acquis une panoplie de gènes bien spécifique au cours de leur histoire évolutive. Ces gènes, aussi appelés gènes auxiliaires de métabolisme, codent souvent pour des fonctions-clés, souvent limitantes, du métabolisme de l'hôte. Le gène le plus étudié, *psbA*, est retrouvé chez un grand nombre de virus de cyanobactéries (aussi appelés cyanophages) et code pour la protéine D1 impliquée dans le transport des électrons du photosystème II. Chez les cyanobactéries, le taux de renouvellement de la protéine D1 est très rapide, ce qui en fait une étape limitante de la photosynthèse. Au cours de l'infection virale, l'expression du gène *psbA* d'origine virale permet de maintenir la photosynthèse durant le cycle d'infection, et donc un niveau énergétique suffisant pour la production de nouveaux virions. L'expression de ces gènes au cours du cycle d'infection permettrait donc de booster ou de reprogrammer le métabolisme de l'hôte infecté, favorisant ainsi la propagation des virus et leur survie dans l'océan (Lindell *et al.*, 2005; Sharon *et al.*, 2007; Sullivan *et al.*, 2006). A l'instar des cyanophages, chez le virus géant EhV qui infecte la microalgue eucaryote *Emiliania huxleyi*, la voie métabolique quasi-complète de biosynthèse des sphingolipides est retrouvée et permettrait une réplication et un assemblage optimal des particules virales (Monier *et al.*, 2009; Wilson *et al.*, 2005)

Dans un système hôte-parasite, les deux partenaires sont en constante évolution en réponse aux changements de stratégies d'attaque et de défense de chacun. Cette force de sélection réciproque fait référence à l'hypothèse de la Reine Rouge, ou à la dynamique de la course aux armements (Van Valen, 1973). Notamment, une des versions de la théorie de la Reine Rouge est « le sexe contre les parasites », où les hôtes auraient développé la reproduction sexuée pour maintenir une diversité génétique face à des parasites évoluant vite grâce à leur temps de génération courts et le grand nombre de progénitures produit (De Bruin *et al.*, 2004). Au sein du phytoplancton, les études illustrant ce concept sont assez rares. En eau douce, des recherches sur le couple formé par la diatomée *Asterionella formosa* et son

parasite chytride *Zygorhizidium planktonicum* ont permis de montré que, plus une population hôte sera diversifiée génétiquement, probablement grâce à de la recombinaison génétique, plus elle sera résistante aux attaques parasitaires (De Bruin *et al.*, 2004, 2008). Cette forte variabilité génétique permet aussi à l'hôte de freiner l'évolution et l'adaptation du parasite. En effet, les hôtes d'une population homogène partagent la même susceptibilité face aux infections mais ils sont aussi facilement sujets à l'arrivée de nouveaux parasites, qui peuvent alors s'installer et s'adapter rapidement dans l'environnement de ces hôtes (De Bruin *et al.*, 2008). Les fortes épidémies parasitaires peuvent ainsi promouvoir la diversification génétique des populations hôtes (De Bruin *et al.*, 2008; Gsell *et al.*, 2013).

Une échappatoire à la pression des parasites sur l'évolution de leurs hôtes a été proposée en milieu marin pour le coccolithophore *Emiliana huxleyi* et son virus EhV. *E. huxleyi* comporte deux phases bien distinctes morphologiquement dans son cycle cellulaire haplo-diploïde, où les cellules diploïdes (immobiles) sont vulnérables aux infections tandis que les cellules haploïdes (flagellées et non calcifiées) sont résistantes aux virus. Frada *et al.* (2008) ont démontré que l'exposition d'*E. huxleyi* aux virus EhV induisait une transition de la phase diploïde à la phase haploïde, entraînant alors un mécanisme d'éviction à l'infection virale, permettant ainsi la transmission des gènes d'un individu à la génération suivante. Cette stratégie de résistance, appelée « Cheshire Cat », représente une force fondamentale pour le maintien de la reproduction sexuée et des cycles de vie dimorphiques (Frada *et al.*, 2008). L'étude de l'association du prasinophyte marin *Ostreococcus tauri* et ses virus OtV illustre probablement l'exemple le plus détaillé de mécanismes de défense d'un hôte phytoplanctonique à l'infection. Le développement de résistance à l'infection virale chez *O. tauri* est observé de façon récurrente et la résistance est maintenue durablement (au moins 2 années) bien qu'elle ait un coût sur le taux de croissance des hôtes immunisés (Thomas *et al.*, 2011). De récentes études proposent que le chromosome 19 d' *O. tauri* (aussi identifié comme Small Outlier Chromosome, SOC) est spécialisé dans la défense contre les infections virales et que la résistance est le plus vraisemblablement induite par la surexpression de différents gènes impliqués dans le métabolisme, la modification et le transport de carbohydrate (glycotransférases) chez l'hôte (Yau *et al.*, 2016).

Ces exemples illustrent la complexité des interactions parasitaires au sein du phytoplancton mais aussi le manque de compréhension des mécanismes moléculaires impliqués. Ces contrôles sur la diversité génétique des hôtes s'établissent sur une large échelle de temps et s'ajoutent aux contrôles à court-terme des parasites sur la biodiversité algale lors des dynamiques saisonnières

- **Parasites : régulateurs de biomasse et de biodiversité**

L'infection d'une micro-algue par un parasite viral, eucaryote ou bactérien conduit le plus souvent à la mortalité de l'organisme infecté et la prolifération du parasite. Les recherches visant à mieux caractériser l'impact des parasites sur la régulation de leurs hôtes se sont principalement focalisées sur des espèces hôtes qui développent des efflorescences

(ou blooms) de forte biomasse, nuisibles ou non pour les écosystèmes (Brussaard, 2004; Nagasaki, 2008; Salomon and Imai, 2006; Tomaru *et al.*, 2015a). Parmi les parasites de phytoplancton, ceux pour lesquels le rôle d'agent de mortalité est le mieux décrit sont les virus. Ces virus vont fortement impacter les dynamiques de leurs hôtes, comme c'est le cas par exemple de *Heterosigma akashiwo* (Raphidophyceae) responsable de marées rouges. Dans les eaux côtières du Japon (Baie d'Hiroshima), le déclin du bloom de cette espèce correspondait à une augmentation soudaine des particules virales, suggérant une désintégration rapide (3 jours) de la marée rouge (Nagasaki *et al.*, 1994). Le dinoflagellé *Heterocapsa circularisquama*, connu pour sa nuisance sur les bivalves, a aussi subi d'importants effondrements de ses efflorescences dus à des infections virales, avec jusqu'à 88% de cellules infectées lors des pics d'abondances maximales (Nagasaki *et al.*, 2004b). Chez l'haptophyte *Phaeocystis globosa* dont les blooms de forte biomasse sont nuisibles pour les activités conchylicoles et touristiques, la mortalité due à la lyse virale représenterait 5 à 66% de la mortalité totale en mer du Nord (Baudoux *et al.*, 2006). Un autre exemple marquant du contrôle qu'exercent les virus sur la dynamique de leurs hôtes, non toxiques mais au développement impressionnant, est celui d'*Emiliana huxleyi* (Bratbak *et al.*, 1993; Holligan *et al.*, 1983). Pour cette micro-algue calcifiante, qui joue un rôle-clé dans le fonctionnement des océans, les virus sont responsables de 25 à 100% de la mortalité (Bratbak *et al.*, 1993; Brussaard *et al.*, 1996; Castberg *et al.*, 2002; Jacquet *et al.*, 2002).

La caractérisation de ces agents de mortalité indique que les virus forment des assemblages complexes et dynamiques en termes de diversité moléculaire et fonctionnelle (Baudoux *et al.*, 2015; Baudoux and Brussaard, 2005; Martinez *et al.*, 2007; Pagarete *et al.*, 2014; Schroeder *et al.*, 2003; Sorensen *et al.*, 2009). En particulier, la forte variabilité des patrons de spécificité des virus isolés suggère que le contrôle de leurs hôtes n'est pas seulement quantitatif mais aussi qualitatif, dans le sens où la composition infra-spécifique de l'hôte peut être affectée. Le suivi à long terme du système *E. huxleyi* – EhV suggère toutefois qu'un même nombre limité d'hôtes et virus associés peuvent persister sur des périodes allant de 3 ans (Martinez *et al.*, 2007) à plusieurs siècles (Coolen, 2011).

Bien que l'impact des virus en tant qu'agent de mortalité porte majoritairement sur la régulation de blooms phytoplanctoniques, un nombre restreint d'études indique qu'à l'échelle de la communauté phytoplanctonique, les virus exercent un contrôle important sur des groupes spécifiques et qu'ils seraient responsables jusqu'à 25% de la mortalité phytoplanctonique totale (Baudoux *et al.*, 2006, 2007, 2008). Une étude récente rapporte des taux de lyse phytoplanctoniques globalement plus importants aux basses latitudes en comparaison des hautes latitudes (Mojica *et al.*, 2015). Les raisons expliquant ces variations ne sont à l'heure actuelle pas élucidées. Sans aucun doute, les communautés virales et microbiennes inféodées à ces milieux contrastés sont différentes. Il est aussi possible que les stratégies de réplication virale diffèrent dans ces environnements. Par exemple, l'environnement thermique a été identifié comme un facteur important qui influence l'intensité de la lyse virale (Mojica and Brussaard, 2014) mais aussi dans les transitions de stratégie de réplication (Demory *et al.*, 2017; Wilson *et al.*, 2001) voire même dans le

développement de résistance à l'infection virale (Demory *et al.*, 2017; Kendrick *et al.*, 2014; Nagasaki and Yamaguchi, 1998).

En ce qui concerne les parasites eucaryotes, un cas impressionnant de contrôle de blooms est celui du dinoflagellé *Alexandrium minutum*. En milieu estuarien (Baie de Penzé), ce dinoflagellé produisait des efflorescences toxiques pendant près d'une dizaine d'année après son introduction, impactant alors les aquacultures locales. Des parasites ont commencé peu à peu à attaquer cette espèce au point de supprimer ses efflorescences quelques années après son introduction. *A. minutum*, toujours présente dans les eaux estuariennes mais à de faibles concentrations, a donc été régulée par des parasites (Chambouvet *et al.*, 2008). L'impact du parasitisme sur les populations marines de dinoflagellés a relativement bien été étudié du fait de nombreuses espèces toxiques. Par exemple, le pathogène *Amoebophrya*, à la distribution géographique très répandue, est responsable du déclin saisonnier de plus 30 espèces de dinoflagellé, avec des taux de mortalité parfois impressionnants (par exemple, 54% de cellules infectées par jour par *Amoebophrya* lors d'une efflorescence de *Gyrodinium uncatenum* (Park *et al.*, 2004)).

Le rôle des bactéries algicides dans les blooms algaux a également été examiné (Mayali and Azam, 2004). Là encore, les interactions liées aux efflorescences toxiques ont plus attiré l'attention du fait des répercussions écologiques et économiques. En milieu naturel, le raphidophyte *Chattonella* provoque de considérables HABs. Au début des années 2000, des chercheurs ont mis en évidence des relations très étroites entre les fluctuations de la bactérie *Cytophaga* sp. souche J18/M01 et l'abondance des espèces *C. antiqua* et *C. marina* (Imai *et al.*, 2001). La densité cellulaire de cette bactérie augmenterait juste après le pic maximum d'abondance de *Chattonella* spp. La désintégration du bloom du raphidophyte serait alors engendrée par l'attaque de la bactérie algicide.

Lors des infections virales, bactériennes ou eucaryotes, l'abondance des pathogènes augmente considérablement après que leurs hôtes aient atteint de fortes concentrations cellulaires. Cela illustre la notion de densité-dépendance dans les interactions hôte-parasite et fait référence à l'hypothèse du « killing the winner » chez les virus (Thingstad, 2000). En effet, plus un hôte sera numériquement dominant, comme dans le cas d'un bloom, plus il y aura de probabilité de rencontre avec le virus. En attaquant préférentiellement les hôtes dominants et compétitifs, les parasites libèrent des niches écologiques alors disponibles pour les espèces moins compétitives pour les ressources et maintiennent ainsi une plus grande biodiversité et coexistence d'espèces. Les lyses des organismes dominants permettent ainsi des successions dans les compositions des communautés microbienne mais aussi virales (Castberg *et al.*, 2001).

Chez les systèmes eucaryotes, Van Donk et Ringelberg ont montré dans un lac oligo-mésotrophe que l'infection de la diatomée *Asterionella formosa* par le chytride *Zygorhizidium planktonicum* favorisait le développement d'autres espèces de diatomées comme *Fragilaria*

crotonensis, Stephanodiscus hantzschii et *S. astraea* (Van Donk and Ringelberg, 1983). *A. formosa* a de fortes affinités pour les éléments nutritifs, comme le phosphore, faisant d'elle une espèce plus compétitive que les trois autres. Lorsqu'elle est infectée, sa population décroit et laisse place aux autres diatomées qui auront accès aux ressources (Van Donk and Ringelberg, 1983). Cet exemple de successions corrobore ainsi la théorie du « killing the winner » chez les virus et souligne le fait que les parasites sont des facteurs importants de la régulation de biomasse algale mais aussi de la composition et diversité des espèces au cours du temps.

En eau douce, le rôle écologique du parasitisme dans la composition et la saisonnalité des communautés phytoplanctoniques a été schématisé par Rasconi *et al.* (2012) (Figure 0-1). En période hivernale, les basses températures empêchent le développement du phytoplancton et des parasites associés. A la fin de l'hiver, la hausse de température et la disponibilité des nutriments favorisent le développement algal, dominé par de grandes diatomées (stratégie K). L'augmentation de la densité des diatomées facilite la rencontre avec les chytrides, il y a alors infection avec production d'une grande quantité de zoospores. Les attaques parasitaires provoquent ensuite le déclin des efflorescences des grandes diatomées, libérant ainsi des niches écologiques pour d'autres espèces phytoplanctoniques. A la fin du printemps, les prédateurs s'établissent alors avec la présence de zoospores et de petites cellules phytoplanctoniques dont ils se nourrissent (« clear water phase » Figure 0-1). En période estivale, les conditions favorables climatiques et hydrologiques permettent le développement d'un complexe d'espèces algales diversifiées. A la fin de l'été, la pression de broutage régule les petites espèces tandis que les parasites régulent les espèces de plus grande taille. A l'automne, les espèces planctoniques coexistent et cette diversité permet le maintien de populations de parasites de faible abondance (Figure 0-1). Ces patrons de successions peuvent varier entre les milieux (marins *vs*. eaux douces, selon le niveau trophique des eaux, etc.) mais ils schématisent relativement bien le rôle structurant des parasites pour les communautés phytoplanctoniques.

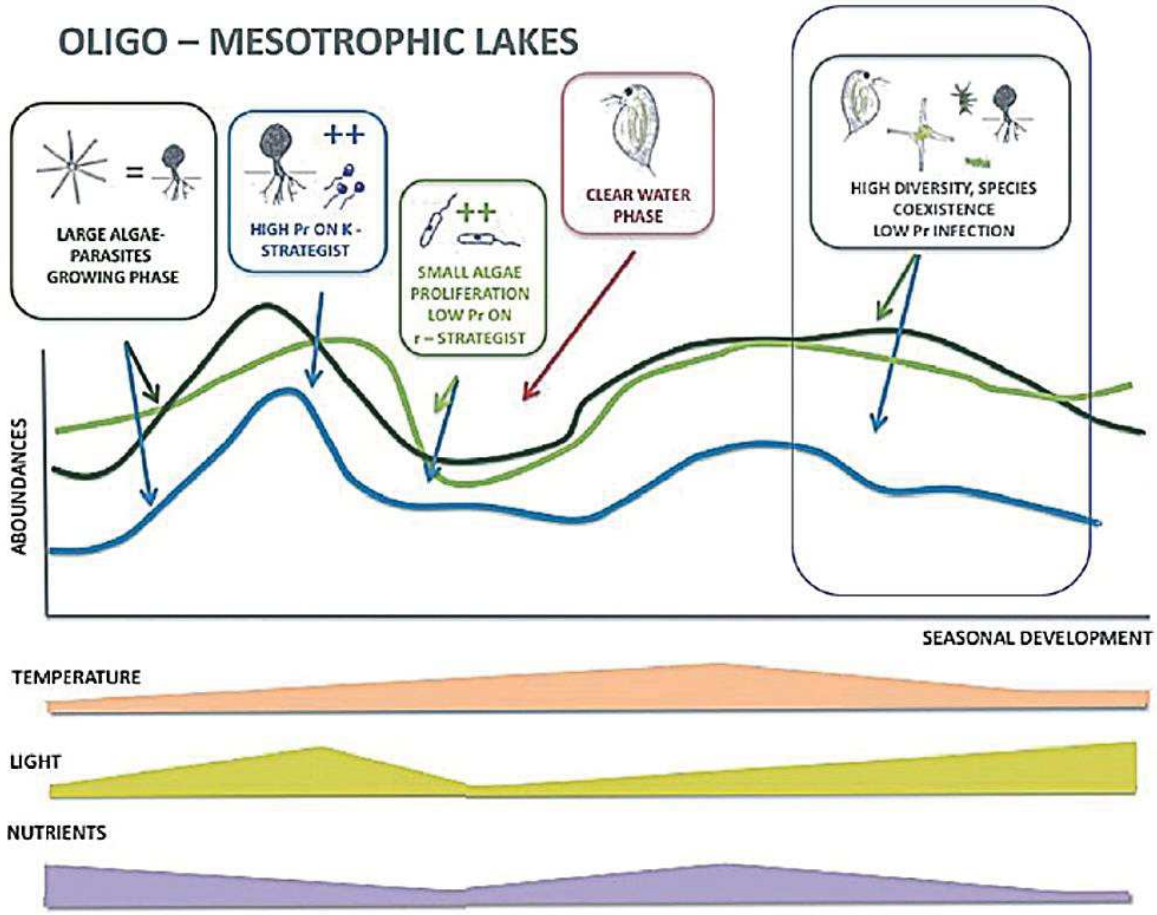

Figure 0-1. Successions saisonnières représentées dans un lac oligo-mésotrophe. La courbe bleue représente les chytrides, la noire les algues de taille large à stratégie K et la courbe verte retrace les petites algues à stratégie r (Rasconi et al.*, 2012)*

- **Parasites : liens importants des réseaux trophiques et des transferts d'énergie**

La mortalité que les virus, bactéries et parasites eucaryotes imposent au phytoplancton a des conséquences directes et indirectes sur la structure et fonctionnement des réseaux trophiques et des cycles biogéochimiques globaux. L'une des conséquences les mieux décrites est que l'infection par un parasite court-circuite les transferts de matière au sein du réseau trophique. Dans la chaîne alimentaire classique, le phytoplancton transforme, via la production primaire, la matière minérale (éléments nutritifs, carbonate) en matière organique sous forme, d'une part, de biomasse et, d'autre part, de matière organique dissoute et particulaire (MOD et MOP) excrétée dans le milieu environnant. La biomasse est transférée aux échelons trophiques supérieurs (par broutage) par la chaîne alimentaire classique. Une partie de la matière organique (labile) sera dégradée et recyclée par les bactéries hétérotrophes dans les eaux de surface. Ce processus est appelé la boucle microbienne (Azam *et al.*, 1983). Une autre partie de la matière organique réfractaire aux transformations bactériennes sédimente de la zone photique vers les couches océaniques profondes et

contribue à la séquestration du carbone. Ce transfert carbone dans les fonds océaniques est aussi appelé la pompe biologique. L'infection par un parasite conduit généralement à la lyse cellulaire de l'hôte infecté et détourne donc la biomasse destinée aux échelons trophiques supérieurs. Le contenu cellulaire de l'hôte lysé est libéré dans le milieu cellulaire sous forme de MOD et MOP labiles et alimente donc le pool de matière organique disponible pour les communautés bactériennes. Chez les virus, ce processus, appelé « viral shunt », résulterait en une diminution de la respiration du microzooplancton et une augmentation nette de la respiration bactérienne, forçant ainsi la boucle microbienne vers une voie régénérative (Wilhelm and Suttle, 1999, Fuhrman 1999). Il est communément accepté que l'ensemble de ces processus conduirait à un ralentissement de la pompe biologique. De récentes études rapportent toutefois que l'infection virale pourrait faciliter l'export de carbone dans les fonds océaniques via la sédimentation des produits de la lyse virale et/ou des cellules infectées (Laber *et al.*, 2018; Lawrence and Suttle, 2004). Chez les parasites eucaryotes, les zoospores acquièrent des nutriments de leur hôte via les processus d'infection. Lorsque les zoospores sont elles-mêmes consommées par des prédateurs, elles transfèrent alors de l'énergie et de la matière des producteurs primaires aux compartiments trophiques supérieurs. Ce phénomène est appelé la « Mycoloop » et présente une alternative dans les dynamiques trophiques lorsque les cellules phytoplanctoniques ne sont pas consommables par les brouteurs, souvent car de trop grandes tailles (Kagami *et al.*, 2007). Cela a été démontré pour les communautés d'eau douce, où l'infection de la diatomée de grande taille *Asterionella* par des Fungis permettait un couplage entre les producteurs primaires et secondaires (Kagami *et al.*, 2007, 2011). De plus, les attaques parasitaires peuvent modifier l'aspect de comestibilité de leurs hôtes pour le zooplancton. Par exemple, la fragmentation des cyanobactéries filamenteuses induite par l'infection d'un chytride peut les rendre plus vulnérables à la prédation des brouteurs (Agha *et al.*, 2016). De la même façon, les cellules d'*E. huxleyi* infectées par des virus peuvent être broutées de façon préférentielle (Evans and Wilson, 2008). L'effet inverse peut cependant se produire : suite à l'infection, les colonies d'*A. formosa* s'agrègent et deviennent alors plus impropres à la consommation par les copépodes (Kagami *et al.*, 2005, 2011).

Les parasites sont essentiellement vus comme les agents de mortalité du phytoplancton, mais ils constituent aussi des ressources nutritives non négligeables pour le zooplancton, soit lorsqu'ils sont consommés avec leur hôte lors d'une infection (prédation concomitante), soit lorsque le stade libre est consommé (Bettarel *et al.*, 2005b; Evans and Wilson, 2008; Frada *et al.*, 2014; Frada and Vardi, 2015; Johnson *et al.*, 2010). Chez les pathogènes eucaryotes, les zoospores (stade libre nageur de petite taille) de chytrides renferment des ressources nutritives, comme des acides gras polyinsaturés (« PUFAs » en anglais) et du cholestérol, essentielles dans la croissance et la reproduction des crustacés comme les Daphnies (Kagami *et al.*, 2007; Müller-Navarra *et al.*, 2000). Les parasites peuvent également représenter une ressource nutritive importante lors de leur décomposition, à l'instar des particules virales dont les protéines et acides nucléiques constituent une source importante de matière labile dans les sédiments marins disponible pour les bactéries

hétérotrophes (Dell'Anno *et al.*, 2015). La valeur qualitative, et non pas simplement quantitative, apparait alors comme un aspect important de ce transfert de matière et fait référence au concept de l'amélioration trophique (Gleason *et al.*, 2008; Sime-Ngando *et al.*, 2011).

Ces diverses implications dans les dynamiques trophiques sont représentées dans la Figure 0-2.

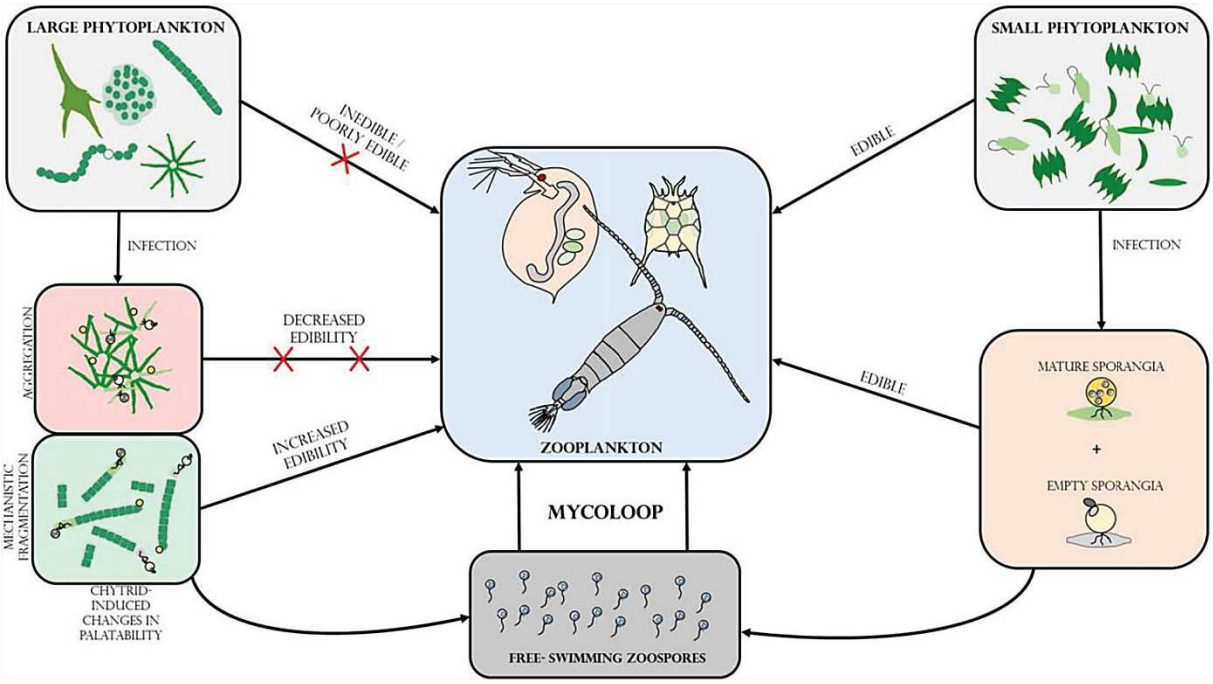

Figure 0-2. Représentation schématique de l'empreinte trophique des parasites eucaryotes, et plus spécifiquement des chytrides dans ce cas. Les colonies et larges cellules phytoplanctoniques sont peu consommables par le zooplancton, comparées à des cellules de plus petite taille. L'infection par des chytrides peut augmenter la vulnérabilité de ces larges cellules au broutage ou au contraire augmenter l'aspect d'agrégat et ainsi rendre encore moins consommables les producteurs primaires. Les chytrides sont aussi des proies pour le zooplancton, soit attachés sur la cellule hôte lors de l'infection (prédation concomitante), soit sous forme libre (zoospores). Schéma de Frenken et al., *2017*

Ainsi, les parasites, selon leur nature et leur stade de vie, ont des implications différentes sur les transferts de matière entre les différents compartiments trophiques. Jusqu'alors, la plupart des études sur les interactions phytoplancton-parasite se sont limitées à des systèmes modèles qui n'incluent qu'un hôte et un type de parasite. Il apparaît pourtant évident que les microalgues sont associées à de multiples parasites. Pour améliorer notre compréhension des implications écologiques, évolutives et biogéochimiques des parasites marins, il est essentiel de mieux caractériser les réseaux parasitaires associés aux groupes taxonomiques dominants dans les écosystèmes. D'un point de vue écologique et biogéochimique, les diatomées sont des organismes primordiaux en milieux marins. La partie suivante développera les aspects majeurs liés à ces microalgues et aboutira dans un troisième temps aux parasites connus de diatomées, avec leur diversité et leur impact sur les blooms et compositions d'espèces.

Les diatomées, groupe majeur du phytoplancton

Les diatomées sont des organismes photosynthétiques unicellulaires, solitaires ou coloniaux, appartenant à la lignée des Straménopiles. Ces microalgues, dont la taille varie entre quelques micromètres et quelques millimètres ont colonisé tous les milieux aquatiques, les eaux douces et eaux marines. Elles peuvent avoir des habitats variés, au mode de vie benthique ou planctonique.

Le terme diatomée vient du grec *diatomos*, qui signifie « coupé en deux » (Figure 0-3, A). En effet, Les diatomées ont la particularité de posséder une paroi siliceuse protégeant la matrice organique, formant ainsi une sorte de boîte de verre appelée le frustule. Ce frustule est composé de deux parties : la partie inférieure, l'hypovalve (=hypothèque) s'emboîte dans la partie supérieure plus grande, l'épivalve (= épithèque). La jonction entre les deux valves, le cingulum, est formée de bandes cingulaires. Les bandes cingulaires supérieures composent l'épicingulum et les bandes inférieures l'hypocingulum (Figure 0-3, C). Le frustule est finement ornementé et porte de nombreux pores (aréoles) et structures siliceuses nommées processus (Figure 0-3, B et C), dont le nombre, la position et la forme sont primordiaux dans la caractérisation des espèces (Graham *et al.*, 2009; Round *et al.*, 1990; Throndsen *et al.*, 2007). Grâce à cet exosquelette siliceux, des fossiles de diatomées bien préservés ont permis de dater leurs origines, de retracer leur histoire et ainsi de mieux comprendre leur rôle dans les cycles biogéochimiques (Armbrust, 2009). Les diatomées seraient apparues au Jurassique (~190 millions d'années), même si des analyses utilisant l'horloge moléculaire estiment leur apparition bien en amont de cette période (~250 millions d'années) (Armbrust, 2009; Medlin, 2016; Sims *et al.*, 2006).

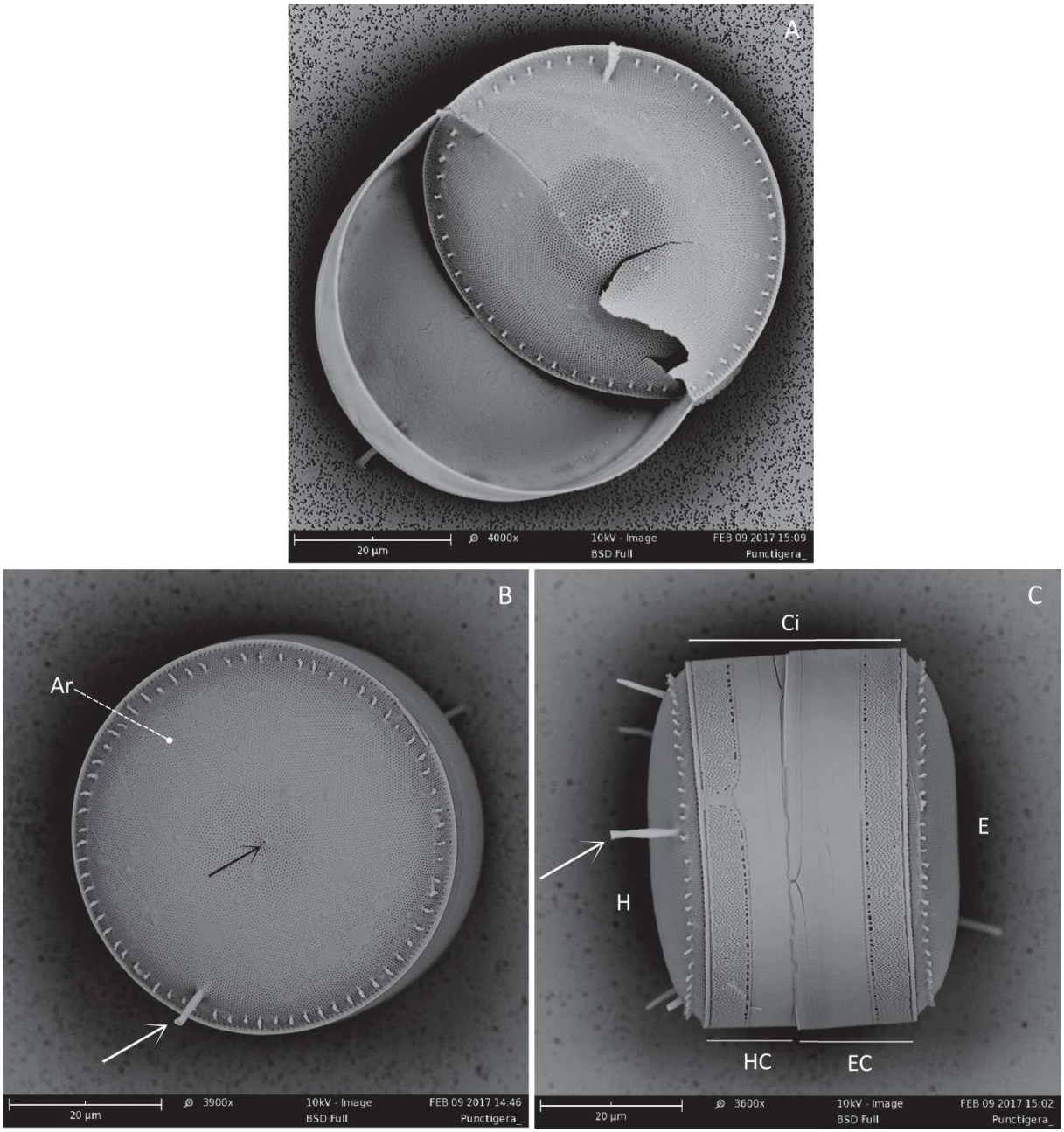

Figure 0-3. Structure d'une diatomée centrique. A. Cellule de Thalassiosira punctigera *cassée mettant en évidence la forme "boîte de pétri" du frustule. B. Vue valvaire. C. Vue cingulaire. Ar : Aréoles (= pores), E : Epivalve, H : Hypovalve, Ci = Cingulum composé de l'épicingulum (EC) et de l'hypocingulum (HC). La flèche noire représente un processus central (fultoportulae) et la flèche blanche le processus labié (rimoportula). Photos personnelles acquises en microscopie électronique à balayage (MEB)*

La classification actuelle des diatomées résulte d'analyses comparatives des caractères morphologiques (essentiellement forme et ornementation du frustule) et génétiques, ainsi que de l'analyse des particularités des cycles de vie (Graham *et al.*, 2009; Kröger and Poulsen, 2008; Medlin, 2016; Medlin and Kaczmarska, 2004; Round *et al.*, 1990; Sabater, 2009) (Figure 0-4). Les diatomées, ou Bacillariophyta, sont actuellement classées au sein de 3 classes, les Coscinodiscophyceae, les Mediophyceae et les Bacillariophyceae (Figure 0-5). Les Coscinodiscophyceae et Mediophyceae correspondent aux diatomées dîtes centriques dont

les valves circulaires ont généralement une forme typique de « boîte de pétri » et surtout, dont les ornementations présentent une symétrie plutôt organisée autour d'un annulus localisé au centre de la valve. La symétrie est radiale pour les Coscinodiscophyceae ou diatomées centriques radiales (Figure 0-4, « radial centric »). Chez les Mediophyceae (Figure 0-4, « polar centric ») des pôles présents à la périphérie des valves modifient la symétrie. L'ornementation des valves présente une symétrie dite bi ou multipolaire et les valves peuvent avoir diverses formes (circulaires, elliptiques, etc.). L'annulus est allongé voire déformé, contrairement à celui des diatomées radiales. Au sein des Mediophyceae cependant, les Thalassiosirales font lieu d'exception, avec leurs valves circulaires et l'absence de symétrie bi/multi polaire.

Les Bacillariophyceae ou diatomées pennées, à la forme souvent allongée, ont des frustules présentant une symétrie bilatérale. Le plan de symétrie est matérialisé sur la valve par une nervure nommée le sternum. Chez les pennées « raphides », le sternum forme un sillon, le raphé, interrompu centralement par un nodule (Figure 0-4, « raphid pennate »). Ces diatomées, généralement benthiques, ont la capacité de se mouvoir sur le substrat grâce à la production d'un mucilage adhésif sécrété via le raphé. Enfin, les diatomées pennées « araphides » ne possèdent pas de raphé et leurs cellules ne sont pas mobiles (Figure 0-4, « araphid pennate »).

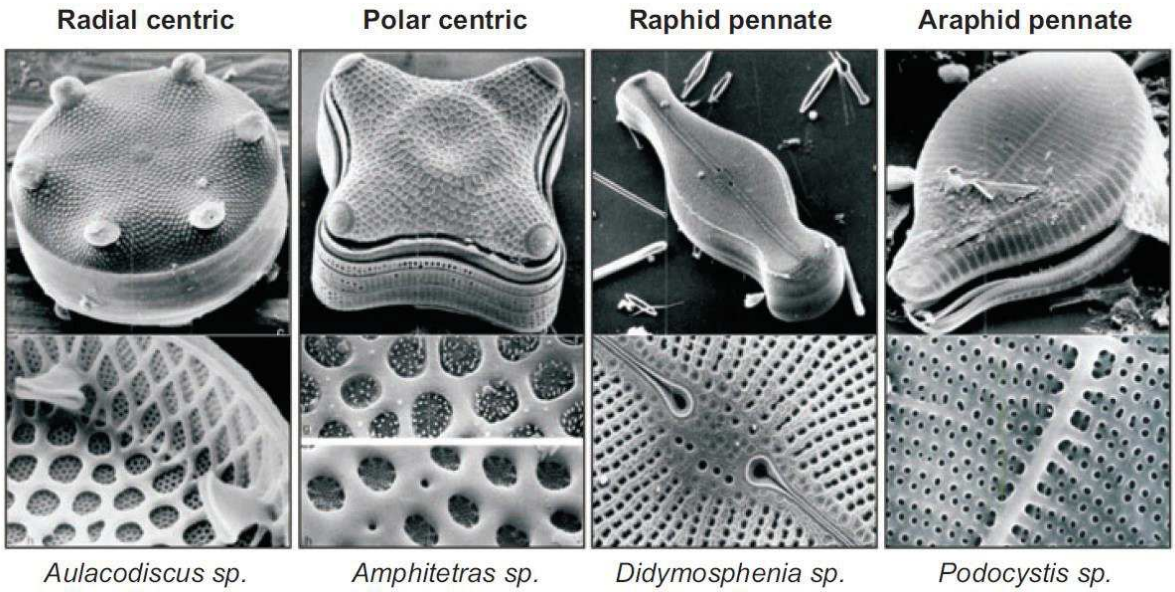

Figure 0-4. Photographies acquises en MEB de diatomées centriques et pennées. Les diatomées centriques se divisent en diatomées à symétrie radiale et aux valves circulaires, et en diatomées aux valves bi ou multipolaires. Les diatomées pennées ont une symétrie bilatérale et peuvent posséder un raphé (diatomées pennées raphides) ou non (diatomées pennées araphides). Les photos inférieures illustrent les diverses ornementations des frustules (Kröger and Poulsen, 2008)

Au total, plus de 15 000 espèces de Bacillariophyta ont été décrites à ce jour (Guiry and Guiry, 2018). Néanmoins, ce nombre sous-estime probablement largement la diversité réelle de ce groupe (de 30 000 espèces à 100 000 voire 200 000 espèces selon les auteurs) (Mann and Droop, 1996; Mann and Vanormelingen, 2013).

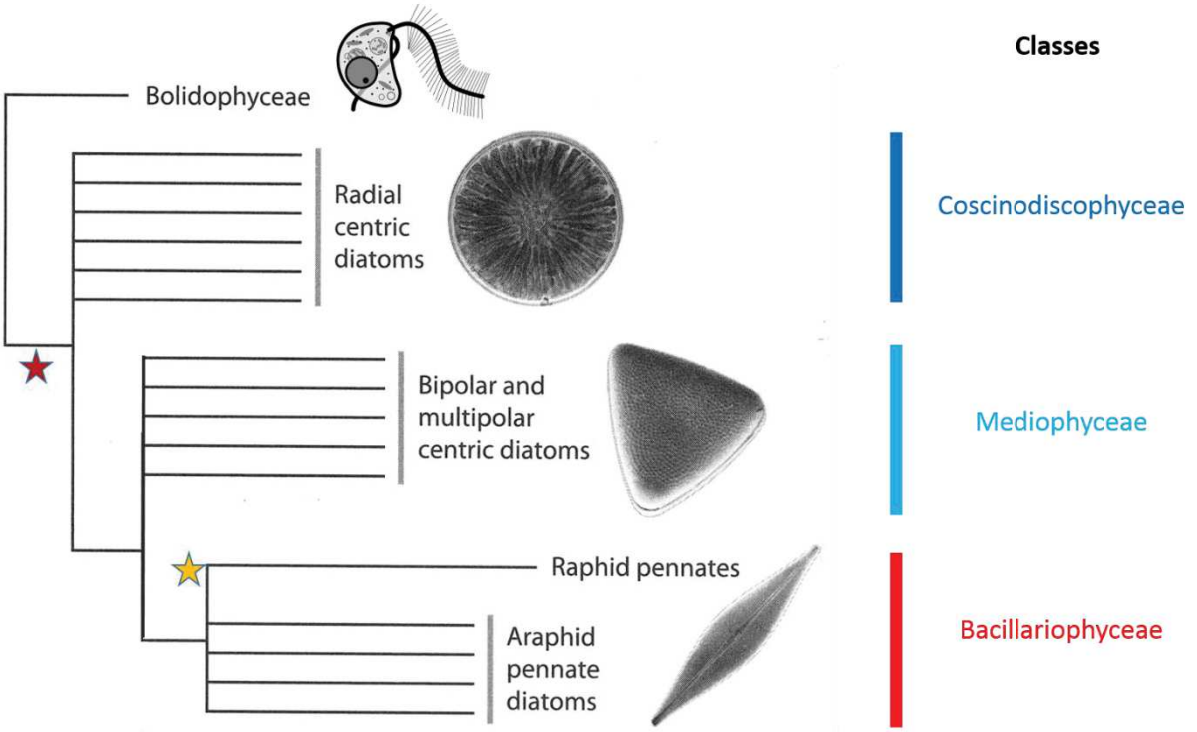

Figure 0-5. Classification phylogénétique schématique des diatomées. La classe des Coscinodiscophyceae correspond aux diatomées centriques radiales et les Mediophyceae correspondent aux diatomées centriques polaires. Les diatomées pennées raphides et araphides sont regroupées dans la classe des Bacillariophyceae. L'étoile rouge représente le 1er fossile de diatomée (Jurassique), L'étoile jaune représente l'apparition du raphé (tertiaire). Schéma modifié à partir de Graham et al. *(2009)*

Les diatomées possèdent un cycle de vie monogénétique diplophasique. Une particularité de leur cycle de vie est liée à leur paroi siliceuse. Les cellules diploïdes entreprennent des divisions mitotiques où chaque cellule fille va recevoir soit l'épithèque soit l'hypothèque de la cellule mère. Chaque progéniture synthétise donc la valve manquante, plus petite (l'hypothèque). De ce fait, la cellule fille ne pourra être plus grande que la cellule initiale. Ce phénomène entraîne donc une diminution graduelle de la taille des cellules. Le déclenchement de la gamétogénèse semble lié, pour de nombreuses espèces, à l'atteinte de la taille minimale (qui dépend des espèces et peut aller jusqu'à 1/3 de la taille maximale) (Round *et al.*, 1990). Le zygote, appelé aussi auxospore, est dépourvu de frustule. Sa croissance cellulaire permet la restauration de la taille maximale pour l'espèce (Figure 0-6). Ce cycle de vie très particulier a probablement des conséquences majeures sur l'écologie des diatomées : la fréquence des évènements de reproduction sexuée a sans doute un impact majeur sur la structure génétique et l'évolution des diatomées (Graham *et al.*, 2009; Loir, 2004; Round *et al.*, 1990; Sabater, 2009).

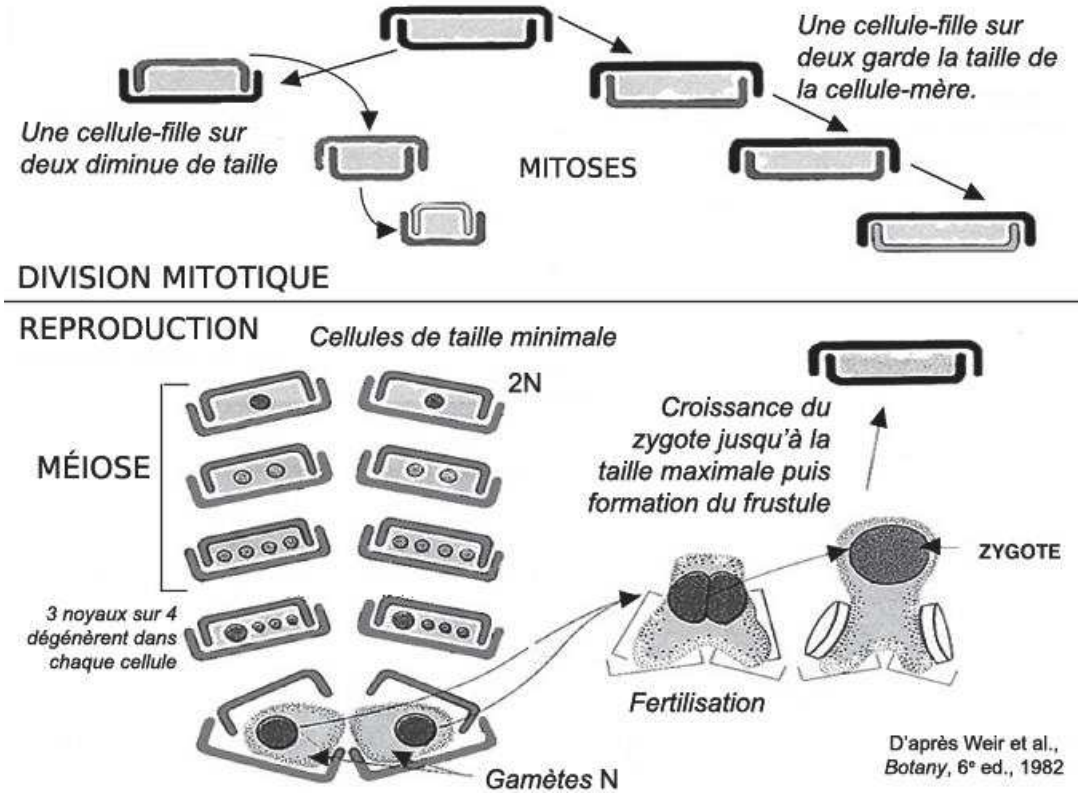

Figure 0-6. Schéma d'un cycle cellulaire chez les diatomées, avec une phase asexuée (division mitotique) et sexuée (reproduction). Schéma pris à partir de C. Langlois

Si les diatomées sont distribuées mondialement dans les océans, des pôles à l'équateur, et des milieux côtiers aux régions centrales oligotrophes des océans, leur contribution à la biomasse phytoplanctonique est particulièrement importante dans les hautes latitudes (Hémisphère nord et Océan Austral), au niveau de l'équateur, dans les régions d'upwellings, de front et en milieux côtiers aux eaux particulièrement mélangées (Armbrust, 2009; Leblanc *et al.*, 2012; Malviya *et al.*, 2016; Tréguer *et al.*, 2018). A l'échelle globale, les diatomées centriques telles que *Rhizosolenia, Chaetoceros* et *Thalassiosira* représentent près 50% de la biomasse totale des diatomées (Leblanc *et al.*, 2012). Les diatomées ont un rôle biogéochimique majeur en étant responsables d'environ 20% de la production primaire totale sur Terre et d'environ 40% de la production primaire de carbone des écosystèmes marins (plus précisément 35% en milieux oligotrophiques et jusqu'à 75% dans les systèmes eutrophiques (Nelson *et al.*, 1995)). Elles produiraient ainsi plus de carbone organique que toutes les forêts tropicales réunies (Field *et al.*, 1998; Leblanc *et al.*, 2012). Elles sont également la principale source de silice biogénique à l'échelle de la planète (Smetacek, 1999; Tréguer *et al.*, 1995). Les diatomées sont aussi considérées comme un moteur de la pompe biologique de carbone (Falkowski *et al.*, 1998; Smetacek, 1999). En effet, le frustule est une structure lourde et épaisse qui confère aux diatomées des taux de sédimentation importants. Il a d'ailleurs été récemment montré que toutes les diatomées n'ont pas le même potentiel d'export de carbone. Leur vitesse de sédimentation dépend de nombreux paramètres comme la taille, la forme, le degré de silicification, la formation de chaînes, ou encore de la production de spores

de dormance (Tréguer *et al.*, 2018). Les exports via des cellules libres, l'agrégation sous forme de neige marine ou de cellules incluses dans les pelotes fécales n'ont pas non plus les mêmes impacts (Sarthou *et al.*, 2005). Par ailleurs, ces taux de sédimentation rapides leur permettent de coloniser d'autres milieux que la surface photique. Les diatomées ont en effet été retrouvées à plus de 2000 m de profondeur, principalement en équateur pacifique, en bon état cellulaire (Agusti *et al.*, 2015). La présence, voire la dominance, de ce groupe phytoplanctonique à si forte profondeur permet ainsi l'injection directe de carbone organique frais dans les fonds marins (Agusti *et al.*, 2015) et l'apport de ressource alimentaire pour les espèces vivant dans ces milieux extrêmes (Armbrust, 2009).

Dans les systèmes marins côtiers, ces organismes forment des efflorescences printanières d'espèces et successions récurrentes d'années en années (Assmy and Smetacek, 2009; Margalef, 1978; Rousseau *et al.*, 2002). Typiquement, un premier assemblage constitué de petites diatomées à croissance rapide, incluant souvent les genres *Thalassiosira*, *Chaetoceros*, ou *Skeletonema,* se développe suite à la remise en suspension des nutriments (par brassage ou upwelling). Un second assemblage dominé par des espèces de plus grande taille telles que *Chaetoceros* spp. apparait ensuite. Puis, à mesure que les nutriments sont consommés, il est remplacé par un troisième assemblage d'espèces assez larges et plus inféodées aux systèmes oligotrophiques telles que les membres des genres *Rhizosolenia* et *Hemiaulus.* La dynamique de ces successions est modulée par des facteurs externes (abiotiques) et de structuration interne, incluant les interactions biotiques telles que le parasitisme. Le rôle des facteurs externes et des interactions de type prédation sur ces blooms a été étudié de façon extensive. L'importance des interactions durables, si elle est aujourd'hui indiscutable, reste toutefois élusive. Un nombre considérable de protagonistes a été identifié (voir partie suivante) mais leur contribution en terme de mortalité demeure mal quantifiée. Par ailleurs, les patrons de successions décrits ci-dessus n'incluent pas les plus petites espèces de diatomées (nanodiatomées) tels que les espèces du genre *Minidiscus*. La prévalence de ces nanodiatomées dans l'océan mondial et leurs implications dans l'export de carbone ont pourtant été soulignées récemment. Il apparaît donc essentiel de mieux caractériser ces blooms et leur facteur de régulation.

L'implication des diatomées dans les cycles biogéochimiques globaux fait de ce groupe un composant majeur et primordial des écosystèmes marins qui a su perdurer et prospérer à travers les temps géologiques. Dans un contexte de changement global, la compréhension de la contribution dans les pompes biologiques de ces taxons clés est nécessaire afin de mieux évaluer les conséquences de l'acidification et du réchauffement des océans contemporains (Armbrust, 2009; Tréguer *et al.*, 2018).

Au cours du temps, le frustule a conféré un avantage évolutif aux diatomées et a offert une protection contre des agressions environnementales, comme les variations de pH ou les attaques UV (voir la revue de Raven and Waite, 2004 pour plus de détails). Outre cela, il a

longtemps été pensé comme une barrière face aux agents biotiques comme les prédateurs, mais aussi imperméable contre les parasites (Hamm *et al.*, 2003; Raven and Waite, 2004; Sarthou *et al.*, 2005). Ces dernières années, le travail intensif de laboratoire, comprenant l'isolement et la caractérisation d'espèces, a permis de mettre à jour des nouveaux pathogènes de diatomées, ouvrant ainsi la voie à de nouveaux axes de recherches. Ces différents parasites sont présentés dans la partie qui suit.

Les parasites de diatomées

1. Les virus associés aux diatomées

Le premier virus de diatomées a été isolé et caractérisé pour la première fois en 2004 sur la diatomée centrique *Rhizosolenia setigera* (Nagasaki *et al.*, 2004a). Ce virus, *Rhizosolenia setigera* RNA Virus (RsRNAV), à la morphologie hexagonale, sans queue et de petite taille (32 nm) (Figure 0-7) était capable de se répliquer au sein du cytoplasme de son hôte. RsRNAV, qui ne pouvait infecter aucune autre espèce phytoplanctonique, a montré une forte spécificité sur certaines souches de *R. setigera*, espèce proliférante sur les côtes du Japon. Le génome de ce premier virus a été complétement séquencé et assemblé (Shirai *et al.*, 2006). Cette structure génomique linéaire à ARN simple brin (ARNsb) positif de moins de 9 kb a montré une organisation particulière, composée de 2 cadres de lecture ouverts (« Open reading frames », ORFs). Le premier ORF représente une poly-protéine codant pour des gènes de réplication tels qu'une hélicace et une « RNA-dependent RNA polymerase » (RdRp), séquence génétique fortement conservée chez les Picornavirus (Koonin *et al.*, 1993) (Figure 0-9, B). Le second ORF quant à lui code pour des protéines structurales de la capside. Les analyses phylogénétiques réalisées dans cette étude ont montré que ce nouveau virus était proche de HaRNAV et SssRNAV, deux virus infectant les Straménopiles *Heterosigma akashiwo* (Tai *et al.*, 2003) et *Schizochytrium* sp. (renommé *Aurantiochytrium* sp., Takao *et al.*, 2005) respectivement, mais n'appartenait à aucun genre ni famille définis (Shirai *et al.*, 2006).

Depuis la description de ce virus, d'autres virus de diatomées centriques ont été isolés et caractérisés, comme montré dans les tableaux 0-1 et 0-2. En plus des virus à génome ARNsb (Kimura and Tomaru, 2015; Shirai *et al.*, 2008; Tomaru *et al.*, 2009, 2013a), l'isolement intensif dans les eaux du Japon notamment a permis de mettre à jour l'existence de virus à ADN simple brin (ADNsb) circulaire (Kimura and Tomaru, 2013, 2015; Nagasaki *et al.*, 2005; Tomaru *et al.*, 2008, 2011c, 2011b, 2013b; Toyoda *et al.*, 2012). De la même façon que les virus à ARN, les virus ADNsb sont de petite taille (< 40 nm), n'ont pas de queue, ont de petits génomes (< 10 kb) mais contrairement aux virus à ARN, ils se répliquent dans le nucléus de l'hôte, où ils ont la capacité à former des « rod-shaped virus-like particles », structures en forme de bâtonnet uniquement observées au sein de la cellule hôte infectée et jamais sous forme libre (Figure 0-8). Les auteurs ont d'ailleurs émis l'hypothèse que ces structures étaient des précurseurs de virions (i.e. virus libres) matures (Tomaru *et al.*, 2015a; Toyoda *et al.*, 2012). Le génome circulaire des virus ADNsb encode également pour une protéine de réplication, une protéine pour la structure de la capside et généralement un ORF à la fonction encore inconnue (Figure 0-9, A). Cependant, une caractéristique propre à ces virus est la présence d'un fragment ADN double brin d'environ 1 kb au sein du génome circulaire (à l'exception de CdebDNAV et CsetDNAV (Tomaru *et al.*, 2008; Tomaru *et al.*, 2013b)). Il est important de noter qu'à ce jour,

les virus ADNsb ont uniquement été reportés chez les diatomées et dans aucun autre groupe de protistes (Tomaru *et al.*, 2015a).

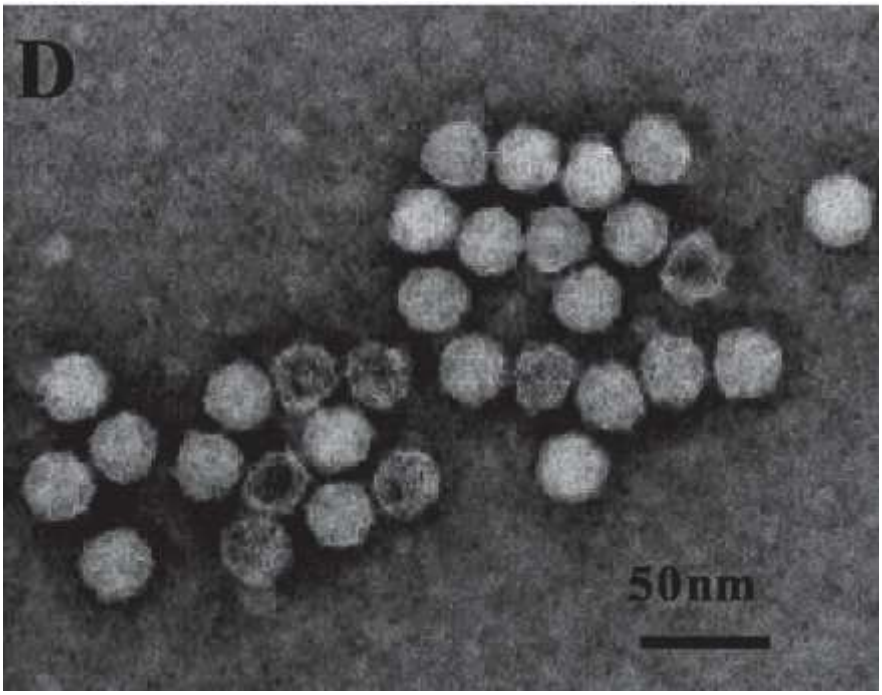

Figure 0-7. Rhizosolenia setigera *RNA virus (RsRNAV), tout premier virus de diatomée isolé en 2004 dans les eaux côtières du Japon (Nagasaki* et al.*, 2004)*

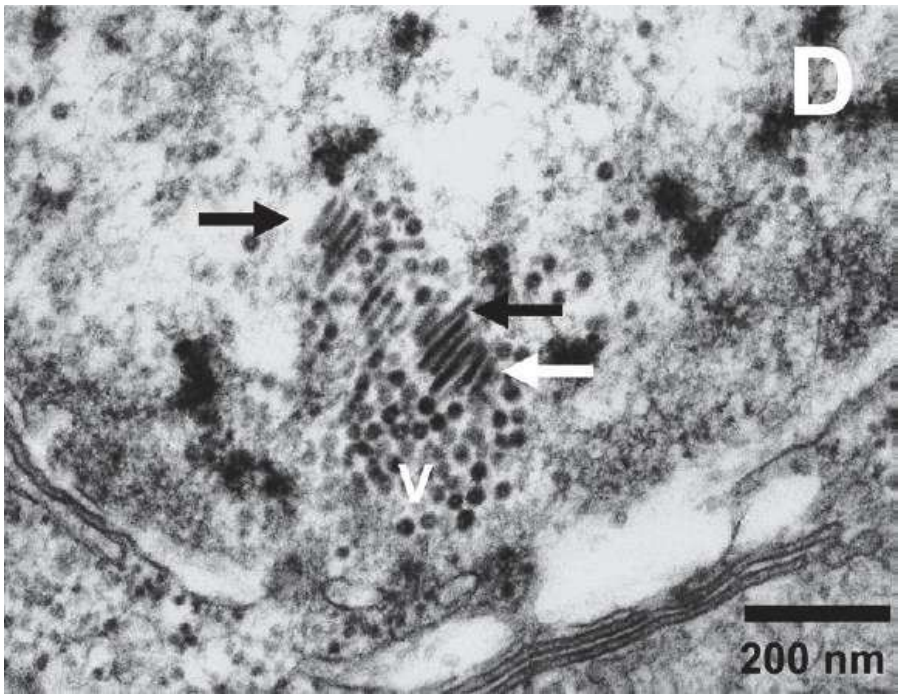

Figure 0-8. Image prise en microscopie électronique à transmission représentant la forme "rod-shaped" des particules virales de Csp05DNAV, virus infectant l'espère Chaetoceros, *dans le nucléus de son hôte (Toyoda* et al.*, 2012)*

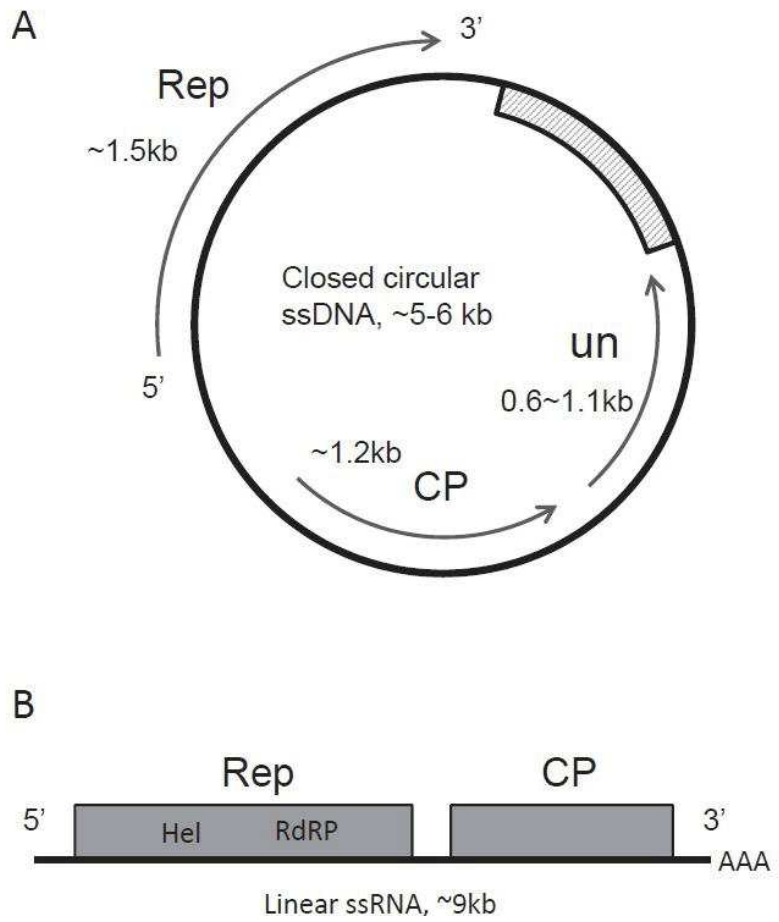

Figure 0-9. Organisation génomique des virus à ADN simple brin (A) et des virus à ARN simple brin (B). A. Génome circulaire ADN d'environ 5-6 kb avec un fragment ADN double brin (rectangle grisé). B. Génome linéaire ARN d'environ 9kb encodant 2 ORFS bien définis (rectangles gris). Le génome peut se terminer par une queue poly A. Rep : Réplication, CP : Protéine de la capside, UN : ORF à fonction inconnue, Hel : Hélicase, RdRp : RNA-dependent RNA-polymerase. Figure de Tomaru et al.*, (2015b)*

Ces dernières années, l'augmentation du nombre d'isolats viraux a permis l'élaboration de comparaisons phylogénétiques plus robustes et ainsi l'attribution des virus ARNsb et ADNsb à des groupes taxonomiques définis. Ainsi, les virus de diatomées à ARN font désormais partie du genre des *Bacillarnavirus*, genre monophylétique (basé sur la RdRp) regroupant uniquement les virus de diatomées et appartenant à l'ordre de *Picornavirales* (International Committee on Taxonomy of Viruses, ICTV, https://talk.ictvonline.org/taxonomy/). Cet ordre regroupe des virus ARNsb infectant une vaste gamme d'organismes, tels que des insectes, des animaux marins, des plantes ou encore des protistes marins avec les genres *Marnavirus* (virus de *Heterosigma akashiwo*) et *Labyrnavirus* (virus d'*Aurantiochytrium* sp.) (Lang *et al.*, 2009). Les *Picornavirales* sont principalement caractérisés par (i) un génome RNA à sens positif avec souvent une queue poly-A en région 3', (ii) une stratégie de traduction du génome en poly-protéines grâce à l'intervention de protéases virales, (iii) des protéines structurales de la capside organisées dans un module contenant trois domaines, formant des petits virions icosaédriques non enveloppés à la une symétrie pseudo T=3, (iv) un module protéique non structurel contenant une hélicase, une protéase (cystéine) et une ARN polymérase ARN dépendante (« RNA-

dependent RNA polymerase », RdRp), codé séquentiellement dans cet ordre (Le Gall *et al.*, 2008).
Quant aux virus à ADNsb, le genre *Bacilladnavirus* avait été proposé pour regrouper tous les membres viraux à ADN associés aux diatomées (ICTV; Tomaru *et al.*, 2011b). Ce genre a été actualisé plus tard à niveau de famille, les Bacilladnaviridae, avec l'ajout de nouveaux représentants infectant des mollusques marins (Kazlauskas *et al.*, 2017). Très récemment, une réorganisation totale de cette famille a eu lieu, avec la création des genres *Diatodnavirus, Kieseladnavirus* et *Protobacilladnavirus,* répartissant les virus de *Chaetoceros* spp. et de mollusques selon les motifs conservés dans les séquences protéiques de réplication (King *et al.*, 2018).

En parallèle des diatomées centriques, les diatomées pennées ont aussi été reportées comme des hôtes potentiels de virus à ADN et ARN (Tomaru *et al.,* 2012), mais avec seulement l'isolement de deux virus sur deux espèces hôtes : *Thalassionema nitzschioides* et *Asterionellopsis glacialis* (tableaux 0-1 et 0-2). Au total, 11 virus ADN et 9 virus ARN ont été décrits pour les diatomées, même si des caractérisations génétiques sont toujours nécessaires dans certains cas (Bettarel *et al.*, 2005a; Eissler *et al.*, 2009; Kim *et al.*, 2015a, 2015b). La grande majorité des virus identifiés ont été isolés sur le genre de diatomée *Chaetoceros* dans les eaux côtières du Japon (tableaux 0-1 et 0-2). Malgré l'effort d'isolement considérable que représentent ces travaux, avec notamment la mise en place de nouveaux protocoles, la restriction de l'aire géographique et des hôtes utilisés pour l'isolement et la sélection des virus laissent à penser qu'une importante diversité virale associée aux diatomées reste à découvrir.

Les études environnementales sont un atout dans l'étude de la diversité et de la répartition des organismes en vue de mieux comprendre leur rôle dans les écosystèmes marins. Des études menées via une approche de gène cible (RdRp), l'analyse du génome viral complet (virome) ou encore des métatranscriptomes ont mis en évidence l'importance des Picornavirus dans les milieux aquatiques, avec des abondances et des diversités totalement sous estimées et encore trop méconnues (Culley, 2018). Notamment, des fragments génétiques et des génomes reconstruits à partir de reads environnementaux provenant des eaux tempérées de Colombie Britannique, des eaux tropicales d'Hawaii ou encore des eaux froides de l'Antarctique, ont montré de fortes homologies avec des membres du genre *Bacillarnavirus* (Culley *et al.*, 2003, 2014; Culley and Steward, 2007; Gustavsen *et al.*, 2014; Miranda *et al.*, 2016; Shirai *et al.*, 2006; Steward *et al.*, 2013). En opposition, les études métagénomiques sur les virus ADNsb sont très limitées. Cependant, Mcdaniel *et al.* (2014) ont réussi à assembler des génomes putatifs de *Bacilladnavirus* à partir de séquences environnementales provenant de Floride.
Les virus infectant les diatomées marines seraient donc globalement distribués, avec des abondances parfois très élevées, et pourraient ainsi être des contributeurs majeurs du plancton au sein de ces écosystèmes. Par ailleurs, les auteurs soulignent le fait que la majorité des séquences génétiques environnementales ne sont pas assignées à des séquences

connues, et que souvent celles-ci ne sont pas détectées au sein de clades taxonomiques définis. Cela suggère donc qu'une importante part de la diversité virale associée aux eucaryotes reste à percer.

Le rôle des virus dans la régulation des dynamiques et succession de diatomées dans l'environnement naturel est, à l'heure actuelle, mal compris. Le suivi des dynamiques diatomées-virus en 2011 dans les eaux côtières du Japon a montré que les espèces de *Chaetoceros* avaient survécu et avaient maintenu leur développement malgré la présence de leurs virus associés (Tomaru *et al.*, 2011a). Une étude plus récente a montré des résultats similaires (Tomaru *et al.*, 2018), appuyant l'hypothèse que les virus de diatomées ne sont pas nécessairement des agents primaires de mortalité de leurs hôtes. Les auteurs proposent des stratégies mises en place par les diatomées pour échapper aux attaques virales, tels que la sédimentation des cellules hôtes infectées, des mécanismes de résistance ou encore une diversité importante dans la sensibilité des hôtes face aux infections virales (Tomaru *et al.*, 2015b). Cependant, le manque de données de terrain empêche les interprétations sur les rôles écologiques de ces virus, confirmant le besoin urgent d'étudier les dynamiques temporelles des systèmes diatomées-virus.

Table 0-1. Caractéristiques morphologiques, physiologiques et génétiques des virus simple brin infectant les diatomées centriques et pennées. CwNIV et CspNIV n'ont pas été totalement décrits mais leurs caractéristiques sont similaires aux ADNsb et sont donc considérés comme appartenant à ce groupe. Tableau modifié à partir de Tomaru et al*., 2015b*

SSDNA VIRUSES OF CENTRIC DIATOMS											
Virus	**Host**	**Particle size (nm)**	**Particle assembly site**	**Rod Shaped virus-like particle**	**Major proteins (kDa)**	**Latent period (h)**	**Burst size (infectious units cell^{-1})**	**Genome length (nt)**	**Complementary fragment length(s) (nt)**	**Accession number**	**Reference**
CdebDNAV	*Chaetoceros debilis*	32	nucleus	ND	37.5, 41	12–24	55	~7 knt not fully sequenced	ND	AB504376	(Tomaru *et al.*, 2008)
ClorDNAV	*Chaetoceros lorenzianus*	34	nucleus	TES	<225	48	2.2×10^4	5813	979	AB553581	(Tomaru *et al.*, 2011c)
CsalDNAV	*Chaetoceros salsugineum*	38	nucleus	ND	43.5, 46	12–24	325	6000	997	AB193315	(Nagasaki *et al.*, 2005)
CsetDNAV	*Chaetoceros setoensis*	33	nucleus	YES	31, 37	48	2.0×10^4	5836	67, 70, 72, 76, 90, 107, 109, 145	AB781089	(Tomaru *et al.*, 2013b)
CtenDNAV type-I	*Chaetoceros tenuissimus*	37	nucleus	YES	38.5	96	320	5639	875	AB597949	(Tomaru *et al.*, 2011b)
CtenDNAV type-II	*Chaetoceros tenuissimus*	37	nucleus	YES	39	<24	1737	5570	669	AB971658	(Kimura and Tomaru, 2015)
Csp05DNAV	*Chaetoceros* sp. strain TG07-C28	33	nucleus	YES	40, 75	<24	ND	5785	890	AB647334	(Toyoda *et al.*, 2012)
Csp07DNAV	*Chaetoceros* sp. strain SS628-11	34	nucleus	YES	38.5	<12	29	5552	827	AB844272	(Kimura and Tomaru, 2013)
CwNIV	*Chaetoceros* cf. *wighamii*	30	nucleus	YES	ND	8	26 396	ND	ND		(Eissler *et al.*, 2009)
CspNIV	*Chaetoceros* cf. *gracilis*	25	nucleus	ND	ND	<24	ND	ND	ND	ND	Bettarel *et al.*, 2005
SSDNA VIRUSES OF PENNATE DIATOMS											
TnitDNAV	*Thalassionema nitzschioides*	35	nucleus	ND	ND	ND	ND	5573	~600 (not sequenced)	AB781284	(Tomaru *et al.*, 2012)

Table 0-2. Caractéristiques morphologiques, physiologiques et génétiques des virus simple brin ARN infectant les diatomées centriques et pennées. SpaIV and ScocV n'ont pas été totalement décrits mais leurs caractéristiques sont similaires aux ARNsb et sont donc considérés comme appartenant à ce groupe. Tableau modifié à partir de Tomaru et al.*, 2015b*

SSRNA VIRUSES OF CENTRIC DIATOMS										
Virus	**Host**	**Particle size (nm)**	**Particle assembly site**	**Major proteins (kDa)**	**Latent period (h)**	**Burst size (infectious units cell^{-1})**	**Genome length (nt)**	**Number of ORFs**	**Accession number**	**Reference**
CtenRNAV type-I	*Chaetoceros tenuissimus*	31	cytoplasm	33.5, 31.5, 30.0	<24	1.0 × 104	9431	2	AB37547	(Shirai *et al.*, 2008)
CtenRNAV type-II	*Chaetoceros tenuissimus*	35	cytoplasm	32.2, 29.0, 26.1	24–28	136	9562	2	AB971661	(Kimura and Tomaru, 2015)
CsfrRNAV	*Chaetoceros socialis* f. *radians*	22	cytoplasm	32.0, 28.5, 25.0	<48	66	9467	2	AB469874	(Tomaru *et al.*, 2009)
Csp03RNAV	*Chaetoceros* sp. strain SS08-C03	32	cytoplasm	42.0, 34.0, 28.0	<48	ND	9417	2	AB639040	(Tomaru *et al.*, 2013a)
RsetRNAV	*Rhizosolenia setigera*	32	cytoplasm	41.5, 41.0, 29.5	48	3100	8847	2	AB243297	(Nagasaki *et al.*, 2004a)
TgraRNAV	*Thalassiosira gravida*	32	ND	ND	ND	ND	~9 knt	ND	LC013477	Unpublished
SpalV	*Stephanopyxis palmeriana*	25-30	cytoplasm	ND	<80	92	ND	ND	ND	(Kim *et al.*, 2015b)
ScosV	*Skeletonema costatum*	45-50	cytoplasm	ND	<48	90-250	ND	ND	ND	(Kim *et al.*, 2015a)
SSRNA VIRUSES OF PENNATE DIATOMS										
AglaRNAV	*Asterionellopsis glacialis*	31	cytoplasm	ND	ND	ND	8842	2	AB973945	(Tomaru *et al.*, 2012)

2. Les parasites eucaryotes

Les parasites eucaryotes de diatomées sont étudiés dans les systèmes marins et d'eau douce depuis seulement quelques décennies. Les méthodes classiques d'échantillonnage, de fixation ou le manque d'expertise rendant souvent leur isolement ou leur caractérisation laborieux (Gleason *et al.*, 2015; Scholz *et al.*, 2015; Schweikert, 2015).

Les pathogènes eucaryotes capables d'infecter les Bacillariophyta peuvent être divisés en deux groupes majeurs : les Opisthochontes et le super groupe des SAR pour Straménopiles, Alveolata et Rhizaria (Adl *et al.*, 2012; Burki *et al.*, 2007) (Figure 0-10). Du fait d'un nombre conséquent d'interactions possibles, seuls les parasites marins seront abordés. Ainsi, environ 18 genres parasites appartenant à près de 10 phylums sont décrits sur plus de 20 genres de diatomées marines.

La plupart de ces parasites de diatomées sont de petite taille et sont couramment désignés « parasites nanoflagellés » (PNF). Ils sont dits zoosporiques, c'est-à-dire qu'ils incluent une phase de cellules mobiles (zoospores) au cours de leur cycle de vie. Dans de nombreux cas, l'analyse de l'ultrastructure de la zoospore, uni flagellée (Opisthochontes) ou biflagellée (groupe SAR), est un élément clef dans le processus d'identification taxonomique de ces parasites. D'autres types de parasites ne présentant pas ce type de structure sporique existent dans la nature (cas du parasite *Rhizamoeba schnepfi* (Kühn, 1996)). Cependant, peu de données étant disponibles, ces derniers ne seront pas abordés dans cette partie.

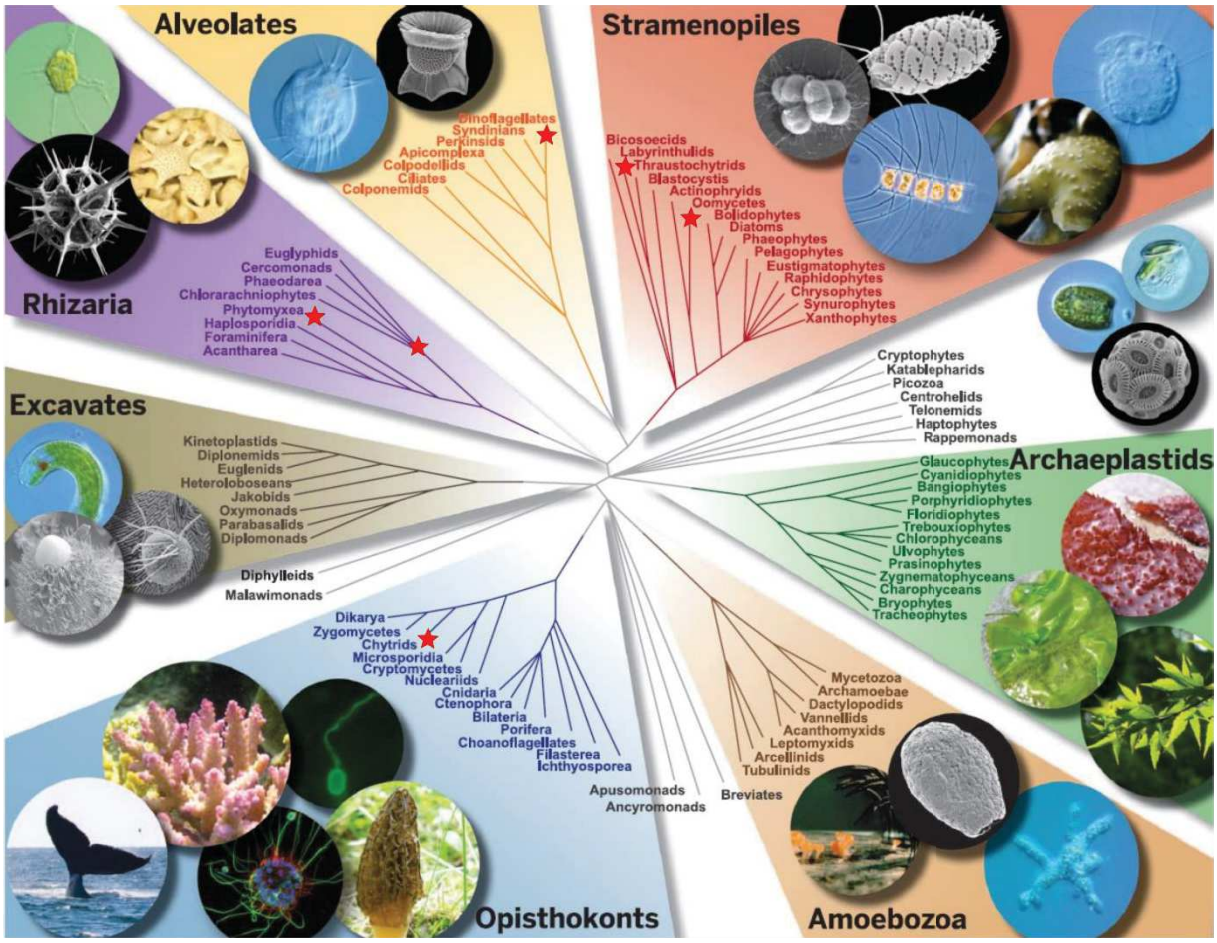

Figure 0-10. Répartition des parasites de diatomées, représentés par une étoile rouge, au sein des majeures lignées eucaryotes. « Tree of life » modifié à partir de (Worden et al.*, 2015). Ces parasites sont répartis parmi les Opisthochontes, les Rhizaria, les Alveolata et les Straménopiles*

L'objectif de cette partie est de donner un aperçu de la diversité des parasites eucaryotes infectant les diatomées, de mettre en avant leurs spécificités, leurs principaux modes d'infection, ainsi que les structures morphologiques et cycles de vie qui les caractérisent. La liste des parasites décrits est fournie dans la Figure 0-14. Il ne s'agit en aucun cas d'une liste exhaustive des parasites eucaryotes zoosporiques de diatomées des milieux marins.

Les Opisthochontes pathogènes de diatomées

Les chytrides (Clade des Chytridiomycota), appelés également vrais Fungis, possèdent une paroi cellulaire faite de chitine, une caractéristique qui permet de les détecter dans les échantillons naturels grâce au marquage avec du Calcofluor White, apparaissant alors en bleu sous lumière UV (Figure 0-12) (Gerphagnon *et al.*, 2013; Rasconi *et al.*, 2009). Associés aux diatomées, ces organismes ont majoritairement été étudiés dans les systèmes aquatiques d'eau douce (Beakes *et al.*, 1992; Ibelings *et al.*, 2004; Rasconi *et al.*, 2012; Van Donk and Ringelberg, 1983) et peu d'interactions ont été signalées en milieu marin. Les genres fongiques *Rhizophydium* et *Chytridium* ont cependant été reportés sur diverses diatomées

planctoniques ou benthiques comme *Achnanthes brevipes, Amphora exigua, Bellerochea malleus, Chaetoceros* sp*., Cylindrotheca closterium, Diploneis didyma, Fragilaria* sp*., Navicula digitoradiata, N. gregaria, Pseudo-nitzchia, Rhizosolenia* sp., *Skeletonema* sp. et *Thalassiosira nordenskioeldii* (Gleason *et al.*, 2011; Gutiérrez *et al.*, 2016; Hanic *et al.*, 2009; Jephcott *et al.*, 2017; Scholz *et al.*, 2014; Schweikert, 2015). Le cycle de vie de *Chytridium* sp. a été détaillé sur *Bellerochea malleus* (Schweikert, 2015). Le chytride, attiré par son hôte par chimiotactisme, va adhérer à la surface du frustule, rétracter son unique flagelle et s'enkyster dans une paroi rigide. Le parasite produit alors un haustorium, appelé aussi rhizoïde ou suçoir intracellulaire, qui va pénétrer la cellule hôte là où la silice est la plus fine. Ce dernier va développer plusieurs branches afin de se nourrir du protoplaste de son hôte par osmotrophie. Les nutriments remontent vers l'extérieur, où le kyste se transforme alors en sporange, contenant de nombreuses zoospores (Figure 0-12 A et B). Lorsqu'une étape de maturation a eu lieu, les zoospores sont relâchées dans le milieu par l'opercule du sporange, pouvant ainsi rencontrer de nouvelles diatomées.

Les Aphelids sont des petits parasites intracellulaires d'algue qui incluent les genres *Aphelidium, Amoeboaphelidium* et le genre marin *Pseudaphelidium* (Karpov *et al.*, 2014). Les Aphelids n'apparaissent pas sur l'arbre des groupes de protistes majeurs établi par Worden et collaborateurs (2015) (Figure 0-10) car ce petit groupe a été récemment classé dans le superphylum Opisthosporidia, avec les Microsporidia et les Cryptomycota (Karpov *et al.*, 2014). L'espèce marine *Pseudaphelidium drebesii* a été caractérisée à la fin des années 1990 sur *Thalassiosira punctigera*, le seul hôte possible recensé à ce jour (Schweikert and Schnepf, 1996, 1997a). Les zoospores ont une taille de 5 µm de long sur 3 µm de diamètre et possèdent un long flagelle de 15 µm. Ces cellules mobiles s'attachent soit au niveau de la jonction des valves, soit directement sur les valves, puis s'enkystent. La vacuole contenue dans la zoospore augmente son volume, exerçant ainsi une pression intracellulaire. Le flagelle forme une structure bien particulière, appelée le tube d'infection, et sous l'effet de la pression, va être « dévaginé ». Toujours sous l'effet de la pression, le tube d'infection et tout le cytoplasme de *P. drebesii* pénètrent la cellule hôte et débutent la phagocytose. Seule la paroi de la zoospore reste à l'extérieur (Figure 0-11). Le parasite envahit complètement la cellule hôte et forme alors un plasmodium. A la fin de la phase trophique, ce plasmodium se divise en cellules ovoïdes qui deviennent amœboïdes et quittent le frustule. Ces cellules amœboïdes s'enkystent (Figure 0-12, D) puis relâchent dans le milieu 2 à 4 zoospores (Schweikert and Schnepf, 1996, 1997a). Le processus d'infection est également schématisé Figure 0-13.

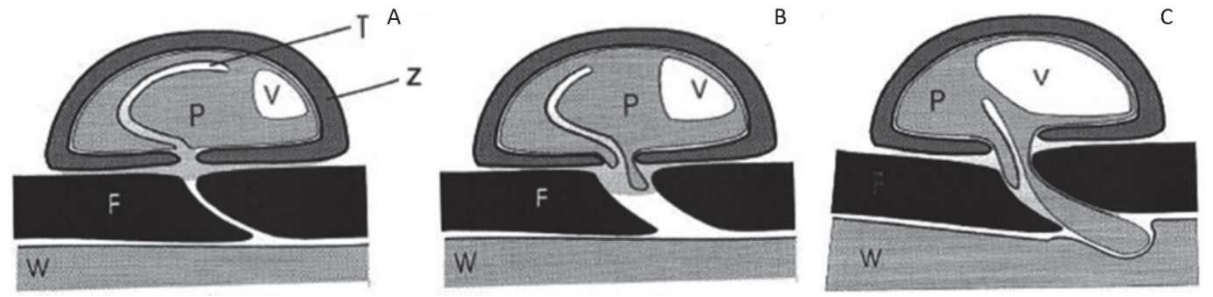

Figure 0-11. Processus d'infection de Pseudaphelidium drebesii*. A. La zoospore s'attache au frustule de* T. punctigera *et s'enkyste. B. L'infection commence, la vacuole augmente de taille et exerce une pression permettant au cytoplasme du parasite de fissurer le frustule. C. Le tube d'infection pénètre la cellule hôte. F : Frustule, P : cytoplasme de* P. drebesii, *T : tube d'infection, V : vacuole, W : cellule hôte, Z : paroi de la zoospore. (Schweikert and Schnepf, 1997a)*

Les principaux membres du super groupe SAR pathogènes de diatomées

- Les Straménopiles

Chez les Oomycètes, 4 genres principaux sont endoparasites de diatomées : *Lagenisma*, infectant plusieurs espèces de *Coscinodiscus* et *Palmeria hardmaniana* (Grahame, 1976; Schnepf *et al.*, 1978a, 1978b; Scholz *et al.*, 2014), *Ectrogella* parasite les espèces *Coscinodiscus granii, Licmophora hyalina* et *Pseudo-nitzschia pungens* (Hanic *et al.*, 2009; Scholz *et al.*, 2014), *Miracula* infecte *P. pungens* et *Olpidiopsis* attaque *Rhizosolenia imbricata* (Buaya *et al.*, 2017). Par exemple, *Lagenisma coscinodiscii* a un cycle assez similaire à celui de *P. drebesii.* Les zoospores s'attachent à la ceinture cingulaire de la diatomée, s'enkystent et germent un tube d'infection. Le parasite se nourrit de son hôte et se développe à l'intérieur de celui-ci sous forme de zoosporange. Les zoospores biflagellées sortent de ce sporange en forme de tube et subissent deux étapes d'enkystement avant d'infecter de nouvelles espèces de *Coscinodiscus* (Figure 0-12, F) (Schweikert, 2015).

Le genre *Pirsonia* (classe des Hyphochytrea) regroupe au total 6 espèces : *P. guinaridiae*, *P. verrucosa, P. formosa, P. diadema, P. eucampiae* et *P. punctigerae* (Kühn *et al.*, 1996; Schnepf *et al.*, 1990; Schweikert and Schnepf, 1997b). L'espèce *P. mucosa* indiquée sur la Figure 0-14 est en réalité l'espèce *Pseudopirsonia mucosa,* et malgré son étonnante ressemblance morphologique avec les membres de *Pirsonia*, des études phylogénétiques ont montré son appartenance non pas au clade des Straménopiles mais des Cercozoa (Kühn *et al.*, 2004).

Les espèces de *Pirsonia* ont des spectres d'hôtes très dissimilaires. *P. formosa* semble être généraliste, infectant les espèces de diatomées *Eucampia zodiacus*, *Guinardia delicatula, Leptocylindrus danicus, Rhizosolenia imbricata* et *R. setigera.* Les autres espèces ont des spectres hôtes plus étroits avec *P. guinardiae* infectant *Guinardia flaccida, P. diadema* sur *Coscinodiscus granii* et *C. wailesii*, *P. eucampiae* sur *E. zodiacus, P. verrucosa* sur *G. delicatula* et *P. punctigerae* sur *Thalassiosira punctigera* et *T. hendeyi.*

De façon générale, la zoospore biflagellée de *Pirsonia* (Figure 0-12, H) s'attache au frustule de son hôte là où la protection siliceuse est faible, le plus souvent au niveau de la jonction des valves ou au niveau des processus externes, et forme un pseudopode qui pénètre alors la cellule hôte. Ce pseudopode va alors former un trophosome à l'intérieur de l'hôte, structure réalisant la phagocytose et contenant une vacuole de digestion. Les nutriments générés sont transférés à l'auxosome, corps resté à l'extérieur et attaché sur le frustule (Figure 0-12, G et Figure 0-13). Grâce à l'apport de ressource, l'auxosome va se diviser tout au long de la phagocytose. Les nouvelles cellules produites vont subir deux autres divisions avant de donner des zoospores. Le nombre de zoospores produites varient d'une espèce à une autre (8 à 60 cellules) ainsi que leur taille (3 à 10 µm de long, 3 à 10 µm de diamètre) (Schweikert and Schnepf, 1997b).

Chez les Straménopiles, la lignée des Labyrinthulomycètes contient 6 clades dont deux majoritaires : les thraustochytrides et le groupe des labyrinthulides et aplanochytrides (description complète dans la récente revue de Bennett *et al.*, 2017). La famille des Thraustochytriacae comporte deux espèces, *Ulkenia visurgensis* et *Schizochytrium* sp*.,* rapportées comme infectant des diatomées telles que *Coscinodiscus* sp., *Grammatophora* sp., *Melosira* sp., *Navicula* sp., *Nitzschia* sp. ou encore *Thalassionema nitzschioides* (Figure 0-12, K) (Bennett *et al.*, 2017; Raghukumar, 1986, 2006). Cependant, peu d'informations sont disponibles, rendant toutes descriptions impossibles. Par ailleurs, l'espèce *Labyrinthula* sp. présentée dans la Figure 0-14 est en réalité un Thraustochytride et les auteurs de l'étude ont conclu ne pas être certains du caractère parasitaire de leur isolat, de fait que celui-ci était préservé dans du formaldéhyde (Riemann and Schaumann, 1993). Le thraustochytride pouvait donc tout autant être un saprophyte comme il a déjà été montré (Bennett *et al.*, 2017; Raghukumar, 2002; Riemann and Schaumann, 1993).

- Les Alveolata

Les dinoflagellés (Dinophyta) sont les seuls membres des Alvéolaires répertoriés comme parasites de diatomées. Les deux seuls genres connus à ce jour, *Paulsenella* et *Gyrodinium,* infectent les diatomées *Helicotheca tamesis* (anciennement *Streptotheca tamesis*), *Chaetoceros decipiens*, *Eucampia zodiacus* et *Odontella aurita* (Figure 0-12, E) (Drebes and Schnepf, 1982, 1988, 1998). Brièvement, le dinoflagellé ectoparasite attaque son hôte au niveau de la région cingulaire et lui insère un tube d'infection afin de phagocyter tout son contenu cytoplasmique. Lorsque la phase trophique se termine, la nourriture est alors digérée dans une grande vacuole, le tube d'infection se rétracte et le trophonte, resté au niveau du frustule, s'enkyste. Une division cellulaire va avoir lieu pour laisser place à un deuxième enkystement. Ce kyste secondaire va alors libérer deux dinospores (= zoospores biflagellées), recommençant alors un nouveau cycle (Figure 0-13) (Drebes and Schnepf, 1982).

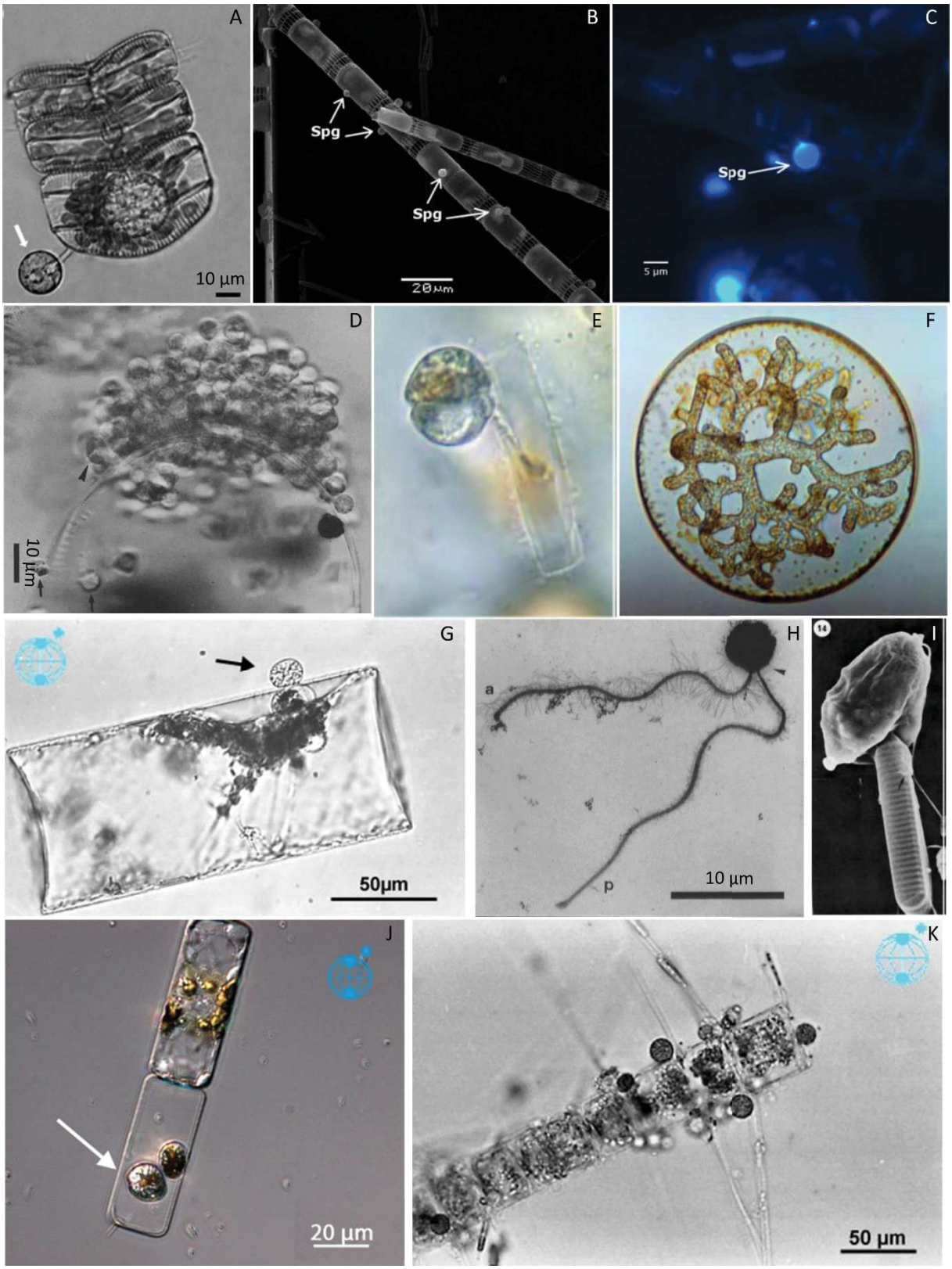

Figure 0-12. Exemples de parasites eucaryotes infectant des diatomées marines. A. Chytride associé à la diatomée benthique Achnanthes brevipes *(Scholz* et al.*, 2014). B et C. Chytride sur le frustule de* Skeletonema *sp. spr : sporange. B : microscopie électronique à balayage, C : microscopie à épifluorescence. La chitine contenue dans la paroi du chytride fluoresce en bleu grâce au calcofluor white (Gutiérrez* et al.*, 2016). D. Cystes de* Pseudaphelidium drebesii *sur* Thalassiosira punctigera *(Schweikert and Schnepf, 1996). E.* Paulsenella *sp. sur un frustule vide. F.* Lagenisma *infectant* Coscinodiscus *sp. E et F : photos de S. Kühn. G.* Pirsonia guinardiae *sur* G. flaccida *(Sabine Ehmen, Plankton Net). H. Zoospore de* Pirsonia punctigerae *avec le flagelle antérieur (a) aux long*

poils et le flagelle postérieur (p) aux poils courts (Schweikert and Schnepf, 1997b). *I.* Cryothecomonas armigera *se nourrissant de la diatomée* Nitzschia cylindrus *en Antarctique (Thomsen* et al.*, 1991). I.* Cryothecomonas aestivalis *dans une cellule vide de* G. delicatula *(Alexandra, Plankton Net). K.* Thraustochytrium *sp. infectant une chaîne de diatomée (Gerhard Drebes, Plankton Net)*

- Les Rhizaria

Les Rhizaires associés aux diatomées sont affiliés principalement au clade des Phytomyxea et au genre *Cryothecomonas* (embranchement des Cercozoa (Kühn *et al.*, 2000)). Ce dernier regroupe deux espèces de parasites : *C. longipes* et *C. aestivalis* (Drebes *et al.*, 1996; Schnepf and Kühn, 2000). D'autres spécimens ont été décrits dans les eaux froides de l'Antarctique et du Danemark, se nourrissant de protistes incluant les diatomées (Figure 0-12, I) (Thomsen *et al.*, 1991). Néanmoins à notre connaissance, leurs caractérisations génétiques n'étant pas disponibles, leur affiliation avec les deux premières espèces est basée uniquement sur la morphologie. *C. aestivalis* a été trouvé uniquement sur *G. delicatula* (Drebes *et al.*, 1996; Peacock *et al.*, 2014) tandis que *C. longipes* infecte de nombreuses espèces comme *Chaetoceros costatus*, *C. debilis, C. didymus, Coscinodiscus granii*, *C. radiatus*, *G. delicatula*, *G. striata*, *Leptocylindrus danicus*, *Navicula* sp., *Pleurosigma* sp., *Rhizosolenia setigera, Thalassiosira rotula, T. punctigera,* et *Cerataulina bergonii* (Schnepf and Kühn, 2000).
Les zoospores de ce genre font entre 9 et 14 µm de long et 4 et 9 µm de large et possèdent deux flagelles de longueurs inégales (Figure 0-12, H). Lorsque la zoospore rencontre son hôte, elle s'attache en général au niveau du cingulum et se transforme en pseudopodium (Figure 0-13). Grâce à cette forme amœboïde, le parasite rentre dans la cellule hôte. La phagocytose prend place, le pseudopodium portant deux petits flagelles, aussi appelé trophonte, occupe alors toute la cellule hôte (Figure 0-12, J). Quand la phase de nutrition s'arrête, le parasite subit 2 à 3 divisions donnant 8 à 32 progénies (= nouvelles zoospores) selon la taille de l'hôte ou la quantité de ressource ingérée. *C. longipes* diffère de *C. aestivalis* dans le sens où le corps principal du parasite reste attaché au frustule lors de la nutrition, ne rentrant dans la cellule hôte qu'un long pseudopodium (Drebes *et al.*, 1996; Schnepf and Kühn, 2000).

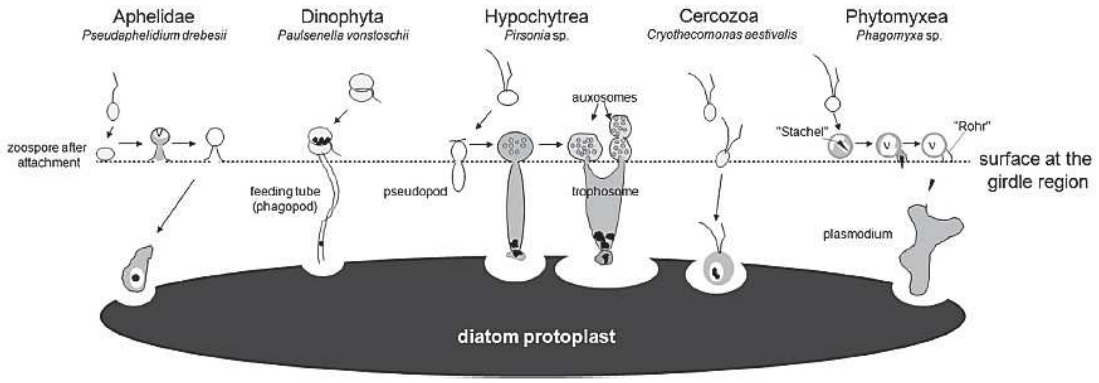

Figure 0-13. Comparaison des divers cycles de vie des parasites infectant les diatomées. Les Aphelidae sont des Opisthochontes représentés par Pseudaphelidium, *endoparasite à zoospores uni-flagellées se nourrissant par un tube d'infection. Les Dinoflagellés du genre* Paulsenella *s'alimentent par phagotrophie via un tube d'infection. Le genre* Pirsonia *(Straménopiles) se nourrit par un pseudopode qui deviendra un trophosome alimentant une*

structure externe, l'auxosome. Cryothecomonas *(Cercozoa) digère son hôte via l'élaboration d'un pesudopodium biflagellé au sein de la cellule hôte et* Phagomyxa *(Phytomyxea) forme un plasmodium (Scholz* et al.*, 2015)*

Les épidémies dues à ces parasites zoosporiques ont été rapportées lors des efflorescences de diatomées, avec souvent d'importants taux d'infection (Peacock *et al.*, 2014; Scholz *et al.*, 2014; Tillmann *et al.*, 1999). Par exemple, *Cryothecomonas aestivalis* a été imagé attaquant *Guinardia delicatula* dans les eaux du Massachusetts (USA) de 2006 à 2013, généralement entre la fin de l'été et le début de l'automne. Les taux d'infection de ces évènements parasitaires récurrents peuvent dépasser les 10% et ainsi représenter une source importante de mortalité pour *Guinardia* (Peacock *et al.*, 2014). Les auteurs suggèrent notamment que les cycles de vie très courts de ce type de parasite (< 24h) peuvent engendrer d'intenses et de nombreux taux d'infection chaque jour, et ainsi constituer des compétiteurs majeurs du zooplancton. Les études proposent également que ces parasites eucaryotes sont d'importants régulateurs de blooms de diatomées jouant un rôle non négligeable dans la succession d'espèces dû à leurs spectres d'hôtes parfois très spécifiques (Peacock *et al.*, 2014; Scholz *et al.*, 2014; Tillmann *et al.*, 1999).
Une étude plus récente soutient ces hypothèses. En effet, Gutiérrez et ses collaborateurs ont montré la co-variation d'abondance entre des chytrides et des diatomées des genres *Skeletonema* et *Thalassiosira* au printemps austral dans une zone d'upwelling productive (courant d'Humboldt au large du Pérou) (Gutiérrez *et al.*, 2016). Les auteurs ont différencié les stades attachés (sporanges) et les stades libres (zoospores) des chytrides et ont constaté l'apparition de sporanges au début de saison printanière, lorsque que les genres *Skeletonema* et *Thalassiosira* prédominaient la communauté de diatomées (Figure 0-12, B et C). A la fin du printemps-début de l'été, la manifestation des stades libres était corrélée à la diminution d'abondance de ces deux genres hôte, avec en parallèle une augmentation de la concentration de *Chaetoceros*. Cet exemple illustre là aussi que la spécificité des infections parasitaires va avoir un rôle dans la composition des communautés de diatomées dans cette région d'upwelling, avec des transitions bien marquées au cours des saisons. Ces auteurs remettent ainsi en cause l'hypothèse selon laquelle la terminaison des blooms de diatomées était uniquement due au manque de nutriments et à la pression de broutage et ajoutent ainsi la responsabilité des Fungi dans le déclin des populations marines de diatomées.

Les descriptions ci-dessus montrent la diversité d'hétérotrophes eucaryotes infectant les diatomées. Cependant, au sein de chaque clade, peu de genres ou d'espèces sont décrits, spécifiquement en milieu marin. Pourtant, des études récentes utilisant des outils moléculaires ont mis en évidence, via des réseaux de co-occurrence et analyses statistiques, que d'autres interactions sont possibles dans le milieu naturel (Christaki *et al.*, 2017a). Cela suggère que de nouvelles espèces restent à isoler et à caractériser afin de mieux comprendre comment les communautés planctoniques sont structurées et comment elles fonctionnent au sein des écosystèmes.

Table 1 – Examples of zoosporic parasites of marine diatoms.

Parasite phylum	Description	Parasite species	Host species	Growth phase	Feeding structure	References of infection
Unikont (opisthokont) zoosporic parasites						
Chytridiomycota	True fungi, characterised by cell walls composed of chitin (with the exception of their zoospores).	Unidentified chytrid species	*Navicula digitoradiata*	epibiotic	rhizoids	Scholz et al. 2014
		(*Rhizophydium* (?)	*N. gregaria*			
		Chytridium (?))	*Achnanthes brevipes*			
			Diploneis didyma			
			Cylindrotheca closterium			
			Amphora exigua			
	The most prominent morphological feature of the thallus is the zoosporangium (James et al., 2006).	Unidentified chytrid species	*Thalassiosira nordenskioeldii*			Gaertner 1979
			Chaetoceros sp.			
		Unidentified chytrid species	*Pseudo-nitzschia pungens*			Hanic et al. 2009
Aphelidae	They have been recently re-classified as Opisthosporidia, a sister group to fungi (Karpov et al., 2014).	*Pseudaphelidium drebesii*	*Thalassiosira punctigera*	endobiotic	infection tube and microfilament	Schweikert and Schnepf 1996, 1997a
Heterokont zoosporic parasites						
Alveolata						
Dinophyta (core dinoflagellates)	The infraphylum Dinozoa is divided into different major groups that included the core Dinophyceae and several basal groups (i.e. Syndinids, Perkinsozoa). Molecular data from ribosomal proteins were used to resolve the deep branching dinoflagellate clades (Bachvaroff et al., 2014). Only a few heterotrophic genera in the core Dinophyceae are parasites of diatoms, and are considered herein. All members of the genus Paulsenella Chatton are ectoparasites on marine planktonic diatoms (Drebes and Schnepf, 1988).	*Paulsenella vonstoschii*	*Streptotheca tamesis* (=*Helicotheca tamesis*)	epibiotic	feeding tube, (phagopod)	Drebes and Schnepf 1988
		P. chaetoceratis	*Chaetoceros decipiens*			
		P. kornmannii	*Eucampia zodiacus*			
		Gyrodinium undulans	*Odontella aurita*			Drebes and Schnepf 1998

Stramenopiles						
Oomycota (basal oomycetes)	Cellulosic cell walls (consisting mainly of 1,3-β-glucans, some1,6-β-glucans and 1,4-β-glucans). Sporangia of different taxa within the Oomycetes have diverse morphology. They may be terminal or intercalary (within a hyphal filament), bulbous or not, and if terminal, caducous (sporangia detach readily) or not. The basal oomycetes that infect diatoms lack the mycelium and sexual reproduction, commonly found in the crown oomycotes.	*Ectrogella perforans* *Ectrogella* sp. *Lagenisma* sp. *Ectrogella* sp. *Lagenisma coscinodisci*	*Licmophora hyalina* *Pseudo-nitzschia pungens* *Coscinodiscus radiatus* *Dimeregramma minor* *Gyrosigma peisonis* *Coscinodiscus granii* *Coscinodiscus centralis* *Coscinodiscus granii* *Coscinodiscus concinnus* *Coscinodiscus* sp.	endobiotic endobiotic endobiotic both endobiotic endobiotic endobiotic	infection tube infection tube infection tube infection tube infection tube	Raghukumar, 1980 a, b Hanic et al., 2009 Scholz et al., 2014 Schnepf et al., 1978 Schnepf et al., 1978 Wetsteyn and Peperzak, 1991 Drebes, 1966, 1968
Hyphochytrea (*Pirsonia* clade)	*Pirsonia* is considered as heterotrophic nanoflagellate. According to Kühn et al. (2004) four species of diatom parasites belonging to the genus *Pirsonia*, clustered together in a clade closely related to *Hyphochytrium catenoides*	*Pirsonia punctigerae* *P. verrucosa* *P. mucosa* *P. formosa* *P. eucampiae* *P. diadema* *P. guinardiae*	*Thalassiosira punctigera* *Rhizosolenia delicatula* (=*Guinardia delicatula* *Rhizosolenia shrubsolei* (=*R. imbricata*) *Rhizosolenia setigera* *Eucampia zodiacus* *Coscinodiscus granii* *C. wailesii* *C. concinnus* *Guinardia flaccida*	endobiotic	pseudopodium at surface, pseudopodia inside	Schweikert and Schnepf, 1997b Kühn et al., 1996 Kühn et al., 1996 Kühn, 1998 Schnepf et al., 1990
Labyrinthulomycota (order Thraustochytriida)	Cell wall is made of dictyosome-derived circular scales, arranged in several layers (Darley et al., 1973; Chamberlain, 1980; Moss, 1985). All species (except the thraustochytrid	*Schizochytrium* *Ulkenia visurgensis*	*Thalassionema nitzschioides* *Navicula* sp. *Nitzschia* sp. *Coscinodiscus* sp. *Melosira* sp. *Grammatophora* sp.	epibiotic epibiotic	pseudopodia	Gaertner, 1979 Raghukumar, 1986

Parasite phylum	Description	Parasite species	Host species	Growth phase	Feeding structure	References of infection
	genus *Althornia* (Jones & Alderman) produce a system of ectoplasmic net (EN) elements from one or more points on the cell (Perkins, 1972, 1973; Porter, 1990). Vegetative stages of thraustochytrids consist of single cells which are globose to subglobose (4-20 μm diam.), growing epibiotically on various substrata (Raghukumar, 1996).					
Bigyra	As far as known for *Labyrinthula* the zoospores may not be the infective agent as it is typical for other parasites described in this review - it infects hosts by direct penetration and osmosis by the vegetative, spindle cells.	*Labyrinthula*	*Nitzschia* sp. *Amphiprora* sp.	both	vegetative, spindle cells	Riemann and Schaumann, 1993
MAST-3 Rhizaria		*Solenicola setigera*	*Leptocylindrus mediterraneus*			Padmakumar et al., 2012
Cercozoa (*Cryothecomonas* clade)	Large and diverse group of amoeboflagellates, with tubular mitochondrial cristae, that cluster together in molecular phylogenies inferred mainly from ribosomal gene sequences (small	*Cryothecomonas aestivalis* *C. longipes*	*Guinardia delicatula* *G. flaccida* *Cerataulina bergonii* (=*C. pelagica* *Chaetoceros costatus* *Ch. debilis* *Ch. didymus* *Coscinodiscus granii* *C. radiatus* *Guinardia delicatula* *G. striata*	epibiotic mostly	pseudopodium	Drebes et al., 1996 Peacock et al., 2014 Schnepf and Kühn, 2000

	and large subunit rDNA) (Thomsen et al., 1991; Chantangsi et al., 2008). Colourless flagellates, in the free, motile stage, oblong to oval, 9-12 × 4-5 μm, two apically inserted flagella, anteriorly directed flagellum 15 μm long, posteriorly directed flagellum up to 25 μm (biflagellate whiplash flagella)	*Heteromita globosa* (a related feeding nanoflagellate)	*Leptocylindrus danicus* *Navicula sp.* *Pleurosigma sp.* *Rhizosolenia setigera* *Thalassiosira rotula* *T. punctigera* *Skeletonema costatum*			Ohno et al., 2013
Phytomyxea	Including Plasmodiophorida ("plasmodio-phorids") and Phagomyxida are a group of parasitic protists belonging to the Rhizaria (Neuhauser et al., 2010, 2012, 2014; Bulman and Braselton, 2014) that form during their life cycle two types of morphologically very similar, heterokont zoosporic stages (Neuhauser et al., 2011a). Motile stages are heterokont, biflagellate, with one whiplash flagellum	*Phagomyxa bellerocheae* *P. odontellae*	*Bellerochea malleus* (=*B. horologicalis*) *Odontella sinensis*	endoiotic	infection tube ("Stachel and Rohr"); plasmodium	Schnepf et al., 2000

Figure 0-14. Exemples de parasites eucaryotes infectant les diatomées marines. Ce tableau est une liste non exhaustive des pathogènes de diatomées et regroupe les organismes les mieux décrits au moment de la publication. Ces organismes produisent des spores mobiles au cours de leur cycle de vie et sont donc appelés "parasites zoosporiques". En raison l'évolution permanente des phylogénies, les affiliations génétiques présentées peuvent ne plus être actuelles. Ce tableau provient de Scholz et al. *(2015)*

3. Les bactéries marines algicides

Les interactions négatives entre les diatomées et les bactéries sont connues depuis de nombreuses décennies. Ces bactéries ont deux façons d'interagir avec la cellule hôte : par contact direct nécessitant une mobilité de la cellule bactérienne et un système d'attachement à la cellule hôte comme des protéines et des polysaccharides, soit de façon indirecte par la détection de molécules dans le milieu environnant, ou chimiotactisme, mais aussi par l'excrétion de composés extracellulaires comme les protéases (Amin *et al.*, 2012; Lee *et al.*, 2000; Mayali and Azam, 2004). Les bactéries en associations négatives avec les diatomées appartiennent principalement aux groupes des Bacteroidetes et des Gammaproteobactéries, impliquant un nombre limité de genres (Amin *et al.*, 2012; Mayali and Azam, 2004; Meyer *et al.*, 2017). La liste ci-dessous des bactéries inhibant la croissance des diatomées est non exhaustive, mais représentative de la diversité de ces interactions, en terme de taxons, de spectres d'hôtes ou encore de mode d'action.

Au début des années 1990, la bactérie *Cytophaga* sp. (phylum des Bacteroidetes) isolée au Japon lors du déclin du bloom de *Skeletonema costatum*, avait la capacité de tuer *S. costatum*, d'autres diatomées comme *Ditylum brightwellii*, *Thalassiosira* sp., et également le raphidophyte *Chattonella antiqua* (Mitsutani *et al.*, 1992). L'action de cette bactérie était une attaque directe, nécessitant un contact physique entre la bactérie et ses hôtes.
Quelques années plus tard, des bactéries marines également isolées à partir des eaux côtières du Japon et appartenant au genre *Pseudoalteromonas* (anciennement *Alteromonas*, classe des gammaproteobactéries, phylum Proteobacteria) ont montré des lyses cellulaires importantes sur les diatomées *S. costatum*, *Thalassiosira* sp., *Eucampia zodiacus* et sur le raphidophyte *C. antiqua*, mais étaient sans effet sur *D. brightwelli* (Kato *et al.*, 1998). Lee *et al.* (2000) se sont penchés plus particulièrement sur la souche *Pseudoalteromonas* A28 et ont démontré qu'une molécule de type sérine protéase qu'elle secrétait était responsable de la lyse algale.
En opposition à ces bactéries à large spectre, la souche SR-14 de l'espèce *Alteromonas colwelliana*, isolée dans les eaux de Corée du Sud, avait un effet algicide très ciblé sur des espèces de *Chaetoceros*, mais sur aucune autre espèce de Bacillariophyta (Kim *et al.*, 1999). Plus récemment, les souches, EC-1 d'*Alteromonas* sp. et EC-2 de *Maribacter* sp. (famille des Flavobacteriaceae, phylum Bacteroidetes), isolées de la station d'observation à long-terme L4 de Plymouth (Manche occidentale), montraient une forte pathogénicité sur *Skeletonema* sp. (Wang *et al.*, 2016). Là encore, l'activité lytique de ces deux bactéries serait due au relargage de composés algicides extracellulaires. Ces études ne font qu'ajouter les diatomées comme hôtes potentiels des bactéries des genres *Pseudoalteromonas* et *Alteromonas,* déjà recensées comme exerçant un fort pouvoir algicide sur de multiples taxons phytoplanctoniques (Mayali and Azam, 2004).

Quatre isolats bactériens incluant *Halobacillus* sp. (famille des Bacillaceae, phylum des Firmicutes), *Muricauda* sp. (Flavobacteriaceae, Bacteroidetes), *Kangiella* sp. (Gammaproteobactéries, Proteobacteria) et *Roseivirga* sp. (famille des Flammeovirgaceae, Bacteroidetes), jusque-là jamais encore décrits comme algicides vis-à-vis des diatomées, ont été rapportés comme tuant également *S. costatum,* augmentant ainsi considérablement la diversité de bactéries pathogènes associées à cette espèce (Shi *et al.*, 2013). Associées à une même espèce hôte, ces quatre bactéries présentaient des modes d'action différents. En effet, *Halobacillus* sp. induisait la lyse cellulaire via la libération d'un composé actif, tandis que les trois autres bactéries pathogènes attaquaient directement *S. costatum.*

D'autres bactéries algicides ont été décrites telles que l'espèce *Saprospira* sp. souche SS98-5 (Bacteroidetes) isolée au Japon tuant *Chaetoceros ceratosporus* (Furusawa *et al.*, 2003) ou encore l'espèce *Kordia algicida* (Flavobacteriaceae) lysant *S. costatum*, *Thalassiosira weissflogii* et *Phaeodactylum tricornutum*, mais sans effet sur *Chaetoceros didymus* (Paul and Pohnert, 2011, 2013). Les actions algicides de ces deux bactéries ont été bien étudiées. *Saprospira* sp., qui a une action directe, se dirige vers son hôte via un mécanisme de glissement (« gliding motility »), s'attache et provoque la lyse cellulaire par la formation de micro-tubules. Comme *Pseudoalteromonas* A28*, K. algicida* produit une sérine protéase qui détruit ses hôtes. L'excrétion de cette molécule n'est pas dépendante de la densité de l'hôte, mais densité-dépendante de *K. algicida*. Ces résultats suggèrent un phénomène de communication dit de quorum sensing (QS) entre les bactéries (Paul and Pohnert, 2011).

Récemment, un autre type de molécule impliqué dans la mortalité des diatomées a été mis en évidence. La bactérie *Chitinimonas prasina* souche LY03 (Betaproteobacteria) était capable de détecter la présence de son hôte par chimiotactisme, de s'attacher au frustule via son flagelle et de produire puis libérer une chitinase ciblant la chitine présente dans cette matrice inorganique et menant ainsi à la mort de *Thalassiosira pseudonana* (Figure 0-15) (Li *et al.*, 2016). Cette étude a montré que seules les diatomées possédant de la chitine dans leur frustule comme *T. pseudonana*, *T. weissflogii*, *C. muelleri* et *S. costatum* étaient impactées par cette bactérie, contrairement à la diatomée sans chitine *Phaeodactylum tricornutum*.

Déterminer le mode d'action des bactéries algicides est important pour mieux comprendre les interactions biotiques au sein des communautés planctoniques à plus large échelle. En effet, selon son mode d'action et les molécules algicides impliquées, le spectre d'hôte d'une bactérie sera plus ou moins large. Les bactéries algicides ont le potentiel de contrôler les dynamiques de leurs hôtes et ainsi d'influencer les successions phytoplanctoniques. Toutefois, l'importance (fréquence des infections, nombre de bactéries impliquées) de ces contrôles n'a, à notre connaissance, jamais été quantifiée dans le milieu naturel.

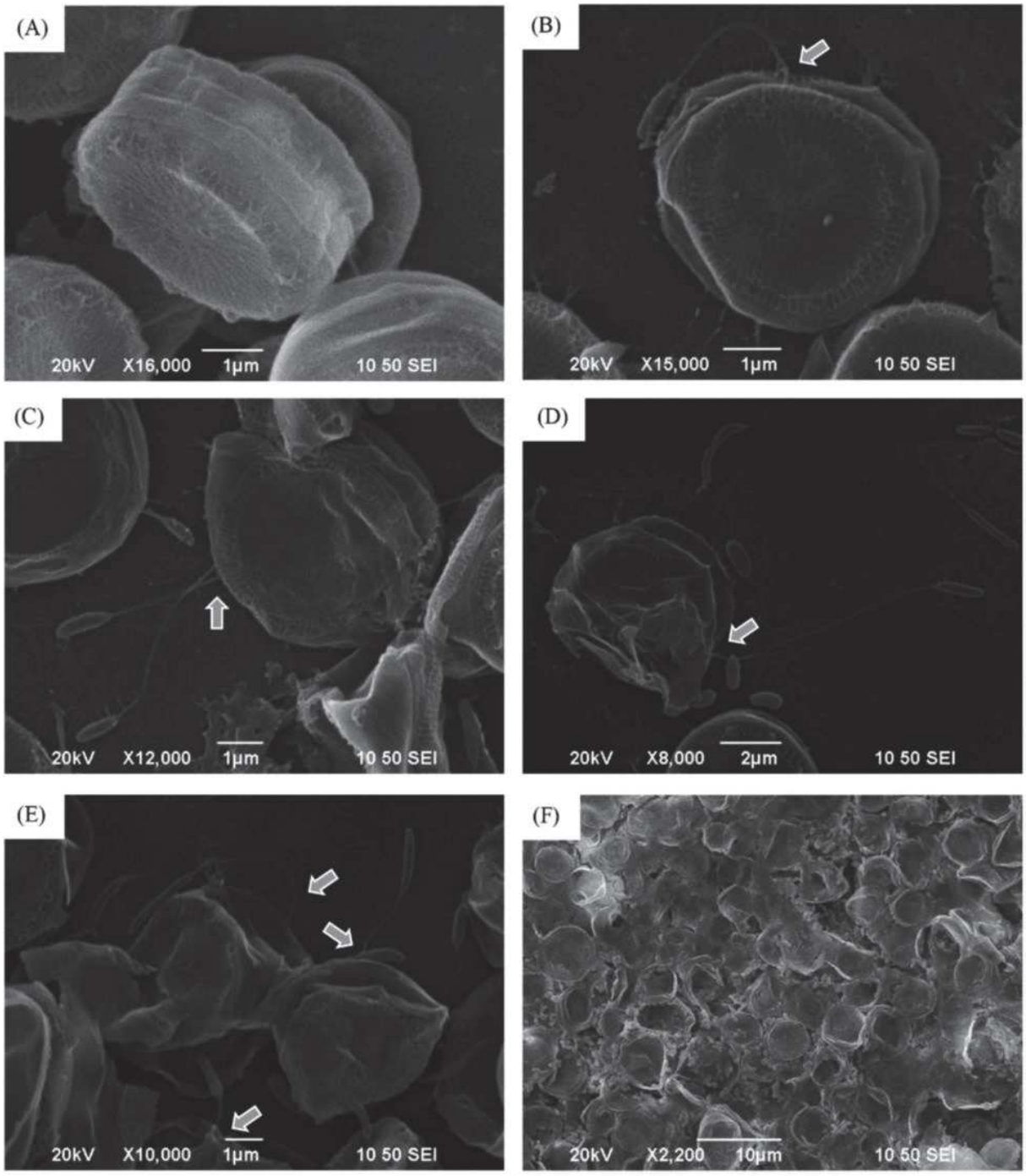

Figure 0-15. Image en microscopie électronique à transmission de Chitinimonas prasina *souche LY03 sur son hôte* Thalassiosira pseudonana. *A. Contrôle sain. B à F : Interactions à 6, 12, 24, 48 et 72h respectivement. Les flèches blanches représentent l'attachement des bactéries sur le frustule de leur hôte (Li* et al.*, 2016)*

OBJECTIFS DE THÈSE

1. Problématique et objectifs principaux

L'introduction qui précède nous a permis de dresser de façon non exhaustive l'état des connaissances actuelles sur le rôle des parasites de phytoplancton dans les milieux aquatiques. Il apparaît que les parasites sont très divers (virus, bactéries, eucaryotes appartenant à plusieurs grandes lignées évolutives). En revanche, leurs rôles écologiques, leurs modes d'action en milieu naturel ou encore leur contribution à la mortalité phytoplanctonique sont souvent encore trop peu compris et encore moins quantifiés. Et cela est d'autant plus marqué en milieu marin. Dans ces écosystèmes, les diatomées forment un groupe prépondérant, et ce depuis les temps géologiques, avec des développements de blooms et de successions d'espèces essentiels d'un point de vue écologique et biogéochimique. La prise de conscience de leur rôle-clé dans le milieu naturel a conduit à de nombreuses études pour comprendre les mécanismes qui contrôlent leurs blooms. Si les contrôles par les facteurs abiotiques et les interactions transitoires (type prédation) font l'objet de nombreuses études, les interactions durables de type parasitisme ont été peu explorées, notamment dans le milieu marin.

Dans ce contexte, l'objectif général de ce projet de thèse était d'identifier le(s) parasite(s) associé(s) aux diatomées prédominantes des côtes françaises de la Manche Occidentale afin de mieux comprendre comment le parasitisme contrôle les proliférations de diatomées. Pour cela, nous avons choisi de travailler sur des modèles constitués chacun d'une espèce d'hôte et de ses parasites, et ce en combinant des approches au laboratoire et des approches *in situ*. Ce sujet de thèse proposait de tester l'hypothèse selon laquelle les parasites forment une communauté structurée qui se développe lors de la prolifération des diatomées et contribue de manière significative à leur déclin et à leurs successions.

2. Modèles d'étude

Pour tester cette hypothèse, nous avons utilisé des systèmes modèles diatomées-parasites que nous avons isolés au cours de la période 2015-2016 à partir d'échantillons obtenus au site SOMLIT-Astan au large de Roscoff, un site d'observation à long terme de la Station Biologique de Roscoff. Par ailleurs, nous avons utilisé des données d'observation obtenues pour ce site (non seulement au cours de la période 2015-2016, mais aussi plus largement depuis 2007) pour analyser les dynamiques des hôtes et parasites dans leur milieu naturel.

Notre choix, en ce qui concerne les hôtes, a porté sur les diatomées du genre *Guinardia* et plus particulièrement sur l'espèce *Guinardia delicatula*, emblématique des blooms printaniers et estivaux au large de Roscoff. Nous avons aussi utilisé comme modèles les

diatomées nanoplanctoniques et en particulier les genres *Minidiscus* et *Thalassiosira*. Des analyses génétiques (par metabarcoding) ont en effet récemment révélé l'importance de ces nanodiatomées tout au long de l'année au site d'observation SOMLIT-Astan (Figure 0-1). Les petites espèces de *Thalassiosira*, non représentées sur la Figure 0-1, étaient parmi les 25 OTUs les plus abondants en termes de reads.

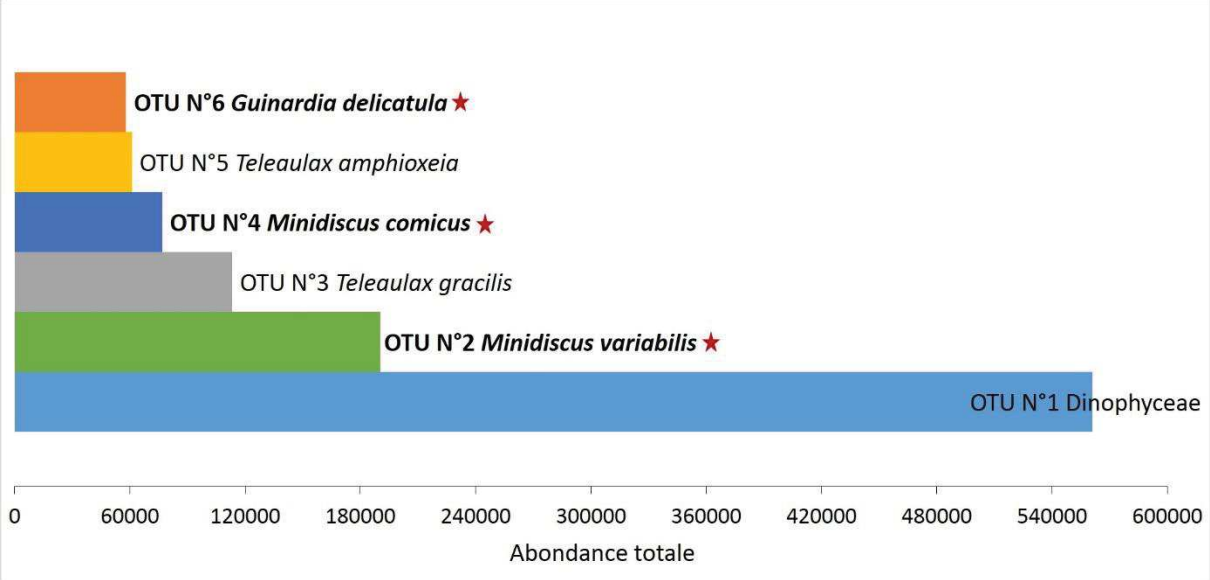

Figure 0-1. Assignation taxonomique 5 premiers OTUs les plus abondants en terme de nombre de reads à SOMLIT-Astan pour la période 2009-2011. L'OTU N°2, N°4 et N°6 ont respectivement été assignés à Minidiscus variabilis, Minidiscus comicus *et* Guinardia delicatula

- **Le genre *Guinardia*, et principalement l'espèce *Guinardia delicatula***

Les espèces du genre *Guinardia* (Coscinodiscophyceae, Rhizosoleniales, Rhizosoleniaceae) sont caractérisées par des cellules cylindriques et allongées, solitaires ou coloniales. Le frustule possède de nombreuses bandes cingulaires ouvertes et ligulées et les valves sont arrondies avec un processus unique. Les cellules possèdent plusieurs plastes. (Kraberg *et al.*, 2010; Throndsen *et al.*, 2007)

G. delicatula (Cleve) Hasle 1997, *G. flaccida* (Castracane) H.Peragallo 1892 et *G. striata* (Stolterfoth) Hasle 1996 sont les plus communes des 6 espèces décrites pour ce genre, et aussi les seules espèces du genre présentes à Roscoff. La forme des colonies (lâches ou avec des cellules accolées), des cellules (cylindres incurvés ou non), et des valves (plates ou convexes) et la localisation et la forme du processus permet une distinction aisée des 3 espèces au microscope (Hasle and Syvertsen, 1997; Kraberg *et al.*, 2010). Ainsi *Guinardia delicatula,* anciennement *Rhizosolenia delicatula* Cleve 1900, possèdent des cellules cylindriques non incurvées (8 et 40 µm de diamètre et de 20 à 70 µm de long), souvent étroitement associées en longues chaînes (Figure 0-2, A, B and C). Les valves sont plates et arrondies sur le pourtour. Elles portent un court processus externe à la marge. Les chloroplastes sont lobés (Hernández-

Becerril, 1995; Kraberg *et al.*, 2010; Yun and Lee, 2011). Ces deux derniers caractères permettent de distinguer *G. delicatula* de *Dactyliosolen fragilissimus*, dont la morphologie est proche (Figure 0-2, D) (Throndsen *et al.*, 2007).

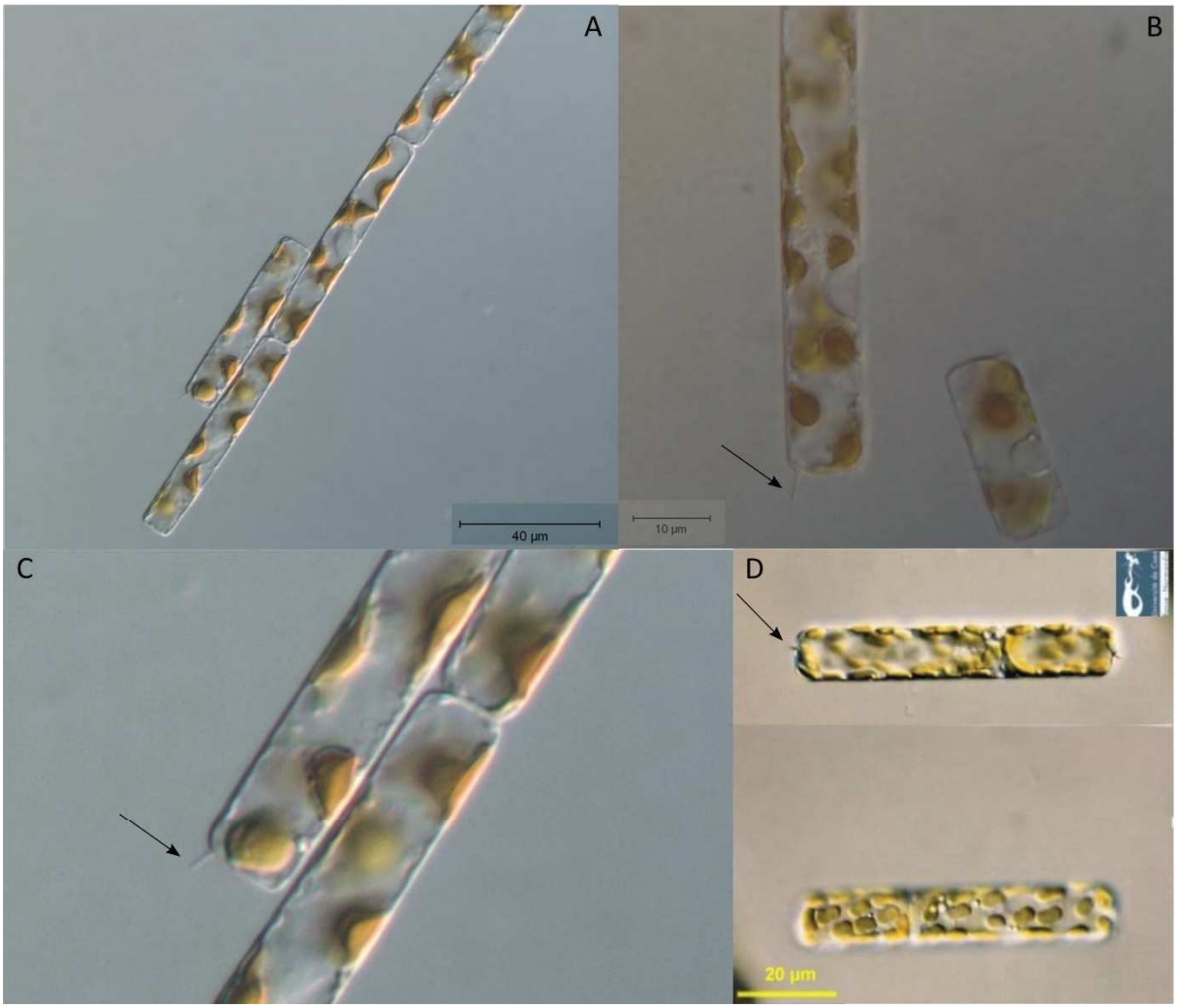

Figure 0-2. Guinardia delicatula*. A and B. Longues chaines et cellules solitaires de la souche RCC3083 en microscopie optique. Cellules montrant plusieurs chloroplastes irréguliers. C. Zoom de la photo A sur le processus externe. A, B et C sont des photos personnelles. D.* Dactyliosolen fragilissimus *avec de nombreux chloroplastes et un tube externe petit et court. Photo de Chantal Billard, Université de Caen Basse-Normandie. Les flèches pointent les processus externes*

G. delicatula est signalée des pôles à l'équateur, essentiellement en zone côtière (base de données OBIS, Guiry and Guiry, 2018; Hernández-Becerril, 1995; Kraberg *et al.,* 2010; Yun and Lee, 2011*)*. En Europe, cette espèce contribue de façon significative aux assemblages de microphytoplancton le long des côtes Atlantiques, en Manche (Gómez and Souissi, 2007; Grall, 1972; Guilloux *et al.*, 2013; Sournia *et al.*, 1987), en Mer du Nord (Wiltshire *et al.*, 2010) et en Mer d'Irlande (Gowen *et al.*, 1999). En Mer du Nord au large de Helgoland (stations de la série temporelle « Helgoland Roads »), *G. delicatula* forme des blooms au printemps, en été et à

l'automne et est considérée comme la diatomée la plus abondante (Kraberg *et al.*, 2010). A Roscoff, où les diatomées dominent largement les assemblages microphytoplanctoniques (83,3 % des cellules phytoplanctoniques dénombrées au microscope pour la période 2007-2016), cette espèce est dominante du milieu du mois de mai jusqu'au mois de septembre (Figure 0-3). Typiquement 3 blooms successifs sont observés au cours de cette période (Figure 0-4).

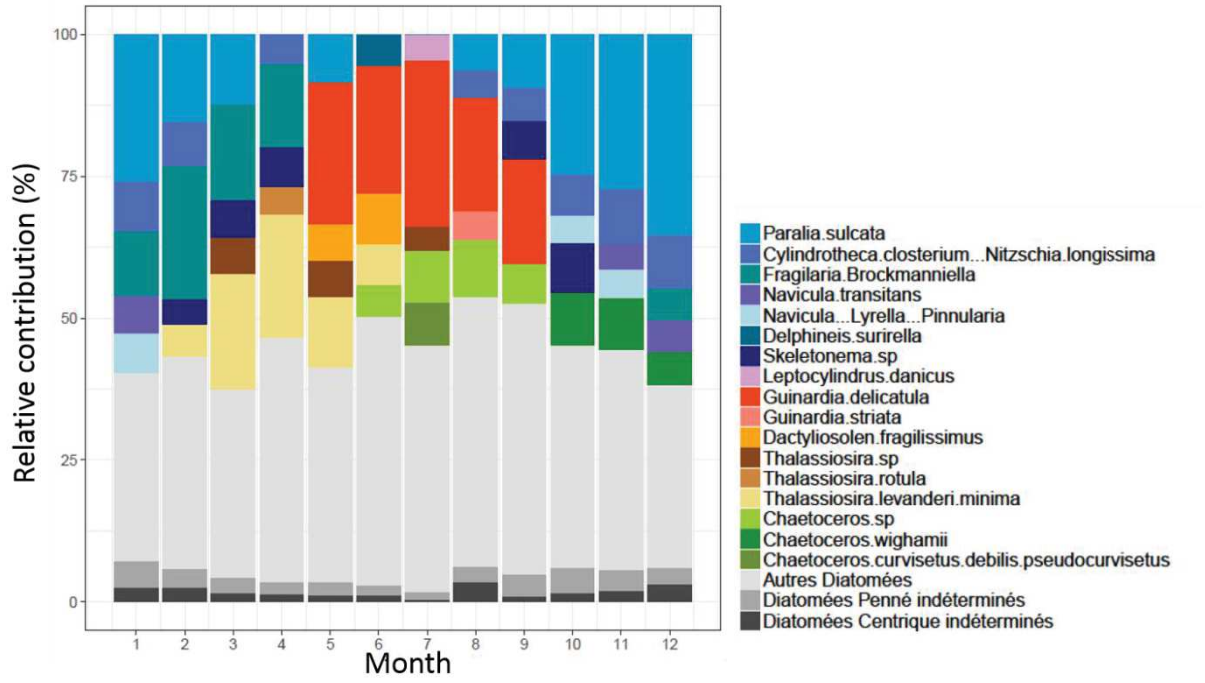

Figure 0-3. Contributions relatives moyennes des taxons de diatomées au cours d'un cycle annuel à la station SOMLIT-Astan pour la période 2007-2016. Pour chaque mois, les contributions moyennes des 5 taxons les plus dominants étaient calculées à partir des comptages taxonomiques (http://abims.sb-roscoff.fr/pelagos/) obtenus pour la période 2007-2016. Figure et légende de Forsans (2018), Master Océanographie et Environnements Marins

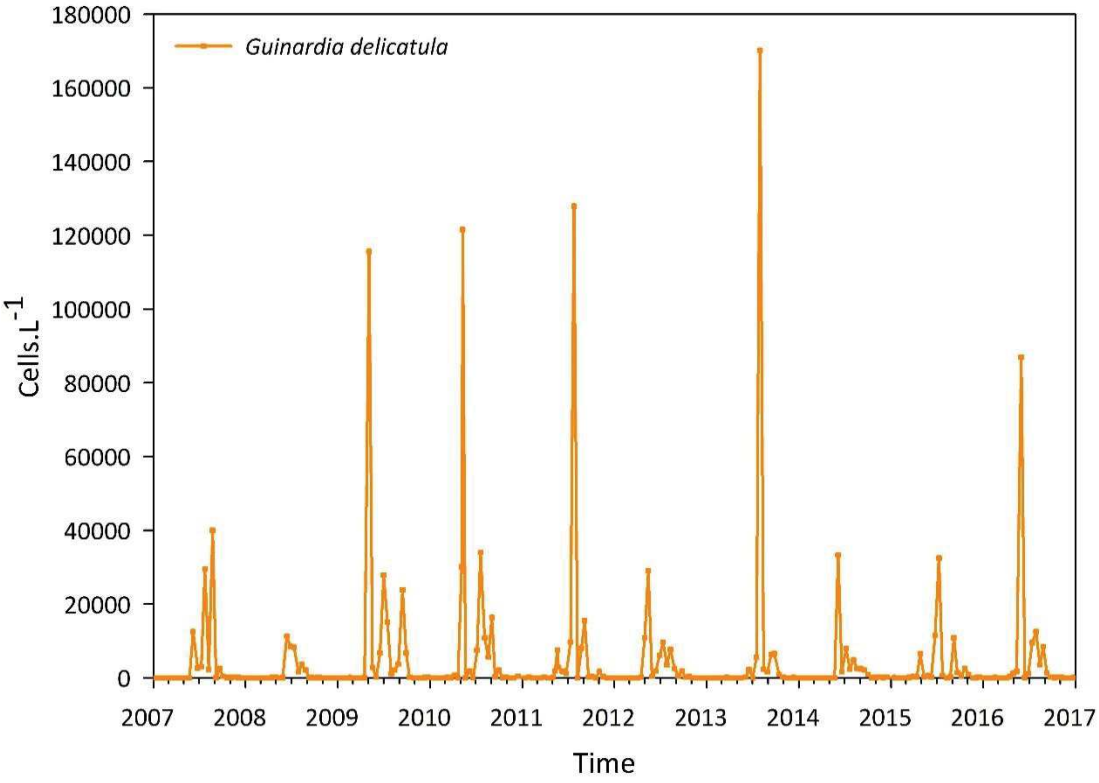

Figure 0-4. Dynamique temporelle de Guinardia delicatula *à la station SOMLIT-Astan durant la période 2007-2016. Les données proviennent de la base de données Pelagos (http://abims.sb-roscoff.fr/pelagos/)*

Dans le cadre de ce projet de thèse, les espèces *Guinardia flaccida* et *Guinardia striata* ont aussi été utilisées comme modèles mais dans une bien moindre mesure ; elles sont donc décrites plus succinctement. *G. flaccida* (anciennement *Rhizosolenia flaccida* Castracane 1886) possède aussi des cellules cylindriques (14 à 95 µm de diamètre, 45 à 160 µm de long) souvent étroitement associées en colonies (Figure 0-5, A). Les chloroplastes sont étoilés et les bandes cingulaires sont souvent aisément observées au microscope tandis que le processus très court est difficile à repérer (Figure 0-5, B) (Hernández-Becerril *et al.*, 2010; Kraberg *et al.*, 2010; Loir, 2004; Yun and Lee, 2011). *G. striata* (anciennement *Rhizosolenia stolterforthii* (Stolterforth) H. Peragallo 1888) possède des cellules cylindriques incurvées et les chaînes forment des spirales (Figure 0-5, C et D). Les cellules (6-53 µm de diamètre, 30-300 µm de long) possèdent de nombreux petits chloroplastes ovoïdes (Figure 0-5, C). Le processus externe qui émerge à la marge de la valve est en forme de crochet et pénètre dans une dépression de la cellule adjacente (Figure 0-5, D et E) (Hernández-Becerril, 1995; Hernández-Becerril *et al.*, 2010; Kraberg *et al.*, 2010; Loir, 2004; Yun and Lee, 2011).

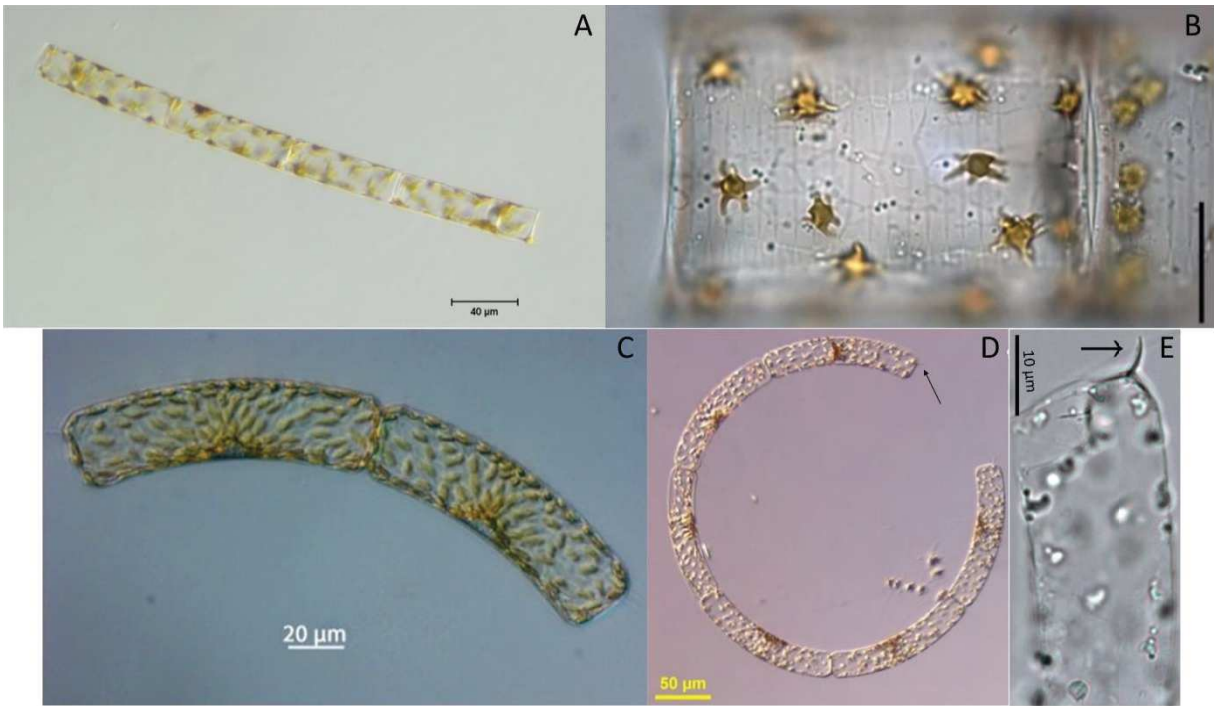

Figure 0-5. A et B: Guinardia flaccida *A. Chaine de 4 cellules. B. Petite et large cellule contenant des chloroplastes étoilés. Les bandes cingulaires bien distinctes peuvent être observées. C à E :* Guinardia striata*. C. Chaines de deux cellules avec de nombreux chloroplastes ovoïdes. D. Début d'une spirale formée par une chaine de cellules. E. Tube externe en forme de crochet. Les flèches indiquent les processus externes. Sources des photos : A : photo personnelle. B : provenant du site web « Iranian Harmful Algal Blooms Defense Committee ». C : Plankton net AWI. D : photo de Fabien Jouenne. E : A partir de Yun and Lee (2011)*

G. flaccida et *G. striata* sont cosmopolites mais leur présence dans les eaux polaires n'a pas jamais été démontrée (Guiry and Guiry, 2018; Throndsen *et al.,* 2007; Yun and Lee, 2011, Hernández-Becerril, 1995; Loir, 2004). En Manche et mers du Nord de l'Europe, ces espèces se développent au printemps et en été (ainsi qu'en automne pour *G. striata*) (Gómez and Souissi, 2007, 2008; Guilloux *et al.* 2013; Kraberg *et al.*, 2010). Au site SOMLIT-Astan au large de Roscoff, *G. flaccida* et G. *striata* forment des blooms en août et septembre (Figure 0-6 et Figure 0-7 respectivement). Les abondances cellulaires atteintes sont bien moindres que celles de *G. delicatula* et varient d'une année sur l'autre.

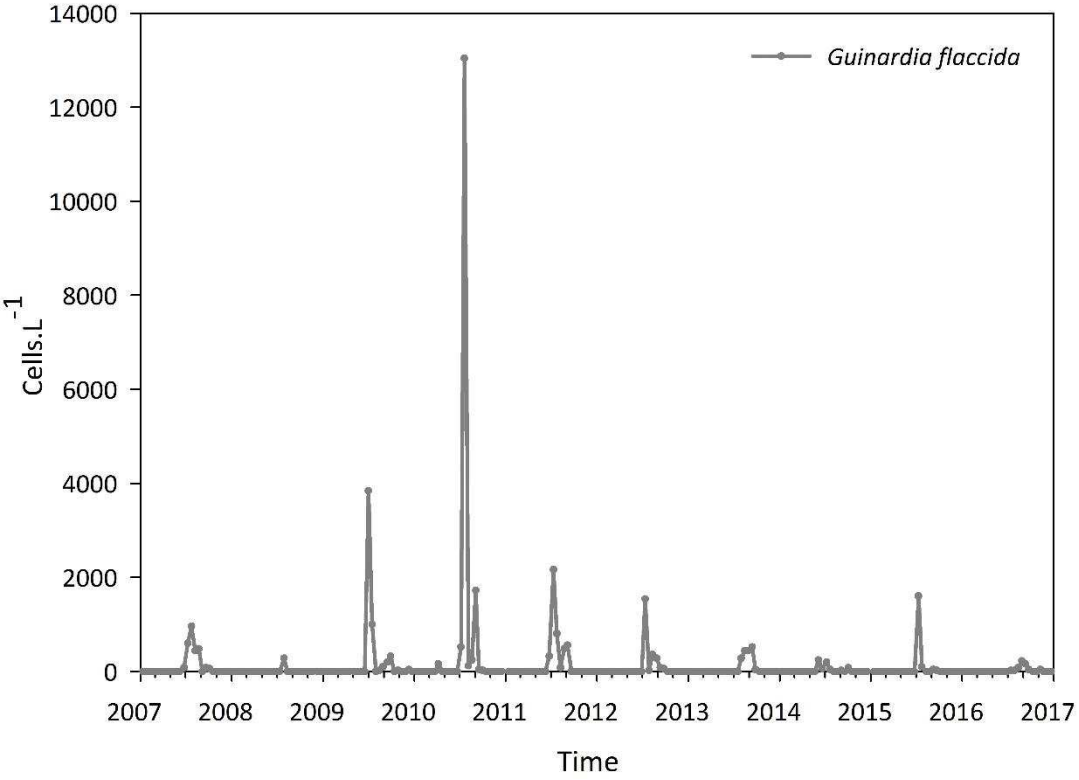

Figure 0-6. Dynamique temporelle de Guinardia flaccida *à la station SOMLIT-Astan durant la période 2007-2016. Les données proviennent de la base de données Pelagos (http://abims.sb-roscoff.fr/pelagos/)*

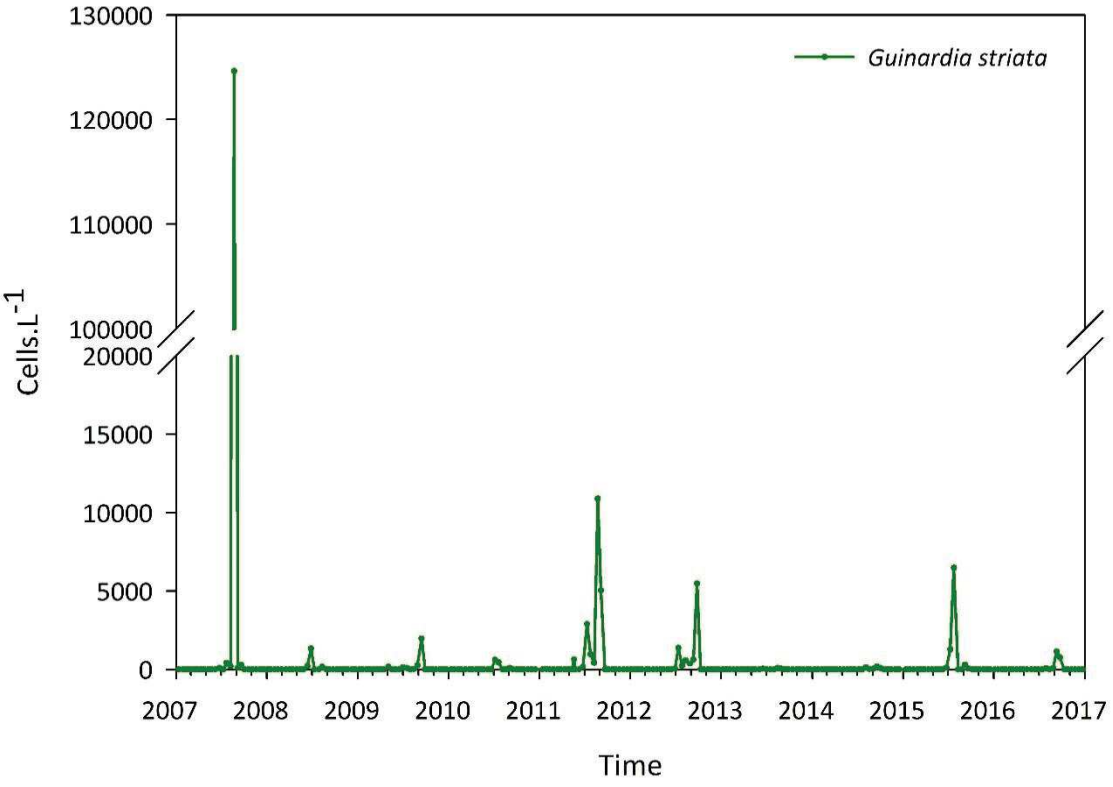

Figure 0-7. Dynamique temporelle de Guinardia striata *à la station SOMLIT-Astan durant la période 2007-2016. Les données proviennent de la base de données Pelagos (http://abims.sb-roscoff.fr/pelagos/)*

- **Nanodiatomées des genres *Minidiscus* et *Thalassiosira***

Le genre *Minidiscus* (Coscinodiscophyceae, Thalassiosirales, Thalassiosiraceae), décrit par Hasle en 1973, comporte 10 espèces dont la taille n'excède pas 10 µm (Aké-Castillo *et al.*, 2001; Gao *et al.*, 1992; Guiry and Guiry, 2018; Hasle, 1973; Kaczmarska *et al.*, 2009; Park *et al.*, 2017; Quiroga and Chretiennot Dinet, 2004; Takano, 1981). Les cellules sont arrondies à cylindriques. Les caractères qui distinguent ce genre des autres Thalassiosirales sont l'absence de processus renforcés (fultoportulae) marginaux, ces processus étant localisés au centre de la valve. Les valves portent un seul processus labié (ou rimoportula) non marginal et souvent présent dans la région subcentrale de la valve (Hasle, 1973). Le genre *Minidiscus* est cosmopolite, il est signalé des pôles à l'équateur (Aké-Castillo *et al.*, 2001; Daniels *et al.*, 2015; Kang *et al.*, 2013; Leblanc *et al.*, 2018; Malviya *et al.*, 2016; Percopo *et al.*, 2011; Quiroga and Chretiennot Dinet, 2004; Takano, 1981; Zingone *et al.*, 2011). Longtemps considéré comme rare, car difficile à détecter et à quantifier à cause de sa taille, *Minidiscus* a récemment été identifié comme un genre majeur de diatomées dans l'océan mondial. Il pourrait aussi contribuer de façon significative à l'export de carbone (Leblanc *et al.*, 2018). En Manche, Quiroga et Chrétiennot-Dinet (2004) ont signalé la présence de 3 espèces : *M. chilensis, M. decoratus* et *M. trioculatus*. Etant donné leur petite taille, ces espèces n'ont pas été dénombrées au microscope et leur dynamique n'est donc pas connue.

Le genre *Thalassiosira* Cleve 1873 comporte aussi des représentants nanoplanctoniques (par exemple *T. curviseriata* Takano (5-14 µm de diamètre), *T. minima* (5-15 µm), *T. profunda* (Hendey) Hasle (2-4 µm), *T. pseudonana* Hasle et Heimdal (2,3- 5,5 µm), *T. mala* Takano (4-10 µm)) (Hasle, 1976; Hasle and Syvertsen, 1997). Ce genre cosmopolite est très diversifié (environ 170 espèces actuelles et de nombreuses espèces fossiles) et comporte des espèces responsables de blooms saisonniers dans les eaux polaires (*T. Antarctica),* tempérées et boréales *(T. angulata*, *T. nordenskioeldii* et *T. rotula*) ainsi que dans les régions d'upwelling (*T. partheneia*) (Assmy and Smetacek, 2009; Hoppenrath *et al.*, 2007; Park *et al.*, 2016b). Le genre, défini au départ par l'espèce type *T. nordenslioldi,* présente une couronne marginale de processus renforcés, un processus renforcé central et un processus labié marginal (Hasle, 1978). Il comprend actuellement de nombreuses espèces dont l'organisation structurale peut varier par rapport à ce schéma. *Thalassiosira* est considéré comme un genre paraphylétique et polyphylétique et aujourd'hui, les relations phylogéniques entre les espèces demeurent mal comprises. Notamment, la description et l'identification des espèces sont encore difficiles à réaliser, en particulier en ce qui concerne les plus petites (Hoppenrath *et al.*, 2007; Jewson *et al.*, 2016).

Au début de ma thèse, et contrairement au genre *Guinardia*, aucun travail n'avait encore été réalisé sur les nanodiatomées du site SOMLIT-Astan. J'ai donc mené un travail d'isolement et de caractérisation des espèces dominantes et j'ai également étudié leur dynamique à partir des données de metabarcoding disponibles au laboratoire. En parallèle, j'ai réalisé un travail très préliminaire sur les parasites qui les infectent.

3. Contenu de la thèse

A travers diverses approches (échantillonnage, culture, biologie moléculaire) décrites dans la **partie I**, ce travail de thèse, totalement exploratoire, a permis de mettre en lumière une diversité jusque-là insoupçonnée des parasites présents dans les milieux marins puisqu'un total de 102 parasites ont été isolés et maintenus entre Août 2015 et Octobre 2016 (**partie I**).

Les parasites associés à *Guinardia delicatula* sont présentés dans la **partie II**. Le **premier chapitre de cette partie II** décrit les premiers virus de *G. delicatula*. La caractérisation fonctionnelle et génomique de ces virus ont permis d'affilier ces parasites à l'ordre des *Picornavirales* et au genre *Bacillarnavirus,* qui inclut d'autres virus de diatomées. Nos analyses suggèrent que ces parasites sont très spécialisés. Ils n'infectent que quelques souches de l'espèce *G. delicatula* et ne représentent probablement pas les agents de mortalité majoritaires durant les blooms de cette diatomée. En effet, la susceptibilité de l'hôte semble varier au cours de son cycle de croissance et nos efforts d'isolement n'ont été fructueux que lors du déclin du bloom estival. Il est donc probable que d'autres contrôles s'exercent durant ces efflorescences massives. Les **chapitres II** et **III de la partie II** indiquent en effet que d'autres parasites généralistes et particulièrement virulents infectent cette diatomée. Le Labyrinthulomycète *Aplanochytrium* sp. (**Chapitre II**) est reporté pour la première fois sur des diatomées. Ce pathogène eucaryote est capable d'attaquer un grand nombre d'espèces algales grâce notamment à son réseau ectoplasmique. *Aplanochytrium* sp. semble se développer plus intensément en hiver et en été, laissant penser à un contrôle sur divers taxons phytoplanctoniques. Enfin, *Kordia* sp. (**Chapitre III**) est une bactérie algicide agissant via l'excrétion de composés extracellulaires responsables de la lyse cellulaire hôte. Les premiers résultats préliminaires semblent montrer que cette bactérie pourrait détecter des signaux provenant de son hôte, lui permettant ensuite de déclencher la production des agents algicides. Cette communication microbienne inter-domaine est très peu reportée en milieux marins et illustre d'autant plus la méconnaissance des interactions biotiques dans ces environnements.

Jusqu'à récemment, les travaux menés sur le contrôle des diatomées se sont exclusivement limités aux espèces microphytoplanctoniques (taille généralement > 10 µm). Une étude récente a pourtant démontré la prépondérance des nanodiatomées marines à l'échelle globale et leur contribution importante dans l'export de carbone. A notre connaissance, les contrôles biotiques régulant ces efflorescences sont inexplorés. Dans la **partie III chapitre I**, une combinaison d'outils microscopiques et moléculaires a mis en évidence que les nanodiatomées, particulièrement certaines espèces des genres *Minidiscus* et *Thalassiosira*, dominent numériquement la communauté phytoplanctonique à SOMLIT-Astan et qu'elles présentent des patrons saisonniers très marqués. Durant cette étude, nous avons conduit la caractérisation morphogénétique de 60 isolats. Ces isolats ont été déposés dans une collection de culture (Roscoff Culture Collection) et sont désormais disponibles pour la communauté scientifique et le grand public. Chacune des espèces décrites apparaît

particulièrement vulnérable aux attaques parasitaires tout au long de l'année (**Partie III - Chapitre I**), puisqu'un total de 82 parasites ont été isolés parmi lesquels une majorité de virus (**Partie III - Chapitre II**).

L'ensemble de ces travaux a permis de générer une collection importante de pathogènes dont seuls environ 3% des isolats ont pu être décrits. Cela démontre qu'une majorité des interactions reste à caractériser et fera éventuellement l'objet de futurs projets recherche (**Perspectives**).

PART I

FROM THE SAMPLING TO THE ISOLATION OF DIATOMS AND PARASITES STRAINS AT THE SOMLIT-ASTAN STATION

CONTEXT OF THE WORK

The SOMLIT-Astan long-term monitoring station has been my playground in particular during the first year of my Ph.D. All the diatom and parasite strains that served for my work were isolated from seawater collected from this station during the period 2015-2016. I also used the hydro-chemical and plankton diversity data (both cell counts and genetic data) acquired at SOMLIT-Astan from 2007 through 2016 in order to understand how these organisms interact in the environment.

In this part, I describe the main characteristics of this sampling station and list the parameters that are regularly measured and provide the protocols associated to these parameters. I also detail the sampling methods and isolation procedures used during the first year of my Ph.D. to obtain the diatom and parasite cultures.

This work has been the subject of a short documentary for the CNRS, Le Journal:
- “Les virus, maîtres méconnus des océans” French version:
https://lejournal.cnrs.fr/videos/les-virus-maitres-meconnus-des-oceans
- “The Viruses that Rule our Oceans”, English version:
https://news.cnrs.fr/videos/the-viruses-that-rule-our-oceans
And of a publication:
Baker, N., 2017. Le royaume des virus. Carnet de sciences, la revue du CNRS. 2, 103-107

Personal contribution:

Between October 2015 and December 2016, I received the help of Anne-Claire Baudoux, Nathalie Simon, Fabienne Rigaut-Jalabert and Florence Le Gall to collect natural seawater (cruises at the SOMLIT-Astan site) and isolate, back to the lab, both diatom hosts and parasites. I achieved by myself more than half of the water sampling. On board, I was helped by Fabienne Rigaut-Jalabert (engineer at the costal observatory service of the Station Biologique de Roscoff), who is in charge of the SOMLIT-Astan plankton series.

Isolation of parasite strains was achieved by Anne-Claire Baudoux, Nathalie Simon and myself. I isolated more than half of the parasite strains and maintained the collection all along the 3 years.

Regarding the isolation and maintenance of the diatom hosts, the work has been exclusively carried out by Florence Le Gall, engineer in the “Diversity and Interactions in Oceanic Plankton” research team.

1. The SOMLIT-Astan sampling station: general context

The SOMLIT-Astan station is located in the Bay of Morlaix, in the Western English Channel (48°46'40'' N, 3°56'15'' W) (Figure I-1). The physico-chemical and biological properties of this station are monitored since 2000 the frame of the SOMLIT national monitoring program (Service d'Observation en Milieu LITtoral, http://somlit.epoc.u-bordeaux1.fr/fr/). The SOMLIT-Astan station is situated 3,500 m off Roscoff and its maximum depth reaches 60 m. The French coastal waters of the Western English Channel are characterized by rather shallow depth and strong tidal currents (Grall, 1972; L'Helguen *et al.*, 1996). Also, these waters are permanently well-mixed and homogeneous throughout the year (L'Helguen *et al.*, 1996; Wafar *et al.*, 1983).

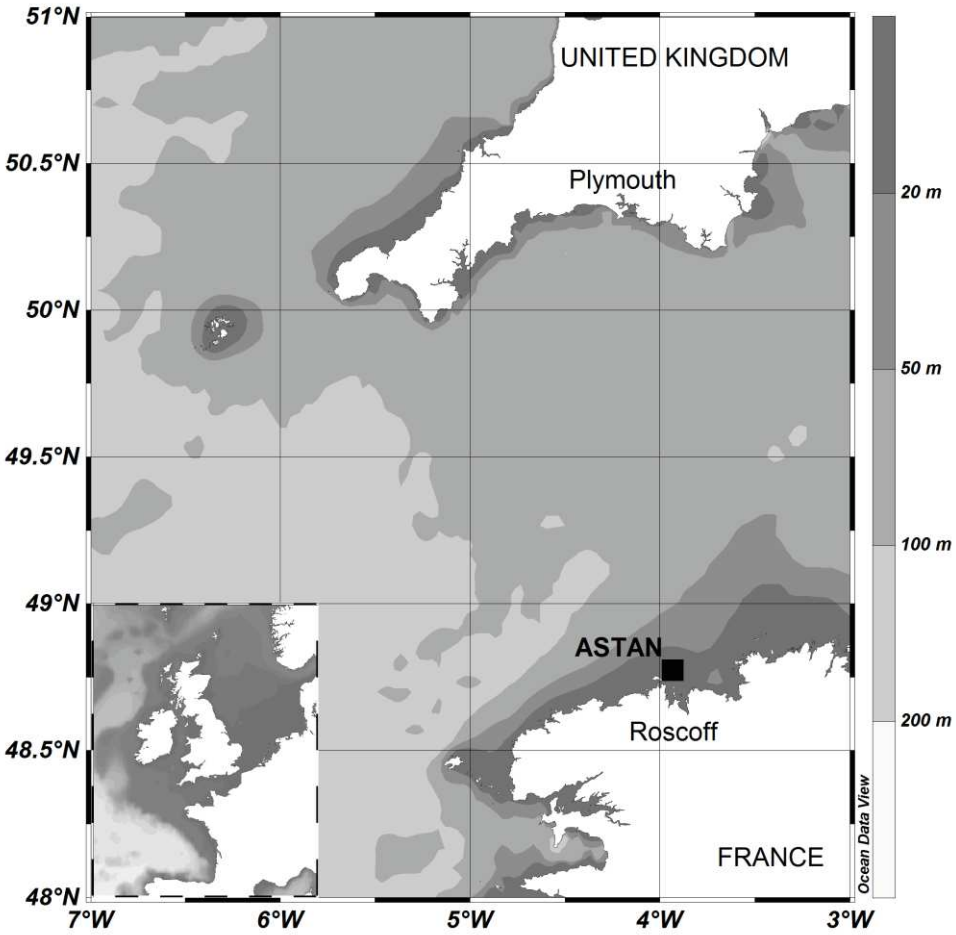

Figure I-1. Map of the Western English Channel. The square represents SOMLIT-ASTAN Station. From Simon et al.*, in prep.*

2. Sampling procedures

For the monitoring of hydrological and biological parameters at the SOMLIT-Astan station, samples are collected twice a month during neap tides since February 2000 (with some interruptions in 2004, 2005 and 2006 for the monitoring of plankton) using a 5 L Niskin bottle. These samples are collected from surface (1 m) and bottom (50 m) waters and are then either processed onboard or brought back to the laboratory for further fixation or analysis (generally about 1-2 h after sampling). Sampling is operated by the Sea and Observatory facility of the SBR ("Service Mer, Service Observation") onboard the research Vessel Neomysis.

In the frame of this PhD thesis, additional surface samples (1 m) were collected either using the 5L-Niskin bottle (5 L samples) or a 20 µm pore-size plankton net (Guilloux *et al.*, 2013) from August 2015 to October 2016. These samples were used in the laboratory for the isolation of model diatoms and parasite strains.

3. Hydrological parameters

Thirteen hydrological parameters are measured from the surface and bottom samples as part of the SOMLIT program. Analyses are performed by the Observatory facility and Marine Chemistry research team of the Station Biologique de Roscoff (Cariou *et al.*, 2002). The detailed protocols used for the parameters listed below are available on the SOMLIT-Astan website (http://somlit.epoc.u-bordeaux1.fr/fr/).

- Temperature (On board thermometer and CTD profile),
- Salinity (Salinometer and CTD profile),
- Oxygen (Winkler)
- pH (PPMetrer),
- Ammonium (Spectrophotometer),
- Nitrates (Autoanalyzer),
- Nitrites (Autoanalyzer),
- Phosphates (Autoanalyzer),
- Silicates (Autoanalyzer),
- Particulate Organic Carbon (Autoanalyzer),
- Particulate Organic Azote (Autoanalyzer),
- Suspended matter (Balance),
- Delta 15N (Isotope)
- Delta 13C (Isotope),
- Chlorophyll *a* (Fluorimeter).

The variations in the hydrology recorded in 2015-2016 are presented in Annexe- 2.

4. Phytoplankton taxa counts

In the laboratory, aliquots (250 mL) of the seawater samples collected for phytoplankton analysis are preserved with acidic Lugol's iodine solution. Phytoplankton counts (for cells above ~10 µm) are obtained from subsamples (50 mL) after sedimentation in Utermöhl settling chambers (For details, see Guilloux *et al.* (2013); NF EN 15024, (2006)). Since 2007, sampling and taxa counts have been mainly conducted by Fabienne Rigaut-Jalabert (Costal observatory service). Microphytoplankton counts are available from the RESOMAR-Pelagos database (http://abims.sb-roscoff.fr/pelagos/).

Seawater samples collected for the examination under scanning electron microscopy were also preserved in order to obtain semi-quantitative data for the nanoplanktonic diatoms and especially the genera *Minidiscus* and *Thalassiosira*. Seawater aliquots of 20, 50 and 200 mL aliquots were filtered through 150 µm and the filtrate was gently concentrated onto 0.8 µm pore size filters (Nuclepore, Whatman) with a low vacuum (< 10 kPa) to avoid cell damages. Filters were rinsed 3 times with 0.2 µm-filtered deionized water and dried for 2 hours at 54°C. Filters were stored at room temperature until observation. Unfortunately, these samples could not be studied in the frame of this project.

5. Isolation of diatom and parasite strains

a. Sampling dates

Samples collected from August 2015 to October 2016 (see the variations of the hydrological parameters encountered during this period in Annex 2) for the isolation of diatoms and parasites were processed in the laboratory. Due to the amount of work needed to isolate and establish parasitic cultures, we decided to decrease the number of sampling during winter and sometimes during summer to one sampling per month. Thus, we carried out 22 natural seawater samples out of the 30 samples collected during this period in the frame of the SOMLIT program (Table I-1).

Table I-1. Comparison of the sampling dates for the SOMLIT program and for the isolation work of diatoms and parasites from the SOMLIT-Astan station

Date	Sampling for the SOMLIT program	Sampling for the host and parasite isolations	Date	Sampling for the SOMLIT program	Sampling for the host and parasite isolations
24/08/2015	YES	YES	01/04/2016	YES	YES
07/09/2015	YES	NO	15/04/2016	YES	YES
21/09/2015	YES	YES	29/04/2016	YES	YES
06/10/2015	YES	YES	13/05/2016	YES	YES
21/10/2015	YES	YES	30/05/2016	YES	YES
04/11/2015	YES	YES	14/06/2016	YES	YES
20/11/2015	YES	YES	28/06/2016	YES	NO
04/12/2015	YES	YES	13/07/2016	YES	YES
18/12/2015	YES	NO	28/07/2016	YES	NO
04/01/2016	YES	YES	12/08/2016	YES	YES
18/01/2016	YES	NO	26/08/2016	YES	YES
02/02/2016	YES	YES	09/09/2016	YES	YES
17/02/2016	YES	NO	23/09/2016	YES	YES
04/03/2016	YES	YES	10/10/2016	YES	NO
17/03/2016	YES	NO	24/10/2016	YES	YES

b. Isolations of diatom strains

In order (1) to characterize the specific and infra-specific diversity of the dominating diatoms (*Guinardia* spp., *Minidiscus* spp. and nanoplanktonic *Thalassiosira* spp.) and (2) to obtain representative strains that thrive in the study site and test their susceptibility to parasites, we implemented different isolation procedures for *Guinardia* spp. and the pico- and nanoplanktonic diatoms (*Minidiscus* spp. and *Thalassiosora* spp.).

For *Guinardia* spp. clonal cultures were established from fresh plankton net samples by a micropipetting method. Briefly, seawater samples were examined using an inverted microscope (Olympus IX71, Olympus Corporation, Tokyo, Japan) and individual cells or chains were picked using a micropipette. The cells (or chains) were rinsed 3 times in sterile seawater and transferred into K+Si medium in a multiwell plate.

Given the numerical dominance of the nanoplanktonic *Minidiscus* spp. and *Thalassiosira* spp. at the SOMLIT-Astan station (see “Modèles d’étude” in the thesis objectives), we used a dilution method to isolate strains of these taxa. Briefly, samples collected from the Niskin bottle were diluted into K+Si medium in multiwell plates in order to reach finally 5 and 10 cells per well. After two weeks of incubation, algal growth and purity of cells were verified by microscopy (Olympus IX71, Olympus Corporation, Tokyo, Japan).

As a result of this work, 18 pure cultures of *Guinardia delicatula*, 4 of *G. flaccida*, 5 of *G. striata* and 49 small diatoms belonging mainly to the genera *Minidiscus* and *Thalassiosira* have been isolated. Some of these strains were lost prior to further analyses. A list of strains that are currently maintained and used during the course of this project is provided in Table I-2.

All diatom cultures isolated were maintained in sterile condition in K+Si medium (Keller *et al.*, 1987) at 18°C, under a 12:12h light:dark cycle of 100 µmol photons.m^{-2}.s^{-1} provided by a white fluorescent light (Philips Master TL_D 18W/865). Diatom cultures were deposited in the Roscoff Culture Collection (RCC, http://roscoff-culture-collection.org/) (Table I-2).

Table I-2. Diatom strains isolated from October 2015 to October 2016 at the SOMLIT-Astan station

Taxon name	Strains (RCC or original code)	Isolation date	Isolation method
Guinardia delicatula	RCC5777	21/10/2015	Pipet
	RCC5778	21/10/2015	Pipet
	RCC5779	21/10/2015	Pipet
	RCC5780	21/10/2015	Pipet
	RCC5781	21/10/2015	Pipet
	RCC5782	04/11/2015	Pipet
	RCC5783	29/04/2016	Pipet
	RCC5784	13/05/2016	Pipet
	RCC5785	13/05/2016	Pipet
	RCC5797	13/05/2016	Pipet
	RCC5786	26/08/2016	Pipet
	RCC5799	26/08/2016	Pipet
	RCC5787	23/09/2016	Pipet
	RCC5788	24/10/2016	Pipet
Guinardia flaccida	RCC5800	09/09/2016	Pipet
	RCC5801	09/09/2016	Pipet
Guinardia striata	RCC5792	09/09/2016	Pipet
	RCC5793	23/09/2016	Pipet
Minidiscus comicus	RCC5839	20/11/2015	Dilution
	RCC5840	04/12/2015	Dilution
	RCC5841	04/12/2015	Dilution
	RCC5842	04/12/2015	Dilution
	RCC5843	04/12/2015	Dilution
	RCC5844	04/01/2016	Dilution
	RCC5845	04/01/2016	Dilution
	RCC5846	02/02/2016	Dilution
	RCC5847	02/02/2016	Dilution
	RCC5848	02/02/2016	Dilution
	RCC5849	04/03/2016	Dilution
	RCC5850	04/03/2016	Dilution
	RCC5851	04/03/2016	Dilution

	RCC5852	01/04/2016	Dilution
	RCC5853	01/04/2016	Dilution
	RCC5854	01/04/2016	Dilution
	RCC5855	01/04/2016	Dilution
	RCC5856	15/04/2016	Dilution
	RCC5857	15/04/2016	Dilution
	RCC5858	13/05/2016	Dilution
	RCC5859	13/05/2016	Dilution
Minidiscus spinulatus	RCC5860	04/03/2016	Dilution
	RCC5861	04/03/2016	Dilution
Minidiscus variabilis	RCC5862	06/10/2015	Dilution
	RCC5863	04/11/2015	Dilution
	RCC5864	04/11/2015	Dilution
	RCC5865	04/11/2015	Dilution
	RCC5866	04/11/2015	Dilution
	RCC5867	04/11/2015	Dilution
	RCC5868	20/11/2015	Dilution
	RCC5869	20/11/2015	Dilution
	RCC5870	04/12/2015	Dilution
	RCC5871	02/02/2016	Dilution
	RCC5872	04/03/2016	Dilution
	RCC5873	01/04/2016	Dilution
	RCC5874	15/04/2016	Dilution
	RCC5875	15/04/2016	Dilution
	RCC5876	30/05/2016	Dilution
	RCC5877	13/07/2016	Dilution
	RCC5878	09/09/2016	Dilution
	RCC5879	24/10/2016	Dilution
	RCC5880	24/10/2016	Dilution
Thalassiosira profunda	RCC5881	20/11/2015	Dilution
	RCC5882	02/02/2016	Dilution
	RCC5883	04/03/2016	Dilution
	RCC5884	29/04/2016	Dilution
	RCC5885	13/05/2016	Dilution
	RCC5886	13/07/2016	Dilution
***Thalassiosira* sp.**	RCC5887	02/02/2016	Dilution

c. Isolations of parasite strains

In order to prospect for parasites in natural seawater collected at the SOMLIT-Astan station between August 2015 to October 2016, we used *Guinardia* spp., *Minidiscus* spp. and nanoplanktonic *Thalassiosira* spp. established in cultures in 2012 and 2015, and deposited in the RCC (Table I-3). These diatom cultures were maintained in sterile condition in K+Si medium

(Keller *et al.*, 1987) at 18°C, under a 12:12h light:dark cycle of 100 µmol photons.m^{-2}.s^{-1} provided by a white fluorescent light (Philips Master TL_D 18W/865). These diatom strains were not fully characterized at the beginning of the PhD project. Their morpho-genetic characterization was conducted during this project (see Part III).

Table I-3. List and origin of the diatom strains used in this project. These cultures were obtained from the Roscoff Culture Collection. EC: English Channel

Genus	Species	RCC number	Isolation area	Isolation date
Guinardia	*delicatula*	RCC3083	Roscoff-Estacade, EC	19/09/12
	flaccida	RCC3088	Roscoff-Astan, EC	19/09/12
		RCC3093	Roscoff-Astan, EC	10/09/12
	striata	RCC2966	Mediterranean Sea	07/03/12
Minidiscus	*comicus*	RCC4660	Roscoff-Astan, EC	26/05/15
		RCC4661	Roscoff-Astan, EC	26/05/15
		RCC4662	Roscoff-Astan, EC	26/05/15
	spinulatus	RCC4659	Roscoff-Astan, EC	26/05/15
	variabilis	RCC4657	Roscoff-Astan, EC	26/05/15
		RCC4658	Roscoff-Astan, EC	26/05/15
		RCC4665	Roscoff-Astan, EC	26/05/15
		RCC4666	Roscoff-Astan, EC	26/05/15
Thalassiosira	*curviseriata*	RCC5154	Roscoff-Astan, EC	26/05/15
	profunda	RCC4663	Roscoff-Astan, EC	26/05/15
	punctigera	RCC4667	Roscoff-Astan, EC	21/10/15
	sp.	RCC4664	Roscoff-Astan, EC	26/05/15

In order to maximize probabilities of successful parasite isolations, we used a host-enrichment method (Figure I-2). This step consists in enriching the seawater sample with prospective host strains and host growth medium to induce the proliferation of parasites. Therefore, natural samples (1 L) collected at the SOMLIT-Astan station were pre-filtered through a 150 µm pore-size nylon filter to remove macro- and micro-zooplankton. 250 mL-aliquots were distributed into seven 270 mL culture flasks, and we added 10% (v/v) of F/2 medium (Guillard, 1975; Guillard and Ryther, 1962) and 5 mL of fresh culture of the prospective host strains (Table I-3). Seven flasks were enriched with the following strains:

- Flask 1: *G. delicatula* RCC3083
- Flask 2: *G. flaccida* RCC3088 and RCC3093
- Flask 3: *G. striata* RCC2966
- Flask 4: *M. comicus* RCC4660, RCC4661 and RCC4662

- Flask 5: *M. variabilis* RCC4657, RCC4658, RCC4667 and RCC4668 and *M. spinulatus* RCC4659
- Flask 6: *Thalassiosira* spp. strains RCC4663, RCC5154, RCC4664 and RCC4667 and *M. variabilis* RCC4666 (NB: RCC4666 had been assigned to the genus *Thalassiosira* at this step of the project. It was later characterized as *M. variabilis*, see Part III)
- Flask 7: no prospective host. Only f/2 medium

The flasks were incubated for two weeks under the culture conditions described above.
After incubation, samples were filtered using different pore size filters in order to isolate parasites from different size fractions targeting specifically viruses, bacteria, and eukaryotes. Enrichment samples were filtered through:

- GF/F filters (Whatman, estimated pore size 0.7 µm) to isolate potential bacterial or picoeukaryotic parasites or viruses
- GF/F filters (Whatman) and then a 0.22 µm PES filter (Whatman) to isolate specifically the viral community
- Nuclepore 5 µm or 3 µm filters in order to isolate nano- or micro-eukaryotic parasites (only for one sampling in June, July and October 2016 for *Guinardia* spp.). Parasites larger than 0.7 µm have indeed been described (see introduction)

Aliquot (0.5 mL) of all the filtered samples were inoculated into 1.5 mL exponentially growing host culture in 24-multiwell plates under the host culture conditions as described above. Untreated host cultures served as controls. Cultures were inspected by light microscopy two weeks after inoculation. If algal lysis was observed, 3 extinction dilution cycles were carried out to clone the pathogens (Suttle, 1993). Briefly, 100 µL aliquots of the lysates were serially diluted in 10-fold increment in 900 µL of exponentially growing diatom culture. Lysates in the last dilution before extinction were transferred to another exponentially host growing culture (Figure I-3). For all treatments, a new filtration on 0.22 µm was repeated to verify their size fractions and the transferability. After establishment, all isolates were maintained in culture by bimonthly transfers in their isolation host under the culture conditions described previously.

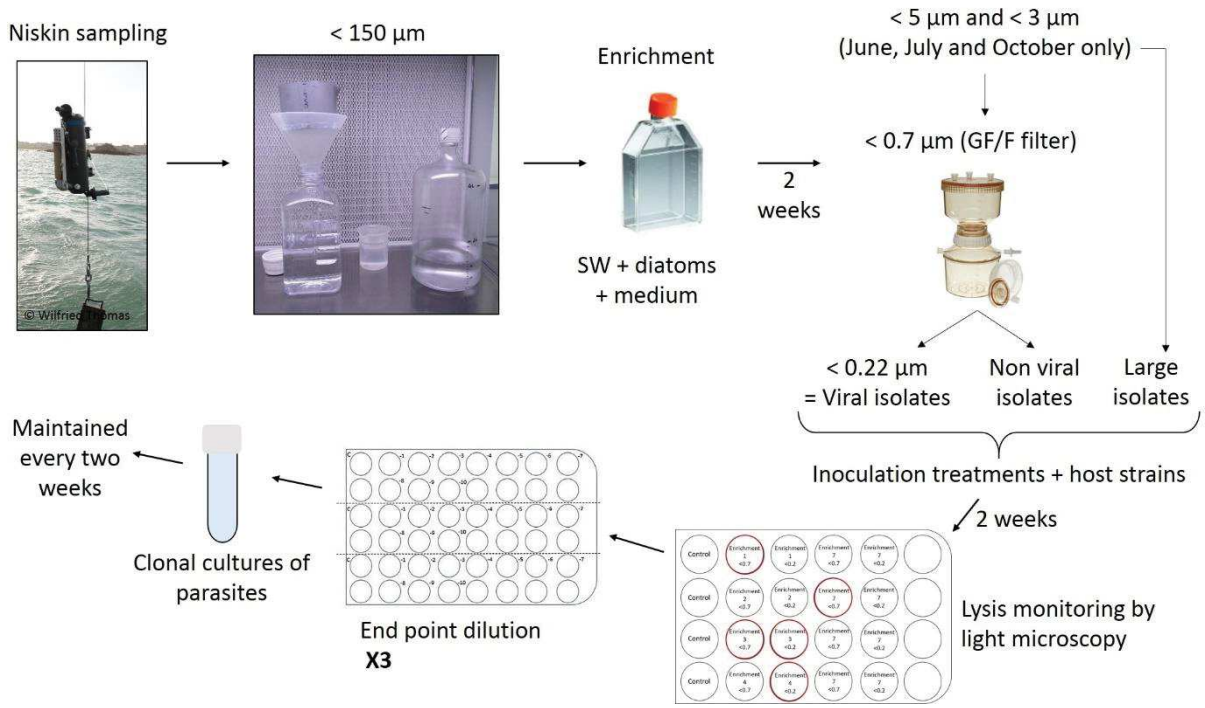

Figure I-2. Sampling and parasitic isolation procedures used during the full seasonal cycle

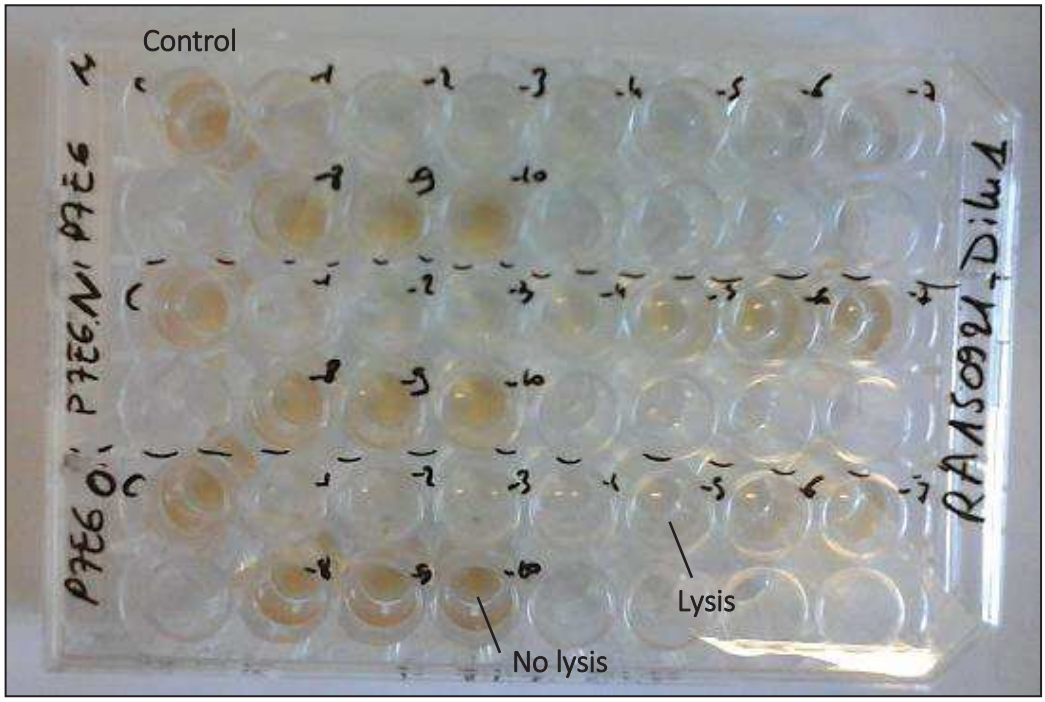

Figure I-3. Example of the end point dilution method in a multiwell plate

In total, 102 clonal cultures of parasites were isolated and maintained in culture including: 15 parasites of *G. delicatula*, 5 of *G. flaccida*, 20 of *M. comicus,* 5 of *M. spinulatus*, 26 of *M. variabilis*, 12 of *T. curviseriata*, 15 of *T. profunda* and 4 of *Thalassiosira* sp. (Table I-4).

It is worth mentioning that no parasite was ever isolated on *Thalassiosira punctigera* RCC4667 although eukaryotic microorganisms infecting this species have been described in the literature (Schweikert and Schnepf, 1996, 1997b).
Also, 2 parasite strains infecting *G. striata* RCC2966 and 3 parasite strains infecting *G. flaccida* RCC3088 were isolated but these diatom strains were lost by the Roscoff Culture Collection and also died in our personal collection. Consequently, we were not able to maintain the pathogens cultures associated to these strains. *G. flaccida* RCC3093 was also lost during the last year of this project. The parasites could be transferred on another *G. flaccida* host RCC5791 isolated in 2017.
In the final table (Table I-4), some parasites were isolated the same day and on the same host. As different treatments were applied (filtered on 0.7 or 0.2 µm, or coming from different enrichment flasks), each isolate was considered as a unique parasite.

From the collection of strains established, a small number of parasites (highlighted in orange, Table I-4) were selected on *Guinardia* species to go further in their characterizations (See Part II).

Table I-4. Final collection of pathogens isolated on the genera Guinardia, Minidiscus *and* Thalassiosira *between the 24/08/2015 and the 24/10/2016. Parasite name corresponds to the host strain RCC code, the isolation date and a letter representing the name of the treatment. Highlighted parasite names in orange were selected for further characterization (See Part II). RA code corresponds to the sampling site (Roscoff-Astan) and the isolation date (year-month-day). ND: Not Determined, Y/N: Yes/No*

Parasite name	Code	Host RCC code	Host name	RA code	Isolation date	Isolator	Lysis after <0.2 µm (Yes/No)
RCC3083-G0921	G0921	RCC3083	*Guinardia delicatula*	RA150921	21/09/2015	LA	N
RCC3083-K0921	K0921	RCC3083	*Guinardia delicatula*	RA150921	21/09/2015	LA	N
RCC3083-A1006	A1006	RCC3083	*Guinardia delicatula*	RA151006	06/10/2015	LA	N
RCC3083-E1006	E1006	RCC3083	*Guinardia delicatula*	RA151006	06/10/2015	LA	N
RCC3083-K1006	K1006	RCC3083	*Guinardia delicatula*	RA151006	06/10/2015	LA	N
RCC3083-E1104	E1104	RCC3083	*Guinardia delicatula*	RA151104	04/11/2015	ACB	ND
RCC3083-G1104	G1104	RCC3083	*Guinardia delicatula*	RA151104	04/11/2015	ACB	ND
RCC3083-E1104 5µ	E1104 5µ	RCC3083	*Guinardia delicatula*	RA151104	04/11/2015	ACB	ND

RCC3083-E1204	E1204	RCC3083	*Guinardia delicatula*	RA151204	04/12/2015	ACB	ND
RCC3083-E0713	E0713	RCC3083	*Guinardia delicatula*	RA160713	13/07/2016	LA	N
RCC3083-F0826	F0826	RCC3083	*Guinardia delicatula*	RA160826	26/08/2016	NS	Y
RCC3083-F0909	F0909	RCC3083	*Guinardia delicatula*	RA160909	09/09/2016	ACB	Y
RCC3083-E0923	E0923	RCC3083	*Guinardia delicatula*	RA160923	23/09/2016	LA	Y
RCC3083-F0923	F0923	RCC3083	*Guinardia delicatula*	RA160923	23/09/2016	LA	Y
RCC3083-$E_5$1024	$E_5$1024	RCC3083	*Guinardia delicatula*	RA161024	24/10/2016	LA	Y
RCC3093-Y0513	Y0513	RCC3093	*Guinardia flaccida*	RA160513	13/05/2016	ACB	N
RCC3093-Y0530	Y0530	RCC3093	*Guinardia flaccida*	RA160530	30/05/2016	ACB	N
RCC3093-$A_3$0614	$A_3$0614	RCC3093	*Guinardia flaccida*	RA160614	14/06/2016	NS	N
RCC3093-$Y_3$0614	$Y_3$0614	RCC3093	*Guinardia flaccida*	RA160614	14/06/2016	NS	N
RCC3093-$Y_3$1024	$Y_3$1024	RCC3093	*Guinardia flaccida*	RA161024	24/10/2016	LA	N
RCC4660-A1006	A1006	RCC4660	*Minidiscus comicus*	RA151006	06/10/2015	LA	N
RCC4660-M1006	M1006	RCC4660	*Minidiscus comicus*	RA151006	06/10/2015	LA	N
RCC4660-M1104	M1104	RCC4660	*Minidiscus comicus*	RA151104	04/11/2015	ACB	N
RCC4660-M0104	M0104	RCC4660	*Minidiscus comicus*	RA160104	04/01/2016	LA	N
RCC4660-M0415	M0415	RCC4660	*Minidiscus comicus*	RA160415	15/04/2016	LA	N
RCC4660-M0428	M0428	RCC4660	*Minidiscus comicus*	RA160428	28/04/2016	NS	Y
RCC4660-M0530	M0530	RCC4660	*Minidiscus comicus*	RA160530	30/05/2016	ACB	N
RCC4660-M0909	M0909	RCC4660	*Minidiscus comicus*	RA160909	09/09/2016	ACB	N
RCC4660-A1024	A1024	RCC4660	*Minidiscus comicus*	RA161024	24/10/2016	LA	N
RCC4661-M1006	M1006	RCC4661	*Minidiscus comicus*	RA151006	06/10/2015	LA	N

RCC4661-N1104	N1104	RCC4661	*Minidiscus comicus*	RA151104	04/11/2015	ACB	Y
RCC4661-N1120	N1120	RCC4661	*Minidiscus comicus*	RA151120	20/11/2015	LA	Y
RCC4661-M0104	M0104	RCC4661	*Minidiscus comicus*	RA160104	04/01/2016	LA	N
RCC4661-N0428	N0428	RCC4661	*Minidiscus comicus*	RA160428	28/04/2016	NS	Y
RCC4661-M0923	M0923	RCC4661	*Minidiscus comicus*	RA160923	23/09/2016	LA	N
RCC4662-M1006	M1006	RCC4662	*Minidiscus comicus*	RA151006	06/10/2015	LA	N
RCC4662-P1006	P1006	RCC4662	*Minidiscus comicus*	RA151006	06/10/2015	LA	Y
RCC4662-M0415	M0415	RCC4662	*Minidiscus comicus*	RA160415	15/04/2016	LA	N
RCC4662-M0826	M0826	RCC4662	*Minidiscus comicus*	RA160826	26/08/2016	NS	N
RCC4662-A1024	A1024	RCC4662	*Minidiscus comicus*	RA161024	24/10/2016	LA	N
RCC4659-Q1006	Q1006	RCC4659	*Minidiscus spinulatus*	RA151006	06/10/2015	LA	N
RCC4659-T1006	T1006	RCC4659	*Minidiscus spinulatus*	RA151006	06/10/2015	LA	Y
RCC4659-Q0530	Q0530	RCC4659	*Minidiscus spinulatus*	RA160530	30/05/2016	ACB	N
RCC4659-Q0909	Q0909	RCC4659	*Minidiscus spinulatus*	RA160909	09/09/2016	ACB	N
RCC4659-A1024	A1024	RCC4659	*Minidiscus spinulatus*	RA161024	24/10/2016	LA	N
RCC4665-A1006	A1006	RCC4665	*Minidiscus variabilis*	RA151006	06/10/2015	LA	N
RCC4665-Q1006	Q1006	RCC4665	*Minidiscus variabilis*	RA151006	06/10/2015	LA	N
RCC4665-Q0204	Q0204	RCC4665	*Minidiscus variabilis*	RA160204	04/02/2016	NS	N
RCC4665-Q0304	Q0304	RCC4665	*Minidiscus variabilis*	RA160304	04/03/2016	LA	N
RCC4665-A1024	A1024	RCC4665	*Minidiscus variabilis*	RA161024	24/10/2016	LA	N
RCC4657-S0921	S0921	RCC4657	*Minidiscus variabilis*	RA150921	21/09/2015	LA	N
RCC4657-A1006	A1006	RCC4657	*Minidiscus variabilis*	RA151006	06/10/2015	LA	N

RCC4657-R0104	R0104	RCC4657	*Minidiscus variabilis*	RA160104	04/01/2016	LA	Y
RCC4657-R0401	R0401	RCC4657	*Minidiscus variabilis*	RA160401	01/04/2016	ACB	Y
RCC4657-A1024	A1024	RCC4657	*Minidiscus variabilis*	RA161024	24/10/2016	LA	N
RCC4658-T1006	T1006	RCC4658	*Minidiscus variabilis*	RA151006	06/10/2015	LA	Y
RCC4658-Q0415	Q0415	RCC4658	*Minidiscus variabilis*	RA160415	15/04/2016	LA	N
RCC4658-Q0513	Q0513	RCC4658	*Minidiscus variabilis*	RA160513	13/05/2016	ACB	N
RCC4658-R0713	R0713	RCC4658	*Minidiscus variabilis*	RA160713	13/07/2016	LA	N
RCC4658-A1024	A1024	RCC4658	*Minidiscus variabilis*	RA161024	24/10/2016	LA	N
RCC4666-X0921	X0921	RCC4666	*Minidiscus variabilis*	RA150921	21/09/2015	LA	Y
RCC4666-B1006	B1006	RCC4666	*Minidiscus variabilis*	RA151006	06/10/2015	LA	Y
RCC4666-V1006	V1006	RCC4666	*Minidiscus variabilis*	RA151006	06/10/2015	LA	N
RCC4666-X1006	X1006	RCC4666	*Minidiscus variabilis*	RA151006	06/10/2015	LA	Y
RCC4666-U1104	U1104	RCC4666	*Minidiscus variabilis*	RA151104	04/11/2015	ACB	N
RCC4666-U1204	U1204	RCC4666	*Minidiscus variabilis*	RA151204	04/12/2015	ACB	N
RCC4666-B0304	B0304	RCC4666	*Minidiscus variabilis*	RA160304	04/03/2016	LA	Y
RCC4666-A0401	A0401	RCC4666	*Minidiscus variabilis*	RA160401	01/04/2016	ACB	N
RCC4666-U0530	U0530	RCC4666	*Minidiscus variabilis*	RA160530	30/05/2016	ACB	Y
RCC4666-U0909	U0909	RCC4666	*Minidiscus variabilis*	RA160909	09/09/2016	ACB	N
RCC4666-A1024	A1024	RCC4666	*Minidiscus variabilis*	RA161024	24/10/2016	LA	N
RCC5154-V0921	V0921	RCC5154	*Thalassiosira curviseriata*	RA150921	21/09/2015	LA	Y
RCC5154-A1006	A1006	RCC5154	*Thalassiosira curviseriata*	RA151006	06/10/2015	LA	Y
RCC5154-U1204	U1204	RCC5154	*Thalassiosira curviseriata*	RA151204	04/12/2015	ACB	N

RCC5154-V0415	V0415	RCC5154	*Thalassiosira curviseriata*	RA160415	15/04/2016	LA	Y
RCC5154-U0428	U0428	RCC5154	*Thalassiosira curviseriata*	RA160428	28/04/2016	NS	Y
RCC5154-V0428	V0428	RCC5154	*Thalassiosira curviseriata*	RA160428	28/04/2016	NS	Y
RCC5154-U0513	U0513	RCC5154	*Thalassiosira curviseriata*	RA160513	13/05/2016	ACB	Y
RCC5154-U0530	U0530	RCC5154	*Thalassiosira curviseriata*	RA160530	30/05/2016	ACB	N
RCC5154-U0614	U0614	RCC5154	*Thalassiosira curviseriata*	RA160614	14/06/2016	NS	N
RCC5154-V0713	V0713	RCC5154	*Thalassiosira curviseriata*	RA160713	13/07/2016	LA	Y
RCC5154-V0812	V0812	RCC5154	*Thalassiosira curviseriata*	RA160812	12/08/2016	LA	Y
RCC5154-U0909	U0909	RCC5154	*Thalassiosira curviseriata*	RA160909	09/09/2016	ACB	N
RCC4663-20824	20824	RCC4663	*Thalassiosira profunda*	RA150824	24/08/2015	ACB	N
RCC4663-30824	30824	RCC4663	*Thalassiosira profunda*	RA150824	24/08/2015	ACB	N
RCC4663-X0921	X0921	RCC4663	*Thalassiosira profunda*	RA150921	21/09/2015	LA	Y
RCC4663-B1006	B1006	RCC4663	*Thalassiosira profunda*	RA151006	06/10/2015	LA	N
RCC4663-V1006	V1006	RCC4663	*Thalassiosira profunda*	RA151006	06/10/2015	LA	N
RCC4663-U1104	U1104	RCC4663	*Thalassiosira profunda*	RA151104	04/11/2015	ACB	Y
RCC4663-V1104	V1104	RCC4663	*Thalassiosira profunda*	RA151104	04/11/2015	ACB	Y
RCC4663-A0204	A0204	RCC4663	*Thalassiosira profunda*	RA160204	04/02/2016	NS	N
RCC4663-A0304	A0304	RCC4663	*Thalassiosira profunda*	RA160304	04/03/2016	LA	N
RCC4663-U0401	U0401	RCC4663	*Thalassiosira profunda*	RA160401	01/04/2016	ACB	Y
RCC4663-U0428	U0428	RCC4663	*Thalassiosira profunda*	RA160428	28/04/2016	NS	N
RCC4663-U0614	U0614	RCC4663	*Thalassiosira profunda*	RA160614	14/06/2016	NS	N
RCC4663-U0713	U0713	RCC4663	*Thalassiosira profunda*	RA160713	13/07/2016	LA	N

RCC4663-U0909	U0909	RCC4663	*Thalassiosira profunda*	RA160909	09/09/2016	ACB	N
RCC4663-A1024	A1024	RCC4663	*Thalassiosira profunda*	RA161024	24/10/2016	LA	N
RCC4664-A1006	A1006	RCC4664	*Thalassiosira* sp.	RA151006	06/10/2015	LA	N
RCC4664-V1006	V1006	RCC4664	*Thalassiosira* sp.	RA151006	06/10/2015	LA	Y
RCC4664-U1104	U1104	RCC4664	*Thalassiosira* sp.	RA151104	04/11/2015	ACB	N
RCC4664-A1024	A1024	RCC4664	*Thalassiosira* sp.	RA161024	24/10/2016	LA	N

6. Plankton genetic diversity

Since 2009, sea surface water is sampled for genetic diversity analysis. The natural samples (5 L) are successively filtered through 3 µm polycarbonate filter (Whatman) and through a 0.22 µm Sterivex filter (PVDF, Millipore), leading to two size fractions (>3 µm and 0.2-3 µm). Filters are preserved in a lysis buffer at -80°C until DNA extraction.

Filters from the two size fractions were first incubated 45 min at 37°C with 100 µL lysozyme 20 mg/mL, and 1h at 56°C with 20 µL proteinase K 20 mg/mL and 100 µL SDS 20%. Nucleic acids were then extracted using a phenol-chloroform method. DNA from fraction > 3µm was purified using filter columns from NucleoSpin® PlantII kit (Macherey-Nagel) following a modified protocol. DNA from the smallest fraction was purified using filter columns Amicon Ultra-4 (Millipore). DNA from both fractions were finally eluted with 100 µL Tris-EDTA 1x pH8 buffer. Environmental DNA extracts were quantified using a Nanodrop ND-1000 Spectrophotometer.

Environmental DNA were used as templates for PCR amplification of the V4 region of the 18S rDNA (~380 bp) using primers TAReuk454FWD1 and TAReukREV3 (Stoeck *et al.*, 2010) that amplify most eukaryotic groups. The forward primer was linked to a tag, and both primers were adapted for Illumina sequencing. PCR reactions (25 µL) contained 1x Master Mix Phusion High-Fidelity DNAPolymerase (Finnzymes), 0.35 µM of each primer, 3% dimethylsulphoxide and 5 ng of DNA. The PCR program had an initial denaturation step at 98°C during 30 s, 10 cycles of 10 s at 98°C, 30 s at 53°C and 30 s at 72°C, then 15 similar cycles but with 48°C annealing temperature, and a final step at 72°C for 10 min. Polymerase chain reaction triplicates were purified and eluted (30 µL) with NucleoSpin Gel and PCR Clean-Up kit (Macherey-Nagel), and quantified with the Quant-It PicoGreen double stranded DNA Assay kit (Invitrogen). About 1 µg of pooled amplicons were sent to Fasteris (https://www.fasteris.com/dna/, Plan-les-Ouates, Switzerland) for high throughput sequencing on a 2x250bp MiSeq Illumina (Simon *et al.*, in prep.).

Sequencing reads were treated by Frédéric Mahé (Cirad, team "Réseaux et Interactions Symbiotiques dans les éco-Agrosystèmes") following the metabarcoding pipeline available online (https://github.com/frederic-mahe/swarm/wiki). Sequences were grouped into Operational Taxonomic Units (OTUs) using the Swarm approach (Mahé *et al.*, 2014). Taxonomical assignment of each OTU was performed using the Protist Ribosomal Reference (PR2) database (Guillou *et al.,* 2013).

In total, the contingency table contained 31 167 OTUs from 180 sampling dates for the >3 µm fraction and 188 sampling dates for the 0.2-3 µm fraction over the 2009-2016 period. Differences in date numbers reflected failures during the filtration or purification procedures (drilled pipe, loss of filter, etc.). These molecular data were used for the dynamic patterns and network analyses.

PART II

PARASITES ASSOCIATED WITH THE DIATOM *GUINARDIA*

CONTEXT OF THE WORK

The second part of this thesis is dedicated to the interactions between the diatom *Guinardia* and parasites isolated at the SOMLIT-Astan time-series station.

The first chapter that describes new single-stranded RNA viruses specific for *G. delicatula* is under revision in Frontiers in Microbiology. Viruses of *G. delicatula* were isolated in 2016 during the first year of my PhD, that was mostly dedicated to field work and isolations of host and parasite strains. These viral isolates demonstrated morphological and phylogenetic relationships with other diatom viruses. They exhibited high affinities for strains of this diatom species, and searches for gene homologies in metagenomics studies revealed a repartition in other temperate coastal systems, where *G. delicatula* occurs as well. In our sampling site, virome survey need to be implemented in order to monitor the temporal dynamics of viruses and evaluate their contribution to the bloom decline of diatoms.

Chapters 2 and 3 correspond to articles in preparation. They describe respectively a eukaryotic parasite (*Aplanochytrium* sp.) and an algicidal bacteria (*Kordia* sp.) that infect *Guinardia* species. Both pathogens have a broad host range, but display different infection strategies. While *Aplanochytrium* sp. needs a direct contact with the host, the bacterium *Kordia* sp. releases an extracellular compound that is responsible for the host lysis.

The infections patterns and modes of action of the three types of parasites suggest multiple controls of *Guinardia* blooms with variable biogeochemical implications in this coastal environment.

CHAPTER I - First viruses infecting the marine diatom *Guinardia delicatula*

This work has been submitted on September 6, 2018 to Frontiers in Microbiology, special issue "The Diversity and Ecology of Aquatic Viruses from Headwaters to the Hadal".
Accepted with minor revisions on October 15, 2016

Laure Arsenieff[1*], Nathalie Simon[1], Fabienne Rigaut-Jalabert[2], Florence Le Gall[1], Samuel Chaffron[3], Erwan Corre[2], Emmanuelle Com[4,5], Estelle Bigeard[1], Anne-Claire Baudoux[1]

[1]Sorbonne Université, CNRS - UMR 7144 - Diversity and interactions in oceanic plankton - Station Biologique de Roscoff, 29860 Roscoff, France
[2]Sorbonne Université, CNRS, Fédération de Recherche FR2424, Station Biologique de Roscoff, 29680 Roscoff, France
[3]Laboratoire des Sciences du Numérique de Nantes (LS2N), CNRS UMR 6004 – Université de Nantes, École Centrale de Nantes, IMT Atlantique, 2 rue de la Houssinière, 44322 Nantes, France
[4]Univ Rennes, Inserm, EHESP, Irset – UMR_S 1085, F-35042 Rennes, France
[5]Protim, Univ Rennes, F-35042 Rennes cedex, France

*Corresponding author:
Laure Arsenieff,
Station Biologique de Roscoff, UMR7144, Place George Teissier, 29680 Roscoff, France
larsenieff@sb-roscoff.fr

Running title:
Characterization of *Guinardia delicatula* viruses

The mass spectrometry proteomics data have been deposited in ProteomeXchange with the dataset identifier PXD009598

Reviewers, please access our data using the following account details:
Project Name: First viruses infecting the marine diatom Guinardia delicatula
Project accession: PXD010967
Project DOI: 10.6019/PXD010967

Reviewer account details:
Username: reviewer83845@ebi.ac.uk
Password: lG1HzGMu

Number of words: < 11 000 words
Number of figures: 8
Number of tables: 4

ABSTRACT

The marine diatom *Guinardia delicatula* is a cosmopolitan species that dominates seasonal blooms in the English Channel and the North Sea. Several eukaryotic parasites are known to induce the mortality of this species. Here, we report the isolation and characterization of the first viruses that infect *G. delicatula*. Viruses were isolated from the Western English Channel (SOMLIT-Astan station) during the late summer bloom decline of *G. delicatula*. A combination of laboratory approaches revealed that these lytic viruses (GdelRNAV) are small tailless particles of 35-38 nm in diameter that replicate in the host cytoplasm where both unordered particles and crystalline arrays are formed. GdelRNAV display a linear single-stranded RNA genome of ~9 kb, including two open reading frames encoding for replication and structural polyproteins. Phylogenetic relationships based on the RNA-dependent-RNA-polymerase gene marker showed that GdelRNAV are new members of the *Bacillarnavirus,* a monophyletic genus belonging to the order *Picornavirales*. GdelRNAV are specific to several strains of *G. delicatula*. They were rapidly and largely produced (< 12h, 9.34×10^4 virions per host cell). We recorded a substantial delay (72h) between virions release and host cell lysis. Our analysis points out the host's variable viral susceptibilities during the early exponential growth phase. Interestingly, we consistently failed to isolate viruses during spring and early summer while *G. delicatula* developed important blooms. While our study suggests that viruses do contribute to the decline of *G. delicatula*'s late summer bloom, they may not be the primary mortality agents during the remaining blooms at SOMLIT-Astan. Future studies should focus on the relative contribution of the viral and eukaryotic pathogens to the control of *Guinardia*'s blooms to understand the fate of these prominent organisms in marine systems.

Keywords:
Single-stranded RNA viruses, Diatoms, Genomics, Host-virus dynamics, Western English Channel

INTRODUCTION

Diatoms are a major component of phytoplankton communities. They have a worldwide distribution (Malviya *et al.*, 2016; Mann and Droop, 1996), occurring in freshwaters and marine habitats from the poles to the tropics (Balzano *et al.,* 2017; Hernández-Becerril *et al.*, 2010; Kellogg and Kellogg, 1996; Sarno *et al.*, 2005; Takano, 1981). They are responsible for 35 to 75% of the marine primary production in the oceans (Nelson *et al.*, 1995) and they play a fundamental role in the transfer of carbon to consumers (Armbrust, 2009). They are also important drivers in the ocean's export production due to their high sinking rate, thus playing a key-role in the functioning of the biological carbon pump (Falkowski *et al.*, 1998; Smetacek, 1999). In nutrient rich coastal ecosystems, diatoms produce recurrent seasonal successions of species and blooms (Assmy and Smetacek, 2009; Sommer *et al.*, 2012). The marine diatom genus *Guinardia* is described as a considerable contributor to micro-phytoplankton assemblages along the Atlantic coasts, in the English Channel (Gómez and Souissi, 2007; Grall, 1972; Guilloux *et al.*, 2013), North Sea (Wiltshire *et al.*, 2010) and western Irish Sea (Gowen *et al.*, 1999). Especially, in the German Bight at Helgoland Roads time series, the bloom-forming species *Guinardia delicatula* is one of the most abundant diatom species, with highest abundances in early summer and autumn. However, a trend towards an earlier and wider period of development in response to environmental variables has been detected (Schlüter *et al.*, 2012; Wiltshire *et al.*, 2010). In the Western English Channel (WEC), *G. delicatula* dominates the seasonal cycle production, where its spring-summer development occurs commonly from May to August/September (Grall, 1972; Guilloux *et al.*, 2013; Simon *et al.*, personal communication).

Decades of research have emphasized the decisive role of physical factors (e.g. light, turbulence and sedimentation), nutrient limitations and predation by zooplankton in pacing the seasonal development of marine diatoms (Sarthou *et al.*, 2005; Schlüter *et al.*, 2012; Smetacek, 1985; Sommer *et al.*, 2012). Parasites have also been identified as potential primary agents that could shape diatom population dynamics (Gleason *et al.*, 2015; Scholz *et al.*, 2015; Tillmann *et al.*, 1999). In the literature, several eukaryotic parasites of the genera *Pirsonia* (Kühn *et al.*, 1996), *Cryothecomonas* (Drebes *et al.*, 1996) and *Rhizamoeba* (Kühn, 1996) were described associated with *G. delicatula*. More recently, viruses have been identified as mortality factors involved in the control of diatoms dynamics. Up to date, about 20 diatom viruses have been described. They are separated into two groups: the single-stranded RNA (ssRNA) viruses (Kimura and Tomaru, 2015; Shirai *et al.*, 2008; Tomaru *et al.*, 2009) and the single-stranded DNA (ssDNA) viruses (Kimura and Tomaru, 2015; Tomaru *et al.*, 2013b; Toyoda *et al.*, 2012). Viruses of diatoms are also highly specific to their hosts, with species-specificity or even strain-specificity (Nagasaki *et al.*, 2004; Tomaru *et al.*, 2008; Toyoda *et al.*, 2012). As a consequence, these mortality agents may play a key role in species or infra-specific groups successions. Nevertheless, the impact of diatom viruses on their host dynamics in natural environments are not clearly understood. More isolations and characterizations are needed to better understand the role of viruses in the regulation of host populations. To our knowledge, no viral particle has been described on *G. delicatula.*

In this study, we isolated four ssRNA viruses causing lysis of *Guinardia delicatula* from the long-term monitoring SOMLIT-Astan station located off Roscoff (Western English Channel,

WEC). The host range, morphological features, lytic cycle, genome structure and phylogenetic position of the representative GdelRNAV-01 (*Guinardia delicatula* ssRNA virus 01) were fully described. These viruses are new members of the *Bacillarnavirus* genus within the *Picornavirales* and share common features with other viruses infecting diatoms. Due to the ecological importance of its host, this discovery raises new questions about the contribution of viruses and other parasites to the interaction network associated with *G. delicatula* in the WEC.

EXPERIMENTAL PROCEDURES

Growth conditions of algal cultures

The marine diatom *Guinardia delicatula* RCC3083 has been used in this study for the isolation of viruses. This clonal strain was provided by the Roscoff Culture Collection (RCC, http://roscoff-culture-collection.org/) and was isolated the 19th September 2012 from surface water at the Roscoff Estacade station in the Western English Channel (48:43:56 N, 3:58:58 W). *G. delicatula* RCC3083 was maintained in sterile condition in K+Si medium (Keller *et al.*, 1987) at 18°C, under a 12:12h light:dark cycle of 100 µmol photons.m^{-2}.s^{-1} provided by a white fluorescent light (Philips Master TL_D 18W/865). These culture conditions were used for all the following experimentations.

Genetic variations among *G. delicatula* strains

Intraspecific variability within *Guinardia delicatula* was examined in the SSU-18S, ITS and partial LSU-28S rDNA genes markers. The primers used were 63F (ACGCTTGTCTCAAAGATTA) and 1818R (ACGGAAACCTTGTTACGA) (Lepere *et al.*, 2011) for the 18S, 329F (GTGAACCTGCRGAAGGATCA) (Guillou *et al.*, 2004) and D1R-R (TATGCTTAAATTCAGCGGGT) (Lenaers *et al.*, 1989) for the ITS, and D1R-F (ACCCGCTGAATTTAAGCATA) (Lenaers *et al.*, 1989) and D3Ca (ACGAACGATTTGCACGTCAG) (Orsini *et al.*, 2002) for the partial 28S D1-D3 region. Briefly, aliquots (2.25 µL) of *G. delicatula* cultures (Table 1) were submitted to 95°C for 5 min. The reaction mixture (30 µL final volume) was then added: Phusion Master Mix (1x final concentration, Thermo Scientific), 3% DMSO and 0.25 µM of each primer. PCR amplifications were performed with the following conditions: an initial incubation step at 95°C for 5 min, followed by 40 cycles of denaturation at 95°C for 1 min, annealing step for 30 sec at 55°, 52° and 57° for the amplifications of the SSU, ITS and LSU respectively, and extension at 72°C for 1 min 30. The 40 cycles were followed by a final extension step at 72°C for 10 min. PCR products were sent to Sanger Sequencing to GATC Biotech (https://www.gatc-biotech.com/en/index.html, Constance, Germany). Sequences were analyzed and aligned using Geneious 9.1.3.

Temporal dynamics of *Guinardia delicatula*

Seasonal variations in abundance of the diatom *G. delicatula* at the long-term monitoring station SOMLIT-Astan off Roscoff (48:46:18 N, 3:58:6 W) were obtained from microscopic counts data (RESOMAR-Pelagos database, http://abims.sb-roscoff.fr/pelagos). Briefly, surface seawater (1 meter depth) collected bi-monthly was preserved in acidic Lugol's

iodine solution. After sedimentation in Utermöhl chambers, cell counts and identifications were performed under an inverted light microscope (Guilloux *et al.*, 2013).

Isolation of viruses

Samplings were conducted every fortnight between October 2015 and October 2016 at SOMLIT-Astan station. This station is representative of the permanently mixed water column of the Western English Channel (L'Helguen *et al.*, 1996; Wafar *et al.*, 1983). Seawater samples of 3L were collected at 1 m depth using a 5 L Niskin bottle. Back in the laboratory, samples were immediately pre-filtered through a 150 µm pore-size nylon filter to remove most of the micro- and mesozooplankton. 250 mL of pre-filtered samples were enriched with F/2 medium (10% v/v) and 5 mL of culture of *G. delicatula* RCC3083. After two weeks of incubation, the enriched samples were successively filtered through a GF/F filter (Whatman) and 0.22 µm PES filter (Whatman) to isolate the viral community.

Aliquot (0.5 mL) of the 0.22 µm-filtered samples were inoculated into 1.5 mL exponentially growing host culture in 24-multiwell plates under the host culture conditions as described above. Untreated host cultures served as controls.

Cultures were inspected by light microscopy two weeks after inoculation. If algal lysis was observed, 3 extinction dilution cycles were carried out to clone the pathogens (Suttle, 1993). Briefly, 100 µL aliquots of the lysates were serially diluted in 10-fold increment in 900 µL of exponentially growing culture of *G. delicatula* RCC3083 (900 µL). Lysates in the last dilution before extinction were transferred to another exponentially growing culture of *G. delicatula* RCC3083 and a new filtration on 0.22 µm was repeated to verify the transferability.

From this procedure, 4 clonal viral isolates lytic to *G. delicatula* strain RCC3083 have been obtained: GdelRNAV-01 (RCC5809), GdelRNAV-02 (RCC5810), GdelRNAV-03 (RCC5811), and GdelRNAV-04 (RCC5812). They were isolated from natural samples collected respectively on the 23th September, 26th August, 09th September and 24th October 2016. They were maintained in culture by bimonthly transfers in *G. delicatula* RCC3083 under the host culture conditions described previously.

Host ranges

To study the host ranges of GdelRNAV-01, GdelRNAV-02, GdelRNAV-03 and GdelRNAV-04, the viral suspensions were filtered on 0.45 µm PES filter (Whatman) and were added to 29 exponentially growing phytoplankton cultures (10% vol/vol), including 27 diatom cultures (Table 1). Untreated phytoplankton cultures served as controls. The experiment has been carried out in triplicate.

Algal growth and lysis were monitored after 7 and 14 days post-inoculation (dpi) under light microscopy. After two weeks incubation, phytoplanktonic cultures where no lysis was detected were not considered as susceptible hosts for these clonal viruses.

Transmission electronic microscopy (TEM)

To inspect the replication site of GdelRNAV-01, an exponential culture of *G. delicatula* RCC3083 host strain was inoculated with a fresh 0.45 µm filtered virus lysate (5% vol/vol).

Uninfected host served as control. Aliquots of the cell suspensions were sampled every 12 hours post-inoculation (hpi), and the algal abundances in the control and infected cultures were monitored by optical microscopy (Sedgewick Rafter, Hausser Scientific, USA). 10 mL of the aliquots were fixed with 1% glutaraldehyde and stored at 4°C until treatment. Pluronic F68 (final concentration 0.01%, Gibco) was added and cells were pelleted by centrifugation. Samples were rinsed twice in K+Si medium and 0.2 M cacodylate buffer (pH=7.53) containing 2% of NaCl were added. Samples were then fixed with 1% OsO4 for 1h at 4°C. After three washings with the cacodylate buffer, samples were progressively dehydrated in ethanol series (from 30% to 100%). Samples were embedded in Spurr's epoxy resin (Low viscosity, Electron Microscopy Sciences) and were polymerized over a week-end at 60°C. Thin sections (40-70 nm) were cut using a Leica ultracut UCT microtome and mounted on copper grids. Sections were stained with 0.4% uranyl acetate and viewed with a JEOL-JEM 1400 electron microscope (JEOL Ltd., Tokyo, Japan) operating at 80 kV.

Morphological features of the virions were also determined by TEM. Briefly, a fresh viral lysate of each four viral strains was filtered through 0.22 µm pore size filter and concentrated by centrifugation (Vivaspin 50 kDa, Sartorius). Concentrated viral suspension was negative stained for 40 s using uranyl acetate (2% w/v) on a copper grid. Appropriate controls (filtrates from uninfected hosts) have been also examined by TEM.

Growth experiment

In order to study the virus growth kinetics, triplicates of exponentially growing cultures of *G. delicatula* RCC3083 were inoculated with a fresh 0.1 µm filtered suspension of GdelRNAV-01 (10% v/v, with a multiplicity of infection of 359.5). An untreated culture of *G. delicatula* RCC3083 served as control. Samples were taken every 12 hours for 8 days to monitor host and virus parameters. Diatom counts were obtained using a Sedgewick Rafter cell (Hausser Scientific, USA) on an inverted microscope. Epifluorescence microscopy (U-MNB2 filter, Olympus BX51, Tokyo, Japan) was used to monitor morphological changes occurring in chloroplasts (using the fluorescence of Chl *a*) and in PicoGreen stained nuclei (Picogreen, final concentration 1x, Molecular Probes).

Viral titer was measured using the extinction dilution method (Suttle, 1993) and was estimated with the software Most Probable Number (MPN; version 2.0, Avineon, U.S Environmental Protection Agency). This experiment was performed in duplicate.

Viral latent period was calculated as the period of time between the viral inoculation and the first increase in viral titer. Burst size (number of viral progenies produced per one host cell lysed) was estimated from the ratio between the increase in viral titer and the decline in host cell concentration for a given period (from 72h to 96h in our case), as:

$$BS = \frac{V_{max} - V_{min}}{H_{max} - H_{min}}$$

where V_{max} and V_{min} are the maximal and minimal viral concentrations respectively, and H_{max} and H_{min} the maximal and minimal host abundances.

Virions thermal stability

The stability of the virions to temperature was determined by incubating 0.5 mL of a 0.2 µm filtered GdelRNAV-01 suspension at -196, -80, - 20, 4, 10, 18, 25, 30, 40, 50 and 60°C.

After 24 hours, samples were thawed or cooled down for 30 min at room temperature and inoculated with *G. delicatula* RCC3083 (10% v/v) in triplicates in 48-multiwell plates. Cultures were inspected by light microscopy at 7 and 14 days dpi to detect lysis.

Sensitivity to chloroform

In order to determine whether GdelRNAV-01 possess a membrane, 10% and 50% (v/v) of chloroform were added to aliquots (1.5 mL) of 0.2 µm filtered lysate. The mixtures were vigorously homogenized by inversion and incubated for 60 min at room temperature. Chloroform was removed by centrifugation, 2,200 *X g* for 20 min at room temperature and the aqueous layers, containing the virions, were transferred to new tubes. Samples were left overnight for evaporation to remove any chloroform contamination. Negative controls of K+Si medium were also taken along. Samples were inoculated with *G. delicatula* RCC3083 (10% v/v) in triplicates in 48-multiwell plates. Cultures were inspected by light microscopy at 7 and 14 days dpi.

Virus purification

A freshly produced GdelRNAV-01 lysate (500 mL) was filtered through 0.45 µm and 0.1 µm PES filters to remove cellular debris and bacteria. Polyethylene glycol 6000 (PEG, Sigma Aldrich) was added to the filtrate (final concentration 10% wt/v) and stored at 4°C overnight as described in Tomaru *et al.* (2004). The mixture was centrifuged at 30,100 *X g*, 4°C, for 2h15 (Avanti J-26XP, Beckman Coulter) and the pellet containing the viruses was washed with 10 mM phosphate buffer (10 mM KH_2PO_4 and 10 mM Na_2HPO_4, pH 7.2). The suspension was transferred to a Falcon tube (polypropylene) and an equal volume of chloroform was added. The sample was vigorously vortexed and centrifuged at 2,200 *X g*, for 20 min at room temperature. The aqueous layer was recovered and the chloroform procedure was repeated 7 times. After ultracentrifugation (207,870 *X g*, 4 h, 4°C, 70 Ti rotor, Optima XPN-80, Beckman Coulter) of the last aqueous phase, the viral pellet was collected and resuspended in 500 µL of Nuclease-Free Water (Life Technologies). This purified virus sample was used for analysis of nucleic acids, genome sequencing and analyses of structural proteins.

Viral nucleic acids

The nucleic acids (300 µL) of the four viral strain suspensions were extracted using the Kit MasterPure complete DNA & RNA purification (Epicentre) according to the manufacturer's instructions. This extraction was performed on a purified viral suspension for GdelRNAV-01 and on non-purified suspensions of GdelRNA-02, GdelRNA-03 and GdelRNA-04. Around 50 mL of lysates were filtered through 0.45 µm and 0.1 µm PES filters and concentrated by centrifugation (Vivaspin 50 kDa, Sartorius).

To determine the nature of viral nucleic acids, enzymatic digestions of nucleic acids extracts were conducted. Aliquots of 4 µL were digested with DNase I (final concentration 0.05 $U.\mu L^{-1}$, Epicentre) at 37°C for 1h, with RNase A (final concentration 0.025 $\mu g.\mu L^{-1}$, Epicentre) or with S1 nuclease (final concentration 0.03 $U.\mu L^{-1}$, Promega) that degrades single stranded nucleic acids, for 30 min at room temperature. An untreated aliquot was kept on ice to serve as control. After incubation, samples were loaded on 1.2% agarose gel, stained with ethidium

bromide and electrophoresed at 100 V for 50 min. The gel was visualized on Imagequant LAS4000 (GE Healthcare, Waukesha, WI, USA).
The ssRNA viral nucleic acids were converted to cDNA using the SuperScript III Reverse Transcriptase (Invitrogen) with random primers (250 ng/µL) following the manufacturer's protocol.

Viral genome sequencing and analyses

The complete viral genome of GdelRNAV-01 was obtained from a 2 x 150 bp paired-end run sequencing on an Illumina NextSeq platform performed by Fasteris (https://www.fasteris.com/dna/, Plan-les-Ouates, Switzerland). A total of 42 872 641 paired reads of 150 nt were quality trimmed using Trimmomatic v. 0.33 with default parameters (Bolger *et al.,* 2014) and normalized using the Diginorm script accessible in the Trinity assembler package (Grabherr *et al.*, 2011). The 443 025 remaining reads were *de novo* assembled into scaffolds with SPAdes version 3.11.0 using a combination of Kmer size 21, 33, 55 and 77 (Bankevich *et al.*, 2012). Scaffolds sequences superior to 8 000 nucleotides were analyzed by megablast against nr database (release February 2018) and blastx against viral section of nr database (release February 2018) leading to the detection of a unique scaffold of 9233 nucleotides matching viral sequences. Genes prediction was performed using NCBI ORFfinder (https://www.ncbi.nlm.nih.gov/orffinder/) and validated by NCBI SmartBLAST (http://blast.ncbi.nlm.nih.gov/smartblast/).

Viral proteins

An aliquot of purified viral suspension (75 µL) was boiled in 4x Laemmli buffer (25 µL) for 5min and laid on ice for 30 min. The mixture was then loaded on SDS-PAGE gel (NuPAGE 4-12% Bis-Tris Protein Gel, Life Technologies) using an XCell SureLock Mini-Cell (Invitrogen, Carlsbad, CA, USA) at 200V for 45 min. After migration, the gel was rinsed 3 times in MilliQ water and stained overnight with ProSieve EX Safe Stain (Lonza Rockland, Inc). The gel was destained in MilliQ water baths and visualized with a white light table. Bands were excised and digested with trypsin for analysis by mass spectrometry using an Orbitrap instrument (LTQ-OrbitrpXL, Thermo Scientific) on Protim platform (https://www.protim.eu/, Rennes, France) as previously described (Lavigne *et al.*, 2012) (see SuplM&M). The mass spectrometry proteomics data have been deposited to the ProteomeXchange Consortium via the PRIDE (Vizcaíno *et al.*, 2016) partner repository with the dataset identifier PXD010967 (project accession) and 10.6019/PXD010967 (project DOI).

Phylogenetic analysis of ssRNA viruses

In order to determine the taxonomic position of GdelRNAV-01, its closest relatives were searched in NCBI non-redundant database (release 01 February 2018) using the helicase, RdRp and ORF2 amino acid sequences as query with the BLASTP tool (https://blast.ncbi.nlm.nih.gov/Blast.cgi). The phylogenetic position of GdelRNAV-01 was inferred from comparative analyses of amino acid sequences encoding the RNA dependent RNA polymerase (RdRp) domain of the replicase polyprotein. The sequence of the GdelRNAV-01 RdRp domain was retrieved from the whole genome sequence using the Basic Local Alignment Search Tool (BLAST, https://blast.ncbi.nlm.nih.gov/Blast.cgi). RdRp domain

sequences of a selection of *Picornavirales* that are representative of different families (International Committee on Taxonomy of Viruses, ICTV, https://talk.ictvonline.org/) were selected. The sequence alignment was generated by the MAFFT version 7 program and the E-INS-I iterative refinement method (https://mafft.cbrc.jp/alignment/server/, Katoh *et al.*, 2017). A phylogenetic tree was constructed by maximum likelihood with PhyML 3.0 (http://www.atgc-montpellier.fr/phyml/, Guindon *et al.,* 2010) with the automatic model selection by SMS (Lefort *et al.*, 2017) and 1000 bootstrap replicates. MEGA7 (Kumar *et al.*, 2016) was used to visualize the final tree.

Comparative analyses of the RdRp gene sequences between *Guinardia delicatula* viruses

Degenerated primers, RdRp_F (TCTTCGTATGCCAGCACAACT) and RdRp_R (WAGAGCTCCATGAATCATYCC), were designed based on the RdRp regions of GdelRNAV-01 and of Csp03RNAV that infects *Chaetoceros* sp. strain SS08-C03 (AB639040), using Geneious 9.1.3 (Biomatters Ltd, NZ). These primers were used to amplify about 500 bp of the RdRp domains of GdelRNA-02, GdelRNA-03 and GdelRNA-04. The PCR reaction mixture (25 µL final volume) consisted of 1x Platinum *Taq* buffer (final concentration, Invitrogen), 2 mM $MgCl_2$, 0.2 mM dNTP, 1 µM of each primer, 2U of Platinum *Taq* and 1 µL of cDNA. PCR amplifications were performed with the following conditions: an initial incubation step at 94°C for 75 sec, followed by 40 cycles of denaturation at 94°C for 45 sec, annealing step at 56°C for 45 sec and extension at 72°C for 1 min. The 40 cycles were followed by a final extension step at 72°C for 9 min. PCR products were sent to Fasteris (https://www.fasteris.com/dna/, Plan-les-Ouates, Switzerland) for an enzymatic purification and for Sanger Sequencing using the degenerated primers RdRp_F and RdRp_R. The sequence alignment was generated by the MAFFT version 7.222 available on Geneious 9.1.3 (Biomatters Ltd, NZ).

Biogeography of GdelRNAV-01 in natural environments

To determine the distribution of GdelRNAV-01, environmental sequences data were downloaded from public databases and bioinformatics workflows were designed under Galaxy instance of the ABIMS platform: http://galaxy3.sb-roscoff.fr (Giardine *et al.*, 2005) in order to search for homologues of GdelRNAV-01 genome sequences. Briefly, when necessary, data were trimmed and quality filtered and reads were mapped against GdelRNAV-01 genome using the Bowtie2 tool with default parameters (Langmead and Salzberg, 2012). In some cases, the GdelRNAV-01 genome or RdRp domain was directly blasted against environmental sequences using Geneious 9.1.3. This was the case for sequences obtained by Culley *et al.* (2003, 2006, 2007) and Culley and Steward (2007) with data volume < 200 sequences.

Accession numbers

The nucleotide sequences of the GdelRNAV-01 genome, GdelRNAV-02, GdelRNAV-03 and GdelRNAV-04 RdRp domains were deposited in the NCBI database under accession number MH706768, MH706769, MH706770 and MH706771 respectively.
Sequences obtained from the eukaryotic nuclear rRNA/ITS for *Guinardia delicatula* strains were also deposited in the NCBI database:

RCC3083 (MH712327), RCC4834 (MH712328), RCC5777 to RCC5789 (MH712329-MH712341) for the 18S, RCC3083 (MH712342), RCC4834 (MH712343), RCC5777 to RCC5787 (MH712344-MH712354) for the partial 28S and RCC3083 (MH714686), RCC4834 (MH714687), RCC5777 to RCC5788 (MH714688- MH714699) for the ITS gene marker.

RESULTS

In situ Guinardia delicatula dynamics and cultural diversity

During the sampling course (Sept 2015 – Oct 2016), we recorded several blooming episodes of *Guinardia delicatula*. A first small peak (2,560 cells.L^{-1}) was detected in October 2015 (Figure 1). In 2016, the diatom bloom that occurred mid-June was dominated by *G. delicatula* (86,960 cells.L^{-1}, 84.7% of the total diatom counts) while 2 smaller peaks were observed during the end of summer (12,540 cells.L^{-1} on the 28th of July, 8,500 cells.L^{-1} on the 26th of August).

During the sampling period, a total of 13 new *G. delicatula* strains were successfully isolated and maintained in culture (RCC5777-RCC5790, Table 1). Sequencing of the SSU-18S, ITS and partial LSU-28S gene markers revealed very low variability among strains. For the 18S rDNA gene, the 1655 bp alignment of the 14 strains indicated 100% of identity between sequences. The ITS gene sequences (646 bp) of 11 of the strains studied were identical while the sequences of RCC4834 (MH714687) and 5783 (MH714694) differed respectively by 2 and 1 position. Concerning the 28S D1-D3 region, 11 strains had identical sequences (833 bp) while a deletion was detected in the RCC5780 sequence (MH712347). The 28S D1-D3 region of strains RCC5788 and RCC5789 were not sequenced (strains lost). Strain RCC5790 was lost before amplification by all three gene markers.

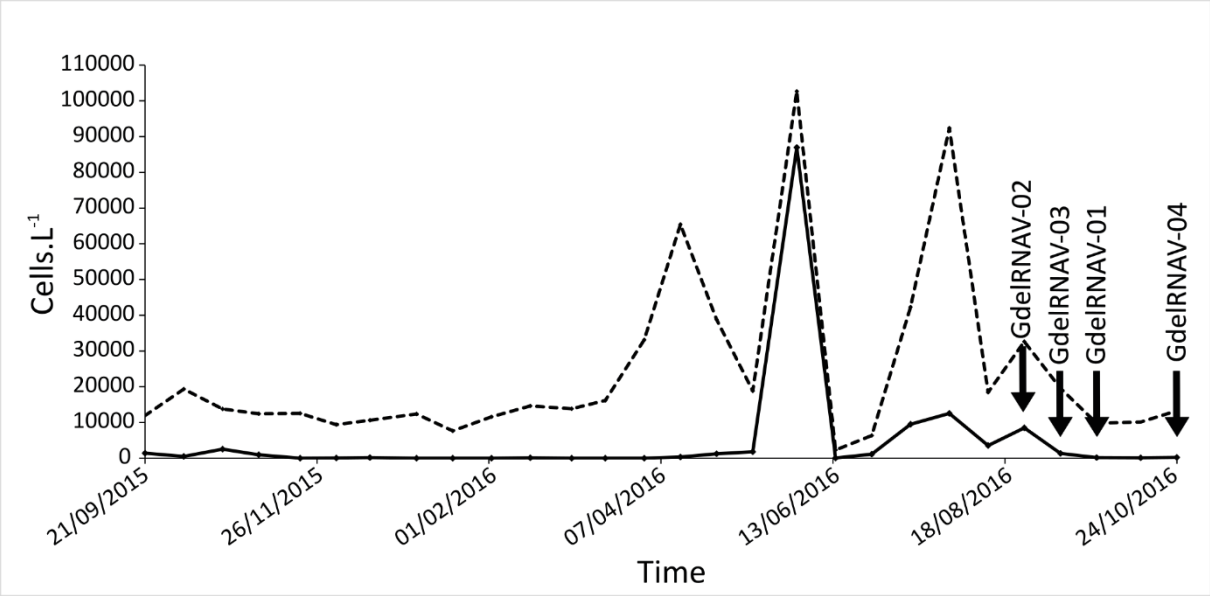

Figure 1. Temporal dynamics of Guinardia delicatula *(solid line) and all diatoms (dash line) at SOMLIT-Astan station (Western English Channel) during the September 2015 – October 2016 period. All along this period a protocol designed for the isolation of viruses lytic to* Guinardia delicatula *was applied to seawater samples collected every fortnight. The arrows point to sampling dates on which the viruses strains GdelRNAV-01 to 04 were successfully isolated.*

Viral isolation

Viruses lytic to *Guinardia delicatula* RCC3083 were isolated between end August 2016 and end October 2016. During this period, four clonal viral strains were successfully isolated and maintained in culture. The inoculation of these viral isolates into fresh host cultures caused the clearance of infected cultures after 2 weeks and led to complete cell degradations (Figure 2).

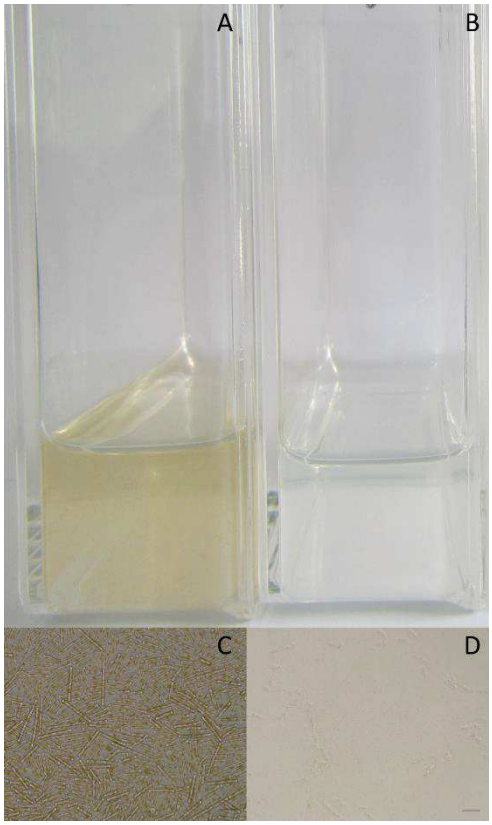

Figure 2. Aspect of healthy and infected cultures of Guinardia delicatula *RCC3083. (**A, C**) Non infected control cultures, (**B, D**) cultures infected by GdelRNAV-01. **A** and **B**: pictures of the flasks, **C** and **D**: light microscopy micrographs showing heathy cells with golden brown plastids (**C**) or cells totally degraded (**D**). All pictures were taken 14 days post infection. Scale bars on pictures **C** and **D**: 40 µm*

Host ranges

Cross infection experiments, using 15 phytoplankton species, indicated that *G. delicatula* was the only species lysed by the four viral isolates. However, all viruses showed clear strain specificity patterns (Table 1). Besides their isolation host (RCC3083), the 4 viruses infected strains RCC5782, RCC5783, RCC5784 and RCC5787 (isolated between October 2015 and September 2016). GdelRNAV-01 was the only virus able to cause lysis of *G. delicatula* RCC5785 (isolated in May 2016). For some host-virus combinations, lysis was not complete (cells with plastids observed in addition to empty frustules 14 dpi). Due to a boarder host range, GdelRNAV-01 that was isolated on the 23rd of September 2016, was chosen for detailed morphological, physiological and genetic characterization.

Morphological features

Thin sections of *G. delicatula* cells showed clear signs of degradation of the cell ultrastructure (few remaining organelles, dispersed traces of cytoplasm) 72h after the inoculation of GdelRNAV-01 compared to a healthy host (Figure 3, A & B). GdelRNAV-01 accumulates in the host cytoplasm where it forms both crystalline arrays and unordered groups of particles (Figure 3, C & D). No viral particle was observed in the control (Figure 3, A).

The TEM examination of GdelRNAV-01 progenies revealed untailed particles of 35 nm ± 2 nm in diameter with a hexagonal outline suggesting an icosahedral symmetry and the absence of outer membrane (Figure 3, E).

Virions of GdelRNAV-02, GdelRNAV-03 and GdelRNAV-04 displayed the same morphological features as GdelRNAV-01 with particles diameter of 38 ± 2 nm, 36 ± 2 nm and 38 ± 1.5 nm respectively (data not shown).

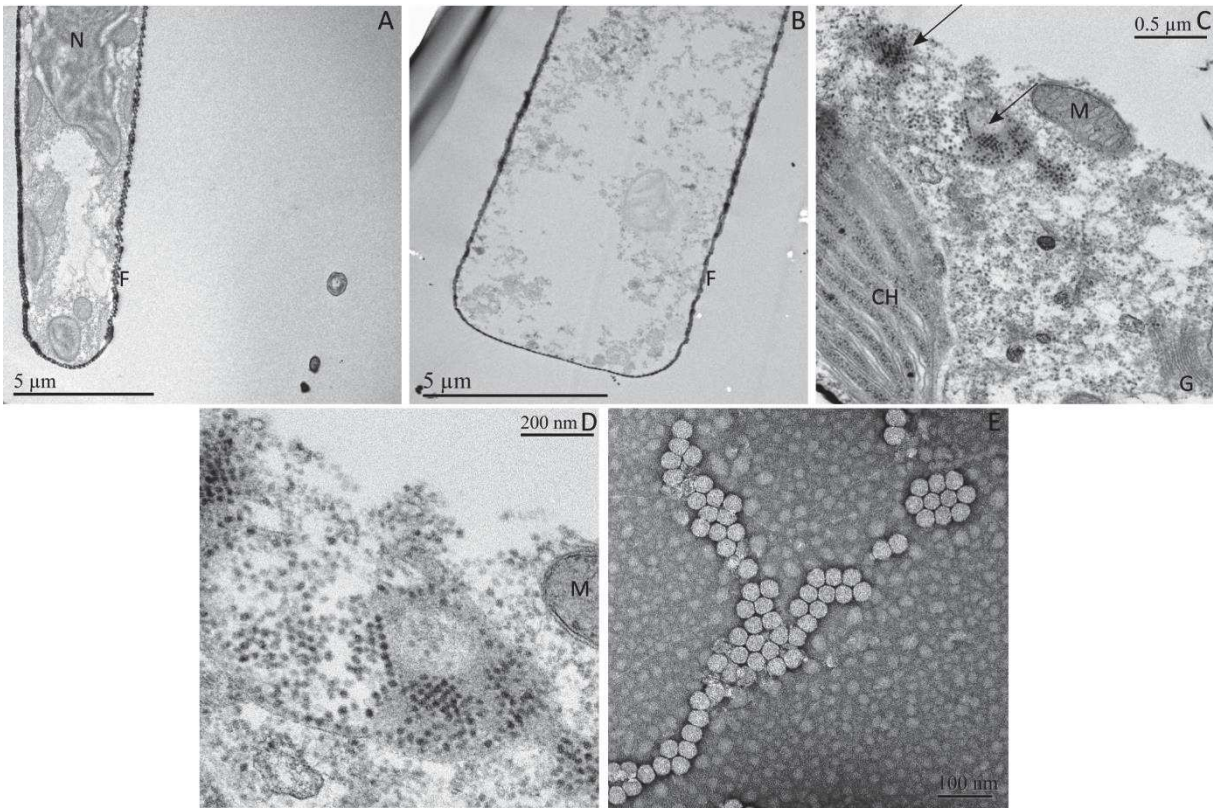

Figure 3. Ultrathin sections of Guinardia delicatula *RCC3083 and negatively stained GdelRNAV-01 particles obtained by TEM. (**A**) Healthy control. (**B, C, D, E**) G. delicatula infected by GdelRNAV-01 at 72 hpi. (**C**) Crystalline arrays and dispersed viral particles accumulated in the host cytoplasm. (**D**) Higher magnification of panel C of GdelRNAV-01 in the host cytoplasm. (**E**) Negatively stained GdelRNAV-01 particles. Arrows: Crystalline arrays. F: Frustule, G: Golgi apparatus, M: Mitochondrion, N: Nucleus, CH: Chloroplast*

Table 1. Host range of GdelRNAV viral strains: lytic activity recorded within the species Guinardia delicatula *and for other phytoplankton species. In bold, host strain used for the isolation of GdelRNAV strains. EC: English Channel. RCC: Roscoff Culture Collection. ++: Complete lysis, +: Partial lysis, -: No lysis*

Phylum	Class	Species	Strain code	Origin of isolation	Date of isolation	Lysis by GdelRNAV-01	Lysis by GdelRNAV-02	Lysis by GdelRNAV-03	Lysis by GdelRNAV-04
Bacillariophyta	Coscinodiscophyceae	*Guinardia delicatula*	**RCC3083**	Roscoff-Estacade, EC	19/09/2012	++	++	++	++
			RCC4834	Penzé estuary, EC	24/05/2015	-	-	-	-
			RCC5777	Roscoff-Astan, EC	21/10/2015	-	-	-	-
			RCC5778	Roscoff-Astan, EC	21/10/2015	-	-	-	-
			RCC5779	Roscoff-Astan, EC	21/10/2015	-	-	-	-
			RCC5780	Roscoff-Astan, EC	21/10/2015	-	-	-	-
			RCC5781	Roscoff-Astan, EC	21/10/2015	-	-	-	-
			RCC5782	Roscoff-Astan, EC	04/11/2015	+	+	+	+
			RCC5783	Roscoff-Astan, EC	29/04/2016	+	+	++	++
			RCC5784	Roscoff-Astan, EC	13/05/2016	+	+	+	+
			RCC5785	Roscoff-Astan, EC	13/05/2016	+	-	-	-
			RCC5787	Roscoff-Astan, EC	23/09/2016	++	++	++	++
			RCC5788	Roscoff-Astan, EC	24/10/2016	-	-	-	-
			RCC5789	Roscoff-Astan, EC	19/05/2017	-	-	-	-
			RCC5790	Roscoff-Astan, EC	02/06/2017	-	-	-	-
		Guinardia flaccida	RCC3093	Roscoff-Astan, EC	19/09/2012	-	-	-	-
		Guinardia striata	RCC5792	Roscoff-Astan, EC	09/09/2016	-	-	-	-
			RCC5793	Roscoff-Astan, EC	23/09/2016	-	-	-	-
		Rhizosolenia sp.	RA170220	Roscoff-Astan, EC	20/02/2017	-	-	-	-
	Mediophyceae	*Thalassiosira punctigera*	RCC4667	Roscoff-Astan, EC	21/10/2015	-	-	-	-
		Thalassiosira curviseriata	RCC5154	Roscoff-Astan, EC	26/05/2015	-	-	-	-
		Thalassiosira sp.	RCC4659	Roscoff-Astan, EC	26/05/2015	-	-	-	-
		Minidiscus variabilis	RCC4657	Roscoff-Astan, EC	26/05/2015	-	-	-	-
		Minidiscus comicus	RCC4660	Roscoff-Astan, EC	26/05/2015	-	-	-	-
		Detonula pumila	RCC5794	Roscoff-Astan, EC	13/07/2016	-	-	-	-
		Chaetoceros peruvianus	RCC2023	Roscoff-Astan, EC	01/09/2010	-	-	-	-
	Bacillariophyceae	*Nitzschia* sp.	RCC80	Roscoff-Estacade, EC	01/06/1997	-	-	-	-
		Pseudo-Nitzschia sp.	RCC3101	Bay of Concarneau	12/06/2012	-	-	-	-
Miozoa	Dinophyceae	*Prorocentrum micans*	RCC3046	Penzé estuary, EC	01/01/2006	-	-	-	-
Haptophyta	Prymnesiophyceae	*Phaeocystis* sp.	RCC1000	MAR4, Marquesas islands	29/10/2004	-	-	-	-

Infection dynamic of GdelRNAV-01

After inoculation of GdelRNAV-01 in cultures of *Guinardia delicatula* strain RCC3083, infected cells grew exponentially as in control cultures until 72 hours post inoculation (5344 cell.mL^{-1} in infected cultured, Figure 4). Cell morphology was similar in infected and control cultures (cells forming colonies with amoeboid-shaped chloroplasts) (Figure 4, optical and epifluorescence pictures). Then, diatom cell abundance decreased rapidly in infected cultures, with a stabilization step between night and day measurements. At the end of the experiment (168 hours), diatom abundance in infected cultures reached 860 cell.mL^{-1} (mean of the 3 replicates) and was lower than at T0 (2140 cell. mL^{-1}). Nuclei and chloroplasts showed signs of degradation (rounded-shaped chloroplasts), and broken frustules heavily colonized by bacteria were observed (Figure 4, optical and epifluorescence pictures). In comparison, diatom cells in control culture exhibited an exponential growth during all the experiment.
The first increase of viral titer occurred at 12 hpi, suggesting that the latent period is shorter than 12h. Periods of increase in virus titer alternated with periods of stagnation suggesting multiple cycles in spite of the high MOI (multiplicity of infection).
The burst size, calculated as the number of viral particles produced per host cell, for a given period, was estimated to be 9.34 x 10^4 infectious units.cell^{-1}.

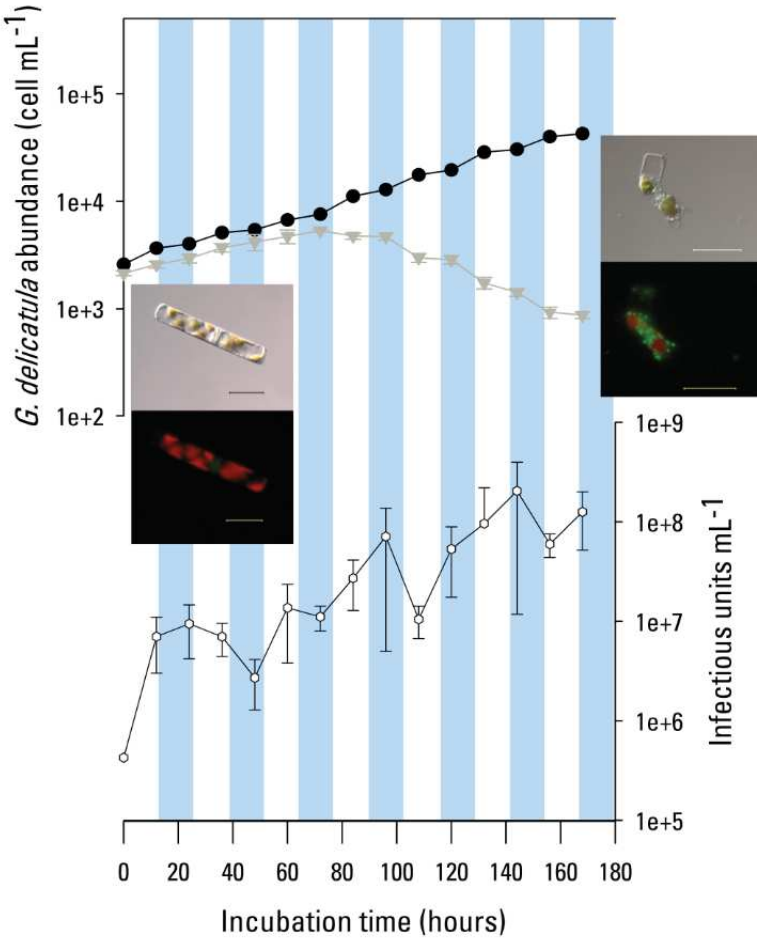

Figure 4. . Infection kinetic of Guinardia delicatula *RCC3083 by GdelRNAV-01. Abundances of diatom hosts in the control culture (black circles) and in infected cultures (grey triangles) were obtained using optical microscopy. Viral titers (open hexagons) were estimated using the MPN method. Error bars were estimated based on counts obtained in triplicates of infected cultures. Blue rectangles represent the dark phases. Pictures obtained using*

transmitted-light and epifluorescence microscopy illustrate the morphology of G. delicatula cells in control and infected cultures at T0 and Tfinal. With epifluorescence microscopy the red natural fluorescence of chloroplasts and green fluorescence of PicoGreen stained nucleic acids are observed. At Tfinal, the green fluorescence is due to the presence of bacteria. Scale bars: 20 µm

Stability of the viral particles

The viral suspension of GdelRNAV-01 has been exposed during 24 hours to a broad range of temperatures (Table 2). The virus remained infectious from -196°C to 45°C showing a high thermal stability. No viral lysis was recorded above 50°C.
GdelRNAV-01 was not susceptible to chloroform since no loss of viral infectivity was reported regardless of the chloroform concentration (Table 2).

Table 2. Viral sensitivity to thermal and solvent treatments. -: no loss of viral infectivity, +: loss of infectivity, +/-: partial loss of infectivity

Treatments	Sensitivity
Temperature (°C)	
-196	-
-80	-
-20	-
4	-
10	-
18	-
25	-
30	-
40	-
45	-
50	+/-
55	+
60	+
Chloroform (%)	
10	-
50	-

GdelRNAV-01 genome

Gel electrophoresis of purified GdelRNAV-01 nucleic acids and enzymatic digestions tests with DNase, RNase and S1 Nuclease, indicated that GdelRNAV-01 possesses a single-stranded RNA genome of about 9 kb (Figure 5). Comparable results were obtained for GdelRNAV-02, delRNAV-03 and GdelRNAV-04 (data not shown), implying that these viruses possess a single-stranded RNA genomes of 9 kb.

The assembled genome of GdelRNAV-01 was 9233 nt in length, excluding a poly(A) tail. The adenine, cytosine, guanine and uracil richness were estimated to be 30.1, 17.6, 19.3 and 33% respectively.
The GdelRNAV-01 genome consisted of a 5’ untranslated region (UTR, 1008 nt), two ORFS separated by an intergenic region (IGR, 574 nt) and a 3’ UTR of 367 nt (Figure 6). The first ORF

was 4959 nt long, representing 53.7% of the whole genome. It clustered two replication-related proteins: a helicase domain (110 amino acids) and a RNA-dependent RNA polymerase (RdRp) domain (291 amino acids) (Figure 6). The BLAST searches (table 3) revealed that both proteins were closely related to *Chaetoceros* sp. RNA virus 03, *Chaetoceros tenuissimus* RNA virus type-II, to Marine RNA virus JP-A, a viral genome reconstructed from metagenomic libraries (Culley *et al.*, 2007), and to Beihai picorna-like viruses and Wenzhou picorna-like virus 50, viruses infecting invertebrates (Shi *et al.*, 2016).
The second ORF (2325 nt, 25.2% of the viral genome) encodes for putative structural proteins of the capsid composed of 3 conserved domains that belong to the CRPV_capsid superfamily, Dicistro_VP4 superfamily, which interspaced domains of the Rhv_like superfamily (Figure 6). As for the first ORF, best hits of ORF2 using BLASTP (774 amino acids) corresponded to sequences of ssRNA viruses (Table 3).
In the IGR, a small conserved region was detected (360 nt, 4% of the whole genome). BLASTn searches revealed two hits belonging to *Chaetoceros* sp. RNA virus 03 (E-value: 2e-88) and Beihai picorna-like virus 4 (E-value: 5e-54). However, no statistically significant matching protein sequence was found using BLASTP searches (119 amino acids).
Overall sequences of the GdelRNAV-01 ORF-1 and ORF-2 showed highest similarities with picorna-like virus sequences (Table 3).

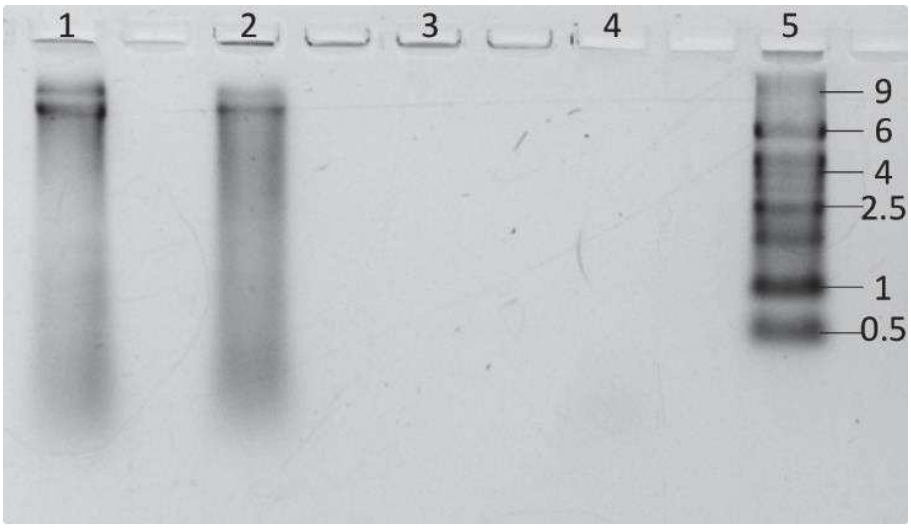

Figure 5. Nucleic acids type of GdelRNAV-01 after extraction. Lane 1: control without treatment, lane 2: Extracts treated with DNase treatment (lane 2), with RNase treatment (lane 3), or with S1 nuclease treatment (lane 4). Lane 5: RNA ladder (kb)

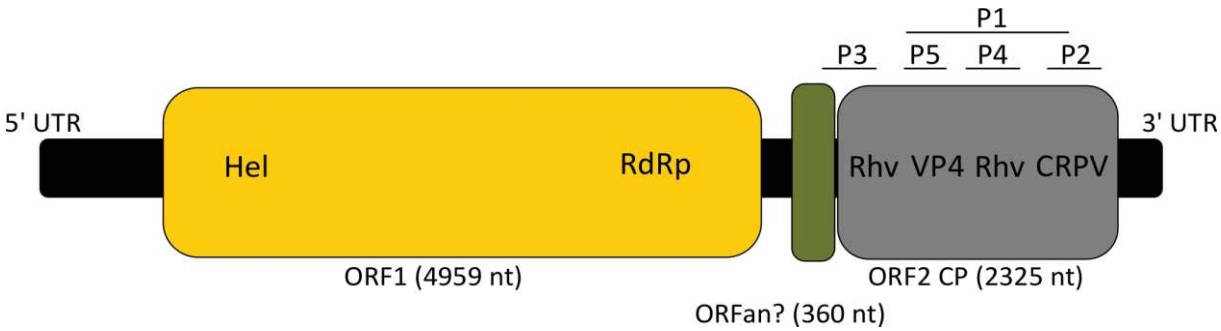

Figure 6. Schematic genome organization of GdRNAV-01 (9233 nt). 5'UTR: 5' untranslated region (1008 nt), 3' UTR: 3' untranslated region (367 nt). The yellow box indicates the replication polyprotein with Hel: Helicase and

RdRp: RNA-dependent RNA polymerase. The grey box represents the capsid proteins (CP) with domains corresponding to the Rhv_like superfamily interspaced by the Dicistro_VP4, and the CRPV_capsid superfamily. The green box indicates the possible ORFan. P1 to P5: structural proteins

Table 3. Best hits from BLASTP results showing significant alignments with the helicase and RdRp domains and the ORF-2 of GdelRNAV-01

Helicase blastp best hits	**Score**	**Query cover**	**E value**	**Identity**	**Accession number**
Beihai picorna-like virus 4	225	100%	4E-66	98%	YP_009333566.1
Chaetoceros sp. RNA virus 3	225	100%	4E-66	98%	BAK40203.1
Wenzhou picorna-like virus 50	190	100%	8E-54	76%	APG78567.1
Marine RNA virus JP-A	182	100%	4E-51	71%	YP_001429581.1
Beihai picorna-like virus 1	176	100%	7E-49	72%	YP_009333509.1
RdRp blastp best hits	**Score**	**Query cover**	**E value**	**Identity**	**Accession number**
Chaetoceros sp. RNA virus 03	585	100%	0	93%	BAK40203.1
Beihai picorna-like virus 4	582	100%	0	92%	YP_009333566.1
Wenzhou picorna-like virus 50	490	100%	2E-158	76%	APG78567.1
Beihai picorna-like virus 1	491	100%	5E-158	76%	YP_009333509.1
Marine RNA virus JP-A	481	100%	1E-154	74%	YP_001429581.1
Chaetoceros tenuissimus RNA virus SS10-45V	411	95%	8E-129	68%	BAP99822.1
Chaetoceros tenuissimus RNA virus SS10-39V	411	95%	9E-129	68%	BAP99820.1
Chaetoceros tenuissimus RNA virus type-II	411	95%	1E-128	68%	YP_009111336.1
ORF2 blastp best hits	**Score**	**Query cover**	**E value**	**Identity**	**Accession number**
Beihai picorna-like virus 4	1088	97%	0	70%	YP_009333567.1
Chaetoceros sp. RNA virus 03	1034	89%	0	73%	BAK40204.1
Marine RNA virus JP-A	904	99%	0	55%	YP_001429582.1
CtenRNAV type-II	894	100%	0	58%	YP_009111337.1
CtenRNAV SS10-39V	893	100%	0	58%	BAP99821.1
CtenRNAV SS10-45V	892	100%	0	58%	BAP99823.1
Beihai picorna-like virus 1	820	90%	0	57%	YP_009333510.1

Structural proteins

Four major capsid proteins of respectively 33.9, 29.8, 27 and 6.8 kDa (P2, P3, P4, and P5, respectively) and one minor protein of 38.6 kDa were detected on the SDS PAGE gel (P1, Figure 7). The amino acid sequences of each protein analyzed by mass spectrometry (MS)

were found in the predicted sequence of the ORF2 (Figure 6 and Table S1 and S2 in Supplementary Information). The smallest protein (P5) (6.8 kDa predicted from the gel and 4.7 kDa from the amino acid sequence) corresponded to the Dicistro_VP4 domain. The predicted peptides of P2 (33.9 kDa on the SDS-PAGE gel, 16.8 kDa based on the amino acid sequence) matched the C-ter region of the CRPV domain. The protein P4 was more central and peptides analyzed by MS corresponded to the N-terminal region of Rhv2 domain. MS analysis of P3 peptides revealed that they matched the upstream region of ORF2 up to Rhv1 domain. The largest and minor protein P1 (33.9 kDa, 51.7 kDa predicted) encompassed VP4, Rhv2, and CRPV domains.

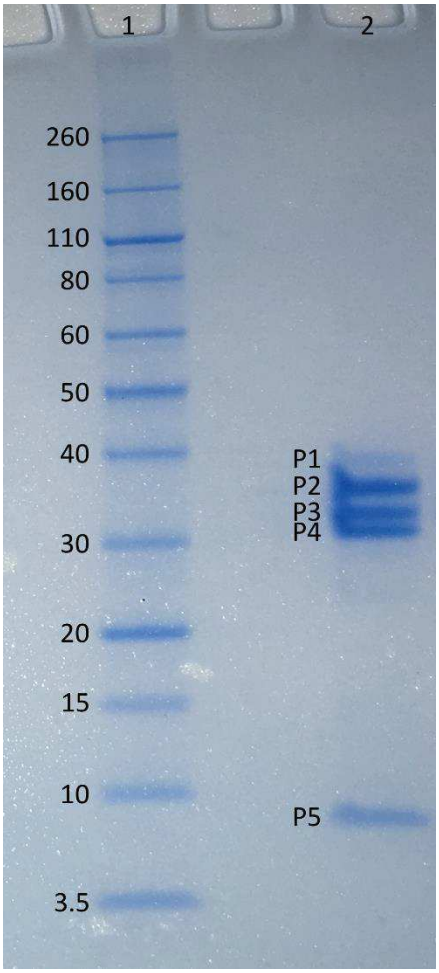

Figure 7. Analysis of the structural proteins of GdelRNAV-01 using SDS-PAGE. Lane 1: Novex sharp unstained protein standard marker (kDa). Lane 2: Denatured proteins of purified GdelRNAV-01. P1 to P5 represent the proteins 1 to 5

Phylogenetic analysis of the *Picornavirales*

Phylogenetic reconstructions based on the analysis of the RdRp amino acid sequences of a selection of *Picornavirales* revealed that GdelRNAV-01 clusters among the monophyletic genus *Bacillarnavirus* (Figure 8). Sequences of these viruses, that infect diatom species, gathered in a clade supported by a high bootstrap value (98%). GdelRNAV-01 was most closely related to *Chaetoceros* sp. number03 RNA virus (Csp03RNAV), a virus infecting the marine diatom *Chaetoceros* sp. (Tomaru *et al.*, 2013a).

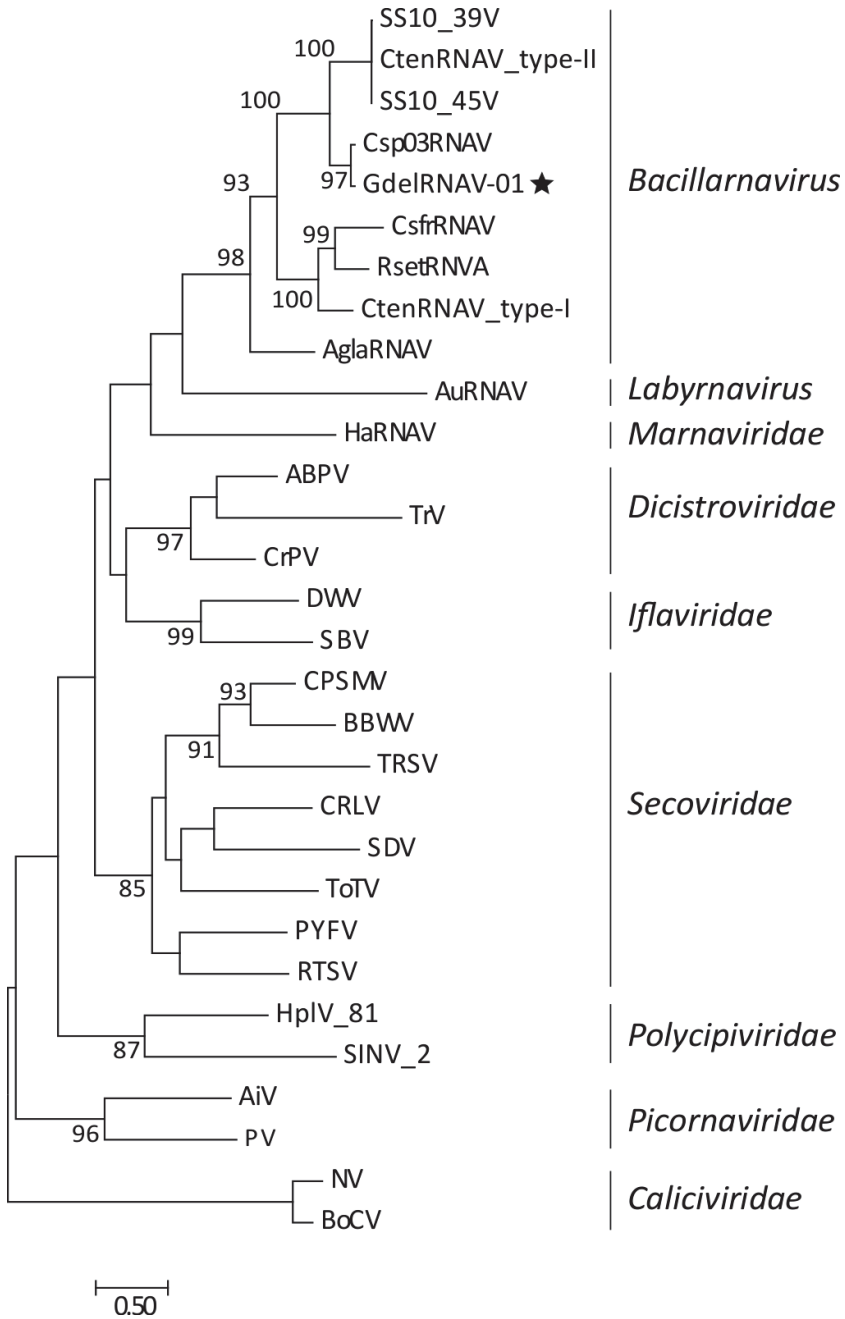

Figure 8. Phylogenetic rooted tree based on RdRp sequences of representative viruses from the Picornavirales *order.* Caliciviridae *viruses were taken as outgroup. The star indicates the position of GdelRNAV-01 in the genus* Bacillarnavirus. *The Maximum Likelihood tree was generated using PhyML 3.0 with 1000 replications and a LG+G+I+F substitution model according to the SMS analyses. Bootstraps values (%) greater than 80 are shown. Scale bar indicates the number of substitutions per site.*

Virus abbreviations: Acute bee paralysis virus (ABPV) NC_002548.1; Aichi virus (AiV), AB010145; Asterionellopsis glacialis *RNA virus (AglaRNAV) NC_024489;* Aurantiochytrium *single-stranded RNA virus (AuRNAV), BAE47143; Bovine enteric calicivirus (BoCV), AJ011099; Broad bean wilt virus 1 (BBW) NC_005289.1;* Chaetoceros socialis *f.* radians *RNA virus (CsfrRNAV), AB469874;* Chaetoceros *sp. number03 RNA virus (Csp03RNAV), AB639040;* Chaetoceros tenuissimus *RNA virus (CtenRNAV type-I), AB375474; CtenRNAV type-II, AB971661; CtenRNAV_SS10V-39V, AB971662; CtenRNAV_SS10V-45V, AB971663; Cherry rasp leaf virus (CRLV), NC_006271.1; Cowpea severe mosaic virus (CPSMV), NC_003545; Cricket paralysis virus (CrPV), NC_003924; Deformed wing virus (DWV), NC_004830;* Heterosigma akashiwo *RNA virus (HaRNAV), NC_005281; Hubei picorna-like virus 81 strain CJLX25805 (HplV-81), KX884540.1; Hubei picorna-like virus 82 (HplV-82) KX883688.1; Human poliovirus 1 Mahoney (PV), V01149; Infectious flacherie virus (IFV) NC_003781.1; Norwalk virus (NV),*

M87661; Parsnip yellow fleck virus (PYFV), D14066; Rhizosolenia setigera *RNA virus (RsRNAV), AB243297; Rice tungro spherical virus (RTSV), AAA66056; Sacbrood virus (SBV), NC_002066; Satsuma dwarf virus RNA 1 (SDV) NC_003785.2;* Solenopsis invicta *virus 2 (SINV-2) EF428566.1; Tobacco ringspot virus RNA 1 (TRSV) NC_005097.1; Tomato torrado virus RNA 1 (ToTV) NC_009013.1; Triatoma virus (TrV), NC_003783*

Intraspecific comparison of GdelRNAV viruses

Nucleotide partial sequences of the RNA-dependent RNA polymerase (RdRp) of GdelRNAV-01, GdelRNAV-02, GdelRNAV-03 and GdelRNAV-04 were highly similar, with 474 identical sites on 478 bp, representing 99.2% of identity (Figure S1). The slight differences between these four RdRp sequences are shown Figure S1 in red frames.

Distribution of GdelRNAV-01 in natural environments

Environmental surveys allowed us to study the natural distribution of GdelRNAV-01 across marine and fresh water environments (Table 4). In total, 18 858 homologous reads (488.2 bp on average) mapped against the GdelRNAV-01 RdRp gene marker. They were exclusively found in temperate coastal water stations off British Columbia. At these stations, deep-sequencing of the RdRp has been carried out to assess the diversity and composition of the ssRNA viral community (Gustavsen *et al.*, 2014).

Table 4. Results of the mapping of the GdelRNAV-01 genome or gene sequences onto environmental data

Reference	Database	Accession number	RdRp amplicons/ Metagenomes	Sampling Site	Region	Number of positive reads mapping	Length (bp) min - mean - max
Culley *et al.,* 2003	GenBank	AY285747 to AY285767	RdRp domain	British Columbia, Canada	Pacific temperate coastal waters	0	0
Culley *et al.,* 2006	NCBI BioProject	PRJNA17367	Genome	British Columbia, Canada	Pacific temperate coastal waters	0	0
Culley *et al.,* 2007	GenBank	NC_009756 to NC_009758	Genome	British Columbia, Canada	Pacific temperate coastal waters	0	0
Culley and Steward, 2007	GenBank	EF591792 to EF591815	RdRp domain	Hawaii and California, USA	Pacific subtropical waters	0	0
Rosario *et al.*, 2009	NCBI BioProject	PRJNA36649	Genome	Manatee County, Florida, USA	Reclaimed waters	0	0
Djikeng *et al.*, 2009	MetaVir	1153 and 1154	Genome	Maryland, USA	Lake, freshwaters	0	0
Culley *et al.*, 2014	GenBank	KC620972 to KC621051	RdRp domain	Hawaii, USA	Pacific tropical waters	0	0
Culley *et al.*, 2014	iMicrobes	CAM_SMPL_000815 and CAM_SMPL_000824	Genome	Hawaii, USA	Pacific tropical waters	0	0
Gustavsen *et al.,* 2014	NCBI BioProject	PRJNA267690	RdRp domain	British Columbia, Canada	Pacific temperate coastal waters	18858	241 - 488,2 - 508
Lõpez-Bueno *et al.*, 2015	Metavir	4488 to 4490	Genome	Livingston Island, Antarctic	Lake, freshwaters	0	0
Miranda *et al.*, 2016	NCBI BioProject	PRJNA266680	Genome	Western Antarctic Peninsula	Antarctic polar waters	0	0

DISCUSSION

The marine diatom *Guinardia delicatula* is a cosmopolitan species that dominates seasonal blooms in the English Channel and the North Sea. In the environment, this species is known to be infected by several eukaryotic parasites. In this study, we described for the first time viruses that infect *G. delicatula*, and probably contribute to the control of its bloom dynamics.

Morphological and genomic analyses indicated that the new *G. delicatula* viruses isolated during this study belong to the genus *Bacillarnavirus* among the *Picornavirales* (Tomaru *et al.*, 2015). This genus includes all ssRNA viruses that infect centric and pennate diatoms and gathers 9 representatives. Like all other viruses of this group, virions are small naked particles (35 nm in diameter) with a hexagonal outline, suggesting an icosahedral symmetry, and they pack a ssRNA genome. During the infection, viral progenies accumulate in the host cytoplasm, where they form both crystalline arrays and unordered particles, before their release by cell lysis. The genome architecture of GdelRNAV-01 is similar to that of other *Picornavirales* (Koonin *et al.*, 2008). The 9 kb genome of GdelRNAV-01- comprises 2 ORFs, coding respectively for replication and structural polyproteins with best hits to sequences of ssRNA viruses of the diatom *Chaetoceros* spp., as well as marine environmental virus genomes (Culley *et al.*, 2007) and viral sequences assembled from transcriptomics (Shi *et al.*, 2016). More precisely, the first ORF includes domains coding for the RNA-dependent RNA-polymerase (RdRp) as well as a helicase. The RdRp is traditionally used as a diversity marker for RNA viruses (Culley *et al.*, 2003; Koonin *et al.*, 1993). The sequencing of this gene showed low genetic variability between the 4 GdelRNAV isolates. The second ORF encodes for the structural polyprotein showing the same conserved protein domains (Rhv_like, Dicistro_VP4, CRPV_capsid) and architecture as the other diatom viruses. According to our proteomic analyses, the GdelRNAV-01 structural polyprotein cleaves into 4 major proteins while other known members of *Bacillarnavirus* have only 3 (Tomaru *et al.*, 2015). The proteomic analyses suggest that each of these major proteins matched with one of the conserved domain regions predicted in the genome sequence. A minor protein, whose amino acid sequence appeared to overlap that of the 3 major proteins, was also detected. This putative protein may correspond to an immature form, which is cleaved into smaller proteins after a maturation process as already observed in noninfectious HaRNAV virions (ssRNA virus infecting *Heterosigma akashiwo* (Lang *et al.*, 2004)).

The functional characterization of GdelRNAV supports the finding that the infection strategy of diatom viruses differs from that of known dsDNA algal viruses. As reported for these viruses, GdelRNAV are strain specific, virions are produced rapidly (in our case, latent period < 12h) and infection ultimately induced host mortality through cell lysis (Brussaard and Martínez, 2008). For GdelRNAV, the estimated burst size reached 9.34 x 10^4 virions per host cell, which is higher than reported values for other ssRNA viruses (<100 - 10^4 virions per cell (Tomaru *et al.*, 2015)). One divergent feature of ssRNA diatom viruses compared to known algal viruses is the simultaneous increase in host and viral concentrations during the first days of incubation (72 h in our case) and the occurrence of multiple viral cycles (Kimura and Tomaru, 2013; Shirai *et al.*, 2008; Tomaru *et al.*, 2009, 2011b, 2014). A theoretical calculation suggests that only 3.3% of *G. delicatula* cells produced viral progenies at the initial time of the kinetics and that the percentage of permissive cells increases along the growth curve (see

Table S3 in Supplementary Information). It is thus likely that the host cell culture, although clonal, exhibited different degrees of viral susceptibility.

Previous studies demonstrated that the physiological status of diatom host cells determines the outcome of viral infection. For example, *Chaetoceros* host population generally became more permissive to viral infection with the progression of the stationary growth (Tomaru *et al.*, 2014). This led to the hypothesis that diatoms with a high growth rate may tolerate viral infection while cells with less vigorous growth rate undergo rapid lysis and do not participate to the bloom formation (Tomaru *et al.*, 2015). Interestingly, we attempted to isolate *G. delicatula* viruses throughout the year but isolation were successful only with samples collected in late summer. We cannot rule out that the host strain used for viral isolation was not permissive to the spring and summer viral populations. Yet, the amplitude of *G. delicatula* late summer bloom is consistently lower compared to spring and early summer blooms at SOMLIT-Astan (our study and RESOMAR Pelagos database). It is tempting to speculate that the late summer environmental conditions were less favorable for the growth of *G. delicatula*, which, in turn, may have been more vulnerable to viral attack. *G. delicatula* is also known to be infected by diverse parasites such as *Pirsonia* (Kühn *et al.*, 1996) and *Cryothecomonas* (Drebes *et al.*, 1996). *G. delicatula* blooms may thus be controlled by a complex network of pathogens, among which viruses may not be the primary cause of bloom disintegration, as already reported for *Chaetoceros* spp. (Tomaru *et al.*, 2011a, 2018). In any case, variability in viral susceptibility of the host is probably contributing to the sustainability of these diatom bloom events in natural habitats.

Isolating and characterizing new viruses infecting ecologically relevant hosts is a prerequisite to advance our understanding of the large amount of environmental sequences collected worldwide. Data-mining of RNA viromes that are publicly available showed that the genome of GdelRNAV-01 recruited homologs in environments where *G. delicatula* is known to develop (based on Ocean Biogeographic Information System (OBIS) database and Hobson and McQuoid (1997)). Although very few RNA viromes are available, these preliminary results suggest that GdelRNAV occur in different temperate coastal waters. Seasonal metagenomic monitoring in the Western English Channel should be considered to investigate the composition, the prevalence and the temporal dynamics of this relevant virus–host model system. It will contribute to have a closer look at the relative contribution of the different pathogens to the control of diatom blooms, necessary to understand the fate of these prominent organisms in marine systems.

ACKNOWLEDGMENTS

The authors would like to thank the crew of the Neomysis ship for their help during the samplings at SOMLIT-Astan station. We are also grateful to Sophie Le Panse from the microscopy platform, for the transmission electron micrographs, to the RCC for the phytoplankton strains provided and also to Sarah Romac for her assistance with molecular biology. Yuji Tomaru who provided protocols and advices on viral purification is acknowledged. Laurianne Gerin is thanked for her English proofreading.

FUNDING

This study was supported by PhD fellowships from the Université Pierre et Marie Curie (Sorbonne Universités) and the Région Bretagne (ARED), the ANR CALYSPO (ANR-15-CE01-0009) and the CNRS-INSU EC2CO CYCLOBS project.

AUTHOR CONTRIBUTIONS STATEMENT

LA designed and conducted the experiments and analyses and wrote the ms. NS designed the study, contributed to the experiments, wrote the ms. FR helped for sampling and for kinetic experiments, and carried out taxonomic counts in the frame of the Roscoff SOMLIT-Astan time series. FL isolated *Guinardia* hosts, performed the PCR and participated to the analyses of the eukaryotic gene marker. SC designed the genome recruitment analysis. ERC assembled the viral genome. EMC performed and analyzed the proteomics data. EB provided technical support. ACB designed the study, contributed to the experiments, wrote the ms.

CONFLICT OF INTEREST STATEMENT

The authors declare that the research was conducted in the absence of any commercial or financial relationships that could be construed as a potential conflict of interest.

REFERENCES

Armbrust, E. V. (2009). The life of diatoms in the world's oceans. *Nature* 459, 185–192. doi:10.1038/nature08057.

Assmy, P., and Smetacek, V. (2009). "Algal Blooms," in *Encyclopedia of Microbiology*, ed. Moselio Schaechter (Oxford: Elsevier), 27–41.

Balzano, S., Percopo, I., Siano, R., Gourvil, P., Chanoine, M., Marie, D., *et al.* (2017). Morphological and genetic diversity of Beaufort Sea diatoms with high contributions from the *Chaetoceros neogracilis* species complex. *J. Phycol.* 53, 161–187. doi:10.1111/jpy.12489.

Bankevich, A., Nurk, S., Antipov, D., Gurevich, A. A., Dvorkin, M., Kulikov, A. S., *et al.* (2012). SPAdes: A New Genome Assembly Algorithm and Its Applications to Single-Cell Sequencing. *J. Comput. Biol.* 19, 455–477. doi:10.1089/cmb.2012.0021.

Bolger, A. M., Lohse, M., and Usadel, B. (2014). Trimmomatic: A flexible trimmer for Illumina sequence data. *Bioinformatics* 30, 2114–2120. doi:10.1093/bioinformatics/btu170.

Brussaard, C. P. D., and Martínez, J. (2008). Algal Bloom Viruses. *Plant Viruses* 2, 1–10. Available at: http://www.globalsciencebooks.info/JournalsSup/08PV_2_1.html.

Culley, A. I., Lang, A. S., and Suttle, C. A. (2003). High diversity of unknown picorna-like viruses in the sea. *Nature* 424, 1054–1057. doi:10.1038/nature01886.

Culley, A. I., Lang, A. S., and Suttle, C. A. (2006). Metagenomic analysis of coastal RNA virus communities. *Science (80-.).* 312, 1795–1798. doi:10.1126/science.1127404.

Culley, A. I., Lang, A. S., and Suttle, C. A. (2007). The complete genomes of three viruses assembled from shotgun libraries of marine RNA virus communities. *Virol. J.* 4, 69. doi:10.1186/1743-422X-4-69.

Culley, A. I., Mueller, J. A., Belcaid, M., Wood-charlson, E. M., Poisson, G., and Steward, G. F. (2014). The Characterization of RNA Viruses in Tropical Seawater Using Targeted PCR and Metagenomics. 5, 1–11. doi:10.1128/mBio.01210-14.Editor.

Culley, A. I., and Steward, G. F. (2007). New genera of RNA viruses in subtropical seawater, inferred from polymerase gene sequences. *Appl. Environ. Microbiol.* 73, 5937–5944. doi:10.1128/AEM.01065-07.

Djikeng, A., Kuzmickas, R., Anderson, N. G., and Spiro, D. J. (2009). Metagenomic analysis of

RNA viruses in a fresh water lake. *PLoS One* 4. doi:10.1371/journal.pone.0007264.

Drebes, G., Kühn, S. F., Gmelch, A., and Schnepf, E. (1996). *Cryothecomonas aestivalis* sp. nov., a colourless nanoflagellate feeding on the marine centric diatom *Guinardia delicatula* (Cleve) Hasle. *Helgoländer Meeresuntersuchungen* 50, 497–515.

Falkowski, P. G., Barber, R. T., and Smetacek, V. (1998). Biogeochemical Controls and Feedbacks on Ocean Primary Production. *Sci. New Ser.* 281, 200–206. doi:10.1126/science.281.5374.200.

Giardine, B., Riemer, C., Hardison, R. C., Burhans, R., Elnitski, L., Shah, P., *et al.* (2005). Galaxy: A platform for interactive large-scale genome analysis. *Genome Res.* 15, 1451–1455. doi:10.1101/gr.4086505.

Gleason, F. H., Jephcott, T. G., Küpper, F. C., Gerphagnon, M., Sime-Ngando, T., Karpov, S. A., *et al.* (2015). Potential roles for recently discovered chytrid parasites in the dynamics of harmful algal blooms. *Fungal Biol. Rev.* 29, 20–33. doi:10.1016/j.fbr.2015.03.002.

Gómez, F., and Souissi, S. (2007). Unusual diatoms linked to climatic events in the northeastern English Channel. *J. Sea Res.* 58, 283–290. doi:10.1016/j.seares.2007.08.002.

Gowen, R. J., McCullough, G., Kleppel, G. S., Houchin, L., and Elliott, P. (1999). Are copepods important grazers of the spring phytoplankton bloom in the western Irish Sea? *J. Plankton Res.* 21, 465–483. doi:10.1093/plankt/21.3.465.

Grabherr, M. G., Haas, B. J., Yassour, M., Levin, J. Z., Thompson, D. A., Amit, I., *et al.* (2011). Full-length transcriptome assembly from RNA-Seq data without a reference genome. *Nat. Biotechnol.* 29, 644–652. doi:10.1038/nbt.1883.

Grall, J. R. (1972). Développement “printanier” de la Diatomée *Rhizosolenia delicatula* près de Roscoff. *Mar. Biol.* 16, 41–48.

Guillou, L., Eikrem, W., Chrétiennot-Dinet, M.-J., Le Gall, F., Massana, R., Romari, K., *et al.* (2004). Diversity of picoplanktonic prasinophytes assessed by direct nuclear SSU rDNA sequencing of environmental samples and novel isolates retrieved from oceanic and coastal marine ecosystems. *Protist* 155, 193–214. doi:10.1078/143446104774199592.

Guilloux, L., Rigaut-Jalabert, F., Jouenne, F., Ristori, S., Viprey, M., Not, F., *et al.* (2013). An annotated checklist of Marine Phytoplankton taxa at the SOMLIT-Astan time series off Roscoff (Western English Channel, France): Data collected from 2000 to 2010. *Cah. Biol. Mar.* 54, 247–256.

Guindon, S., Dufayard, J. F., Lefort, V., Anisimova, M., Hordijk, W., and Gascuel, O. (2010). New algorithms and methods to estimate maximum-likelihood phylogenies: Assessing the performance of PhyML 3.0. *Syst. Biol.* 59, 307–321. doi:10.1093/sysbio/syq010.

Gustavsen, J. A., Winget, D. M., Tian, X., and Suttle, C. A. (2014). High temporal and spatial diversity in marine RNA viruses implies that they have an important role in mortality and structuring plankton communities. *Front. Microbiol.* 5, 703. doi:10.3389/fmicb.2014.00703.

Hernández-Becerril, D. U., Herrera-Hernández, P., Pérez-Mendoza, A., and Gerardo A Ceballos-Corona, J. (2010). Marine planktonic diatoms of the order Rhizosoleniales (Bacillariophyta) From the tropical Mexican pacific. *Vie milieu - life Environ.* 60, 95–107.

Hobson, L. A., and McQuoid, M. R. (1997). Temporal variations among planktonic diatom asseblages in a turbulent environment of the southern Strait of Georgia, British Columbia, Canada. *Mar. Ecol. Prog. Ser.* 150, 263–274.

Katoh, K., Rozewicki, J., and Yamada, K. D. (2017). MAFFT online service: multiple sequence alignment, interactive sequence choice and visualization. *Brief. Bioinform.*, 1–7. doi:10.1093/bib/bbx108.

Keller, M. D., Seluin, R. C., Claus, W., and Guillard, R. R. L. (1987). Media for the culture of oceanic ultraphytoplankton. *J. Phycol.* 23, 633–638. doi:10.1016/0198-0254(88)92621-0.

Kellogg, D. E., and Kellogg, T. B. (1996). Diatoms in South Pole ice: Implications for eolian contamination of Sirius Group deposits. *Geology* 24, 115–118. doi:10.1130/0091-7613(1996)024<0115:DISPII>2.3.CO;2.

Kimura, K., and Tomaru, Y. (2013). Isolation and characterization of a single-stranded DNA virus infecting the marine diatom *Chaetoceros* sp. strain SS628-11 isolated from western Japan. *PLoS One* 8, e82013. doi:10.1371/journal.pone.0082013.

Kimura, K., and Tomaru, Y. (2015). Discovery of Two Novel Viruses Expands the Diversity of Single-Stranded DNA and Single-Stranded RNA Viruses Infecting a Cosmopolitan Marine Diatom. *Appl. Environ. Microbiol.* 81, 1120–1131. doi:10.1128/AEM.02380-14.

Koonin, E. V., Dolja, V. V., and Morris, T. J. (1993). Evolution and Taxonomy of Positive-Strand RNA Viruses: Implications of Comparative Analysis of Amino Acid Sequences. *Crit. Rev. Biochem. Mol. Biol.* 28, 375–430. doi:10.3109/10409239309078440.

Koonin, E. V, Wolf, Y. I., Nagasaki, K., and Dolja, V. V (2008). The Big Bang of picorna-like virus evolution antedates the radiation of eukaryotic supergroups. *Nat. Rev. Microbiol.* 6, 925–939. doi:10.1038/nrmicro2030.

Kühn, S. F. (1996). *Rhizamoeba schnepfii* sp. nov, a naked amoeba feeding on marine diatoms (North Sea, German Bight). *Arch. Fur Protistenkd.* 147, 277–282. doi:10.1016/S0003-9365(97)80054-1.

Kühn, S. F., Drebes, G., and Schnepf, E. (1996). Five new species of the nanoflagellate *Pirsonia* in the German Bight, North Sea, feeding on planktonic diatoms. *Helgoländer Meeresuntersuchungen* 50, 205–222.

Kumar, S., Stecher, G., and Tamura, K. (2016). MEGA7: Molecular Evolutionary Genetics Analysis Version 7.0 for Bigger Datasets. *Mol. Biol. Evol.* 33, 1870–1874. doi:10.1093/molbev/msw054.

L'Helguen, S., Madec, C., and Le Corre, P. (1996). Nitrogen Uptake in Permanently Well-mixed Temperate Coastal Waters. *Estuar. Coast. Shelf Sci.* 42, 803–818. doi:10.1006/ecss.1996.0051.

Lang, A. S., Culley, A. I., and Suttle, C. A. (2004). Genome sequence and characterization of a virus (HaRNAV) related to picorna-like viruses that infects the marine toxic bloom-forming alga *Heterosigma akashiwo*. *Virology* 320, 206–217. doi:10.1016/j.virol.2003.10.015.

Langmead, B., and Salzberg, S. L. (2012). Fast gapped-read alignment with Bowtie 2. *Nat. Methods* 9, 357–359. doi:10.1038/nmeth.1923.Fast.

Lavigne, R., Becker, E., Liu, Y., Evrard, B., Lardenois, A., Primig, M., *et al.* (2012). Direct Iterative Protein Profiling (DIPP) - an Innovative Method for Large-scale Protein Detection Applied to Budding Yeast Mitosis. *Mol. Cell. Proteomics* 11, M111.012682. doi:10.1074/mcp.M111.012682.

Lefort, V., Longueville, J. E., and Gascuel, O. (2017). SMS: Smart Model Selection in PhyML. *Mol. Biol. Evol.* 34, 2422–2424. doi:10.1093/molbev/msx149.

Lenaers, G., Maroteaux, L., Michot, B., and Herzog, M. (1989). Dinoflagellates in evolution. A molecular phylogenetic analysis of large subunit ribosomal RNA. *J Mol Evol* 29, 40–51.

Lepere, C., Demura, M., Kawachi, M., Romac, S., Probert, I., and Vaulot, D. (2011). Whole-genome amplification (WGA) of marine photosynthetic eukaryote populations. *FEMS Microbiol. Ecol.* 76, 513–523. doi:10.1111/j.1574-6941.2011.01072.x.

Lõpez-Bueno, A., Rastrojo, A., Peirõ, R., Arenas, M., and Alcamí, A. (2015). Ecological

connectivity shapes quasispecies structure of RNA viruses in an Antarctic lake. *Mol. Ecol.* 24, 4812–4825. doi:10.1111/mec.13321.

Malviya, S., Scalco, E., Audic, S., Vincent, F., Veluchamy, A., Poulain, J., *et al.* (2016). Insights into global diatom distribution and diversity in the world's ocean. *Proc. Natl. Acad. Sci.* 113, 1516–1525. doi:10.1073/pnas.1509523113.

Mann, D. G., and Droop, S. J. M. (1996). 3 . Biodiversity , biogeography and conservation of diatoms. *Hydrobiologia* 336, 19–32.

Miranda, J. A., Culley, A. I., Schvarcz, C. R., and Steward, G. F. (2016). RNA viruses as major contributors to Antarctic virioplankton. *Environ. Microbiol.* 00. doi:10.1111/1462-2920.13291.

Nagasaki, K., Tomaru, Y., Katanozaka, N., Shirai, Y., Nishida, K., Itakura, S., *et al.* (2004). Isolation and characterization of a novel single-stranded RNA virus infecting the bloom-forming diatom *Rhizosolenia setigera*. *Appl. Environ. Microbiol.* 70, 704–711. doi:10.1128/AEM.70.2.704.

Nelson, D. M., Tréguer, P., Brzezinski, M. A., Leynaert, A., and Quéguiner, B. (1995). Production and dissolution of biogenic silica in the ocean: Revised global estimates, comparison with regional data and relationship to biogenic sedimentation. *Global Biogeochem. Cycles* 9, 359–372. doi:10.1029/95GB01070.

Orsini, L., Sarno, D., Procaccini, G., Poletti, R., Dahlmann, J., and Montresor, M. (2002). Toxic *Pseudo-nitzschia multistriata* (Bacillariophyceae) from the Gulf of Naples: morphology, toxin analysis and phylogenetic relationships with other *Pseudo-nitzschia* species. *Eur. J. Phycol.* 37, 247–257. doi:10.1017/S0967026202003608.

Rosario, K., Nilsson, C., Lim, Y. W., Ruan, Y., and Breitbart, M. (2009). Metagenomic analysis of viruses in reclaimed water. *Environ. Microbiol.* 11, 2806–2820. doi:10.1111/j.1462-2920.2009.01964.x.

Sarno, D., Kooistra, W. H. C. F., Medlin, L. K., Percopo, I., and Zingone, A. (2005). Diversity in the genus *Skeletonema* (Bacillariophyceae). II. An assessment of the taxonomy of *S. costatum*-like species with the description of four new species. *J. Phycol.* 41, 151–176. doi:10.1111/j.1529-8817.2005.04067.x.

Sarthou, G., Timmermans, K. R., Blain, S., and Tréguer, P. (2005). Growth physiology and fate of diatoms in the ocean: A review. *J. Sea Res.* 53, 25–42. doi:10.1016/j.seares.2004.01.007.

Schlüter, M. H., Kraberg, A., and Wiltshire, K. H. (2012). Long-term changes in the seasonality of selected diatoms related to grazers and environmental conditions. *J. Sea Res.* 67, 91–97. doi:10.1016/j.seares.2011.11.001.

Scholz, B., Guillou, L., Marano, A. V., Neuhauser, S., Sullivan, B. K., Karsten, U., *et al.* (2015). Zoosporic parasites infecting marine diatoms – A black box that needs to be opened. *Fungal Ecol.* 19, 59–76. doi:10.1016/j.funeco.2015.09.002.

Shi, M., Lin, X. D., Tian, J. H., Chen, L. J., Chen, X., Li, C. X., *et al.* (2016). Redefining the invertebrate RNA virosphere. *Nature* 540, 539–543. doi:10.1038/nature20167.

Shirai, Y., Tomaru, Y., Takao, Y., Suzuki, H., Nagumo, T., and Nagasaki, K. (2008). Isolation and Characterization of a Single-Stranded RNA Virus Infecting the Marine Planktonic Diatom *Chaetoceros tenuissimus* Meunier. *Appl. Environ. Microbiol.* 74, 4022–4027. doi:10.1128/AEM.00509-08.

Smetacek, V. (1999). Diatoms and the ocean carbon cycle. *Protist* 150, 25–32. doi:10.1016/S1434-4610(99)70006-4.

Smetacek, V. S. (1985). Role of sinking in diatom life-history cycles: ecological, evolutionary

and geological significance. *Mar. Biol.* 84, 239–251. doi:10.1007/BF00392493.

Sommer, U., Adrian, R., De Senerpont Domis, L., Elser, J. J., Gaedke, U., Ibelings, B., *et al.* (2012). Beyond the Plankton Ecology Group (PEG) Model: Mechanisms Driving Plankton Succession. *Annu. Rev. Ecol. Evol. Syst.* 43, 429–448. doi:10.1146/annurev-ecolsys-110411-160251.

Suttle, C. A. (1993). "Enumeration and Isolation of Viruses," in *Handbook of Methods in Aquatic Microbial Ecology*, eds. P. F. Kemp, B. F. Sherr, E. B. Sherr, and J. J. Cole (Boca Raton: Lewis Publisher), 121–137.

Takano, H. (1981). New and rare diatoms from Japanese marine waters – VI. Three new species in Thalassiosiraceae. *Bull. Tokai Reg. Fish. Res. Lab.* 105, 34–43.

Tillmann, U., Hesse, K. J., and Tillmann, A. (1999). Large-scale parasitic infection of diatoms in the Northfrisian Wadden Sea. *J. Sea Res.* 42, 255–261. doi:10.1016/S1385-1101(99)00029-5.

Tomaru, Y., Fujii, N., Oda, S., Toyoda, K., and Nagasaki, K. (2011a). Dynamics of diatom viruses on the western coast of Japan. *Aquat. Microb. Ecol.* 63, 223–230. doi:10.3354/ame01496.

Tomaru, Y., Katanozaka, N., Nishida, K., Shirai, Y., Tarutani, K., Yamaguchi, M., *et al.* (2004). Isolation and characterization of two distinct types of HcRNAV , a single-stranded RNA virus infecting the bivalve-killing microalga *Heterocapsa circularisquama*. *Aquat. Microb. Ecol.* 34, 207–218. doi:10.3354/ame034207.

Tomaru, Y., Kimura, K., and Yamaguchi, H. (2014). Temperature alters algicidal activity of DNA and RNA viruses infecting *Chaetoceros tenuissimus*. *Aquat. Microb. Ecol.* 73, 171–183. doi:10.3354/ame01713.

Tomaru, Y., Shirai, Y., Suzuki, H., Nagumo, T., and Nagasaki, K. (2008). Isolation and characterization of a single-stranded DNA virus infecting the marine planktonic diatom *Chaetoceros debilis*. *Aquat. Microb. Ecol.* 50, 103–112. doi:doi: 10.3354/ame01170.

Tomaru, Y., Takao, Y., Suzuki, H., Nagumo, T., Koike, K., and Nagasaki, K. (2011b). Isolation and characterization of a single-stranded DNA virus infecting *Chaetoceros lorenzianus* Grunow. *Appl. Environ. Microbiol.* 77, 5285–5293. doi:10.1128/AEM.00202-11.

Tomaru, Y., Takao, Y., Suzuki, H., Nagumo, T., and Nagasaki, K. (2009). Isolation and characterization of a single-stranded RNA virus infecting the bloom-forming diatom *Chaetoceros socialis*. *Appl. Environ. Microbiol.* 75, 2375–2381. doi:10.1128/AEM.02580-08.

Tomaru, Y., Toyoda, K., and Kimura, K. (2015). Marine diatom viruses and their hosts: Resistance mechanisms and population dynamics. *Perspect. Phycol.* 2, 69–81. doi:10.1127/pip/2015/0023.

Tomaru, Y., Toyoda, K., and Kimura, K. (2018). Occurrence of the planktonic bloom-forming marine diatom *Chaetoceros tenuissimus* Meunier and its infectious viruses in western Japan. *Hydrobiologia* 805, 221–230. doi:10.1007/s10750-017-3306-0.

Tomaru, Y., Toyoda, K., Kimura, K., Takao, Y., Sakurada, K., Nakayama, N., *et al.* (2013a). Isolation and characterization of a single-stranded RNA virus that infects the marine planktonic diatom *Chaetoceros* sp. (SS08-C03). *Phycol. Res.* 61, 27–36. doi:10.1111/j.1440-1835.2012.00670.x.

Tomaru, Y., Toyoda, K., Suzuki, H., Nagumo, T., Kimura, K., and Takao, Y. (2013b). New single-stranded DNA virus with a unique genomic structure that infects marine diatom *Chaetoceros setoensis*. *Sci. Rep.* 3, 3337. doi:10.1038/srep03337.

Toyoda, K., Kimura, K., Hata, N., Nakayama, N., Nagasaki, K., and Tomaru, Y. (2012). Isolation and characterization of a single-stranded DNA virus infecting the marine planktonic

diatom *Chaetoceros* sp. (strain TG07-C28). *Plankt. Benthos Res.* 7, 20–28. doi:10.3800/pbr.7.20.

Vizcaíno, J. A., Csordas, A., Del-Toro, N., Dianes, J. A., Griss, J., Lavidas, I., *et al.* (2016). 2016 update of the PRIDE database and its related tools. *Nucleic Acids Res.* 44, D447–D456. doi:10.1093/nar/gkv1145.

Wafar, M. V. M., Le Corre, P., and Birrien, J. L. (1983). Nutrients and primary production in permanently well-mixed temperate coastal waters. *Estuar. Coast. Shelf Sci.* 17, 431–446. doi:10.1016/0272-7714(83)90128-2.

Wiltshire, K. H., Kraberg, A., Bartsch, I., Boersma, M., Franke, H.-D., Freund, J., *et al.* (2010). Helgoland Roads, North Sea: 45 Years of Change. *Estuaries and Coasts* 33, 295–310. doi:10.1007/s12237-009-9228-y.

Supplementary:

Note: Tables S1 and S2 are too large to be included in this manuscript

```
                1         10         20         30         40         50         60
                |         |          |          |          |          |          |
GdelRNAV-01     CATCAATGCTGCTTTTGCCGCTTTAATAGAAATTGCGGAAAAATGTGGCAGATATACCAA
GdelRNAV-02     CATCAATGCTGCTTTTGCCGCTTTAATAGAAATTGCGGAAAAATGTGGCAGATATACCAA
GdelRNAV-03     CATCAATGCTGCTTTTGCCGCTTTAATAGAAATTGCGGAAAAATGTGGCAGATATACCAA
GdelRNAV-04     CATCAATGCCGCTTTTGCCGCTTTAATAGAAATTGCGGAAAAATGTGGCAGATATACCAA

GdelRNAV-01     TGATGATCTTACGATTATGAGAGGTATTGCAACAGAAATTGCTTATTCATGCGTAGCTTA
GdelRNAV-02     TGATGATCTTACGATTATGAGAGGTATTGCAACAGAAATTGCTTATTCATGCGTAGCTTA
GdelRNAV-03     TGATGATCTTACGATTATGAGAGGTATTGCAACAGAAATTGCTTATTCATGCGTAGCTTA
GdelRNAV-04     TGATGATCTTACGATTATGAGAGGTATTGCAACAGAAATTGCTTATTCATGCGTAGCTTA

GdelRNAV-01     TAATGGAGATATTATTATCCATAAAGGATCAAATCCATCAGGACAAAATTTAACGGTATA
GdelRNAV-02     TAATGGAGATATTATTATCCATAAAGGATCAAATCCATCAGGACAAAATTTAACGGTATA
GdelRNAV-03     TAATGGAGATATTATTATCCATAAAGGATCAAATCCATCAGGACAAAATTTAACGGTATA
GdelRNAV-04     TAATGGAGATATTATTATCCATAAAGGATCAAATCCATCAGGACAAAATTTAACGGTATA

GdelRNAV-01     TATTAACTGTCTCGTTAATTCTTTGCTATTAAGATGTGCATATTTTCACCTTTGGCCTAA
GdelRNAV-02     TATTAACTGTATCGTTAATTCTTTGCTATTAAGATGTGCATATTTTCACCTTTGGCCTAA
GdelRNAV-03     TATTAACTGTATCGTTAATTCTTTGCTATTAAGATGTGCATATTTTCACCTTTGGCCTAA
GdelRNAV-04     TATTAACTGTATCGTTAATTCTTTGCTATTAAGATGTGCATATTTTCACCTTTGGCCTAA

GdelRNAV-01     ACACCTAGGTCAGCCAAAACCTTTTCGTGAGGTTTGTGCTATTATGACTTATGGTGATGA
GdelRNAV-02     ACACCTAGGTCAGCCAAAACCTTTTCGTGAGGTTTGTGCTATTATGACTTATGGTGATGA
GdelRNAV-03     ACACCTAGGTCAGCCAAAACCTTTTCGTGAGGTTTGTGCTATTATGACTTATGGTGATGA
GdelRNAV-04     ACACCTAGGTCAGCCAAAACCTTTTCGTGAGGTTTGTGCTATTATGACTTATGGTGATGA

GdelRNAV-01     TGTTAAAGGTTCTGTAAAGGAAGGCTATGATTGGTTTAATCATATTTCATATGCTGATTT
GdelRNAV-02     TGTTAAAGGTTCTGTAAAGAAAGGCTATGATTGGTTTAATCATATTTCATATGCTGATTT
GdelRNAV-03     TGTTAAAGGTTCTGTAAAGGAAGGCTATGATTGGTTTAATCATATTTCATATGCTGATTT
GdelRNAV-04     TGTTAAAGGTTCTGTAAAGGAAGGCTATGATTGGTTTAATCATATTTCATATGCTGATTT

GdelRNAV-01     CTTAAGAGAACGTGATATGGTTTTTACTATGCCAGATAAAGAATCTGAACCTACCCCATA
GdelRNAV-02     CTTAAGAGAACGTGATATGGTTTTTACTATGCCAGATAAAGAATCTGAACCTACCCCATA
GdelRNAV-03     CTTAAGAGAACGTGATATGGTCTTTACTATGCCAGATAAAGAATCTGAACCTACCCCATA
GdelRNAV-04     CTTAAGAGAACGTGATATGGTTTTTACTATGCCAGATAAAGAATCTGAACCTACCCCATA

GdelRNAV-01     CATGAATGATCTCGAAGCTGATTTTTTGAAGCGTGAGAATATATTTAATGAGGATACT
GdelRNAV-02     CATGAATGATCTCGAAGCTGATTTTTTGAAGCGTGAGAATATATTTAATGAGGATACT
GdelRNAV-03     CATGAATGATCTCGAAGCTGATTTTTTGAAGCGTGAGAATATATTTAATGAGGATACT
GdelRNAV-04     CATGAATGATCTCGAAGCTGATTTTTTGAAGCGTGAGAATATATTTAATGAGGATACT
```

Figure S1. Nucleotide alignment of the partial sequences of the RNA-dependent RNA polymerase of GdelRNAV viruses. Differences between sequences are enclosed in a red frame. RdRp sequences were aligned using MAFFT on Geneious 9.1.3.

Table S3. Estimated percentages of permissive host cells during the infection kinetics. For each putative lytic cycle the number of permissive cells was calculated by dividing the number of viruses produced (maximum number of viruses minus number of viruses at the beginning of the lytic cycle) by the burst size (see material and methods for calculation of burst size). The % of permissive cells was calculated in relation to the abundance of diatom cells at the beginning of each lytic cycle.

Incubation time (hours) corresponding to the beginning of each putative lytic cycle	Permissive host cells (%)
0	3.3
48	2.8
72	12
108	69.4

CHAPTER II - *Aplanochytrium* sp., a novel eukaryotic parasite

Laure Arsenieff[1], Alexandre Epinoux[1], Sébastien Colin[2], Frédéric Mahé[3], Fabienne Rigaut-Jalabert[4], Hanna Dehmer[1], Martin Tournier[1], Marie Latimier[1], Anne-Claire Baudoux[1], Nathalie Simon[1]

[1]Sorbonne Université, CNRS, UMR 7144 - Diversity and Interactions in Oceanic Plankton, Station Biologique de Roscoff, 29860 Roscoff, France
[2]Sorbonne Université, CNRS, UMR 7144 - Evolution of Plankton and Pelagic Ecosystems, 29680 Roscoff, France
[3]CIRAD, UMR LSTM, 34000 Montpellier, France
[4]Sorbonne Université, CNRS, Fédération de Recherche FR2424, Station Biologique de Roscoff, 29680 Roscoff, France

Author contributions

Laure Arsenieff, Anne-Claire Baudoux, Nathalie Simon designed the study, conducted the samplings, the experiments and analyses. Alexandre Epinoux conducted the experiments and analyses. Sébastien Colin performed the confocal microscopy. Frédéric Mahé carried out the metabarcoding bioinformatics analyses. Fabienne Rigaut-Jalabert conducted the samplings and participated to the production of the metabarcoding data. Hanna Dehmer, Martin Tournier, Marie Latimier conducted preliminary characterization.

INTRODUCTION

Labyrinthulomycota, also designated as Labyrinthulomycetes, are marine heterotrophic protists that belong to Stramenopiles (Adl *et al.*, 2012). They are characterized by their rhizoid-like ectoplasmic nets, produced by an unusual membrane organelle, called the bothrosome (Iwata *et al.,* 2017; Perkins, 1973). This ectoplasmic network consists of cytoplasmic threads that provide adhesion to surfaces, and can be used for locomotion, or even to penetrate organic particles (Bennett *et al.*, 2017; Raghukumar, 2002). Two groups prevail among the Labyrinthulomycota: the thraustochytrids and the group composed of aplanochytrids and labyrinthulids. These organisms are differentiated based on the 18 rDNA gene and also according to the cell shape and the life cycle (Honda *et al.*, 1999; Leander *et al.*, 2004; Leander and Porter, 2001).

Members of Labyrinthulomycetes are ubiquitous in marine environments, from coastal to oceanic waters, from pelagic to benthic regions and from the surface to the deep sea (Bennett *et al.*, 2017; Bochdansky *et al.,* 2016; Collado-Mercado *et al.*, 2010; Perkins, 1973; Raghukumar, 2002; Ueda *et al.*, 2015). They have a wide biogeographic distribution, and occur in polar, tropical and temperate marine regions (Damare and Raghukumar, 2010; FioRito *et al.*, 2016; Mystikou *et al.*, 2014). Some specimens also occur in mangroves, freshwater and terrestrial habitats (Honda *et al.*, 1998; Takahashi *et al.*, 2014). Most Labyrinthulomycetes are osmotrophic or phagotrophic. They develop on a wide range of substrates such as marine plants and algae, and take part in diverse biotic associations (Bennett *et al.*, 2017; Raghukumar, 2002; Raghukumar and Damare, 2011). Most species are known for their saprotrophic lifestyle, feeding on dead and decaying organic matter but some are parasitic. For instance, *Labyrinthula zosterae* is a parasite that causes the "wasting disease" in the eelgrass *Zostera marina* (Muehlstein *et al.*, 1988). The aplanochytrid *Aplanochytrium haliotidis* is responsible for mortality of the juveniles of abalone (Bower, 1987a, 1987b). More recently, three species belonging to the aplanochytrid-labyrinthulid group (*Stellarchytrium dubum, Oblongichytrium porteri* and *A. blankum*) were isolated from sea stars exhibiting disease symptoms (FioRito *et al.*, 2016), suggesting a case of parasitism. Besides invertebrates and plants, some thraustochytrids were found attached to live or dead diatoms (Bennett *et al.*, 2017; Raghukumar, 1986, 2002; Takao *et al.*, 2015).

Although Labyrinthulomycetes are cosmopolitan and have the potential to cause massive mortalities on invertebrates and plants, their ecology and impacts on protists are largely unaddressed. Several studies have monitored their diversity, abundance and dynamics through diverse approaches in sediments, estuaries and coastal waters (Collado-Mercado *et al.*, 2010; Raghukumar and Damare, 2011; Ueda *et al.*, 2015), showing that carbon biomass during Labyrinthulomycetes development can overtake bacterial biomass. But to our knowledge, their direct interaction with the phytoplankton community is understudied. To date, their industrial use (Caamaño *et al.*, 2017; Marchan *et al.*, 2017) has more attention than their ecological influence in natural habitats. Indeed, thraustochytrids synthetize omega-3 polyunsaturated fatty acids (PUFAs) and docosahexaenoic acid (DHA) (Lewis *et al.*, 1999), which are molecules of great biotechnological interest (aquaculture and biofuels). These natural high lipid contents in thraustochytrids may also represent valuable food source for predators (Raghukumar, 2002; Raghukumar and Damare, 2011).

Here, we report on *Aplanochytrium* sp., a novel pathogen of diatoms. *Aplanochytrium* sp. A3 RA160614 was isolated from the marine diatom *Guinardia flaccida* from the SOMLIT-Astan long-term monitoring station. Using morphological observations and molecular data, we demonstrated that our isolate was related to the genus *Aplanochytrium* among the aplanochytrid-labyrinthulid clade. The life cycle of *Aplanochytrium* sp. A3 RA160614 slightly differs from the classic one with the formation of motile zoospores. This parasite may use the conspicuous ectoplasmic network to penetrate the host cell and transfer the nutritive resource to the main body. According to cross infection tests, this generalist parasite induced

the mortality of a broad range of phytoplankton taxa, which may explain its occurrence all the year at the SOMLIT-Astan station.

MATERIAL AND METHODS

Isolation of the *Aplanochytrium* strain

The *Aplanochytrium* strain A3 RA160614 was obtained in the context of a larger project that aimed at isolating parasites that infect diatoms in the Western English Channel between August 2015 and October 2016 (see Part I). Briefly, the sample from which this strain was isolated was collected on the June 14, 2016 at the SOMLIT-Astan time-series site (48:46:18 N, 3:58:6 W) at 1 m depth, using a 5 L Niskin bottle. Back in the laboratory, a subsample (3 L) was immediately pre-filtered through a 150 µm pore-size nylon filter to remove most of the micro- and mesozooplankton and 250 mL of this pre-filtered sample was enriched with F/2 medium (10% v/v) and 5 mL of culture of the diatom *G. flaccida* RCC3093. After two weeks of incubation, the enriched sample was gently filtered through a 3 µm polycarbonate membranes (Millipore Isopore and Whatman respectively). An Aliquot (0.5 mL) of the < 3 µm sample was inoculated into 1.5 mL exponentially growing host culture in 24-multiwell plates under the host culture conditions described below and 3 extinction dilution cycles were carried out to clone the pathogens (Suttle, 1993). For this purpose, 100 µL aliquots of the lysates were serially diluted in 10-fold increment in 900 µL of exponentially growing culture of *G. flaccida* RCC39093. Lysates in the last dilution before extinction were transferred to another exponentially growing culture of *G. flaccida* RCC3093.

Last, to estimate the size range of the infectious cells, fresh lysates were filtered through 5 µm, 3 µm, 1.2 µm, 0.45 µm and 0.2 µm pore size nuclepore filters and filtrates were inoculated to *G. flaccida* RCC3093 cultures. Hosts inoculated with unfiltered lysate and an untreated host served as positive and negative controls respectively.

Culture conditions

The *Aplanochytrium* strain A3 RA160614 was maintained by bimonthly transfer in fresh host culture (0.1 mL of fresh lysate in 10 mL of a healthy diatom culture). Because the *Guinardia flaccida* RCC3093 strain was lost during the year 2016, the parasite was transferred and maintained on *Guinardia delicatula* strain RCC3083 (Table II-1). Both *Guinardia* strains were isolated from coastal waters off Roscoff.

All the phytoplankton strains used in the frame of this study were provided by the Roscoff Culture Collection (RCC, http://roscoff-culture-collection.org/) and cultures were maintained in sterile condition in K+Si medium (Keller *et al.*, 1987) at 18°C, under a 12:12h light:dark cycle of 100 µmol photons.m^{-2}.s^{-1} provided by a white fluorescent light (Philips Master TL_D 18W/865).

Molecular and phylogenetic analyses

A fresh lysate containing *Aplanochytrium* strain A3 RA160614 was clarified through a 5 µm PVDF filter (Millex, Merck) in order to remove the remaining host cells. Pluronic F68 (final concentration 0.01%, Gibco) was added and cells were pelleted by centrifugation at 10 000 rpm for 10 min at RT. Nucleic acids were extracted using the Kit MasterPure complete DNA & RNA purification (Epicentre) according to the manufacturer's instructions.

Genomic DNA was amplified by PCR using the universal eukaryote primers 63F (ACGCTTGTCTCAAAGATTA) and 1818R (ACGGAAACCTTGTTACGA) targeting the 18S rDNA gene (Lepere *et al.*, 2011). The reaction mixture (30 µL final volume) included: 1x Green GoTaq Flexi Buffer, 1.5 mM of $MgCl_2$ solution, 0.4 mM of dNTP, 0.3 µM of each primer, 0.25 U of GoTaq G2 Flexi (Promega) and 2.5 µL of extracted DNA. PCR amplifications were performed with the following conditions: an initial incubation step at 95°C for 5 min, followed by 39 cycles of denaturation at 95°C for 30 sec, annealing step for 30 sec at 52° and extension at 72°C for 1 min 30, followed by a final extension step at 72°C for 10 min. PCR products were sent to Macrogen Europe (Amsterdam, The Netherlands) for Sanger Sequencing using the 1818R and 63F and internal primers S30F (CGCGGTAATTCCAGTCYA) and S69R (ACCAGACTTGCCCTCC).

Best sequence matches were searched in GenBank using the BLASTn tool (https://blast.ncbi.nlm.nih.gov/Blast.cgi). According to BLASTn searches, closest relatives and additional sequences from the literature were selected. 24 sequences, as well as outgroup sequences (*Thraustochytrium* and *Labyrinthula*) served to produce an alignment using MAFFT (version 7) and automatic alignment (the L-INS-i iterative refinement method was calculated for both genes) (https://mafft.cbrc.jp/alignment/server/, Katoh *et al.*, 2017). Ambiguously or poorly aligned regions were eliminated with Gbloks (Castresana, 2000) using the less stringent options (allowing smaller final blocks, gap positions within the final blocks and less strict flanking positions). A phylogenetic reconstruction was performed on the 1575 aligned nucleotides by maximum likelihood with PhyML 3.0 (http://www.atgc-montpellier.fr/phyml/, Guindon *et al.,* 2010) with the automatic model selection by SMS (Lefort *et al.*, 2017) and 100 00 bootstrap replicates. MEGA7 (Kumar *et al.*, 2016) was used to visualize the final tree.

Morphological characterization

In order to characterize the morphological features of *Aplanochytrium* sp. during the course of the infection, diatom cultures infected with *Aplanochytrium* sp. A3 RA160614 were monitored using inverted and confocal microscopes. Uninfected host cultures served as a controls.

Observations were first obtained after inoculation of *Aplanochytrium* sp. A3 RA160614 to an exponentially growing culture of *G. flaccida* (1% vol/vol). Infections were monitored using epifluorescence microscopy and confocal microscopy. For epifluorescence microscopy, aliquots of the control and infected cultures were sampled every day and were fixed with 0.5% glutaraldehyde. Cells were then stained with the nucleic acid dye Sybr Green I 50x (Final concentration 0.4%). 5% (vol/vol) Citifluor AF1 (antifading) were added. Stained samples were observed using an Olympus BX51 epifluorescence microscope (Olympus Corporation, Japan),

with a blue light excitation. Confocal imaging was used for a sample collected 5 days after inoculation. 1 mL of live sample was stained with 1.5 µM of DioC6 (D273, Molecular Probes Invitrogen) and 10 µM of Hoechst 33342 (H21492, Molecular Probes Invitrogen). DiocC6 (Ex488nm/Em500-530nm) targets active membranes and Hoechst (Ex405nm/Em415-475nm) stains DNA. Autofluorescence of chlorophyll *a* (Ex405nm/em670-720nm) was also recorded. Observations were performed using an inverted SP8 laser scanning confocal microscope (Leica Microsystem, Germany).

A second batch of confocal images was produced for culture of *G. delicatula* infected with *Aplanochytrium* sp. A3 RA160614. For this purpose, 40 mL of *G. delicatula* RCC3083 was inoculated with 1% vol/vol *Aplanochytrium* sp. A3 RA160614. Again, an uninfected host culture was kept as negative control. Every 24 hours for 8 days, aliquots of 1 mL were sampled and they were transferred into a 4 wells Lab Tek II chambered cover glass (Nunc 155382; Thermo Fisher Scientific, MA, USA) with well bottom coated with poly-L-lysine (Sigma). Live samples were stained with 0.32 µM DioC6, 5.68 µM Hoechst 33342 and with 0.5 $\mu g.\mu L^{-1}$ Nile Red (working solution: 0.1 $mg.mL^{-1}$ in acetone, ref.72485, Sigma Aldrich, Ex515–530nm/Em525–605nm) which has high affinities with lipids. Observations were performed using the same confocal microscope equipped with a compact supply unit which integrates a LIAchroic scan head and several laser lines (405 nm, 488 nm, 552 nm, 638 nm), and 4fluo+1trans photomultiplier tube detectors. Details of the procedure are described in Colin *et al.* (2017). Unfortunately, the 3D pictures produced could not be analyzed due to of lack of time.

Cross infections experiment

To study the host range, *Aplanochytrium* strain A3 RA160614 was added to 19 phytoplanktonic hosts, including 14 diatom strains (Table II-1). Most of the tested strains originated from sea surface water collected off Roscoff. Untreated phytoplankton cultures served as controls. Algal growth and lysis were monitored after 7 and 14 days post-inoculation (dpi) under light microscopy. As complete algal cell death can be arduous to ascertain, chlorophyll *a* fluorescence intensity was measured simultaneously, with an excitation wavelength at 430 nm and an emission wavelength at 670 using a microplate reader (Spark, Tecan, Männedorf, Switzerland). After two weeks incubation, lysis were considered effective when the host fluorescence intensity was lower than 50% to that of the uninfected control. The experiment has been carried out in triplicate.

Temporal dynamics

To study the seasonal variations of the pathogen and its *Guinardia* hosts, OTUs with a V4-18S rDNA gene sequence 100% similar to that of respectively *Aplanochytrium* strain A3 RA160614, *G. delicatula* strains RCC3083 and of *G. flaccida* RCC3093 were retrieved from the SOMLIT-Astan metabarcoding dataset using the BLASTn tool on Geneious 9.1.3. As explained in the Part I of this thesis, this dataset corresponds to a contingency table of 31 167 OTUs for which read abundances have been obtained bimonthly for two size fractions over the 2009-

2016 period. For this study, OTUs from the >3 µm fraction and with total cumulated abundance higher than 10 reads were selected (8 788 OTUs). Metabarcoding data corresponding to 25 sampling dates were deleted from the dataset (total number of reads very low compared to that of other dates). Most of these dates corresponded to a period between 2014 and 2015.

Cryopreservation

Aplanochytrium strain A3 RA160614 was tested for cryopreservation following the RCC procedure. Briefly, 10% DMSO (final concentration) were added to 1 mL of culture in a cryogenic tube. The culture was progressively frozen with an incubation at 20°C, a decrease of temperature of 1°C per minute until -40°C, which was maintained for 10 min. Sample was transferred to liquid nitrogen before storage at -150°C for one month. After this period of time, the culture was thawed in a 25°C water bath for 3 min and was transferred to 20 mL of fresh culture of *G. delicatula* RCC3083. Cell lysis was monitored for two weeks by optical microscopy (Day and Brand, 2005; Roscoff Culture Collection http://roscoff-culture-collection.org/protocols/cryopreservation).

Accession numbers

SSU sequence of *Aplanochytrium* strain A3 RA160614 will be deposited in the NCBI database.

RESULTS

Impact of *Aplanochytrium* sp. strain A3 RA160614 on the host used for isolation and size range of infectious cells

Complete clearance of *Guinardia flaccida* RCC3093 strain was observed within 3-4 days after inoculation of the lysate maintained on the same strain. Filtrates of this lysate had the same effect on the diatom strain for pore size filters above 1.2 µm (Figure II-1).

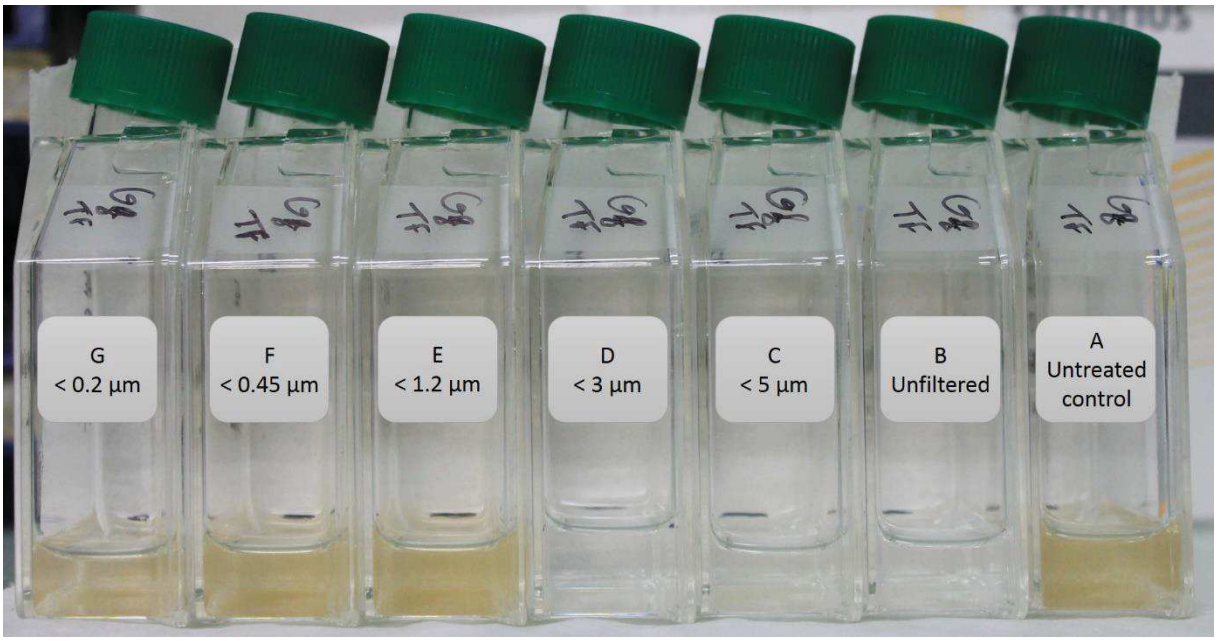

Figure II-1. Determination of size range of Aplanochytrium *sp. A3 RA160614. From right to left: (A) healthy and untreated control* Guinardia flaccida *RCC3093, (B) infected* G. flaccida *RCC3093 culture by* Aplanochytrium *sp. A3 RA160614. (C-G)* Aplanochytrium *sp. A3 RA160614 culture filtered through 5 µm (C), 3 µm (D), 1.2 µm (E), 0.45 µm (F) and 0.2 µm (G) and inoculated to* Guinardia flaccida *RCC3093*

Phylogenetic affiliation of the isolated algicidal strain

A preliminary ML phylogenetic analysis based on the 18S rDNA showed that all *Aplanochytrium* strains clustered together (Figure II-2), although the bootstrap value was rather low (below 80%). Also, relationships among aplanochytrid strains chosen were poorly resolved. The sequence of *Aplanochytrium* sp. strain A3 RA160614 was 100% identical to that of *Aplanochytrium* sp. strain SEK717 (1 650 aligned nucleotides), its closest relative, isolated from Japanese coastal sea surface waters (Ueda *et al.*, 2015).

Other strains used for sequence comparisons were also found living in association with diverse organisms. *A. stocchinoi* and *Aplanochytrium* sp. strains ANT10.3, PR1-1 and PR12-3 were isolated from the surface of macroalgae and seagrasses (Moro *et al.*, 2003; Mystikou *et al.*, 2014), *Aplanochytrium* sp. strains S1961, S19610 and S2122 to S2129 were isolated from zooplankton samples (Damare and Raghukumar, 2010) and *A. blankum* originated from dermal tissue of sea stars (FioRito *et al.*, 2016). Interestingly, seagrasses-associated *Aplanochytrium* sp. strains PR15-1, PR24-1 and SC24-1 (Leander *et al.*, 2004) grouped together with high bootstrap support (98%).

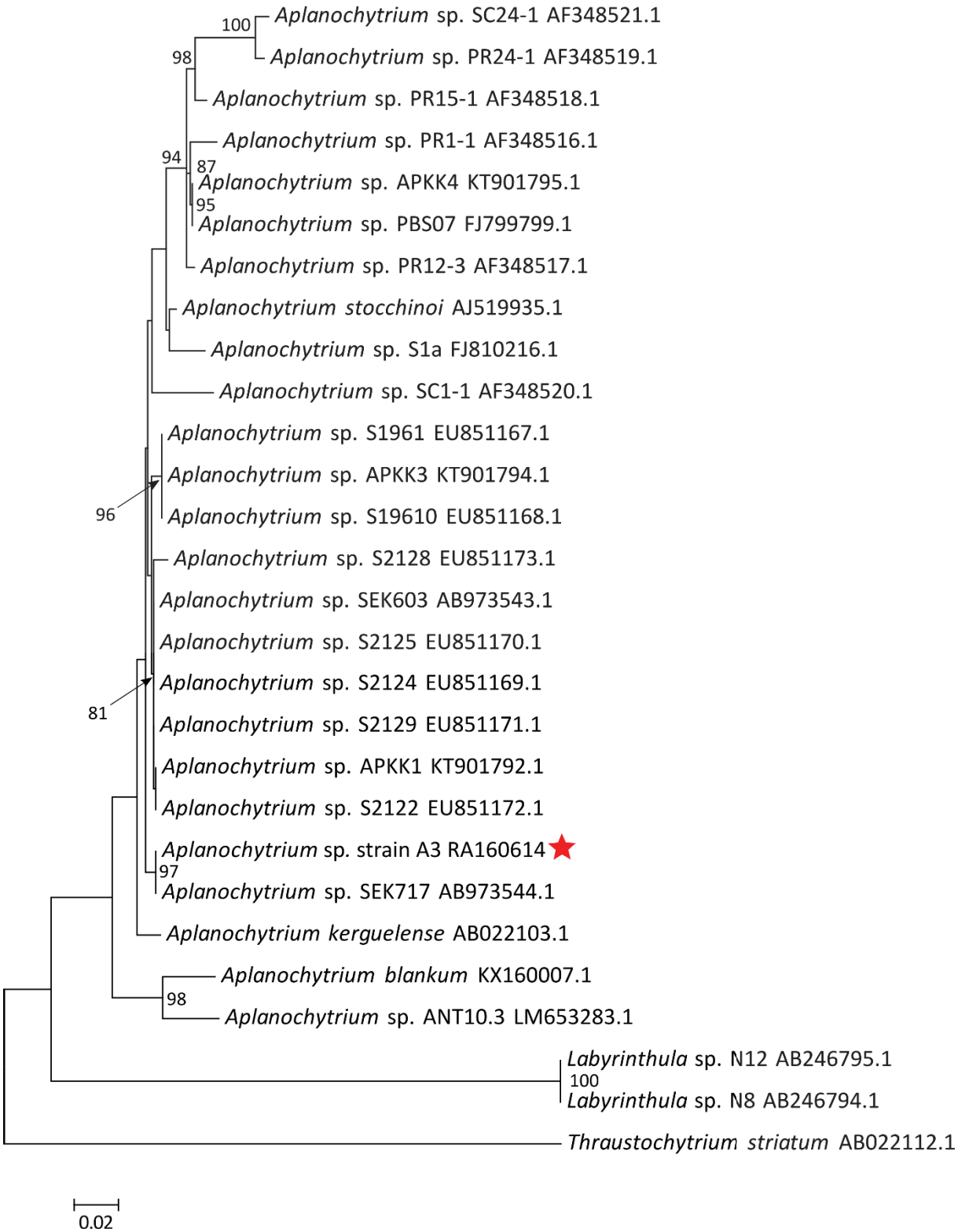

Figure II-2. Phylogenetic tree inferred from the alignment of 18S rDNA gene sequences (1575 positions). Thraustochytrium striatum served as outgroup. The red star indicates the position of Aplanochytrium *sp. A3 RA160614. The ML tree was generated using PhyML 3.0 with 10 000 replications and a TN93+G+I substitution model. Bootstraps values (%) greater than 80 are shown. Scale bar indicates the number of substitutions per site*

Morphological features of *Aplanochytrium* sp. A3 RA160614

Microscopic observations of infected *G. flaccida* strain RCC3093 and *G. delicatula* strain RCC3083 cultures revealed several types of cells that most probably corresponded to different stages of the life cycle of this *Aplanochytrium* species.

- First, biflagellate free-living motile cells, referred to as “zoospore”, with a size between 3.5 µm and 4.5 µm (3 individuals measured) (Figure II-3). Zoospores were visualized once the lysis of *G. flaccida* was totally effective, swimming fast among the frustule detritus.

- A second non-flagellated stage was observed in contact with host cells (Figure II-4, A and B). The corresponding cell appeared spherical (mean cell diameter 4.3 µm, for 100 cells measured) and staining with Sybr Green I revealed only one nucleus per cell. These cells were preferentially attached to the girdle region or to the extremities of the valves of *G. flaccida* and *G. delicatula.*

- A third stage attached to the diatom frustule corresponded to a spherical structure composed of several cells, the “sporangium” (8- 12 µm in diameter, 3 individuals measured) (Figure II-4, C and D).

Figure II-3. Biflagellate zoospore of Aplanochytrium *sp. A3 RA160614 observed under light microscopy (LM). Arrows point out the flagella*

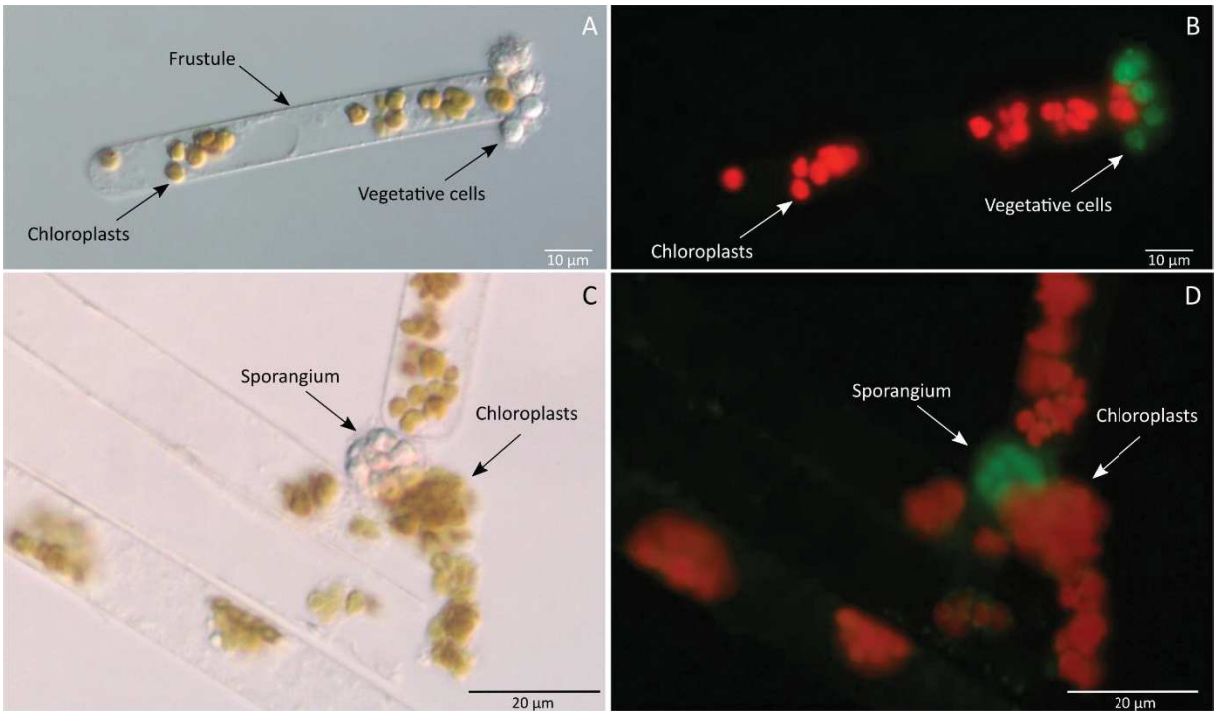

Figure II-4. Life stages of Aplanochytrium *sp. A3 RA160614 in LM (**A** and **C**), and in epifluorescence microscopy after staining with Sybr Green I (**B** and **D**). (**A, B**) Vegetative cells attached to the extremity of* G. flaccida *frustule. (**C, D**) Sporangium stage. In green: nuclei of* Aplanochytrium *sp.. In red: autofluorescence of chloroplasts*

The confocal microscopic observations using a set of dyes allowed to describe in more details the structure of the parasite. The membrane specific fluorochrome Dioc6 highlighted an impressive ectoplasmic network that emerged from fixed vegetative cells or sporangia (Figure II-5, A, B and C). This ramified structure was widely spread around the host cell and penetrated into the frustule (data not shown). The sporangium contained many nuclei usually in even number (from 4 to 12 observed, or more, according the infection progress) (Figure II-6, A and C). Staining with DioC6 also revealed small structures within the sporangium (Figure II-5, D, Figure II-6, B) and in vegetative cells (Figure II-5, D). These structures were also stained by Nile Red, suggesting that they contained lipid droplets (data not shown).

Observations carried out under the microscope also showed important structural rearrangement in host cell upon infection. The host nucleus was the first component to be destroyed during the infection process, as shown in Figure II-4 A and B, and Figure II-5, A and B. Often, we could observed the vegetative cells attached in the frustule close to the region of the nucleus. Also, chloroplasts of infected cells became rounded and disorganized and were located in the vicinity of the parasite's fixation site during the late infection stages (Figure II-5, B, C and D). Infections of a single diatom cell by several vegetative cells or sporangia were also observed (Figure II-4 A, Figure II-5 D). Analysis of pictures obtained from the second batch of infection experiments will help to clarify the different steps of the life cycle of *Aplanochytrium* sp. A3 RA160614.

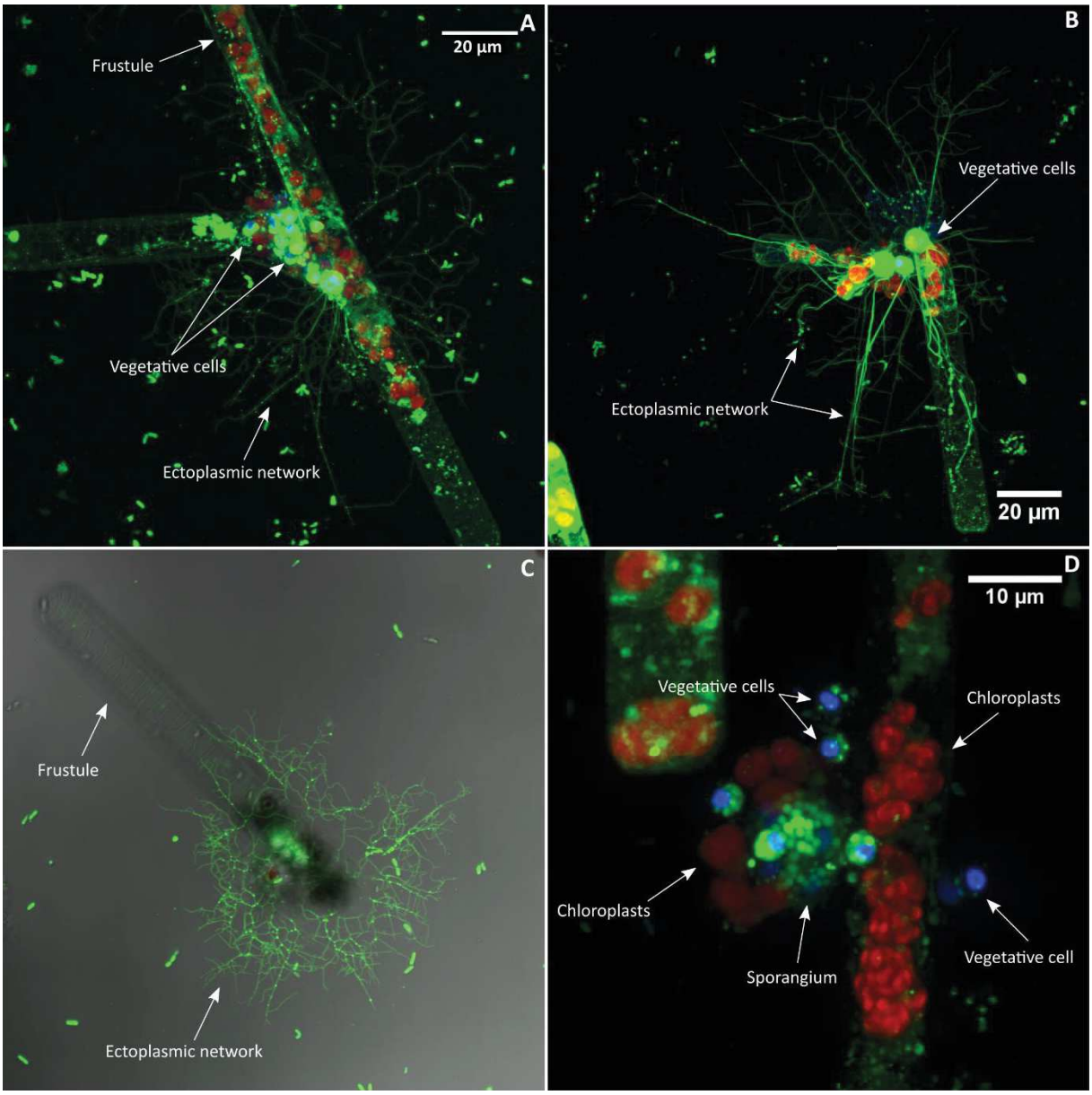

Figure II-5. Life stages of Aplanochytrium *sp. A3 RA160614 obtained in 3 dimensions.* ***A, B*** *and* ***C****. The parasite develops an ectoplasmic network (stained with the DioC6) from the vegetative cells attached to the dead cells of* G. flaccida*. Micrographs obtained with the confocal microscopy.* ***D****. Sporangium stage. In green: membrane structures labeled with DioC6. In blue: Hoechst-labeled nucleic acids. In red: autofluorescence of chloroplasts. Scale for picture* ***C*** *not available*

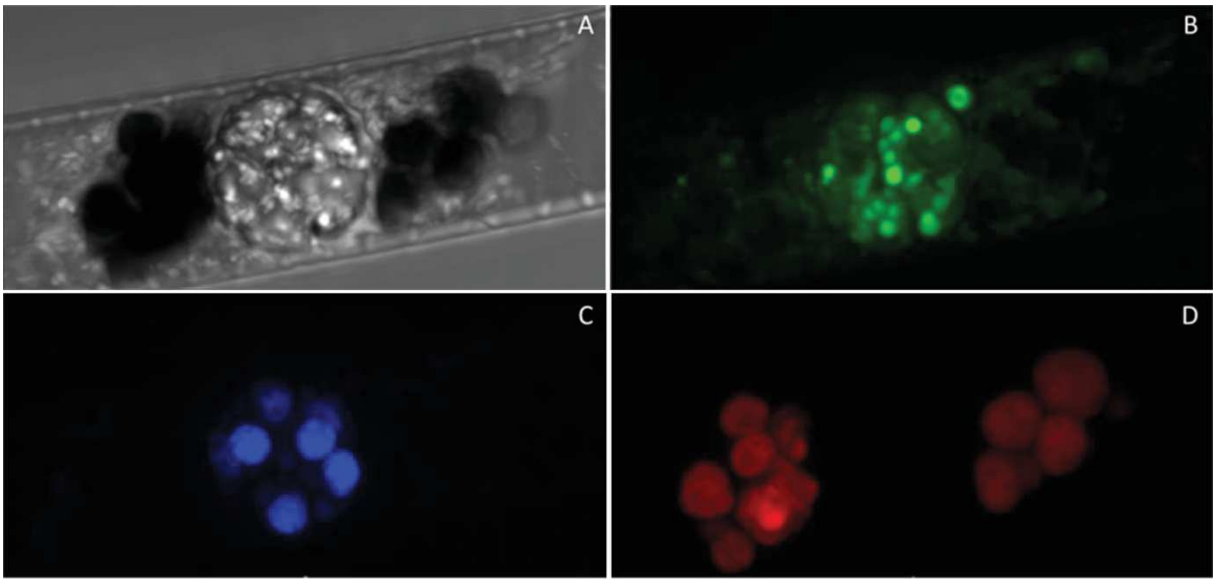

Figure II-6. Sporangium of Aplanochytrium *sp. A3 RA160614 inside or on the frustule of* G. flaccida *observed in confocal microscopy.* ***A****. Sporangium containing many cells, LM,* ***B****. Membrane structures labeled with DioC6 (green fluorescence).* ***C****. Hoechst-labeled nucleic acids (blue fluorescence).* ***D****. Autofluorescence of* G. flaccida *chloroplasts*

Host specificity

Fourteen phytoplankton strains out of the 19 tested, representing in total 18 species, were lysed by *Aplanochytrium* sp. A3 RA160614 (Table II-1). This parasite was able to kill the three species of the genus *Guinardia* and also all other diatom species except *Skeletonema costatum.* Indeed, despite the use of two methods (microscopy and fluorescence intensity measurement), infectious effect on *S. costatum* was no clear. The two strains were not lysed by *Aplanochytrium* sp. A3 RA160614 but displayed slight modifications in their cell chain morphologies. Besides diatoms, *Aplanochytrium* sp. A3 RA160614 was responsible for cell mortality of *Micromonas pusilla* and *Ostreococcus lucimarinus*, two picoeukaryote species. *Heterocapsa* sp. (dinoflagellate) and *Heterosigma akashiwo* (raphidophyte), which were not isolated from waters off Roscoff, were not susceptible to this pathogen.

Table II-1. Host range of Aplanochytrium *sp. A3 RA160614. Cell lysis were recorded after 14 days under light microscopy and by spectrophotometer measuring the host fluorescence intensity. EC: English Channel, NA: not applicable, ND: Not determined, +: Lysis, -: No lysis*

Phylum	Class	Species	Strain code	Origin of isolation	Date of isolation	Lysis by *Aplanochytrium* sp.
Bacillariophyta	Coscinodiscophyceae	*Guinardia delicatula*	RCC3083	Roscoff Estacade, EC	19/09/2012	+
		Guinardia flaccida	RCC5791	Roscoff-Astan, EC	02/02/2017	+
		Guinardia striata	RCC5792	Roscoff-Astan, EC	09/09/2016	+
	Mediophyceae	*Chaetoceros peruvianus*	RCC2023	Roscoff-Astan, EC	01/09/2010	+
		Conticribra weissflogii	RCC3389	North Sea	10/09/2012	+
		Minidiscus comicus	RCC4660	Roscoff-Astan, EC	26/05/2015	+
		Minidiscus variabilis	RCC4657	Roscoff-Astan, EC	26/05/2015	+
		Skeletonema costatum	RCC75	Caen	NA	-[a]
		Skeletonema costatum	RCC1716	Roscoff-Astan, EC	13/05/2008	-[b]
		Thalassiosira curviseriata	RCC5154	Roscoff-Astan, EC	26/05/2015	+
		Thalassiosira profunda	RCC4663	Roscoff-Astan, EC	26/05/2015	+
		Thalassiosira punctigera	RCC4667	Roscoff-Astan, EC	21/10/2015	+
	Bacillariophyceae	*Cylindrotheca closterium*	RCC1713	Roscoff-Astan, EC	13/05/2008	+
		Nitzschia sp.	RCC80	Roscoff Estacade, EC	01/06/1997	+
Miozoa	Dinophyceae	*Heterocapsa sp.*	RCC5157	Bay of Biscay	26/07/2016	-
Haptophyta	Prymnesiophyceae	*Phaeocystis* sp.	RCC1719	Roscoff-Astan, EC	13/05/2008	ND
Chlorophyta	Mamiellophyceae	*Micromonas pusilla*	RCC465	Roscoff-Astan, EC	13/06/2001	+
		Ostreococcus lucimarinus	RCC756	Roscoff Dourduff	13/06/2001	+
Heterokontophyta	Raphidophyceae	*Heterosigma akashiwo*	RCC1502	La Rochelle	NA	-

[a]: No significant loss of fluorescence intensity (as measured using the microplate reader) in infected cultures but broken cell chains were observed in microscopy compared to the control

[b]: 43% of fluorescence intensity loss in infected cultures after 14 days. Broken cell chains were observed in microscopy compared to the control

Temporal dynamics

Among the 8 788 OTUs identified in the metabarcoding dataset, three OTUs had 100% sequence identity with the V4 sequences of *G. delicatula* RCC3083, *G. flaccida* RCC3093 and *Aplanochytrium* sp. A3 RA160614 respectively.

Aplanochytrium sp. exhibited rather low read abundances in the water column all year round (relative abundance always lower than 800 reads and with 0.04% of contribution to total read counts). No clear recurrent seasonal pattern of development could be deduced from analyses of the metabarcoding data. Also the peaks of read abundances did not generally match with that of *Guinardia* spp. (Figure II-7), for which blooms are observed in May, July and August-September at this station (Figure II-7 and Guilloux *et al.* (2013)). In 2009, 2013, 2014, 2015 and 2016, peaks of read abundances occurred in winter, outside the period of blooms of *Guinardia* (as indicated by the variations in abundance of reads for OTUs corresponding to both *G. delicatula* and *flaccida*). However, summer peaks were also detected in 2010 and 2011 along with blooms of *G. delicatula* and *G. flaccida*. In 2015 and 2016, relative abundances of the OTU related to the aplanochytrid peaked after the proliferation of *Guinardia* (November 2015, end of September 2016).

Interestingly, during the sampling period (October 2015-October 2016), the *Aplanochytrium* sp. A3 RA160614 strain was isolated from a sample collected in June 2016, which corresponds to the season of the lowest relative abundance of the OTU related to this strain. Conversely, strains of *Aplanochytrium* were not isolated in winter 2015, when OTU read abundances were the highest.

Cryopreservation

Aplanochytrium sp. A3 RA1606014 culture was stored for one month at -150°C with 10% DMSO as cryoprotectant. After thawing out, this pathogen was able to induce *G. delicatula* mortality in less than 2 weeks, meaning that long-term preservation of this organism is possible without maintenance and transfer in fresh host culture.

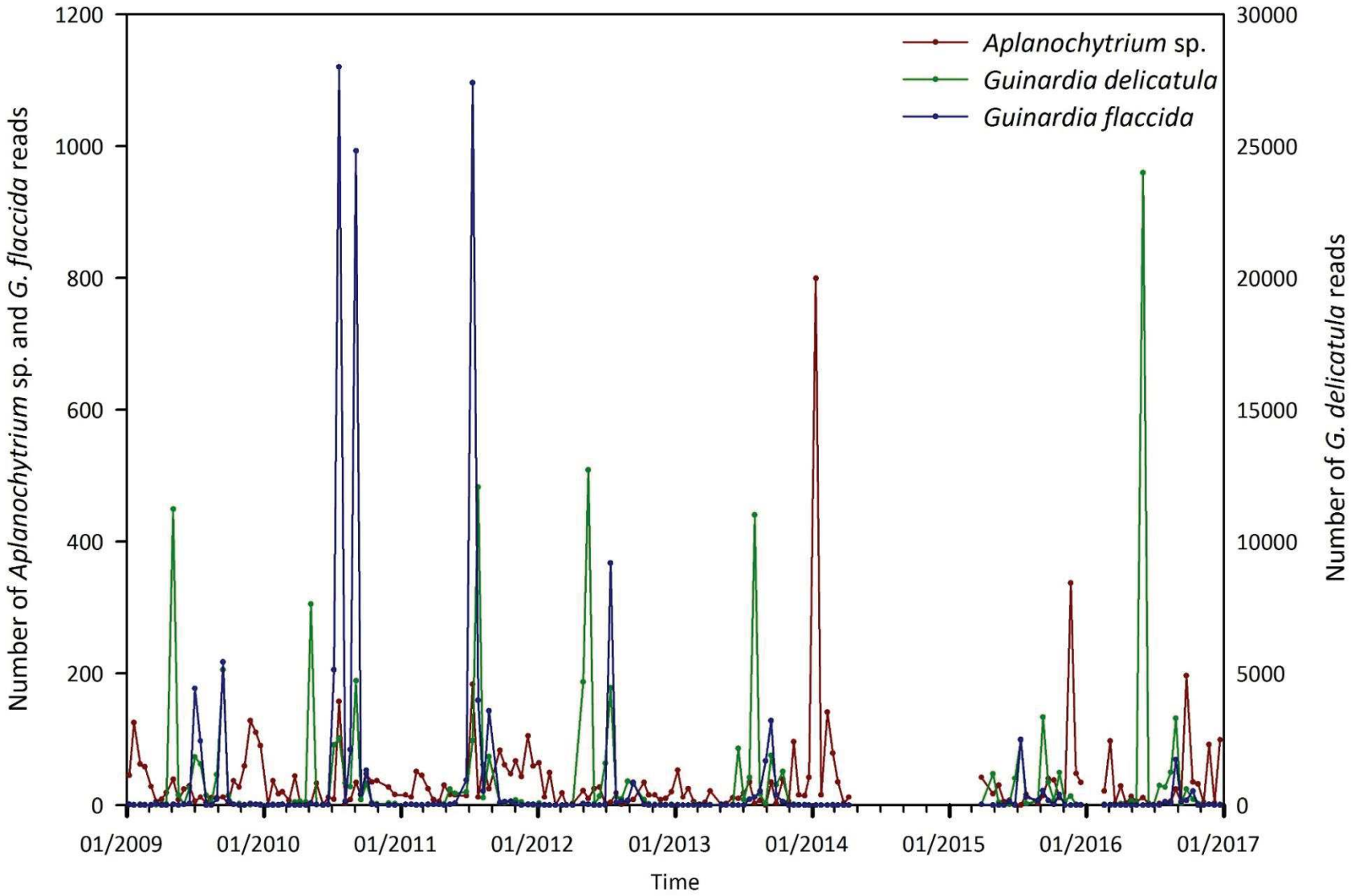

Figure II-7. Temporal dynamics of the OTUs related to Aplanochytrium *sp. (red line),* G. delicatula *(green line) and* G. flaccida *(blue line) at the SOMLIT-Astan station during the period 2009-2016. Note that metabarcoding data corresponding to 25 sampling dates (mainly between 2014 and 2015) were deleted from the dataset*

DISCUSSION

In this study, we report on an aplanochytrid strain that was isolated and maintained on cultures of the diatom *Guinardia*. This *Aplanochytrium* sp. isolate displayed strong algicidal effects on *Guinardia* species. Its preliminary life cycle was studied using confocal imaging which allowed us to unveil a conspicuous ectoplasmic network which may operate during the infection process. Metabarcoding data obtained from samples collected at the SOMLIT-Astan time-series station during the period 2009-2016 years suggested large seasonal and interannual variations in abundances of this aplanochytrid. Peaks in read abundances of this species do not seem to be systematically occurring during *Guinardia* summer blooms. These seasonal patterns raise interesting questions about the putative hosts of this parasite in the natural habitat and its implication in the regulation of their populations.

Characterization of *Aplanochytrium* sp. A3 RA160614, a novel species?

Our algicidal strain clearly shows genetic and morphological features that are characteristic of the genus *Aplanochytrium*. It also shows peculiarities and may represent a new species for the genus *Aplanochytrium*.

Within the Labyrinthulomycota, the aplanochytrids (that currently contain the single genus *Aplanochytrium*) are characterized by the formation of crawling spores, called also aplanospores. These structures refer to non-flagellate spores which are able to glide on substrate via an ectoplasmic net, that does not completely enrobe the cell in the genus *Aplanochytrium* (Leander *et al.*, 2004; Leander and Porter, 2001). Some species, namely *A. yorkensis*, *A. minuta*, *A. haliotidis* and *A. thaisii* are also able to produce biflagellate spores (only in the commensal host tissue and not on agar medium for *A. thaisii*, according to Cox and Mackin (1974)), a particularity originally described as a distinctive feature of thraustochytrids. Like these later species, our strain was apparently able to produce these two cell types. However, we were not able to observe the crawling movement of aplanospores. Observation of such movements may require a transfer of the cells from liquid seawater medium to solid medium. Indeed, *Aplanochytrium* species are generally described based on observations recorded for cells cultured on agar medium. In fact, *Aplanochytrium*, and more generally Labyrinthulomycetes possess plastic features which can be modified depending on the medium substrate or the growth conditions (Damare and Raghukumar, 2006; Doi and Honda, 2017; Leander *et al.*, 2004), which complicates comparative studies.

Comparisons of the 18S rDNA sequence of our isolate with references retrieved from public databases confirmed its position in the *Aplanochytrium* radiation. According to the BLATSn searches conducted against the non-environmental sequences of the NCBI, and according to the phylogenetic analyses, our isolate is most closely related to *Aplanochytrium* sp. strain SEK717 (which morphological description is not provided) isolated from the water column in Japanese coastal waters (Ueda *et al.*, 2015). The 18S rDNA gene of these two strains was identical, suggesting that they belong to the same species. But more detailed studies of intraspecific and interspecific genetic variations are needed to support such a conclusion.

More generally, in order to progress on the phylogenetic position of this strain within the *Aplanochytrium* clade, and on its taxonomic status, more detailed morphogenetic analyses of described strains and species are needed. Indeed, the genus *Aplanochytrium* gathers nine species but the complete or partial 18S rDNA gene sequences of only six of these species (*A. blankum, A. haliotidis, A. kerguelense, A. minuta, A. stocchinoi* and *A. yorkensis*) are available in public databases. The production of reference sequences (from species for which morphological and ecological features have been studied in depth) are also needed for a better description and understanding of the ecological importance of this group through the use of metagenomics data (Pan *et al.*, 2017).

Another argument in favor of the affiliation of our strain to a new species is its capacity to grow on live phytoplankton cells, a unique feature among aplanochytrids described to date. *Aplanochytrium* sp. A3 RA160614 was indeed isolated using a diatom host culture and was able to complete its life cycle very rapidly (a few days) when inoculated in live cultures of microalgae that belong to different phyla (diatoms, dinoflagellates and chlorophytes). Described aplanochytrids are most often associated to dead and decaying material, although some species are known to be pathogens of invertebrates and plants (Leander *et al.*, 2004). For example, *A. schizochytrops* (Quick, 1974) was responsible for brown patches on marine grass leaves, and *A. haliotidis* is responsible for important mortalities on abalone (Bower, 1987a).

Hypothetical parasitic lifecycle

Given the ability of *Aplanochytrium* sp. A3 RA160614 to grow on healthy diatom strains, causing their death within a few day, we suspect that this strain exhibits a parasitic rather than (or in addition to) a saprophytic behavior. Using 3D imaging technologies, we clearly demonstrated that our algicidal strain produces spherical cells and sporangia that are attached to diatoms, entailing their death.

The ectoplasmic filaments developed by *Aplanochytrium* sp. A3 RA160614 were observed both on the diatom frustule and within cells, suggesting a role of the cytoplasmic threads in the feeding process. Such penetration within substrate has mainly been observed for thraustochytrids (Raghukumar, 2002). In the literature, the ectoplasmic net of aplanochytrids is considered as a structure mainly involved in locomotion (Leander *et al.*, 2004). Penetration of the ectoplasmic net in the diatom cells may involve specific mechanisms such as the production of enzymes. Aplanochytrids and thraustochytrids are indeed able to produce extracellular enzymes, such as proteases or cellulases (Damare and Raghukumar, 2006; Nagano *et al.*, 2011) involved in the degradation and remineralization of organic matter in marine systems (Raghukumar, 2002; Raghukumar and Damare, 2011). We can hypothesize that the release of such enzymes is also involved in the parasitic strategy developed by *Aplanochytrium* sp. A3 RA160614. Production of such enzymes could also explain the generalist nature of *Aplanochytrium* sp. A3 RA160614, that infects a large range of phytoplankton taxa.

Our study also suggests that the dispersal of our *Aplanochytrium* strain is ensured by the liberation of biflagellate spores. As explained above, this strategy has been described mostly for thraustochytrids and for some *Aplanochytrium* species, in addition to crawling aplanospores. Overall, the life cycle of *Aplanochytrium* A3 RA160614 resembles that described for some thraustochytrid species such as *Monorhizochytrium globosum,* that develops on macroalgae (Doi and Honda, 2017). Based on it, we tried to reconstruct a hypothetical life cycle our parasitic *Aplanochytrium* strain A3 RA160614 (Figure II-8). We hypothesize that small biflagellate zoospore of *Aplanochytrium* sp. liberated from sporangia settles on diatom frustule and retracts or looses its flagella before developing an ectoplasmic network that penetrates the host cell. While feeding on diatom, the globose vegetative cells would divide by mitotic divisions, producing small cells enclosed in a sporangium. The production of flagellates would occur in sporangia (stage not observed in our case) and are released in the environment after rupture of the sporangium wall. After completion of the complete life cycle, only empty frustules of infected cells are remaining. Further experiments and observations using confocal microscopy are required to obtain details concerning the life cycle of this strain and in particular concerning the mechanisms by which the ectoplasmic network penetrates into diatom cells. It would also be interesting to study the strategies used by this strain to feed on other phytoplankton species.

Last, we were not able, in the frame of this thesis, to test other carbon sources and in particular dead cells. Labyrinthulomycota are known for their diverse ecological strategies, that include saprophytism, parasitism or even commensalism. In many cases, the exact relationships with their hosts are not always clear (Bennett *et al.*, 2017). For example, *A. haliotidis*, causing mortalities of abalone, is also able to survive in artificial media (Bower, 1987b). This species is thus considered as a facultative parasite. Similar results were found for *Stellarchytrium dubum*, *Oblongichytrium porteri*, and *A. blankum*, isolated during epidemics of sea stars, as they were able to grow on solid media (FioRito *et al.*, 2016). Determining the trophic strategy of these organisms and evaluating their fate and role in food webs is a relevant issue. In order to determine if *Aplanochytrium* sp. A3 RA1606014, isolated in this study, is a facultative parasite, we will attempt to cultivate it on solid medium designed for thraustochytrids such as Serum Seawater Agar medium containing horse serum (Leander *et al.*, 2004). If *Aplanochytrium* sp. A3 RA1606014 can grow and complete its life cycle on solid medium, we will consider that live organic matter is not mandatory to sustain the life cycle of this species and that it can switch from parasitic to saprophytic strategies.

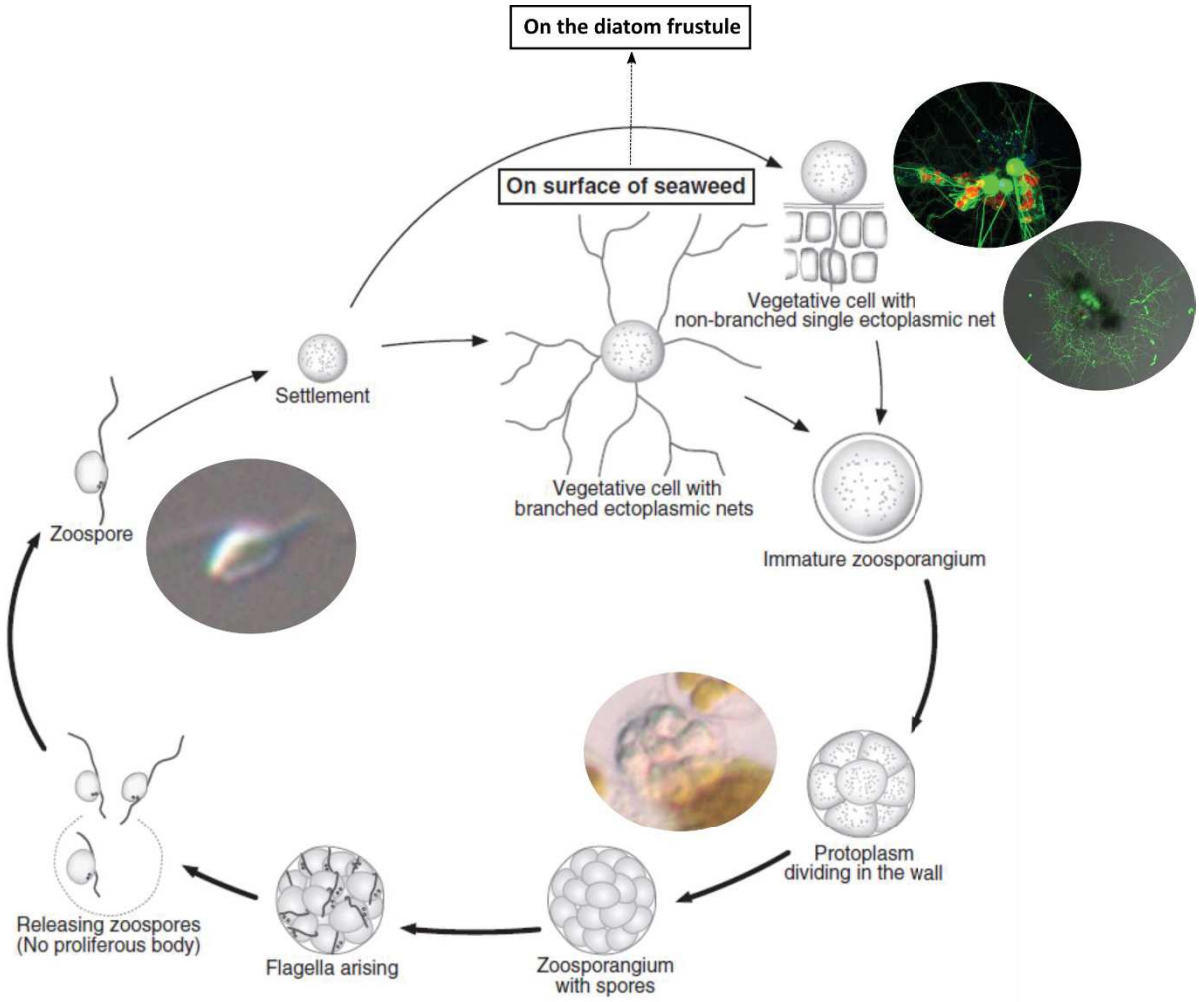

Figure II-8. Hypothetical lifecycle of Aplanochytrium *sp. A3 RA160614 associated to* Guinardia *sp. in liquid medium. The biflagellate zoospore settles and develops an ectoplasmic network. This network favors the encounter with a healthy host cell and is used to penetrate the host cell. While feeding on the diatom, the vegetative cell divides by mitotic divisions, producing small cells enclosed in a sporangium. Cells within the sporangium become flagellate (stage not observed) and are released in the environment. Adapted from the lifecycle of* Monorhizochytrium globosum, *a thraustochytrid which can grow on seaweed surface* (Doi and Honda, 2017)

Ecological role of the new *Aplanochytrium* sp. in the natural environment

Time-series offer a good opportunity to study variability of organisms in their natural habitats. Using the 8 years of molecular survey at the SOMLIT-Astan station we showed that sequences 100 % similar to that of *Aplanochytrium* sp. A3 RA160614 could be present in winter and/ or summer. These peaks did not always co-occur with blooms of *Guinardia*, the host used for parasite isolation. However, as *Aplanochytrium* sp. can attack a large range of phytoplankton species in culture, we posit that this parasite can shift from a host to another to support its growth all year round.

Abrupt decreases in *Aplanochytrium* sp. abundance could reflect crashes of host populations but also predation on this parasite. After Nile red staining, microscopic observations showed that immobile stages were rich in lipids. Like chytrid parasites, thraustochytrids are known for their PUFA production and their importance as nutritive

resource for predators (Kagami *et al.*, 2007; Raghukumar and Damare, 2011). Likewise, aplanochytrid may also represent an essential source of nutrition for zooplankton. Aplanochytrids could then appear as important agents for the transfer of organic carbon from diatoms to grazers. By feeding on aplanochytrids, zooplankton could indeed benefit from diatom blooms and avoid or bypass the defense strategies developed by this highly successful group (such as mechanical defenses represented by the frustule (Smetacek, 2001) and chemical defenses (Ianora *et al.*, 2004). This form of predation, in which grazers consume the parasite with its host, refers to a concomitant predation (Johnson *et al.*, 2010). However, to our knowledge, predation on aplanochytrids has not been studied in the natural environment. Viral infections may also explain in part the variations in *Aplanochytrium* sp. abundances suggested by the molecular data. Viruses infecting Labyrinthulomycetes have already been reported in Japanese coastal waters (Takao *et al.*, 2005, 2007).

To help deciphering the role of these organisms in the environment, the metabarcoding dataset will be used to reconstruct co-occurrence networks (EC2CO CYCLOBS project). With a similar strategy using the SOMLIT-Station C metabarcoding dataset obtained from the Eastern English Channel, significant positive connections were identified between OTUs assigned to the Labyrinthulomycetes and diatom and dinoflagellate OTUs (Christaki *et al.*, 2017b). In order to better understand the global ecology of the species that we isolated, homologous sequences will also be searched in other molecular datasets such as Tara Oceans or Malaspina.

In conclusion, we isolated the first *Aplanochytrium* infecting live marine diatoms. Phytoplankton populations thus appear as new ecological niches for this group of heterotrophic protists. The impact and fate of aplanochytrids in planktonic systems remain to be unveiled.

CHAPTER III - Species of the genus *Kordia* exert differential algicidal activity on marine diatoms

Laure Arsenieff[1], Raphaël Lami[2], Dominique Marie[1], Dominique Bœuf[3], Anne-Claire Baudoux[1], Nathalie Simon[1] and Christian Jeanthon[1]

[1]Sorbonne Université, CNRS, UMR 7144, Station Biologique de Roscoff, 29860 Roscoff, France
[2]Sorbonne Université, CNRS, LBBM, Observatoire Océanologique, 66650 Banyuls-sur-Mer, France
[3] Daniel K. Inouye Center for Microbial Oceanography: Research and Education, University of Hawai'i at Manoa, Honolulu, HI 96822

Author contributions
Laure Arsenieff designed the study, conducted the samplings, the experiments and analyses. Raphaël Lami performed the quorum sensing biotests and the *in silico* analyses. Dominique Marie provided technical support. Dominique Bœuf designed specific probes. Anne-Claire Baudoux and Nathalie Simon designed the study and conducted the samplings. Christian Jeanthon designed the study, conducted the experiments and contributed to the analyses.

INTRODUCTION

In marine environments, phytoplankton blooms development and seasonal successions are essential processes involved in the maintenance of ecosystem functioning. Decades of research have emphasized the role of algicidal bacteria in regulating algal bloom dynamics, by active cell lysis or growth inhibition (Mayali *et al.*, 2008; Mayali and Azam, 2004). Algicidal bacteria have been particularly studied in cases of harmful algal blooms (Imai *et al.*, 2001; Lovejoy *et al.*, 1998; Salomon and Imai, 2006; Skerratt *et al.*, 2002), with the final aim to use these pathogens for biological control of phytoplanktonic species (Cai *et al.*, 2016). A broad range of microalgae are targeted by algicidal bacteria, such as raphidophytes, dinoflagellates and also diatoms (Mayali and Azam, 2004). Among them, diatoms are a large component of marine biomass and produce about 20% of the total CO_2 fixed on Earth (Field *et al.*, 1998; Nelson *et al.*, 1995). These key ecological players of the modern ocean have been described as one of the most diverse groups of phytoplankton (Armbrust, 2009; Mann and

Droop, 1996). Thus, studying the biological factors involved in the regulation of diatom population dynamics is a major concern.

Bacteria that kill diatoms belong mainly to the Bacteroidetes and Gammaproteobacteria (Mayali and Azam, 2004; Meyer *et al.*, 2017) but Betaproteobacteria and Firmicutes are also reported (Li *et al.*, 2016; Shi *et al.*, 2013). Bacteria use fundamentally two different lines of attack to kill their microalgal hosts: one requires attachment or close proximity of the algicidal bacteria with the host while the other relies on indirect interaction via the excretion of algicidal compounds. The contact-based algicidal activity are reported for numerous bacteria (Mayali and Azam, 2004; Mitsutani *et al.*, 1992) while the mechanisms involved in non-contact interactions are less documented (Paul and Pohnert, 2011).

The nature of the excreted compounds varies considerably according to the bacteria. Metabolites can be heat labile or thermal resistant, span from low or high molecular weight, and target a specific host or be more generalist (Kim *et al.*, 1999; Paul and Pohnert, 2011; Shi *et al.,* 2013; Wang *et al.,* 2016). Algicidal enzymes known to lyse diatoms are for instance chitinase (Li *et al.*, 2016) or serine-protease (Lee *et al.* 2000). The later authors have demonstrated that the release of a serine-protease molecule by *Pseudoalteromonas* strain A28 (Gammaproteobacteria) was responsible for the mortality of diatoms such as *S. costatum*, *Thalassiosira* sp., *Eucampia zodiacus* and the raphidophyte *Chattonella antiqua*. The flavobacterium *Kordia algicida* (Bacteroidetes) isolated in Korea during a *S. costatum* proliferation (Sohn *et al.*, 2004) produces a serine-protease as algicidal agent to kill its diatom hosts (Paul and Pohnert, 2011). Paul and Pohnert (2011) further discovered that production and excretion of the inhibitory molecule were triggered by the bacterial cell density and not by the host density. These authors suggested that quorum sensing (QS), a density-dependent based mechanism, was involved in the independent regulation of algicidal enzymes. In Gram-negative bacteria, QS is mediated through diverse types of signaling molecules. Among them, the well-studied acyl homoserine lactones (AHLs, AI-1, autoinducer type 1) are synthesized by an autoinducer synthase LuxI and bind to a LuxR receptor. This transcription factor regulates diverse type of bacterial genes, and interestingly, may also regulate the production and the excretion of the algicidal principles (Rolland *et al.*, 2016). Some bacterial strains do not produce AHLs but rely on other modes of quorum sensing, like those involved in AI-2 (autoinducer type 2, furanosyl diester borate) or CAI (Cholerae autoinducers family)-based communication (Bassler, 1999; Skerratt *et al.*, 2002). However, despite the acquisition of new bacterial genomes, determining the nature and biosynthesis of signaling compounds remains a challenge and the downstream regulation of gene expression of these molecules in bacteria-diatom interactions is still poorly understood.

In this study, we isolated a bacterial strain exerting a strong algicidal effect against *Guinardia delicatula*, a diatom forming annual blooms in coastal waters off Roscoff (France) (Guilloux *et al.*, 2013). We compared the host spectrum of this strain affiliated to the genus *Kordia* to that of all described *Kordia* species. Our results demonstrated that *Kordia* strains have different infection patterns, which might reflect distinct modes of action. Our new isolate was able to attack diatoms and other microalgae by excreting an extracellular compound. We

further investigated communication between cells. Using biotests and published genomes, we tested the hypothesis that *Kordia* spp. might be involved in a quorum sensing mode of chemical signaling, in particular for the control of its protease activities. Analyses and experimentations are still ongoing but preliminary results of this study highlight the fact that *Kordia*-diatom interactions are more complex than previously thought.

MATERIAL AND METHODS

Growth conditions of algal and bacterial cultures

The xenic culture of the marine diatom *Guinardia delicatula* RCC3083 was used in this study for the isolation of potential pathogens. This clonal strain isolated from Roscoff coastal waters in 2012 was provided by the Roscoff Culture Collection (RCC, http://roscoff-culture-collection.org/) and was cultivated in sterile conditions in K+Si medium (Keller *et al.*, 1987) at 18°C, under a 12:12h light:dark cycle of 100 µmol photons.m^{-2}.s^{-1} provided by a white fluorescent light (Philips Master TL_D 18W/865). These culture conditions were used during isolation of parasites and following experimentations.

Reference *Kordia* strains used in this study were obtained from the Japanese Collection of Microorganisms, Ibaraki, Japan (*K. aquimaris* JCM 18556^T), from the Korean Collection for Type Cultures, Jeonbuk, Korea (*K. jejudonensis* KCTC 3426^T, *K. periserrulae* KCTC 22801^T, *K. antarctica* KCTC 32292^T, *K. zosterae* KCTC 52268^T), from the Marine Culture Collection of China, Xiamen, China (*K. ulvae* MCCC 1A01772^T and *K. zhangzhouensis* MCCC 1A00726^T) and from the Nite Biological Resource Center, Tokyo, Japan (*K. algicida* NBRC 100336^T). Unless otherwise stated, all strains were grown on Marine Agar (Difco) and in Marine Broth (Difco) at 18°C.

Screening of *Guinardia* parasites and isolation of algicidal bacteria

Samplings were conducted every fortnight between October 2015 and October 2016 at the SOMLIT-Astan station, the long-term monitoring time-series off Roscoff in the Western English Channel (60 m depth, 48°46’18” N-3°58’6”W). Surface seawater samples (3 L) were collected at 1 m depth using a 5 L Niskin bottle. Back in the laboratory, samples were immediately pre-filtered through a 150 µm pore-size nylon filter to remove most of the micro- and mesozooplankton. Pre-filtered samples (250 mL) were enriched with F/2 medium (10% v/v) and supplemented with 5 mL of an exponential culture of *G. delicatula* RCC3083. After two weeks of incubation, the enriched samples were filtered through a GF/F filter (Whatman) to isolate the pathogen community. To detect the presence of pathogens, aliquots (0.5 mL) of filtered samples were transferred into fresh host culture (1.5 mL) in 24-multiwell plates. After two weeks of incubation, cultures were inspected by light microscopy and compared to untreated host cultures used as controls. When algal lysis was observed, 3 dilution-to-extinction cycles were carried out to purify the involved pathogenic organisms (Suttle, 1993). Briefly, aliquots of the lysates (100 µL) were serially diluted in fresh *G. delicatula* RCC3083

cultures (900 µL). Lysates from the last dilution before extinction were further transferred to another fresh culture of *G. delicatula* RCC3083.

Two algicidal cultures, K-RA151006 and E-RA160713, have been selected for further investigations. They were isolated from natural samples collected respectively on the 06th October 2015 and 13th July 2016. In order to determine the nature of these pathogenic agents, lysates were filtered through 5 µm, 3 µm, 1.2 µm, 0.45 µm and 0.2 µm. Besides, lysates (10 mL) were filtered through 5 µm and centrifuged at 10000 *X g* for 15 min. Pelleted material was stored at -20°C for further molecular characterization. Genomic DNA was isolated using the Kit MasterPure complete DNA & RNA purification (Epicentre) according to the manufacturer's instructions, and amplifications targeting the 18S rRNA gene were performed.

To select for potential algicidal bacteria, antibiotic treatments were carried out on *G. delicatula* RCC3083 cultures inoculated with K-RA151006 and E-RA160713. This selection procedure was performed by adding algicidal cultures (1% vol/vol) to the algae and two different antibiotic mixtures at increasing concentrations. Stock solutions of the antibiotic mixtures consisted in (i) cefotaxime (5 mg/mL), carbenicillin (5 mg/mL), kanamycin (2 mg/mL), and augmentin (2 mg/mL) and (ii) penicillin (5,000 units/ml), neomycin (5 mg/mL), and streptomycin (10 mg/mL) (PNS solution, Sigma). Cultures for which algal lysis occurred were plated on 1/2 diluted Marine Agar (2.5 g peptone, 0.5 g yeast extract, 35 g sea salts dissolved in 1 L Milli-Q water and 15 g agar). After bacterial growth, the dominant phenotypes were transferred into *G. delicatula* RCC3083 cultures to confirm algicidal activity. Bacterial isolates were further maintained in MA medium. Isolate E-RA160713 was deposited into the Roscoff Culture Collection with accession number RCC5776.

Molecular and phylogenetic analyses

Genomic DNA extraction and amplification of the 16S rRNA gene of strain RCC5776 were performed as described in Crenn *et al.* (2016). Sanger sequencing of the PCR product was performed by GATC Biotech (Konstanz, Germany). Bacterial taxon was identified by the homologous 16S gene sequence in Genbank using BLAST (Altschul *et al.*, 1990). Phylogenetic analyses of 16S rRNA gene sequences were performed using the neighbour joining and maximum-likelihood tree methods implemented in Geneious 9.1.3. 1000 bootstrap replicates and Jukes-Cantor substitution model were applied for both trees.

Host ranges determination

To study the host ranges of *Kordia* species, fresh bacterial cultures (10^6 cells.mL^{-1}) were added to 19 exponentially growing algal hosts that encompassed mostly diatoms but also some dinoflagellates, haptophytes, chlorophytes and raphidophytes (Table S1- 1). Most of these phytoplanktonic cultures provided by the RCC have been isolated from surface waters off Roscoff. Untreated phytoplankton cultures served as controls. Cross infection experiments were carried out in triplicate. Algal growth and lysis were monitored after 7, 14 and 18 days post-inoculation (dpi) under light microscopy. As complete algal cell death can be arduous to ascertain, chlorophyll *a* fluorescence intensity (FI) was measured simultaneously (excitation

wavelength, 430 nm; emission wavelength, 670) using a microplate reader (Spark, Tecan, Männedorf, Switzerland). Lysis was considered positive when the host FI was lower than 50% of that of the uninfected control after 18 days of incubation.

Modes of action of algicidal agents

To determine if the susceptibility patterns of algal cultures according to *Kordia* strains required contact between partners, or were due to the bacterial production of proteases and possibly inducible, the following experimentations based on the methods of Paul and Pohnert (2011) were conducted on all the *Kordia* strains against *Guinardia flaccida*. Additional tests included *Kordia* sp. RCC5776 and *K. antarctica* against *G. striata* and *K. periserrulae* against *Minidiscus comicus*.

Exponentially growing *Kordia* strains were inoculated into MB/10 medium (Marine Broth diluted in natural seawater). After the cultures reached optical density (540 nm; UVmc2 spectrophotometer, Safas Monaco) > 0.25, bacterial cultures (300 µL) were diluted into 15 mL of K+Si medium and into 15 mL of exponentially growing algal cultures. When an onset of lysis was observed in cocultures (after 24 to 96h depending on the strains), aliquots of both conditions (*Kordia* in K+Si medium and *Kordia*-algae cocultures) were filtered through 0.2 µm PES filter (Whatman). Serine-protease inhibitor phenylmethanesulphonylfluoride (PMSF; Sigma, Munich, Germany) was tested for evaluating its ability to reduce algicidal activity against algae. A stock solution (100 mM in isopropanol) was added to each active cell-free bacterial filtrate (final PMSF concentration of 1mM). After incubation for 30 min in the dark at 15°C, the cell-free filtrates were applied to each corresponding algae. To test the potential toxicity of PMSF on the algal growth, PMSF was also added to K+Si medium.
The unfiltered suspensions, the filtered suspensions, and the filtered-PMSF treated suspensions were inoculated to diatoms in a 48-multiwell plates (10% vol/vol). K+Si medium with PMSF was also inoculated as positive control. Algal growth and lysis were monitored after 2, 3, 5, 7, 10 and 14 days post-inoculation (dpi) under light microscopy and measuring the fluorescence intensity. The experiment has been carried out in triplicate.

Additional experimentations were carried out in the above conditions on *Kordia* sp. strain RCC5776, *K. algicida* and *K. periserrulae*. Algicidal modes of the two first strains were tested against the diatoms *G. delicatula*, *G. flaccida*, *G. striata*, *M. comicus* and *Skeletonema costatum*. Due to its narrow host range, *K. periserrulae* was tested only against *G. flaccida* and *M. comicus*. Tests between *K. algicida* and *Skeletonema costatum* were also performed to mimic the bioassays conducted by Paul and Pohnert (2011). All protease inhibition experiments were carried out in triplicate.

Searching for quorum sensing autoinducer synthases

The supernatant of *Kordia* sp. RCC5776 was tested for the production of quorum sensing autoinducers using biosensor assays, following previously described protocols based on *Pseudomonas putida*- and *Escherichia coli*-based biosensors (Andersen *et al.*, 2001; Riedel *et al.*, 2001). Briefly, *P. putida* F117 (pRK-C12; Kmr; *ppuI*::*npt*) and *E. coli* MT102 (pJBA132)

were used for the detection of long-chain and of short-chain AHLs, respectively. *E. coli* MT102 and *P. putida* F117 were cultivated overnight with continuous shaking (200 rpm), in Luria–Bertani (LB) Broth (Sigma L3022) at 37°C supplemented with tetracycline (25 µg.mL^{-1}) and at 30°C supplemented with gentamicin (20 µg.mL^{-1}), respectively. An overnight culture of each biosensor strain (200 µL) was inoculated in 9.8 µL of fresh LB medium with the appropriate antibiotics. The fresh biosensor cultures were dispensed into 96-well microplates (180 µL per well). Then *Kordia* sp. RCC5776 supernatant (20 µL) collected at mid- and end-exponential growth was added in each well in triplicate. Microplates were incubated at 30°C and 37°C depending of growth optimum of the selected biosensor strain, without shaking. After 0, 5 and 24 h of incubation, fluorescence was determined with a Victor1420 Multilabel Counter (Perkin–Elmer) at an excitation wavelength of 485 nm and a detection wavelength of 535 nm. OD620 was also measured to control for biosensor cell growth. Negative controls were biosensor cultures without extracts, and sterile LB medium. Biosensor cultures with addition of commercial AHLs (C6-HSL for *E. coli* MT102 and oxo-C10-HSL for *P. putida* F117) were used as positive controls.

***In silico* analysis of quorum sensing autoinducer synthases and receptors**

The genome of *K. algicida* OT1^T, fully accessible online (PRJNA19315), was used to detect *in silico* potential quorum sensing autoinducer synthases and receptors. First, the detection of AI-1 synthases was conducted by sequence homology searches using the BLAST algorithm and our AI synthase databases as the query sequences (fully described in Doberva *et al.* (2015)). A *de novo* annotation of *K. algicida* OT1^T genome was also performed using the RAST server to confirm the results obtained using BLAST. In addition, the presence of potential AI synthases was examined in the InterPro Database *v*69.0, with the query "IPR001690 - autoinducer synthase". InterPro is a meta-database which contains sequences from diverse other bases (CATH-Gene3D, TIGRFAMs, PROSITE, Pfam, PANTHER, etc.) (Mitchell *et al.*, 2015). Similar searches where performed using the genome browser MaGe, included in the MicroScope platform (Médigue *et al.*, 2017).

Potential LuxR proteins were detected in the genome of *K. algicida* OT1^T using the InterPro *v*69.0 database with the entry "Transcription regulator LuxR, C-terminal" (IPR000792). Protein domains were then identified using SMART 7 using software (Letunic *et al.*, 2015). LuxR were aligned using the ClustalW algorithm under MEGA software (Higgins *et al.*, 2007) with *V. fisheri* LuxR and *Agrobacterium* TraR sequences to check potential conserved amino-acids. The prediction of ligand binding on LuxR proteins was performed to test whether or not all identified LuxR proteins could effectively be involved in quorum sensing. The ligands were identified using COACH-D software available in I-TASSER package (Wu *et al.*, 2018) that identifies the potential ligands using both a structure-based approach (TM-SITE) and an evolution-based (S-SITES) based approach. The *de novo* RAST based annotation that we conducted for *K. algicida* OT1^T genome allowed us to identify some of the genes present in the same genomic region than LuxR genes. Their presence in a similar operon was checked using FGENSB software FGENSB (http://www.softberry.com/berry.phtml).

Accession numbers

The 16S rRNA gene sequence of *Kordia* sp. RCC5776 is available in GenBank database under the accession number MH999446.

RESULTS

Isolation and purification of algicidal bacteria

Two seawater samples collected at SOMLIT-Astan station on 6th October 2015 (RA151006) and 13th July 2016 (RA160713) induced complete lysis of *G. delicatula* RCC3083. Further experiments revealed that no lysis occurred after filtration of both lysates below 0.45 µm and no eukaryotic DNA amplification was possible, indicating that both algicidal agents were neither viral nor eukaryotic. Antibiotic treatments showed that lysis of *G. delicatula* RCC3083 also occurred in PNS-treated cultures (final concentration 1X) derived from both samples while algal growth was still observed in cultures with other antibiotic mixtures. Lysates of PNS1X-treated cultures of K-RA151006 and E-RA160713 were plated on MA allowing the growth of yellow bacterial colonies after about one week. When cell suspensions of yellow bacterial colonies were inoculated into fresh *G. delicatula* RCC3083 cultures, algicidal activity was observed after 4 days for colonies obtained from E-RA160713 lysate (Figure II-9). The resulting strain (E-RA160713=RCC5776) was selected for further investigations. None of the bacteria isolated from K-RA151006 lysate induced algal lysis when using the same procedure.

Figure II-9. G. delicatula *RCC3083 cultivated without (left) and with* Kordia *sp. RCC5776 (on the right)*

Phylogenetic relationships

A nearly full-length 16S rRNA gene sequence (1,440 bp) was obtained from strain RCC5776. The closest relatives of strain RCC5776 were *K. ulvae* SC2^T (98.7%), *K. zosterae* ZO-23T^T (98.6%), *K. antarctica* IMCC3317^T (97.6%) and *K. algicida* OT-1^T (97.2%). Using both maximum-likelihood and neighbor-joining methods, strain RCC5776 formed a distinct lineage within the highly supported clade comprising *Kordia* species (with a bootstrap resampling value of 100%) and joined the cluster that included *K. ulvae* SC2^T, *K. antarctica* IMCC3317^T and *K. zosterae* ZO2-23^T (Figure II-10).

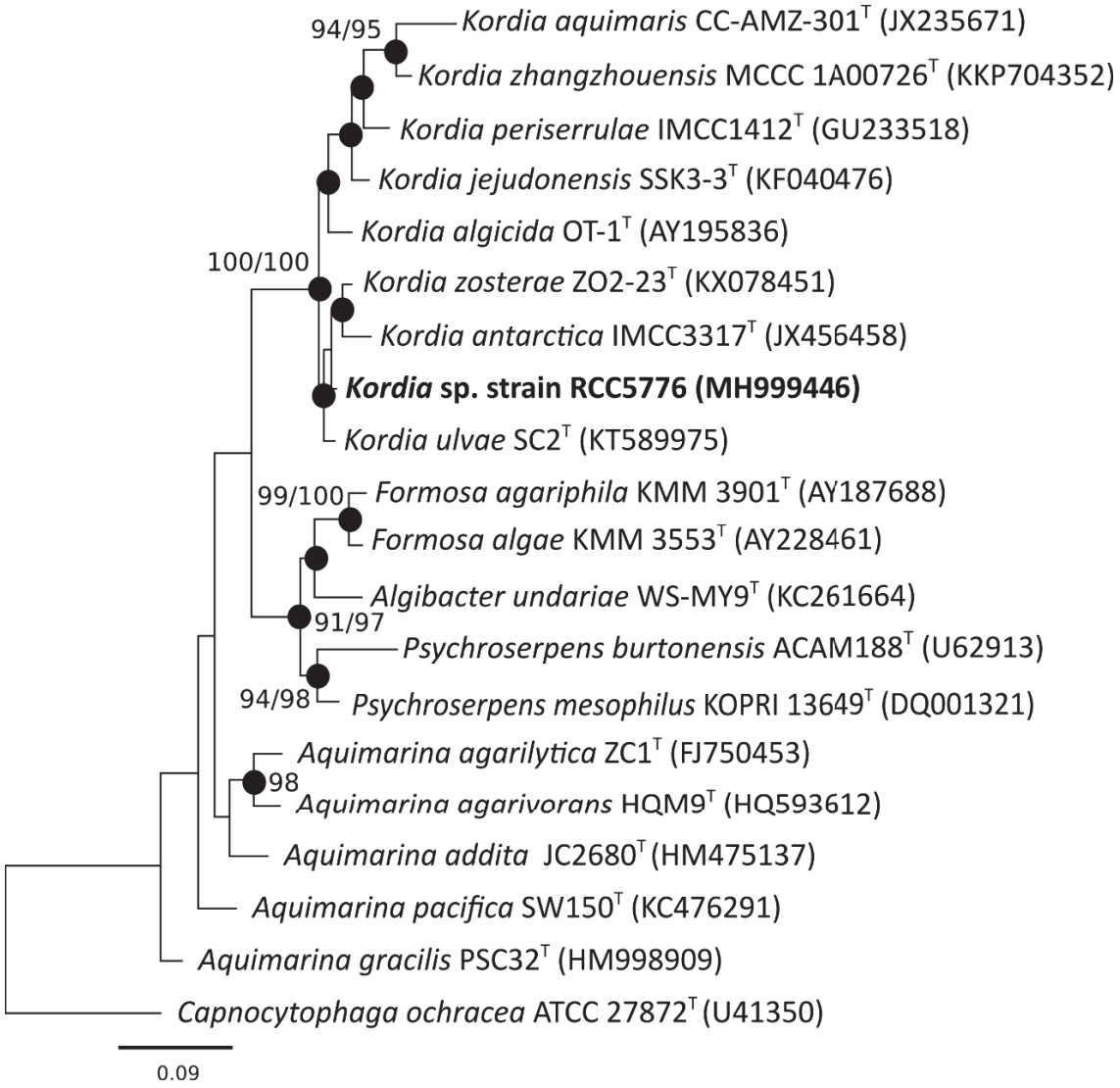

Figure II-10. Maximum-likelihood tree based on 16S rRNA gene sequences showing the position of Kordia *sp. RCC5776 (in bold). Only bootstrap values (expressed as percentages of 1000 replications) > 80% are shown. Filled circles indicate that the corresponding nodes were also recovered using the neighbor-joining algorithm.* Capnocytophaga ochracea *ATCC 27872^T was used as outgroup. Scale: substitutions per nucleotide position.*

Algicidal activities of *Kordia* strains

Microscopic examinations of co-cultures showed that complete algal lysis was mostly obtained after 14 days of incubation. However, since residual fluorescence was measured by spectrophotometry for some algal species, suggesting that algal mortality was incomplete, the algicidal activity was recorded after 18 days of incubation to better accommodate the differences (Table II-2).

A clear difference of host ranges was observed between the 9 *Kordia* strains (Table II-2). *Kordia* sp. RCC5776, *K. algicida*, *K. jejudonensis*, *K. zhangzhouensis* and *K. zosterae* were generalists, with a broad range of phytoplanktonic hosts, while *K. aquimaris*, *K. antarctica* and *K. periserrulae* were able to infect only a restricted number of diatoms. It is noteworthy that *K. antarctica* showed algicidal effect only on *Guinardia* species. *K. ulvae* showed an

intermediate algicidal activity, exerted mainly against diatom species. It is worth to notice that all *Kordia* strains were able to lyse the three *Guinardia* species, except *K. periserrulae*.

The two methods used to record algal cell lysis in the co-cultures (microscopy and FI measurements) were not congruent in all cases. As an example, when *Thalassiosira profunda* and *Cylindrotheca closterium* were exposed to *K. antarctica* and *K. zosterae* respectively, partial or complete cell lysis was observed microscopically while remaining chloroplasts spread in the wells still emitted fluorescence, resulting in slight difference of fluorescence signal compared to the control. In *Heterocapsa* cultures, the algicidal activity of bacteria was not easy to notice. Indeed, motility of *Heterocapsa* cells was reduced or inhibited when compared to the control but no cell burst occurred. However, FI measurements corroborated the unhealthy status of this alga. Similar results were found for the dinoflagellate *Lingulodinium polyedrum* infected by algicidal bacteria from the family Flavobacteriaceae (Mayali *et al.*, 2008).

A few algae demonstrated peculiar susceptibility patterns. *Guinardia flaccida* was susceptible to all *Kordia* strains while no algicidal activity was detected against *Chaetoceros peruvianus, Thalassiosira punctigera*, and *Heterosigma akashiwo*.

Table II-2. Algicidal activities of Kordia *sp. RCC5776 and the 8 validly described species of genus* Kordia*. Cell lysis were inspected after 18 days under light microscopy and quantified by spectrophotometry. ND: Not determined, +: Lysis, -: No lysis*

Class	Species	***Kordia* sp. RCC5776**	***K. aquimaris***	***K. algicida***	***K. antarctica***	***K. jejudonensis***	***K. periserrulae***	***K. ulvae***	***K. zhangzhouensis***	***K. zosterae***
Coscinodiscophyceae	*Guinardia delicatula*	+	+	+	+[a]	+	-	+	+	+
	Guinardia flaccida	+	+	+	+	+	+	+	+	+
	Guinardia striata	+	+	+	+	+	-	+	+	+
Mediophyceae	*Chaetoceros peruvianus*	-	-	-	-	-	-	-	-	-
	Conticribra weissflogii	+	-	-	-	+	-	-	-	-
	Minidiscus comicus	+	+	+	-	+	+	+	+	+
	Minidiscus variabilis	+	ND	+	-	+	-	+	+	+
	Skeletonema costatum	+	-	+	-	+	-	+	+	+
	Skeletonema costatum	+	+	+	-	+	-	+	+	+
	Thalassiosira curviseriata	+	-	+	-	+	-	+	+	+[a]
	Thalassiosira profunda	+	-	+	-[b]	+	+	+[a]	+	+[a]
	Thalassiosira punctigera	-	-	-	-	-	-	-	-	-
Bacillariophyceae	*Cylindrotheca closterium*	+	-	+	-	+	-	-	+	+[b]
	Nitzschia sp.	+	-	+	-	+	-	-	+	-
Dinophyceae	*Heterocapsa* sp.	+	-	+	-	+	-	+	+	+
Prymnesiophyceae	*Phaeocystis* sp.	+	-	+	-	-	-	-	-	+
Mamiellophyceae	*Micromonas pusilla*	-	-	+	-	-	-	-	+	-
	Ostreococcus lucimarinus	-	-	+	-	-	-	-	+	-
Raphidophyceae	*Heterosigma akashiwo*	-	-	-	-	-	-	-	-	-

[a]: Incomplete lysis (40-47% of FI loss in infected cultures compared to the control)

[b]: No change of FI in the infected cultures but partial or total lysis observed by microscopy

Modes of action of algicidal agents

Comparison between different* Kordia *host ranges. The narrow to wide host ranges exhibited by *Kordia* strains suggested different types of interactions between *Kordia* species and microalgae. To test if the algicidal modes of *Kordia* sp. RCC5776 (wide host range), *K. antarctica* and *K. periserrulae* (narrow host ranges) against their respective host was indirect (mediated by diffusible compounds), possibly due to a protease and inducible, the algicidal effects of the *Kordia* and *Kordia*-algae cell-free filtrates, and of a protease inhibitor were tested.

The three *Kordia* species pre-cultivated alone or with their respective host strongly affected the subsequent growth of their respective host (Figure II-11, A, B and C). Cell-free filtrates of *Kordia* sp. RCC5776 and *K. antarctica* alone or in co-cultures with *G. striata* significantly inhibited the algal growth (Figure II-11, A and B). For instance, almost no FI (0.7% of the control) was detected for *G. striata* inoculated with *Kordia* sp. strain RCC5776 after 7 days (Figure II-11, A). The cell-free filtrate of *K. periserrulae*/*M. comicus* cocultures resulted in a conspicuous reduction of the FI (-43%) in comparison to the control, while no growth inhibition was observed with *K. periserrulae* filtrate, suggesting that a contact with the host is required (Figure II-11, C).

Addition of PMSF in the *Kordia* sp. RCC5776 filtrate decreased the growth inhibition of *G. striata* (59% of FI loss) but did not fully restored it (Figure II-11, A). Interestingly, algal growth was fully inhibited after addition of PMSF in the filtrate of *Kordia* sp. RCC5776/*G. striata* coculture (Figure II-11, A). PMSF treatment did not affect the algicidal action of *K. antarctica* against *G. striata* whatever the filtrate (Figure II-11, B). Addition of PMSF did not change the inhibition patterns of *K. periserrulae* against *M. comicus* (Figure II-11, C). In both cases, *K. periserrulae* filtrates showed no inhibition while the filtrate of *K. periserrulae*/*M. comicus* coculture induced a significant release of bacterial proteases (51% of FI loss).

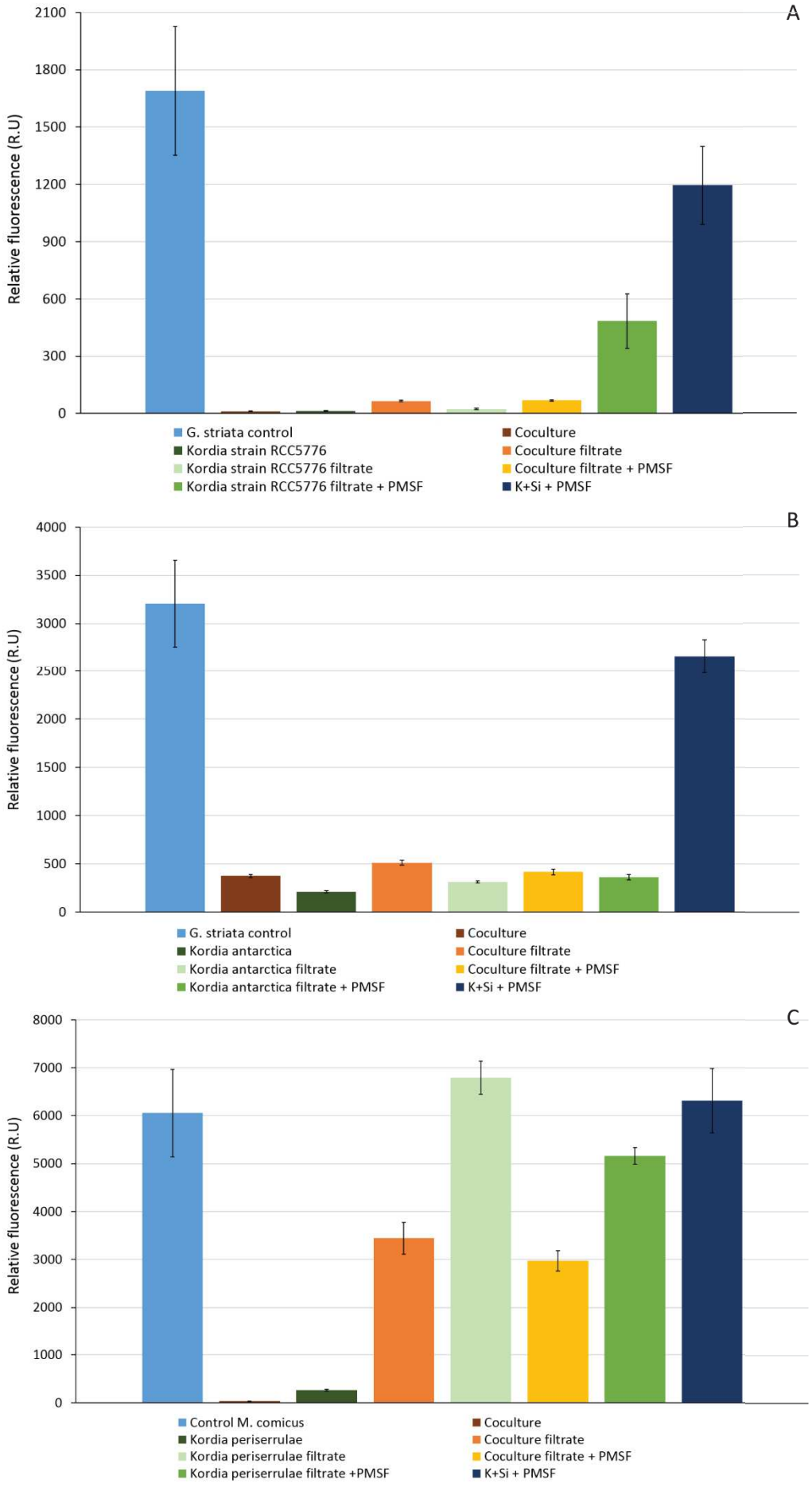
A
Relative fluorescence (R.U)
2100
1800
1500
1200
900
600
300
0
G. striata control
Kordia strain RCC5776
Kordia strain RCC5776 filtrate
Kordia strain RCC5776 filtrate + PMSF
Coculture
Coculture filtrate
Coculture filtrate + PMSF
K+Si + PMSF
B
Relative fluorescence (R.U)
4000
3500
3000
2500
2000
1500
1000
500
0
G. striata control
Kordia antarctica
Kordia antarctica filtrate
Kordia antarctica filtrate + PMSF
Coculture
Coculture filtrate
Coculture filtrate + PMSF
K+Si + PMSF
C
Relative fluorescence (R.U)
8000
7000
6000
5000
4000
3000
2000
1000
0
Control M. comicus
Kordia periserrulae
Kordia periserrulae filtrate
Kordia periserrulae filtrate +PMSF
Coculture
Coculture filtrate
Coculture filtrate + PMSF
K+Si + PMSF

Figure II-11. Algicidal effects of Kordia *sp. RCC5776 (A) and* K. antarctica *(B) on* G. striata *and* K. periserrulae *on* Minidiscus comicus *(C). Data were recorded after 7 days (A, B) and 14 days (C). For each test, the relative FI of the uninfected control and treatments was measured by spectrophotometry. Coculture refers to the pre-incubation of* Kordia *spp. with their respective host. Note that* G. striata *growth was slightly affected by the addition of PMSF.*

***The algicidal activities of* Kordia *species against* G. flaccida.** *G. flaccida* was the unique algal culture tested whose growth was affected by all the *Kordia* strains (Table II-2). We used the previous suite of experiments to test if all *Kordia* strains had the same mode of action. With the exception of *K. periserrulae*, all strains displayed the same response to the different treatments (Figure II-12, A). Raw suspensions of the active *Kordia* and of the *Kordia*/*G. flaccida* coculture resulted in cell mortality of *G. flaccida*. However, filtration and PMSF treatments did not affect the diatom growth (Figure II-12, A), suggesting that algicidal agents produced were not diffusible and not inducible.
Unexpectedly, growth of *G. flaccida* was not significantly inhibited in the presence of *K. periserrulae* in comparison to the control regardless the treatment (Figure II-12, B).

As results obtained on *G. flaccida* differed from the one obtained on *G. striata* and *M. comicus*, we set up a new experiment with several host-bacteria combinations. Experimentations are ongoing in the laboratory and results were not yet available before the submission of this manuscript.

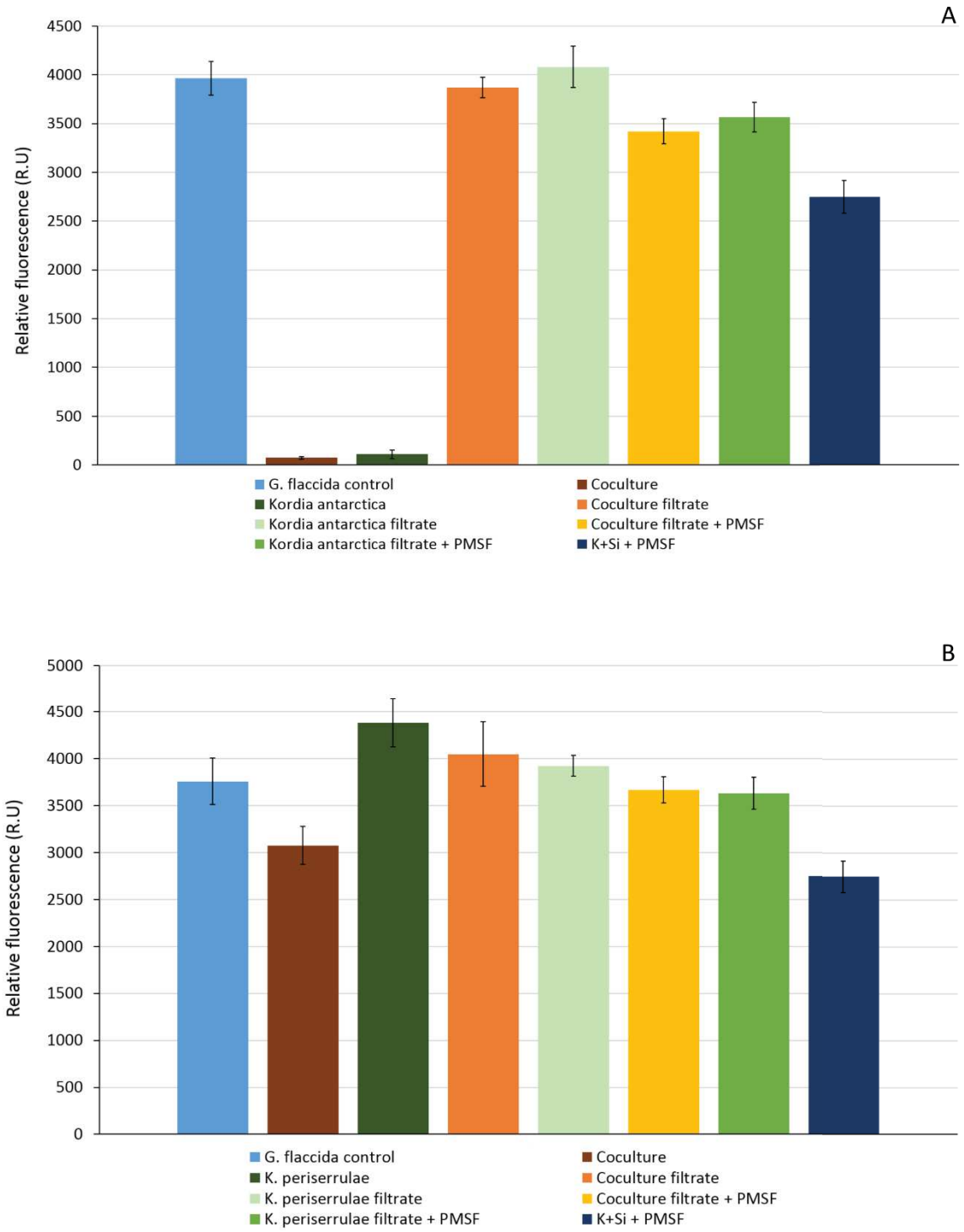

Figure II-12. Algicidal modes of K. antarctica *(A) and* K. periserrulae *(B) on* G. flaccida *after 14 days of incubation. For each test, the relative FI of the uninfected control and treatments was measured by spectrophotometry. Coculture refers to the pre-incubation of* Kordia *with* G. flaccida. *Note that growth of* G. flaccida *was slightly altered after the PMSF addition*

Searching for quorum sensing autoinducer synthases and quorum sensing LuxR type receptors

Our biotests based on two different specialized biosensors, indicated the absence of autoinducer synthases. No *luxI* genes were also found in the genome of *K. algicida* OT1^{T}. By

contrast, the analysis of the Interpro database revealed the presence of a total of 16 LuxR type genes in *K. algicida* OT1^T genome. This pattern is typical of "LuxR solo" or "LuxR orphans", i.e. when *luxR* genes are detected in a genome but without any cognate *luxI* gene. Similar analyses could not be conducted on the 4 other available *Kordia* genomes (*K. jejudonensis* SSK3-3, *K. periserrulae* DSM 25731, *Kordia* sp. NORP58 and *K. zhangzhouensis* MCCC 1A00726^T) since they were not accessible into InterPro and MaGe databases.

***In silico* analysis LuxR-type receptors**

The Interpro and SMART analysis of *K. algicida* OT1^T LuxR protein sequences confirmed that they all harbor the typical LuxR DNA-binding helix-turn-helix (HTH) domain at their C-terminal region. On the N terminal region, 10 sequences presented a signal transduction response regulator (IPR001789), one a tetratricopeptide repeat-containing domain (IPR013026), one a RNA polymerase sigma-70 (IPR007627) and 4 showed N terminal domains which were not possible to affiliate to any known type of protein domain. However, none of them presented the autoinducer binding domain (IPR005143).

Two of these *luxR* genes were contained in operons where a few genes where annotated. The first LuxR (WP_007094024 in the CBI genome) was linked to a chitinase (EC 3.2.1.14) (WP_007094023.1 in NCBI, annotated with RAST) and a Mg2+ related chelatase/ComM related protein (WP_007094022.1 in NCBI). The second LuxR (WP_007096707) was linked with a C14 peptidase catalytic unit p20 (WP_083777331.1).

Using a COACH-D approach, we further examined the potential ligands for these 2 LuxR receptors identified in connection with the genes encoding a caspase subunit and the one encoding a chitinase. The potential ligands appeared very similar for both LuxR and presented similar Cscore for both proteins: manganese (Cscore=0.63), beryllium trifluoride ion (0.25), peptides (0.03) and c-di-GMP (0.02). However, none of the amino-acids known to be involved in autoinducers binding were detected when aligned with *Agrobacterium* TraR sequence and *Vibrio fischeri* LuxR sequence (Venturi *et al.*, 2018).

DISCUSSION

Algal-microbial parasitism has been the subject of extensive research in marine systems, most particularly in the context of potential use of algicidal bacteria in harmful algal bloom control (Cai *et al.*, 2016; Doucette *et al.*, 1999; Ramanan *et al.*, 2016; Salomon and Imai, 2006). For example, several parasitic microorganisms including a virus (Kim *et al.*, 2015a), several bacteria (Kato *et al.*, 1998; Mitsutani *et al.*, 1992; Paul and Pohnert, 2011; Shi *et al.*, 2013) and an eukaryote (Ohno *et al.*, 2013) have been reported to kill the red tide forming diatom *Skeletonema costatum*. To our knowledge, except for the haptophyte *Emiliania huxleyi* for which viruses and bacteria could be involved in bloom decline and termination (Barak-Gavish *et al.*, 2018; Bratbak *et al.*, 1993; Frada *et al.*, 2008; Segev *et al.*, 2016), much less is known regarding biotic factors possibly affecting proliferation of non-toxic species. The non-

toxic diatom *G. delicatula* is the dominating species during the spring-summer bloom in temperate coastal waters off Roscoff and is a major contributor to phytoplankton spring bloom in diverse Atlantic coastal and estuarine systems (Guilloux *et al.*, 2013 and references therein).

In the present study, we report on the first algicidal prokaryote isolated during a summer bloom of *G. delicatula*. The isolated strain belongs to the genus *Kordia* that contains eight validly described species originating from diverse habitats such as surface seawater (*K. algicida* (Sohn *et al.*, 2004), *K. aquimaris* (Hameed *et al.*, 2013) and *K. antarctica* (Baek *et al.*, 2013)), from a zone where oceanic waters marine and a freshwater spring meet (*K. jejudonensis* (Park *et al.*, 2014)), from freshwater (*K. zhangzhouensis* (Du *et al.*, 2015)) but also associated with macroalgae (*K. ulvae* (Qi *et al.*, 2016) and *K. zosterae* (Kim *et al.*, 2017)) and with a polychaete (*K. periserrulae* (Choi *et al.*, 2011). So far, only the algicidal activity of *K. algicida* against several microalgae had been reported (Paul and Pohnert, 2011; Sohn *et al.*, 2004) but the parasitic lifestyle of all other *Kordia* species was unknown. Our host range laboratory experiments revealed that *Kordia* species displayed an algicidal effect on diatoms, and in a lesser extent, on Dinophyceae, Prymnesiophyceae and Mamiellophyceae. To our knowledge, *Kordia* is the only marine bacterial genus for which all species act as parasites.
Kordia strains did not share similar infection patterns that ranged from broad (generalists) to narrow (specialists) spectra, especially on diatoms. We posited that this difference in host spectra might reflect difference in algicidal modes, i.e. by direct contact or by release of diffusible compounds.

First experiments on *G. striata* demonstrated that both cell-free filtrates of *Kordia* sp. RCC5776 and *K. antarctica* inhibited algal growth, suggesting the presence of a small-sized and diffusible agent. Our results indicated however that the two strains did not produce the same types of inhibitory compounds. Indeed, their responses to PMSF treatments may imply that *Kordia* sp. RCC5776 synthetizes a protease but not *K. antarctica.* Pre-cultivation of *Kordia* strains with *G. striata* was not necessary to trigger algal growth inhibition, suggesting that the protease is not induced by the presence of the host. Contrary to cell-free filtrate of *Kordia* sp. RCC5776 alone, cell-free filtrate of *Kordia* sp. RCC5776/*G. striata* coculture completely inhibited algal growth in the presence of PMSF. One possible explanation is that the protease synthesis was strongly induced in the coculture preventing the inhibitory effect of PMSF observed in the bacterial preculture alone. It is also possible that the PMSF concentration in this experiment was not sufficient to have an inhibitory effect. Similarly to *K. antarctica*, the algicidal activity of *K. periserrulae* was not restored by PMSF, suggesting a protease was not involved in the presence of *Minidiscus comicus*. However, our results indicated that a contact between *K. periserrulae* and the diatom is required to initiate lysis. Although the cell-free coculture filtrates inhibited algal growth, complete lysis of the algal culture was not observed. Further experimentations are needed to explain this phenomenon.

G. flaccida was the only host for which all *Kordia* strains exert algicidal activity. A second run of experimentations was carried out to determine the algicidal modes of all *Kordia*

strains on the same host. Unexpectedly, our results did not corroborate those of the first analysis. Diatom growth inhibition occurred in presence of raw suspensions of all *Kordia* and all *Kordia*/*G. flaccida* cocultures but cell-free filtrates with and without PMSF treatment had no algicidal effect. This discrepancy between both run of experiments was obvious for *Kordia* sp. RCC5776 and *K. antarctica* that clearly showed two different responses according to the host. Likewise, contrary to Paul and Pohnert (2011) who found that a protease was involved in the algicidal action of *K. algicida* against *S. costatum,* we were not able to show that a protease was also involved against *G. flaccida*. In the case of *K. periserrulae*, contrary to the results obtained with *Minidiscus comicus* and for the host range determination, lysis was barely observed in the raw coculture condition. It has already been documented that a bacterium could exhibit different algicidal modes according to algal taxa (Skerratt *et al.*, 2002). Nevertheless, we cannot rule out that these discrepancies are due problems that occurred during handling of the cultures. To overcome this issue, new experimentations are in progress in the laboratory.

Based on the first experimentation on *Kordia* sp. RCC5776 and *G. striata*, we confirmed that the interaction was mediated via a protease and was not host-dependent. Thus, we assumed that the released protease was dependent on the bacterial density as previously shown for *K. algicida* (Paul and Pohnert, 2011). Although these authors suggested a quorum sensing dependent excretion of the protease, they did not detect AHL in the cell free supernatant of *K. algicida.* We investigated the ability of *Kordia* sp. RCC5776 to produce quorum sensing autoinducers by using laboratory biotests, but we did not detect any. Further genome analysis confirmed the lack of *luxI* genes in *K. algicida* genome but highlighted the presence of *luxR* genes. These receptors, when lacking a LuxI AHL synthase, are called LuxR solos or orphans (Fuqua, 2006; Subramoni and Venturi, 2009). Many LuxR solos can bind endogenous (intraspecies) AHLs or AHLs produced by diverse bacteria (interspecies) from their close environment (Subramoni and Venturi, 2009). However, in the last few years, LuxR solos were also found to be able to detect other types of host signals (González and Venturi, 2013). These receptor proteins do not possess the typical autoinducer-binding domain but instead carry amino acid modifications in their sequence (González and Venturi, 2013; Venturi *et al.*, 2018). With the ability to bind to different types of ligands, these LuxR receptors have thus the particularity to play a role in intraspecies and interspecies bacterial-communication or in interkingdom communication. Signalization between organisms of different domains was specially studied for mutualistic and pathogenic plant-bacteria interactions (Venturi and Fuqua, 2013). Recently, researches on terrestrial systems have pointed out that an non-bacterial inducer binded to the LuxR solos from a root endophyte *Pseudomonas* sp., and activated all the downstream virulence gene expression (Coutinho *et al.*, 2018). Authors indicated the signal molecule was present in the tree tissues, necessary for plant physiological processes. In our study, identified LuxR solos did not present the classic autoinducer-binding domain. Thus, we can emit the hypothesis that LuxR receptors from *K. algicida* are not activated by a bacterial signal but they may sense host metabolites instead.

In-depth genome analysis has revealed two LuxR receptors were linked to two enzymes, a chitinase and a caspase respectively. Chitin associated to diatom cell wall has been already identified (Durkin *et al.*, 2009). Among the three diatom classes, Mediophyceae is the one with the most chitin producers reported, such as *Thalassiosira* and *Skeletonema* (Amato and Ferrante, 2018; Durkin *et al.,* 2009). Also, chitin threads are suspected to connect cells in chain-forming species of *Minidiscus* (Kaczmarska *et al.*, 2009). However, little is known for Bacillariophyceae or Coscinodiscophyceae as *Guinardia*. Although we can imagine that fixation of the ligand on LuxR solos may indirectly activate the biosynthesis of chitinase, a complex regulation of gene expressions may exist for the production and secretion of algicides. For instance, *C. weissflogii* and *T. punctigera* are known to produce chitin (Durkin *et al.*, 2009). However, the first diatom was only attacked by *Kordia* sp. RCC5776 and by *K. jejudonensis* and *T. punctigera* was not susceptible to any *Kordia* strains.

Our preliminary results on specificity and algicidal modes of all *Kordia* species shed light on their variable nature and possible contributors in the regulation of diatom blooms in the Western English Channel. Analysis of their mode of communication may suggest an interkingdom interplay barely inspected in marine environments. However, this outcome was determined only by genomic analyses and should be interpreted with caution. Ongoing laboratory experiments and *in-silico* analyses searches will bring more information about these pathogens and how their algicidal agents are regulated.

ADDITIONAL EXPERIMENTS FOR MANUSCRIPT COMPLETION

To complement the results obtained before the submission of this manuscript, two main approaches will investigate the relevance of *Kordia*-diatoms in marine environments.

- Environmental samplings throughout the year at the SOMLIT-Astan observatory site led to the isolations of several *G. delicatula* pathogens belonging to different microorganisms ranging from viruses (Arsenieff *et al.*, submitted), eukaryotes to bacteria (Arsenieff, 2018). In order to study the seasonal dynamics of the genus *Kordia* and compare it with that of diatoms and other parasites present in this coastal system, we designed several *Kordia* genus specific 16S rRNA probes using ARB (Ludwig *et al.*, 2004). Their specificity will be first evaluated and the most efficient one will be used to quantify by qPCR the abundance of *Kordia* in 2015 and 2016 DNA samples extracted from SOMLIT-Astan.

- The global spatial distribution and temporal dynamics of the genus *Kordia* and *Guinardia* will be studied using open access metabarcoding datasets (V4-V5 of 16S rRNA for prokaryotes, 18S rRNA V4 for eukaryotes) and/or metagenomes from the Tara Oceans circum-oceanic expeditions (de Vargas *et al.*, 2015; Sunagawa *et al.*, 2015), Malaspina (Villarino *et al.*, 2018), Geotraces cruises (Biller *et al.*, 2018), the Ocean Sampling Day dataset (covering coastal environments) and long-term monitoring stations such as ALOHA (North Pacific) and BATS (Atlantic) (Biller *et al.*, 2018), respectively. To predict potential associations between *Kordia*

and *Guinardia*, classical statistical co-occurrence analyzes (Friedman and Alm, 2012) and large Gaussian graphical models (Kurtz *et al.*, 2015) will be used. When the depth of sequencing allows, such as for the Tara and Malaspina expeditions, the inference of associations using the same marker genes will be directly extracted from the metagenomes, thus limiting the PCR amplification biases of the metabarcoding data sets.

Supplementary:

Table S1- 1. List and origin of the phytoplankton taxa used as potential hosts for Kordia *species. EC: English Channel, NA: not applicable*

Phylum	Class	Species	Strain code	Origin of isolation	Date of isolation
Bacillariophyta	Coscinodiscophyceae	*Guinardia delicatula*	RCC3083	Roscoff Estacade, EC	19/09/2012
		Guinardia flaccida	RCC5791	Roscoff-Astan, EC	02/02/2017
		Guinardia striata	RCC5792	Roscoff-Astan, EC	09/09/2016
	Mediophyceae	*Chaetoceros peruvianus*	RCC2023	Roscoff-Astan, EC	01/09/2010
		Conticribra weissflogii	RCC3389	North Sea	10/09/2012
		Minidiscus comicus	RCC4660	Roscoff-Astan, EC	26/05/2015
		Minidiscus variabilis	RCC4657	Roscoff-Astan, EC	26/05/2015
		Skeletonema costatum	RCC75	Caen	NA
		Skeletonema costatum	RCC1716	Roscoff-Astan, EC	13/05/2008
		Thalassiosira curviseriata	RCC5154	Roscoff-Astan, EC	26/05/2015
		Thalassiosira profunda	RCC4663	Roscoff-Astan, EC	26/05/2015
		Thalassiosira punctigera	RCC4667	Roscoff-Astan, EC	21/10/2015
	Bacillariophyceae	*Cylindrotheca closterium*	RCC1713	Roscoff-Astan, EC	13/05/2008
		Nitzschia sp.	RCC80	Roscoff Estacade, EC	01/06/1997
Miozoa	Dinophyceae	*Heterocapsa* sp.	RCC5157	Bay of Biscay	26/07/2016
Haptophyta	Prymnesiophyceae	*Phaeocystis* sp.	RCC1719	Roscoff-Astan, EC	13/05/2008
Chlorophyta	Mamiellophyceae	*Micromonas pusilla*	RCC465	Roscoff-Astan, EC	13/06/2001
		Ostreococcus lucimarinus	RCC756	Roscoff Dourduff	13/06/2001
Heterokontophyta	Raphidophyceae	*Heterosigma akashiwo*	RCC1502	La Rochelle	NA

PART III

NANODIATOMS AND THEIR PATHOGENS AT THE SOMLIT-ASTAN STATION

CONTEXT OF THE WORK

The third part of this PhD research focuses on the dominant nanoplanktonic diatoms and their putative parasites in the Western English Channel (WEC). In comparison to large diatoms, the role and dynamics of nanoplanktonic diatoms (also referred to as nanodiatoms) in marine environments has been largely overlooked. However, few studies have shown that they develop massive blooms in multiple locations and that they contribute significantly to carbon export.

In this context, the first chapter describes a 13 month-field work (Oct 2015 – Oct 2016), which led to the isolation of about 60 cultures of the numerically dominant nanodiatoms at the study site. The combination of microscopic and molecular tools showed that they belonged to 6 different species of the genera *Minidiscus* and *Thalassiosira*. Barcodes corresponding to these species were retrieved from an 8 year genetic survey at SOMLIT-Astan station. This analysis revealed that nanodiatoms, and more specifically *Minidiscus* species, are prominent members of the phytoplankton community in the WEC, as they ranked in the top 3 of the most abundant diatoms at the study site. The reconstruction of their temporal dynamics over 8 years showed contrasted seasonal patterns. To begin to address the drivers that control nanodiatom dynamics, we have attempted to isolate pathogens (from two size fractions > 0.2 µm and < 0.2 µm) throughout the sampling period. This intense isolation effort led to a unique collection of 82 parasites, among which many viruses. Parasites could be isolated from the 6 nanodiatoms species and all year round, which arises questions about their contribution in diatom regulation. This chapter is a preliminary draft of a scientific article and will be submitted for publication after analyses completion.

The second chapter describes a preliminary characterization of several viruses that infect *Minidiscus* and *Thalassiosira* species. These partial characterizations were done during the first year of the Ph.D. and will probably be part of a new scientific project.

CHAPTER I - Diversity and dynamics of relevant nanoplanktonic diatoms in the Western English Channel

Targeted journal: Environmental microbiology / Applied and Environmental Microbiology

Laure Arsenieff[1], Florence Le Gall[1], Fabienne Rigaut-Jalabert[2], Frédéric Mahé[3], Diana Sarno[4], Léna Gouhier[2], Anne-Claire Baudoux[1], and Nathalie Simon[1]

[1]Sorbonne Université, CNRS, UMR 7144 - Diversity and Interactions in Oceanic Plankton, Station Biologique de Roscoff, 29860 Roscoff, France
[2]Sorbonne Université, CNRS, Fédération de Recherche FR2424, Station Biologique de Roscoff, 29680 Roscoff, France
[3]CIRAD, UMR LSTM, 34000 Montpellier, France
[4]Stazione Zoologica Anton Dohrn, Villa Comunale, 80121 Naples, Italy

Author contributions
Laure Arsenieff, Florence Le Gall, Anne-Claire Baudoux and Nathalie Simon designed the study. Laure Arsenieff, Fabienne Rigaut-Jalabert, Florence Le Gall, Anne-Claire Baudoux and Nathalie Simon sampled onboard and isolated the nanodiatoms and/or parasites. Laure Arsenieff, Florence Le Gall and Fabienne Rigaut-Jalabert, performed the molecular analyses on the nanodiatoms and/or environmental samples and analyzed the results. Laure Arsenieff and Florence Le Gall conducted the morphological characterization. Frédéric Mahé was in charge of the metabarcoding bioinformatics analyses. Diana Sarno brought her expertise in diatom taxonomy. Léna Gouhier was in charge of the cryopreservation. Laure Arsenieff, Anne-Claire Baudoux, Nathalie Simon and Florence Le Gall wrote the ms.

INTRODUCTION

In the context of global change, understanding the mechanisms that influence the dynamics of carbon export from the photic layers to the ocean floors is of prime importance. Diatoms, that form massive blooms, have long been recognized as major drivers of the biological pump, especially in productive marine ecosystems (Leblanc *et al.*, 2012; Nelson *et al.*, 1995; Smetacek, 1999). All diatoms do not contribute equally to the export of carbon

(Tréguer *et al.*, 2018). Sinking rates depend on diverse parameters such as the cell size, the shape, the degree of valve silicification, or also the ability to produce chains (Tréguer *et al.*, 2018). It is therefore crucial to accurately determine the diatom diversity composing the seasonal proliferations and to better understand the drivers shaping their dynamics and species successions.

Studies on the diatom dynamics and its long-term variability have mainly focuses on large sized species (> 20µm) that belong to the micro-phytoplanktonic community (see for example Gómez and Souissi, 2007; Guilloux *et al.*, 2013; Schlüter *et al.*, 2012; Widdicombe *et al.*, 2010 for communities of the English Channel and North Sea). By comparison, nanoplanktonic diatoms, also referred to as nanodiatoms, are globally overlooked. These tiny organisms, mostly assigned to the genus *Minidiscus*, appear to be more frequent and abundant in the ocean than previously thought (Leblanc *et al.*, 2018; Percopo *et al.*, 2011; Ribera d'Alcalà *et al.*, 2004). *Minidiscus* is one of the smallest known marine diatom (Jewson *et al.*, 2016) with a cell size ranging generally from 2 to 5 µm (Kaczmarska *et al.*, 2009; Quiroga and Chretiennot Dinet, 2004; Takano, 1981). It includes 10 species (Aké-Castillo *et al.*, 2001; Gao *et al.*, 1992; Guiry and Guiry, 2018; Hasle, 1973; Kaczmarska *et al.*, 2009; Park *et al.*, 2017; Quiroga and Chretiennot Dinet, 2004; Takano, 1981) and is widespread in the world ocean (Aké-Castillo *et al.*, 2001; Daniels *et al.*, 2015; Kang *et al.*, 2013; Leblanc *et al.*, 2018; Malviya *et al.*, 2016; Percopo *et al.*, 2011; Quiroga and Chretiennot Dinet, 2004; Takano, 1981; Zingone *et al.*, 2011). Locally, *Minidiscus* can comprise up to 92% of the total diatom abundance as reported in the Northwestern Mediterranean sea (Leblanc *et al.*, 2018). At global scale, according to recent estimations based on metagenomic data, *Minidiscus* ranks in the top 20 most abundant diatom genera (Malviya *et al.*, 2016). Its ability to form aggregates favors high sinking rates, which allow to reach deep sea layers and fast injection of carbon (Leblanc *et al.*, 2018). Altogether, this studies highlight the necessity of considering nanodiatoms for a better understanding of ocean functioning.

Up to date, nanodiatoms have been largely overlooked due to their small size and their difficult detection by routine analyses. As a result, few representatives have been brought into culture, and the large majority of this group is not characterized genetically. To our knowledge, genetic markers exist only for 2 of the 10 known *Minidiscus* species (*M. trioculatus* and *Minidiscus* sp.) in the expert protistan database PR2 (Guillou *et al.*, 2013). This lack of sequence information hinders the detection of *Minidiscus* species in environmental metabarcoding surveys and implies that the global significance of nanodiatoms is most likely underestimated.

In this study, we characterized the dominant nanodiatoms that thrive at the long-term monitoring SOMLIT-ASTAN station located off Roscoff (Western English Channel, WEC) and investigated their dynamics using metabarcoding data obtained from 2009 to 2016. Using a combination of morphological and genetic approaches, we showed that species of the genera *Minidiscus*, and in a lesser extent nanoplanktonic *Thalassiosira,* dominate the diatom community at this sampling station. *Minidiscus* and *Thalassiosira* species showed distinct seasonal patterns. The large collection of parasites, including viruses, isolated from these

diatom genera indicates that pathogens may exert an important biotic pressure at this sampling station.

MATERIAL AND METHODS

Environmental isolations and growth conditions of diatom cultures

Diatom strains were isolated from natural seawater samples collected at 1 m depth using a 5 L Niskin bottle at the long-term monitoring SOMLIT-Astan station in the Western English Channel (48:46:18 N, 3:58:6 W) on May 26, 2015 and over a full seasonal cycle (October 2015 - October 2016). Strains were isolated either using flow cytometry single cell sorting or dilutions. For isolation using flow cytometry, natural seawater samples were filtered (< 50 µm) and diatoms were single cell sorted by flow cytometry, as described in Marie *et al.* (2017). For strain isolation using dilution, monthly or bimonthly seawater samples were analyzed by flow cytometry to determine the cell concentrations. Samples were diluted into K+Si medium in multiwell plates in order to obtain a final concentration of 5 and 10 cells per well. After two weeks of incubation, algal growth was monitored under an inverted microscope (Olympus IX71, Olympus Corporation, Tokyo, Japan). Cultures that appeared monospecific were selected. These cultures were maintained in sterile condition in K+Si medium (Keller *et al.*, 1987) at 18°C, under a 12:12h light:dark cycle of 100 µmol photons.m^{-2}.s^{-1} provided by a white fluorescent light (Philips Master TL_D 18W/865). Diatom cultures were deposited in the Roscoff Culture Collection (RCC, http://roscoff-culture-collection.org/) (Table III-1).

Molecular analysis

The SSU-18S, ITS and partial LSU-28S rDNA genes markers were amplified by PCR directly on diatom cultured cells. The primers used were 63F (ACGCTTGTCTCAAAGATTA) and 1818R (ACGGAAACCTTGTTACGA) (Lepere *et al.*, 2011) for the 18S, 329F (GTGAACCTGCRGAAGGATCA) (Guillou *et al.*, 2004) and D1R-R (TATGCTTAAATTCAGCGGGT) (Lenaers *et al.*, 1989) for the ITS, and D1R-F (ACCCGCTGAATTTAAGCATA) (Lenaers *et al.*, 1989) and D3Ca (ACGAACGATTTGCACGTCAG) (Orsini *et al.*, 2002) for the partial 28S D1-D3 region.

Aliquots (2.25 µL) of diatom cultures in exponential growth phase were submitted to 95°C for 5 min. The reaction mixture (30 µL final volume) was then added: Phusion Master Mix (1x final concentration, Thermo Scientific), 3% DMSO and 0.25 µM of each primer. PCR amplifications were performed with the following conditions: an initial incubation step at 95°C for 5 min, followed by 35 (18S-28S) or 40 (ITS) cycles of denaturation at 95°C for 1 min, annealing step for 30 sec at 55°, 52° and 57° for the amplifications of the 18S, ITS and 28S respectively, and extension at 72°C for 1 min 30. The cycles were followed by a final extension step at 72°C for 10 min. PCR products were sent to Sanger Sequencing to GATC Biotech (https://www.gatc-biotech.com/en/index.html, Constance, Germany). Sequences were analyzed using Geneious 9.1.3 and relative were searched in GenBank using the BLASTn tool (https://blast.ncbi.nlm.nih.gov/Blast.cgi).

Table III-1. Diatom strains isolated in May 2015 and from October 2015 to October 2016 at the SOMLIT-Astan station. When indicated, morphological and genetic identifications were carried out. In bold, representative strains for each taxon. RCC: Roscoff Culture Collection, LM: Light microscopy, SEM: Scanning Electronic Microscopy

Species	Strains	Isolation date	Isolation method	Morphological identification	SSU-18S	ITS	LSU-28S D1-D3 region
Minidiscus comicus	**RCC4660**	26/05/2015	Flow cytometry	LM, SEM	Complete	Complete	Complete
	RCC4661	26/05/2015	Flow cytometry	LM, SEM	Complete	Complete	Complete
	RCC4662	26/05/2015	Flow cytometry	LM, SEM	Complete	Complete	Complete
	RCC5839	20/11/2015	Dilution		Complete	Complete	
	RCC5840	04/12/2015	Dilution		Complete	Complete	
	RCC5841	04/12/2015	Dilution		Complete	Complete	
	RCC5842	04/12/2015	Dilution		Complete	Complete	
	RCC5843	04/12/2015	Dilution		Complete		
	RCC5844	04/01/2016	Dilution		Complete	Complete	
	RCC5845	04/01/2016	Dilution		Complete	Complete	
	RCC5846	02/02/2016	Dilution		Complete		
	RCC5847	02/02/2016	Dilution		Complete	Complete	
	RCC5848	02/02/2016	Dilution		Partial	Complete	
	RCC5849	04/03/2016	Dilution		Complete		
	RCC5850	04/03/2016	Dilution		Complete	Complete	
	RCC5851	04/03/2016	Dilution		Partial	Complete	
	RCC5852	01/04/2016	Dilution		Complete	Complete	
	RCC5853	01/04/2016	Dilution		Complete	Complete	
	RCC5854	01/04/2016	Dilution		Partial	Complete	
	RCC5855	01/04/2016	Dilution		Partial	Complete	
	RCC5856	15/04/2016	Dilution		Partial	Complete	
	RCC5857	15/04/2016	Dilution		Partial	Complete	
	RCC5858	13/05/2016	Dilution		Partial	Complete	
	RCC5859	13/05/2016	Dilution		Complete	Complete	
Minidiscus spinulatus	**RCC4659**	26/05/2015	Flow cytometry	LM, SEM	Complete	Complete	Complete
	RCC5860	04/03/2016	Dilution		Partial	Complete	
	RCC5861	04/03/2016	Dilution		Partial	Complete	
Minidiscus variabilis	**RCC4657**	26/05/2015	Flow cytometry	LM, SEM	Complete	Complete	Complete
	RCC4658	26/05/2015	Flow cytometry	LM, SEM	Complete	Complete	Complete
	RCC4665	26/05/2015	Flow cytometry	LM, SEM	Complete	Complete	Complete

	RCC4666	26/05/2015	Flow cytometry	LM, SEM	Complete	Complete	Complete
	RCC5862	06/10/2015	Dilution		Complete		
	RCC5863	04/11/2015	Dilution		Complete	Complete	
	RCC5864	04/11/2015	Dilution		Partial		
	RCC5865	04/11/2015	Dilution		Complete		
	RCC5866	04/11/2015	Dilution		Complete		
	RCC5867	04/11/2015	Dilution		Complete	Complete	
	RCC5868	20/11/2015	Dilution		Complete	Complete	
	RCC5869	20/11/2015	Dilution		Complete	Complete	
	RCC5870	04/12/2015	Dilution		Complete	Complete	
	RCC5871	02/02/2016	Dilution		Complete	Complete	
	RCC5872	04/03/2016	Dilution		Partial	Complete	
	RCC5873	01/04/2016	Dilution		Partial	Complete	
	RCC5874	15/04/2016	Dilution		Partial	Complete	
	RCC5875	15/04/2016	Dilution		Partial	Complete	
	RCC5876	30/05/2016	Dilution		Complete	Complete	
	RCC5877	13/07/2016	Dilution		Complete	Complete	
	RCC5878	09/09/2016	Dilution		Partial	Complete	
	RCC5879	24/10/2016	Dilution		Complete		
	RCC5880	24/10/2016	Dilution		Complete		
Thalassiosira curviseriata	**RCC5154**	26/05/2015	Flow cytometry	LM, SEM	Complete	Complete	Complete
Thalassiosira profunda	**RCC4663**	26/05/2015	Flow cytometry	LM, SEM	Complete	Complete	Complete
	RCC5881	20/11/2015	Dilution		Partial		
	RCC5882	02/02/2016	Dilution		Partial		
	RCC5883	04/03/2016	Dilution		Complete	Complete	
	RCC5884	29/04/2016	Dilution		Partial	Complete	
	RCC5885	13/05/2016	Dilution		Partial	Complete	
	RCC5886	13/07/2016	Dilution		Partial	Complete	
***Thalassiosira* sp.**	**RCC4664**	26/05/2015	Flow cytometry	LM, SEM	Complete	Complete	Complete
	RCC5887	02/02/2016	Dilution		Partial		

Phylogenetic analysis

In order to determine the taxonomic positions of the diatom strains, new DNA sequences of the 18S and of the partial 28S rDNA gene markers were aligned with sequences of other Thalassiosirales (Table III-2). The sequence alignments for each gene were generated by the MAFFT version 7 program and with automatic alignment strategy (the L-INS-i iterative refinement method was calculated for both genes) (https://mafft.cbrc.jp/alignment/server/, Katoh *et al.*, 2017). For each gene, a phylogenetic reconstruction was performed on the 1590

and 534 aligned nucleotides (18S and 28S respectively) by maximum likelihood with PhyML 3.0 (http://www.atgc-montpellier.fr/phyml/, Guindon *et al.,* 2010) with the automatic model selection by SMS (Lefort *et al.*, 2017) and 1000 bootstrap replicates. MEGA7 (Kumar *et al.*, 2016) was used to visualize the final tree. For the concatenated tree (18S+28S), a GTR model was applied to the alignments with 1000 bootstrap replicates.

Table III-2. Species of Thalassiosirales used for the phylogenetic analyses. Porosira pseudodenticulata *(Thalassiosirales) and* Lithodesmium undulatum *(Lithodesmiales) were used as outgroups.*

Species	Culture strain	SSU accession number	LSU accession number	Reference
Bacterosira bathyomphala	NB04_B6	DQ514894	DQ512444	Alverson *et al.*, 2007
Bacterosira constricta (formerly *Thalassiosira minima*)	CCMP991	DQ514877	DQ512426	Alverson *et al.*, 2007 Luddington *et al.*, 2012
Bacterosira constricta (formerly *T. constricta*)	SMDC01286	KT692951	KT692948	Park *et al.*, 2016
Thalassiosira angulata	BEN02_35	DQ514867	DQ512416	Alverson *et al.*, 2007
Thalassiosira anguste lineata	BEN02_30	DQ514865	DQ512414	Alverson *et al.*, 2007
Thalassiosira antarctica	CCMP982	DQ514874	DQ512423	Alverson *et al.*, 2007
Thalassiosira cf pacifica	FB02_35	DQ514888	DQ512438	Alverson *et al.*, 2007
Thalassiosira curviseriata	-	HM991690	HM991675	Direct submission by Park *et al.*, 2010
Thalassiosira eccentrica	BER02_09	DQ514868	DQ512417	Alverson *et al.*, 2007
Thalassiosira gessneri	ANO2_08	DQ514864	DQ512413	Alverson *et al.*, 2007
Thalassiosira minima	CCMP990	DQ514876	DQ512425	Alverson *et al.*, 2007
Thalassiosira minuscula	CCMP1093	DQ514882	DQ512431	Alverson *et al.*, 2007
Thalassiosira nodulolineata	BEN02_33	DQ514866	DQ512415	Alverson *et al.*, 2007
Thalassiosira nordenskioeldii	FB02_19	DQ514886	DQ512436	Alverson *et al.*, 2007
Thalassiosira profunda	X9III12	KC284713	Not available	Alverson, 2014
Thalassiosira pseudonana	CCMP1057	DQ514880	DQ512429	Alverson *et al.*, 2007
Thalassiosira punctigera	FB02_06	DQ514885	DQ512435	Alverson *et al.*, 2007
Thalassiosira rotula	CCMP1812	DQ514884	DQ512433	Alverson *et al.*, 2007
Thalassiosira sp.	CCMP1065	DQ514881	DQ512430	Alverson *et al.*, 2007
Thalassiosira sp.	CCMP353	DQ514871	DQ512420	Alverson *et al.*, 2007
Thalassiosira tumida	CCMP1469	DQ514883	DQ512432	Alverson *et al.*, 2007
Minidiscus comicus	SC72	Not available	JQ657759	Gu *et al.*, 2012
Minidiscus comicus	MCXM01	Not available	JQ657758	Gu *et al.*, 2012
Minidiscus proschkinae	SMDC305	KY912618	KY912621	Park *et al.*, 2017
Minidiscus spinulatus	SMDC050	Too short	KY912619	Park *et al.*, 2017
Minidiscus spinulatus	SMDC303	KY912617	KY912620	Park *et al.*, 2017
Minidiscus spinulosus	SSND12	Not available	JQ657760	Gu *et al.*, 2012
Minidiscus trioculatus	CCMP496	FJ590768	Not available	Kaczmarska *et al.*, 2009

M. trioculatus var. *monoculatus*	MiniNova	FJ590769	Not available	Kaczmarska *et al.*, 2009
Minidiscus variabilis (formerly *M. trioculatus*)	CCMP495	DQ514872	DQ512421	Alverson *et al.*, 2007 Kaczmarska *et al.*, 2009
Skeletonema grethae (Labeled in GenBank as *S. costatum*)	CCAP1077/3	AY684941	DQ512445	Alverson and Kolnick, 2005
Skeletonema grevillei	CCMP1685	DQ396512	DQ396495	Sarno *et al.*, 2007
Skeletonema japonicum (Labeled in GenBank as *S. costatum*)	NB02_45	AY684968	DQ512450	Alverson and Kolnick, 2005
Skeletonema menzelii	CCMP787	DQ011161	DQ512449	Alverson and Kolnick, 2005
Skeletonema potamos	AJA010_19	KJ081747	KJ081744	Direct submission by Alverson (2014)
Skeletonema pseudocostatum	CCAP1077/7	AY684952	DQ512447	Alverson and Kolnick, 2005
Skeletonema subsalsum	CCAP1077/8	AY684962	DQ512448	Alverson and Kolnick, 2005
Outgroups				
Lithodesmium undulatum	CCMP1806	DQ514846	DQ512393	Alverson *et al.*, 2007
Porosira pseudodenticulata	CCMP1433	DQ514848	DQ512396	Alverson *et al.*, 2007

Morphological characterization

Cultures in exponential growth phase were observed under a light microscope (Olympus BX51, Tokyo, Japan) with 40x or 100x objectives and a differential interference contrast. Cultures were imaged with a SPOT RT-slider camera (Diagnostics Instruments, Sterling Heights, MI, USA).

Besides, cultures were harvested by gravity on a 0.8 µm polycarbonate filter (Nuclepore, Whatman), dried for 2h at 56°C, and coated with a metallization process. The filters were mounted on stubs and adhesive paper and observed using a scanning electronic microscopy (SEM, Phenom G2 Pro, PhenomWorld) operating at 10 kV. Cell diameters were estimated from the SEM pictures.

Temporal dynamics

To study the seasonal dynamics of nanoplanktonic diatoms, we used the SOMLIT-Astan eukaryotic (V4 region of the 18S ribosomal RNA gene, ~380 bp) metabarcoding dataset obtained for the >3 µm size fraction (see Part I for detailed protocols of data acquisition). This dataset consists of OTU abundance reads data for 188 dates over the period 2009-2016. OTUs showing a total abundance higher than 10 reads were selected (8 788 OTUs). Read abundances of OTUs for which sequences were 100 % similar to those of *Minidiscus* and *Thalassiosira* nanoplanktonic strains isolated from our monitoring station were retrieved from this dataset using the blastn tool on Geneious 9.1.3. Note that metabarcoding data corresponding to 25 sampling dates were deleted from the dataset (total number of reads very low compared to that of other dates). Most of these dates corresponded to a period between 2014 and 2015.

Isolations of parasites

In order to test for the presence of parasites infecting nanoplanktonic diatoms at the SOMLIT-Astan monitoring station, we used established isolates of *Minidiscus* spp. and *Thalassiosira* spp. (Table III-1, diatoms in bold from May 2015) both to amplify and isolate potential lytic biological agents (for details, see Part I). Briefly, prefiltered (150 µm) natural seawater was enriched with F/2 medium and fresh diatom cultures and incubated for 2 weeks under the hosts culture conditions described above. This enrichment culture was clarified by filtration (GF/F filters, Whatman, estimated pore size 0.7 µm and 0.22 µm PES filter, Whatman). 0.5 mL of GF/F and 0.22 µm filtered aliquots were added to 1.5 mL host cultures in 24-multiwell plates. Cultures were inspected by light microscopy two weeks after inoculation. If algal lysis was observed, 3 extinction dilution cycles were carried out to clone the pathogens (Suttle, 1993). Parasite prospection was conducted using samples collected between October 2015 and October 2016. Isolates obtained after a 0.2 µm filtration were considered as potential viruses while those obtained after a filtration through GF/F filters could not be assigned to any specific parasite group. New filtrations on 0.22 µm were repeated to verify the transferability and the size range of clonal parasites.

Cryopreservation

Resistance to cryopreservation was tested on a subset of diatom strains. Briefly, 10% DMSO (final concentration) were added to 1 mL of culture in a cryogenic tube. Cultures were progressively frozen with an incubation at 20°C, a decrease of temperature of 1°C per minute until -40°C, which was maintained for 10 min. Samples were transferred to liquid nitrogen before storage at -150°C for one month. After this period of time, cultures were thawed in a 25°C water bath for 3 min. The 1 mL cultures were transferred to 20 mL of K+Si and kept at 18°C and in the dark to avoid light stress. After 24h, culture were placed in optimal light conditions and growth was monitored for one month by optical microscopy (Day and Brand, 2005; Roscoff Culture Collection http://roscoff-culture-collection.org/protocols/cryopreservation).

Accession numbers

Sequences obtained from the eukaryotic nuclear rRNA/ITS will be deposited in the NCBI database.

RESULTS

Morphogenetic characterization of nanoplanktonic diatoms from the French coasts of the Western English Channel

Three species of *Minidiscus* (*M. comicus, M. spinulatus* and *M. variabilis*) and three species of *Thalassiosira* (*T. curviseriata*, *T. profunda* and *Thalassiosira* sp.) were identified based on the morphogenetic characterization of 11 strains isolated in May 2015 from the SOMLIT-Astan time-series station (Table III-1).

Minidiscus comicus

Morphological features of RCC4660, RCC4661 and RCC4662 were identical to that of *M. comicus* (Jewson *et al.*, 2016; Takano, 1981): cells were solitary or aggregated in pairs (Figure III-1, A and B) and had an ovoid shape when observed in girdle view (Figure III-1, A and C). The valve was circular and 4.8 ± 0.6 µm (n=71) in diameter (Figure III-1, B). The doomed valve face was covered by areolae (Figure III-1, B and D). A long and central rimoportula was surrounded by 3-4 fultoportulae. A maximum of 5 strutted processes have been observed on some specimens. External tubes of the fultoportulae were shorter than the one of the rimoportula. Excretion of mucilaginous threads by the fultoportulae allowed connections between cells (Figure III-1, A and D).

In our phylogenetic analyses of the 18S, partial 28S and concatenated 18S+28S sequences, the strains RCC4660, RCC4661 and RCC4662 (100% identical 18S sequences) appeared as a distinct branch in a clade that contained ribosomal sequences of *Skeletonema* (Figure III-3, A and B, Figure III-4). The partial 28S rDNA gene sequences of these three *M. comicus* isolates (sequence similarity 99.9%) gathered with *M. comicus* SC72 and MCXM01 with a high bootstraps (100% value). They formed, together with a sequence belonging to *M. spinulosus* SSBH12*,* a highly supported sub-clade (100% bootstraps value) in a clade that included sequences of the genus *Skeletonema* (Figure III-3, B).

Minidiscus spinulatus

Morphological features of RCC4649 was identical to that of *M. spinulatus* (Park *et al.*, 2017). Cells were solitary or aggregated in colonies of 2-3 cells (Figure III-1, E). As described in Park *et al.* (2017) valve face was flat, with a circular shape and was 5.3 ± 0.4 µm (n=16) in diameter (Figure III-1, F). On the valve face, true areolae were absent and were replaced by granules or Y-shaped ribs according to the silicification of the frustule (Figure III-1, F, G and H). A sub-central rimoportula with an ellipsoidal shape was adjacent to a central fultoportula. External tube of the fultoportula was short and surrounded by a hyaline flange. On the valve margin, the cell possessed a ring of 5-8 fultoportulae (Figure III-1, F, G and H). *M. spinulatus* is the only species within this genus with a marginal ring of strutted processes (Park *et al.*, 2017).

In phylogenies reconstructed based on the 18S rDNA, partial 28S rDNA sequences and on the concatenation of both genes, RCC4659 clustered with two other strains of *M. spinulatus* (91% bootstrap value) and were closely related to sequences of the species *M. proschkinae* (97%) and *M. variabilis* (Figure III-3, B, Figure III-4).

Minidiscus variabilis

The morphological of RCC4657, 4758, 4665 and 4666 strains fitted with that of *M. variabilis* or *trioculatus* (Kaczmarska *et al.*, 2009). Solitary cells (Figure III-1, I) had with a cylindrical shape and a wide and marginal hyaline flange (Figure III-1, J, K and L). The valve (3.4 ± 0.3 µm in diameter, n=63) was covered by loculate areolae with a tangential-linear organization. The valve presented a sub-central and small labial process and a varying number of fultoportulae (2-4 and very rarely 5). For most cells, one fultoportula was located in the

central region of the valve while the others were dispersed throughout the valve face. Ornamentations in the base of each fultoportula were lacking. Even if the majority of the cells had a tangential-linear areolation (a feature of *M. trioculatus* according to (Kaczmarska *et al.* (2009)), some specimens showing radial areolation (a feature of *M. variabilis* according to Kaczmarska *et al.*, (2009) were observed (Figure III-1, L).

The 18S rDNA gene sequences of strains RCC4657, RCC4658, RCC4665, RCC4666 showed 100% of identity with sequences of *M. variabilis* CCMP495 (Figure III-3, A). Similarly, the 28S rDNA gene sequences of the four strains (that were 100 % identical) were also identical to that of *M. variabilis* CCMP495 (Figure III-3, B).

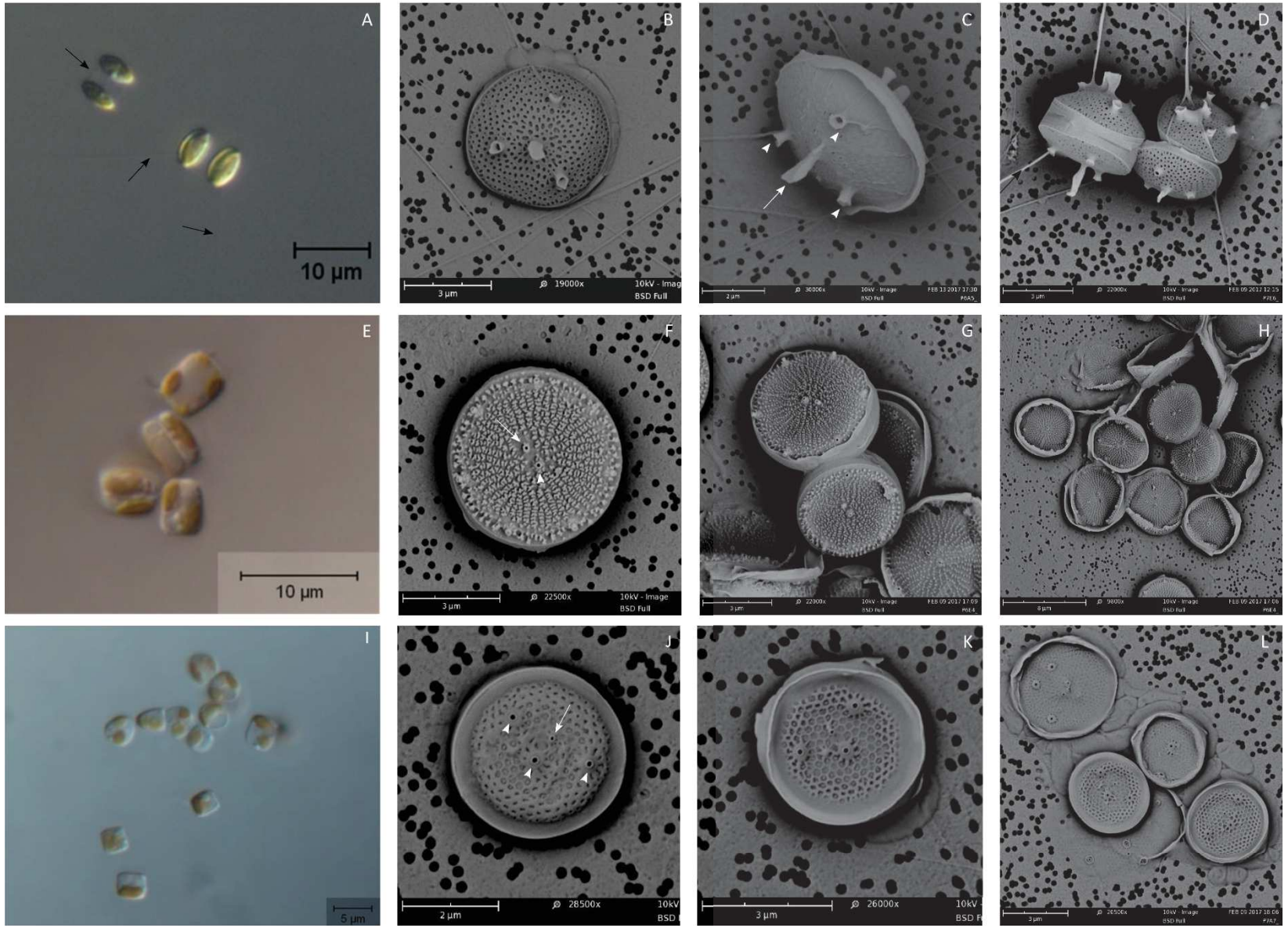

Figure III-1. LM and SEM micrographs of Minidiscus *species. **A** to **D**.* M. comicus. ***A**. Pairs of cells connected by mucilaginous threads (LM). **B, C, D**. External views of solitary cells (SEM). **E** to **H**.* M. spinulatus. ***E**. Aggregated and solitary cells (LM). **F, G, H**. Valves views. Note the Y-shaped ribs and the fultoportulae ring on the margin (SEM). **I** to **L**.* M. variabilis. *I. Solitary cells (LM). **J, K, L**. External view valves. Black arrows: threads connecting cells. White arrow: Rimoportula. White arrowheads: Fultoportulae*

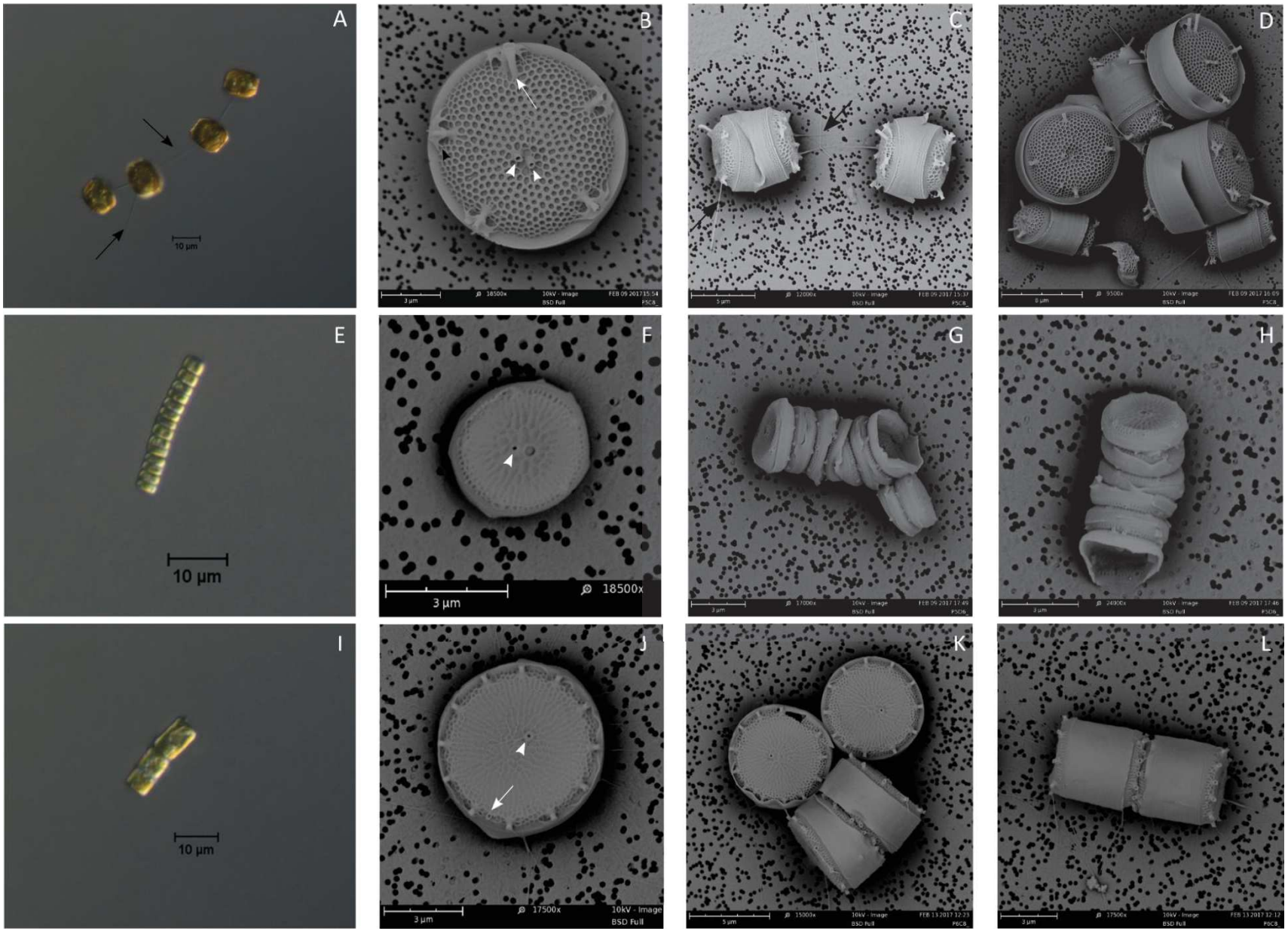

Figure III-2. LM and SEM micrographs of Thalassiosira *species.* ***A*** *to* ***D.*** T. curviseriata*.* ***A****. Chain of cells connected by thread (LM).* ***B****. External valve view of solitary cells (SEM). Black arrowhead indicates the winged fultoportulae.* ***C****. Girdle view of connected cells.* ***D****. External view of large and small cells of* T. curviseriata *(SEM).* ***E*** *to* ***H****.* T. profunda*.* ***E.*** *Long chain of cells (LM).* ***F****. Solitary cell in a valve view. Note the large areola adjacent to the central fultoportula (SEM).* ***G*** *and* ***H****. Girdle views of chains (SEM).* ***I*** *to* ***L.*** Thalassiosira *sp..* ***I****. Chains of cells (LM).* ***J****. Valve external view of a solitary cell (SEM).* ***K*** *and* ***L****. External views of solitary and cells associated in pair (SEM). Black arrows: threads connecting cells. White arrow: Rimoportula. White arrowheads: Fultoportulae*

Thalassiosira curviseriata

The morphological features of strain RCC5154 fitted with that described by Takano (1981) for *Thalassiosira curviseriata*. Cells (6.7 ± 2.4 µm in diameter, n=9) were connected in chains by threads (Figure III-2, A and C). As described in Takano (1981) the circular valve possessed a radial areolation and was encircled by a hyaline mantle. Strutted processes (1-2) were in the central region while a ring of 3-5 fultoportulae was disposed on the margin of the cell. Two conspicuous wings were attached in the middle of each fultoportula. A unique and long labial process was located close to a marginal fultoportula (Figure III-2, B). The micrograph D illustrates the size and ornamentation variabilities that can occur in culture conditions.

Ribosomal DNA gene sequences of *T. curviseriata* RCC5154 clustered with other published sequences of *Thalassiosira curviseriata* in the 18S and 28S rDNA gene phylogenetic trees (99% and 98% bootstrap values respectively) (Figure III-3, A and B).

Thalassiosira profunda

The morphological features of strain RCC4663 fitted with that of *Thalassiosira profunda* (Hallegraeff, 1984; Park *et al.*, 2016b). Cells were tightly associated to form long chains and appeared rectangular in girdle view (Figure III-2, E). As in Park *et al.* (2016b), valve face was flat, 3-3.3 µm (n=2) in diameter and was covered by a radial lines of areolae. A ring of marginal areolae was also present (Figure III-2, F). In the central region, a single fultoportula was adjacent to a large areola (F and H). A ring of fultoportulae was disposed on the margin (Figure III-2, F, G and H). No rimoportula could be observed.

The 18S rDNA gene sequence of *T. profunda* RCC4663 was 99% similar to that of *Thalassiosira profunda* X9lll12. The two sequences formed a highly supported clade (100% bootstrap support) that emerged in a clade containing *T. anguste lineata*, *T. nodulolineata* and *T. pacifica* (Figure III-3, A).

Thalassiosira sp.

Strain RCC4664 had morphological features that fitted with that of the genus *Thalassiosira* (Hasle, 1978). Valves of the cylindrical cells (5.6 ± 0.7 µm, n=16) that were associated in chains (Figure III-2, I and L) possessed a sub central fultoportula and one ring of 8-15 marginal fultoportulae. A short marginal rimoportula was also present between two fultoportulae (Figure III-2, J, K and L). These features did not correspond to that of any described species of *Thalassiosira*.

Our phylogenetic analyses did not provide any additional information on the affiliation of this strain to known species in the Thalassiosirales radiation (Figure III-3, A and B, Figure III-4).

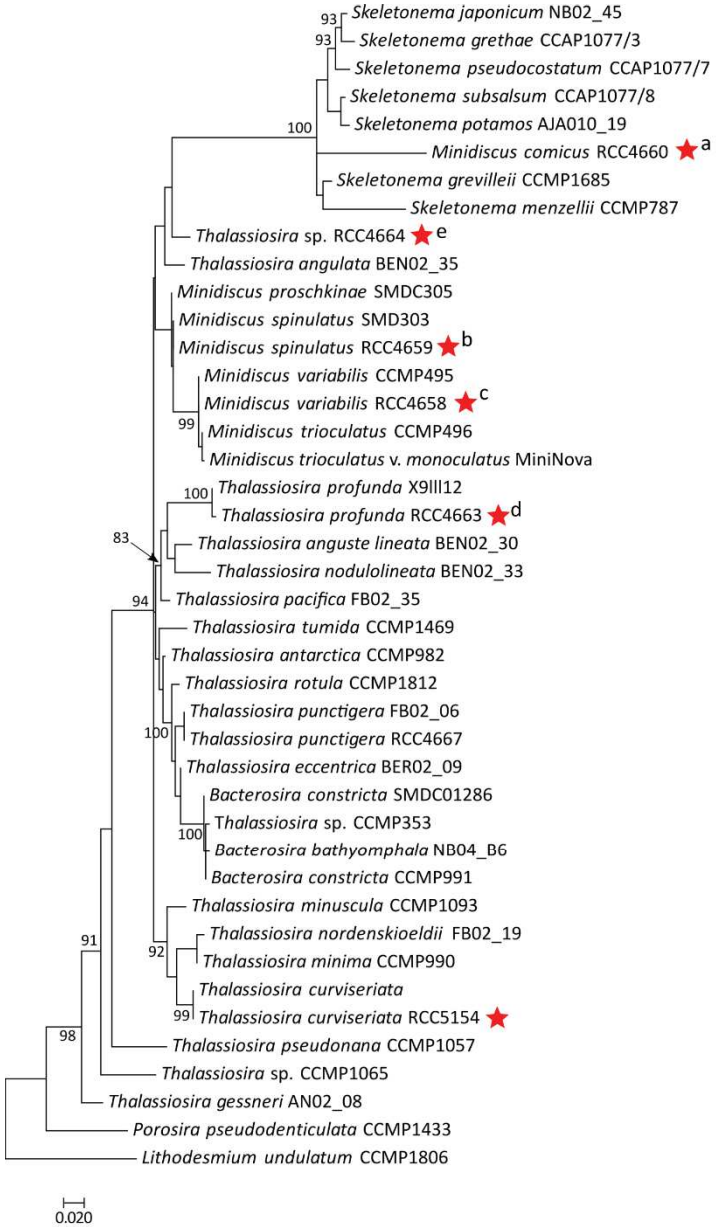

*Figure III-3. Phylogenetic rooted tree based on the 18S (**A**) and partial 28S (**B**) sequences of diatoms from the Thalassiosirales order.* Porosira pseudodenticulata *and* Lithodesnium undulatum *were taken as outgroups. The red stars indicate the positions of strains for which morphogenetic characterizations were achieved in the frame of this study. Both Maximum Likelihood trees were generated using PhyML 3.0 with 1 000 replicates and a GTR+G+I substitution model according to the SMS analyses. Bootstraps values (%) greater than 80 are shown. Scale bars indicate the number of substitutions per site. Letters in superscript indicate that several strains had identical sequences.* [a]*:* Minidiscus comicus *strains RCC4660, RCC4661, RCC4662 and RCC5839 to RCC5859.* [b]*:* Minidiscus spinulatus *strains RCC4659, RCC5860 and RCC5861.* [c]*:* Minidiscus variabilis *strains RCC4657, RCC4658, RCC4665, RCC4666 and RCC5862 to RCC5880.* [d]*:* Thalassiosira profunda *strains RCC4663 and RCC5881 to RCC5886.* [e]*:* Thalassiosira *sp. RCC4664 and RCC5887*

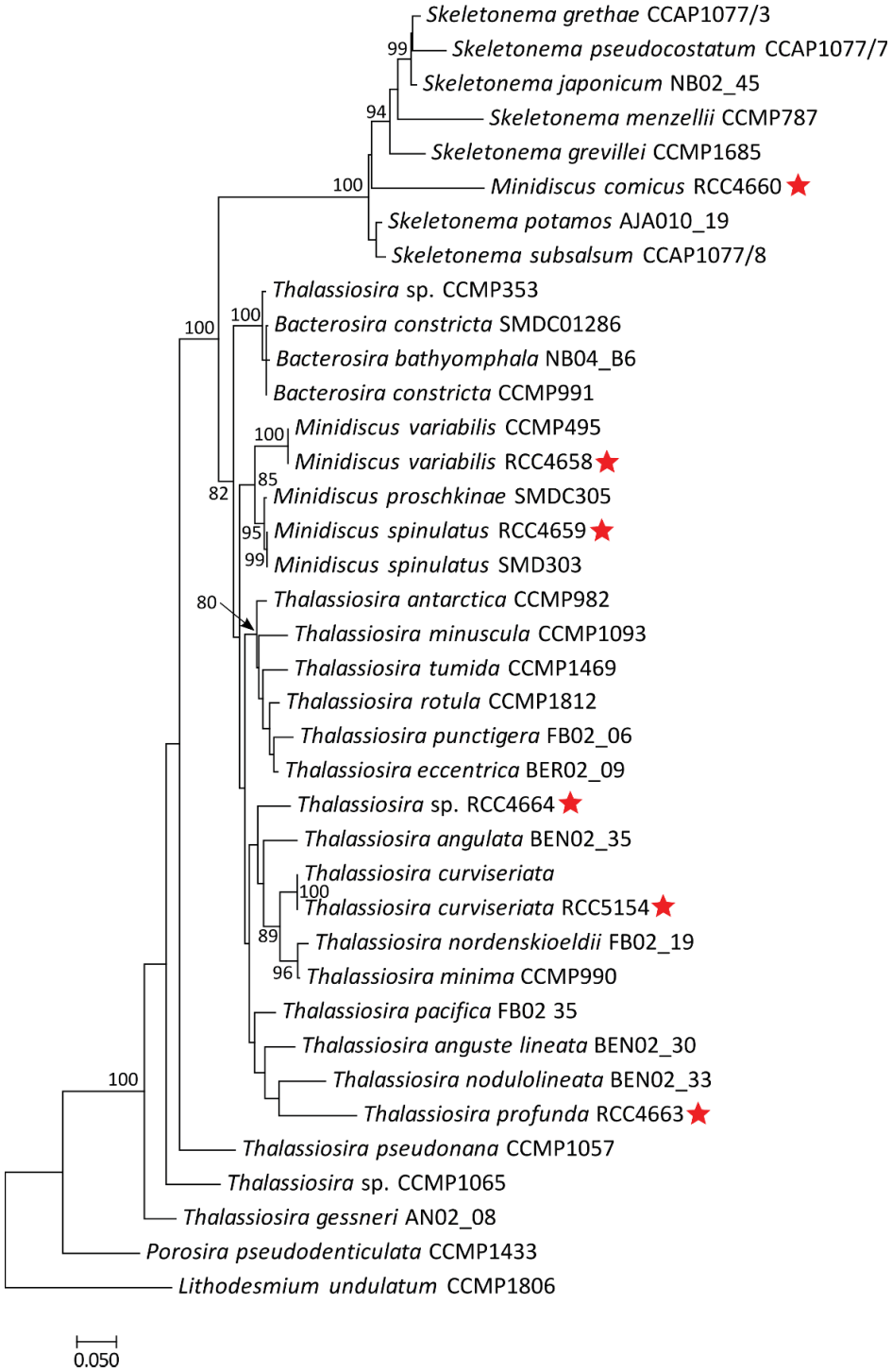

Figure III-4. Phylogenetic rooted tree based on concatenation of the 18S and partial 28S sequences of diatoms from the Thalassiosirales order. Porosira pseudodenticulata *and* Lithodesmium undulatum *were taken as outgroups. The red stars indicate the positions of the reference strains. The Maximum Likelihood tree was generated using PhyML 3.0 with 1000 replications and a GTR substitution model. Bootstraps values (%) greater than 80 are shown. Scale bar indicates the number of substitutions per site*

Prevalence and seasonal dynamics of nanoplanktonic diatoms over the 2009-2016 period

In order to get a sense of the contribution of nanoplanktonic diatoms to the diatom assemblage over a seasonal cycle at our SOMLIT-Astan station, we used two strategies. The first one consisted of analyzing eukaryotic metabarcoding data obtained for this station over the period 2009-2016 (*in situ* approach). More precisely we analyzed the temporal dynamics of abundances of OTUs of which sequences corresponded to those of the nanoplanktonic diatoms described above. Our second strategy was to conduct isolations and genetic characterizations of diatom strains along a full seasonal cycle (October 2015 to October 2016) (culture approach).

For the *in situ* approach, exact matches of the V4-18S sequences of the *Minidiscus* and *Thalassiosira* strains described in this study were searched in the metabarcoding dataset obtained at the SOMLIT-Astan station over the period 2009-2016 (8 788 OTUs and 14 292 629 reads in total). The contribution of OTUs related to diatoms (608 in total) accounted for 17% of the total number of reads in the whole dataset. OTUs with sequences 100% similar to that of *M. variabilis* and of *M. comicus* ranked first and second in read abundances (comprising 13.2% and 7.5% of reads assigned to diatoms, respectively) (Figure III-5). The OTU assigned at 100% to *M. spinulatus* RCC4659 contributed 1.3 % to total diatom reads while OTUs related to *Thalassiosira curviseriata* (100% identity with strain RCC5154), *T. profunda* RCC4663 (with 99.7% sequence similarity), and *Thalassiosira* sp. RCC4664 (100%) contributed respectively to 1.9%, 1.6%, and 1.2% of the total diatom reads abundance. Contribution of these nanoplanktonic diatoms to the total eukaryotic read pool was also significant. For example, the OTU assigned to *M. variabilis* ranked as the fifth position in terms of read abundance (2.2% of all eukaryotic read counts).

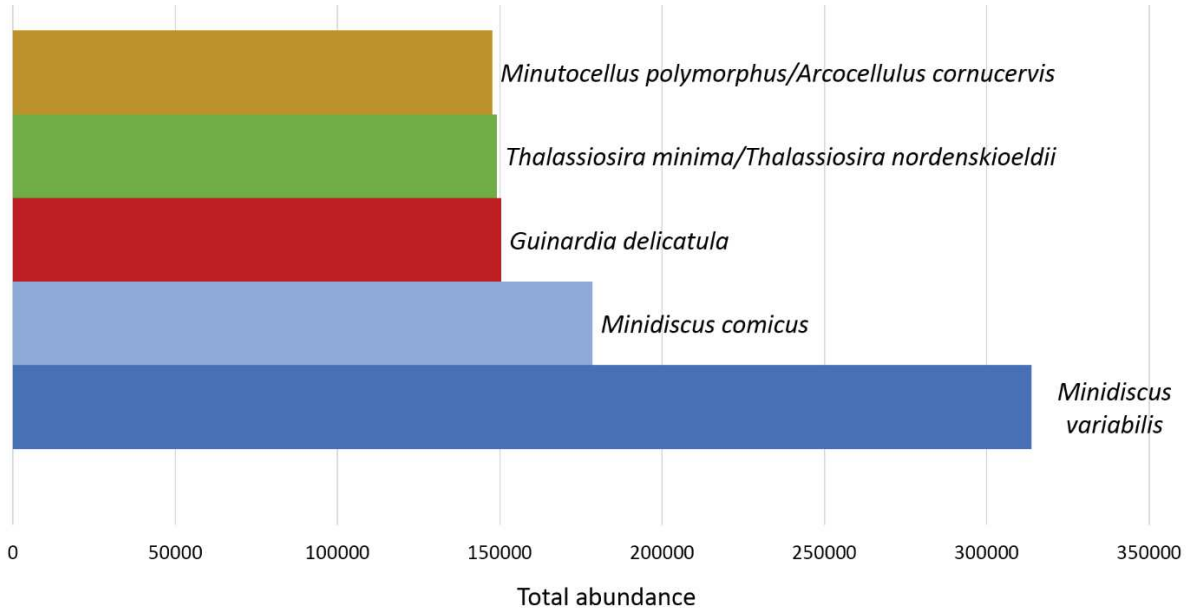

Figure III-5. Taxonomic assignations of the 5 most abundant OTUs related to Bacillariophyta at SOMLIT-Astan. The total abundance represents the reads number for 8 years of metabarcoding survey. Minidiscus variabilis *and* Minidiscus comicus *were related respectively to the first and second most abundant OTUs*

Abundances of reads assigned to *M. variabilis* appeared highly variable at the SOMLIT-Astan station over the period studied and no clear seasonal patterns of variations were detected (Figure III-6, C). However, variations in read abundances of all other nanoplanktonic diatoms studied showed clear seasonal patterns. *M. comicus* read abundances peaked during winter, generally from January to March, while very low abundances were recorded during the rest of the year for the OTU related to this species (Figure III-6, A). *M. spinulatus* seemed to develop from autumn to early spring while lower abundance values were recorded during summer (Figure III-6, B).

According to the molecular analyses, *T. curviseriata* development occurred mainly during spring (late March to early June) (Figure III-7, A) while abundances of the OTU related to *T. profunda* peaked principally during winter (Figure III-7, B). The seasonal signal associated to variations in abundances of the OTU related to *Thalassiosira* sp. RCC4664 was less clear. Peaks were generally recorded during winter (January-February) and during summer (end of June-early July) (Figure III-7, C).

All the species demonstrated fluctuations in the amplitude of their seasonal peaks from year to year. For example, the OTUs related to the three *Minidiscus* species reached exceptionally high read abundances in February 2012 (12 524, 10 891, and 1 267 reads respectively for *M. comicus, M. variabilis* and *M. spinulatus* (Figure III-6, A-C)). Similarly, read abundances related to *T. curviseriata* were relatively low all along the year in 2013 (no spring peak) while exceptionally high abundances were recorded in March 2015 (5 380 reads) (Figure III-7, A). For the OTU related to *T. profunda,* abundances recorded during the period 2009-2011 were comparatively lower than those recorded during the period 2012-2016 (Figure III-7, B).

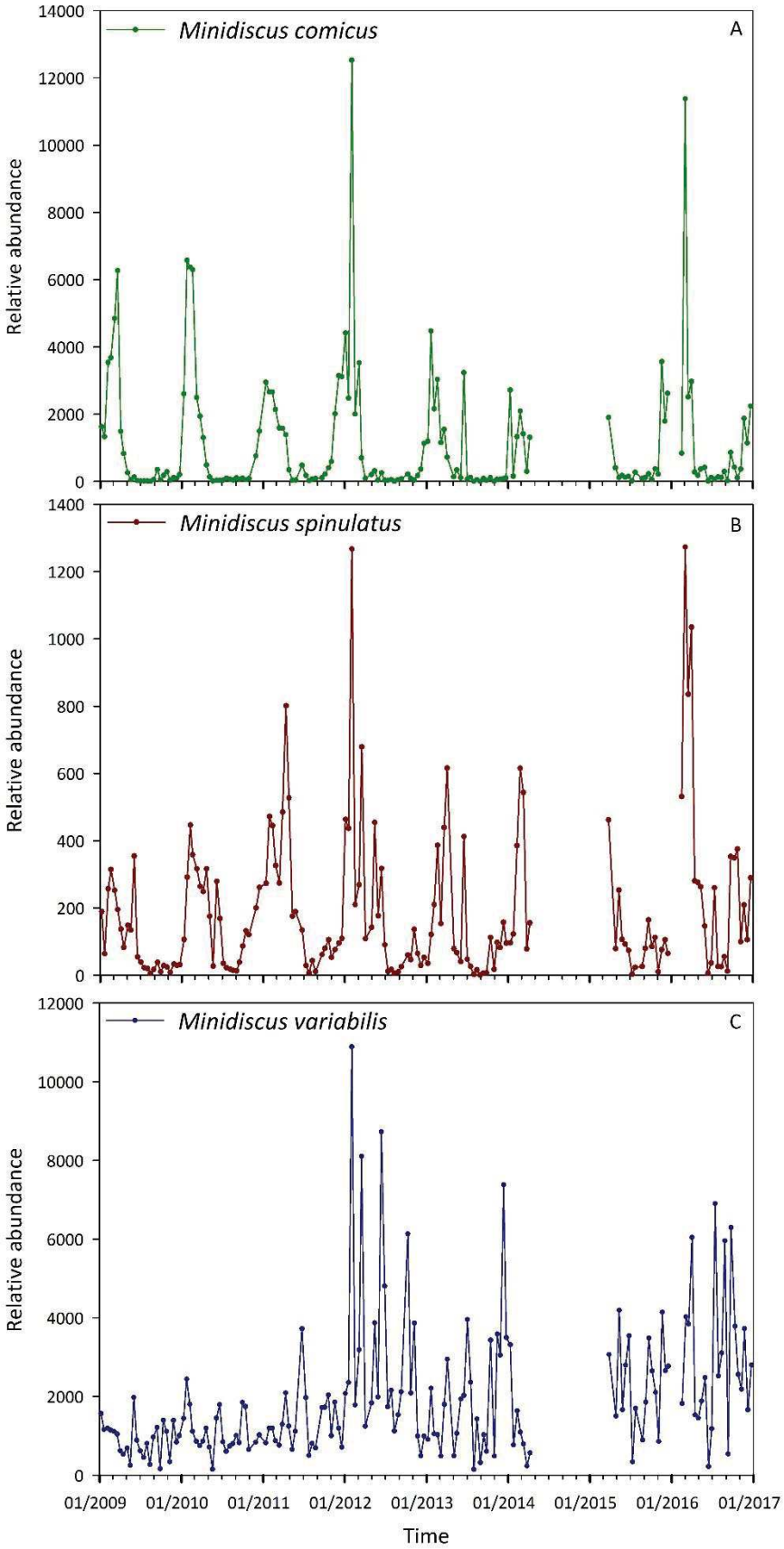

Figure III-6. Temporal dynamics of the OTUs related to ***A***. Minidiscus comicus*,* ***B***. Minidiscus spinulatus*, and* ***C***. Minidiscus variabilis *at the SOMLIT-Astan station during the period 2009-2016. Note that metabarcoding data corresponding to 25 sampling dates (mainly between 2014 and 2015) were deleted from the dataset*

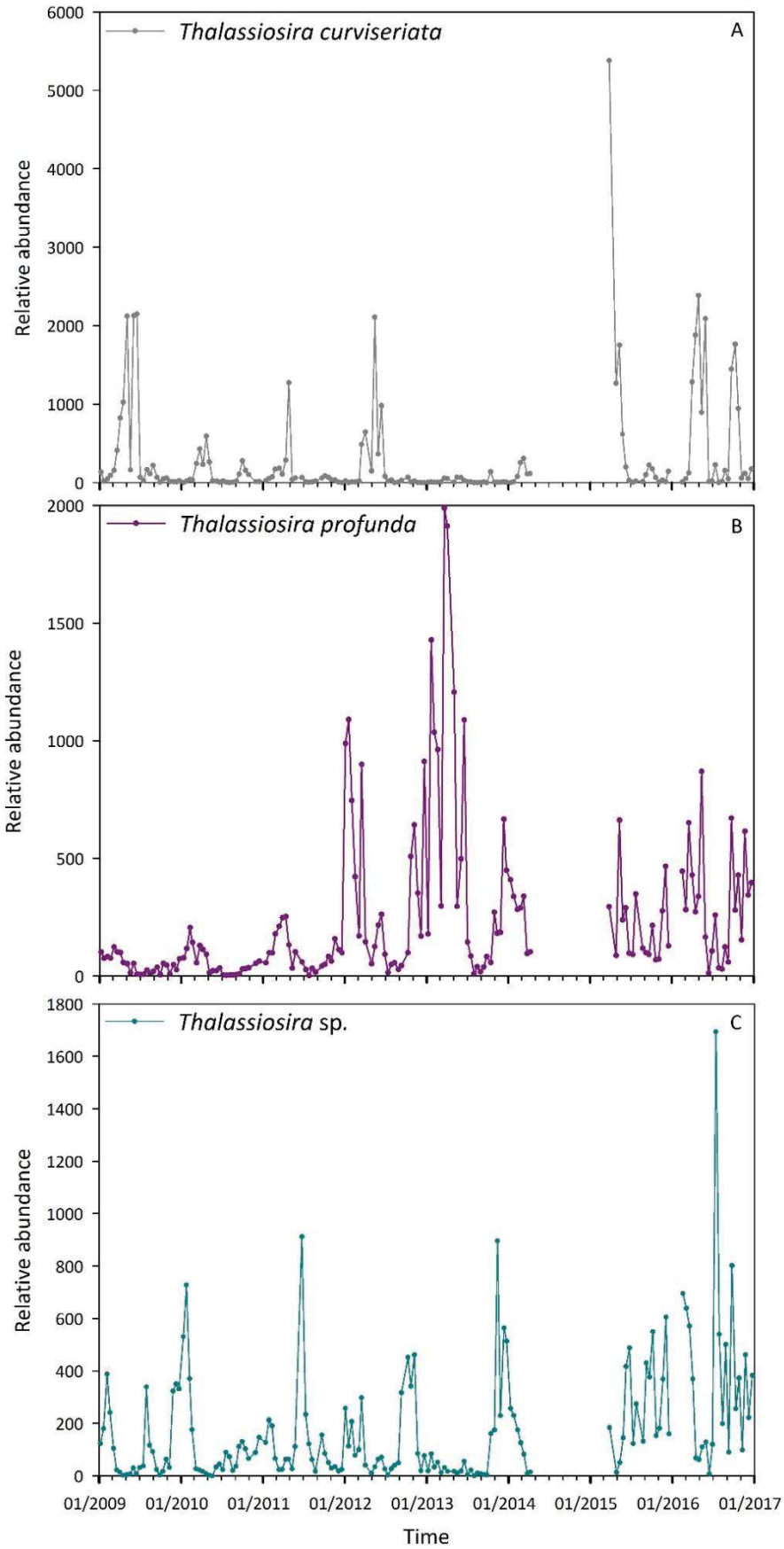

*Figure III-7. Temporal dynamics of the OTUs related to **A**.* Thalassiosira curviseriata*, **B**.* Thalassiosira profunda*, and **C**.* Thalassiosira *sp. at the SOMLIT-Astan station during the period 2009-2016. Note that metabarcoding data corresponding to 25 sampling dates (mainly between 2014 and 2015) were deleted from the dataset*

The temporal patterns described above rely on the correct assignment of OTUs to the targeted species, i.e. on the assumption that the chosen barcode is sufficiently variable to distinguish between species, which appears to be the case for the studied nanoplanktonic diatoms. However, a second strategy was developed using culture approaches and sequencing of the full 18S rDNA gene and ITS spacer. This strategy was adopted to confirm that the three species of *Minidiscus* and the three species of *Thalassiosira* that we identified were present at our sampling station, at least during the periods when peaks of read abundances of the corresponding OTUs were recorded. It also allowed us to study the infra-specific genetic variability of each species over a seasonal cycle. In total, 49 new nanoplanktonic isolates were obtained from which the 18S rDNA gene sequences and ITS spacer sequences were analyzed and compared to those of the fully characterized nanoplanktonic species recorded at SOMLIT-Astan (Table III-1).

With this strategy, we obtained isolates of the three *Minidiscus* species as well as of *Thalassiosira profunda* and *Thalassiosira* sp. RCC4664 (Figure III-8 and Figure III-9). 19 new isolates whose 18S rDNA gene sequences were 100 % similar to those of *M. variabilis* RCC4657, RCC4658, RCC4665 and RCC4666 as well as to that of strain CCMP495 were obtained (Table III-1, Figure III-3, A). Cells were isolated all along the seasonal cycle, corroborating the dynamics of OTU reads (Figure III-8, A and B). The 17 ITS sequences obtained for isolates of *M. variabilis* showed very low variability (only two strains demonstrated one variable nucleotide in the 522 bp alignment). Isolates for which 18S rDNA gene sequences matched 100% with that of *M. comicus* RCC4660, RCC4661 and RCC4662 (21 isolates) and of *M. spinulatus* RCC4659 (2 isolates) were obtained respectively in winter and spring (between end of November 2015 and May 2016) and in March (Table III-1, Figure III-3, A and Figure III-8, B). These periods corresponded to blooms of the corresponding species, as suggested by the metabarcoding data (Figure III-8, A). The *M. comicus* strains isolated from our SOMLIT-Astan sampling station (RCC4660, RCC4661, RCC4662 and RCC5839 to RCC5859) showed 99.6% identity between ITS sequences, with only 2 divergent nucleotide sites (540 bp). ITS sequences of *M. spinulatus* RCC4659, RCC5860 and RCC5861 were also highly similar (97.6% identity, 537 bp alignment).

Despite the several peaks of *T. curviseriata*, no culture could be established from October 2015 to October 2016 (Figure III-9, A and B). 6 isolates identical to *T. profunda* (18S sequence similarity 100%) were isolated from winter, spring and early July when OTU related to this species was detected in the metabarcoding dataset (Figure III-9, A and B). ITS sequences analysis of strains RCC4663 and RCC5883 to RCC5886 revealed 95.7% of identity in the 571 bp alignment. Over one year, only one culture related to *Thalassiosira* sp. RCC4664 (18S sequences 100% identical) could be isolated in February 2016. However, the lack of molecular data hindered the link between field and laboratory works (Figure III-9, A and B). The 614 bp alignment of *Thalassiosira* sp. RCC4664 and RCC5887 indicated a rather high divergence with only 91.9% of identity, mainly due to an insertion of 46 nucleotides in the ITS sequence from RCC4664.

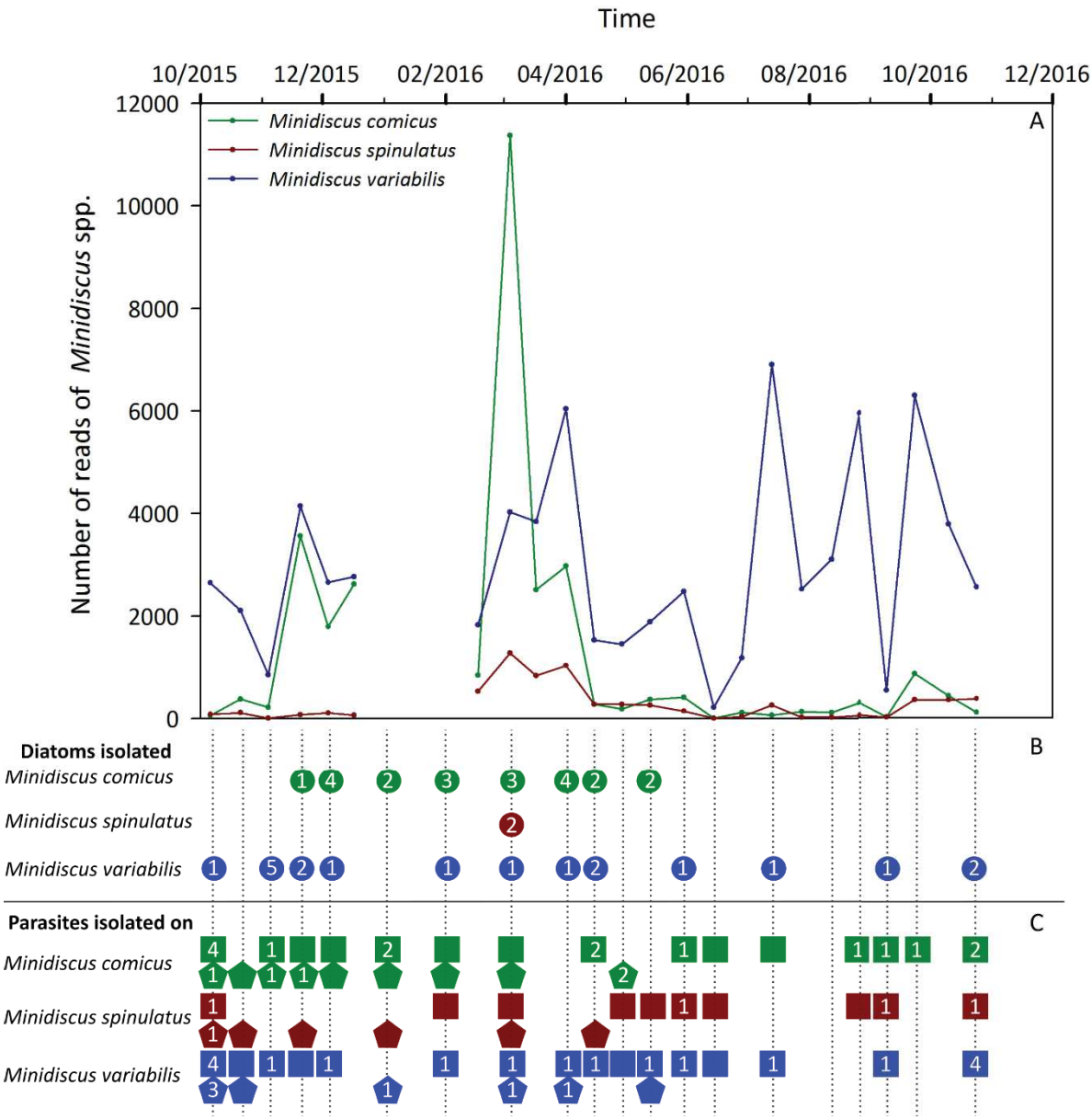

Figure III-8. ***A****. Temporal dynamics of the OTUs related to* Minidiscus comicus *(green line),* Minidiscus spinulatus *(red line), and* Minidiscus variabilis *(blue line) at the SOMLIT-Astan station during the 2015-2016 period. Ambiguous sequence abundances were removed from the dataset.* ***B****. Isolations of diatoms indicated by encircled numbers. Vertical dashed lines correspond to dates for which cell isolations were carried out.* ***C****. Isolations of parasites from* Minidiscus *species represented by squares and by pentagons (originated from fractions > 0.2 µm and < 0.2 µm respectively). Numbers indicate the parasites still maintained in the laboratory while empty squares and pentagons represent the cultures lost during the project*

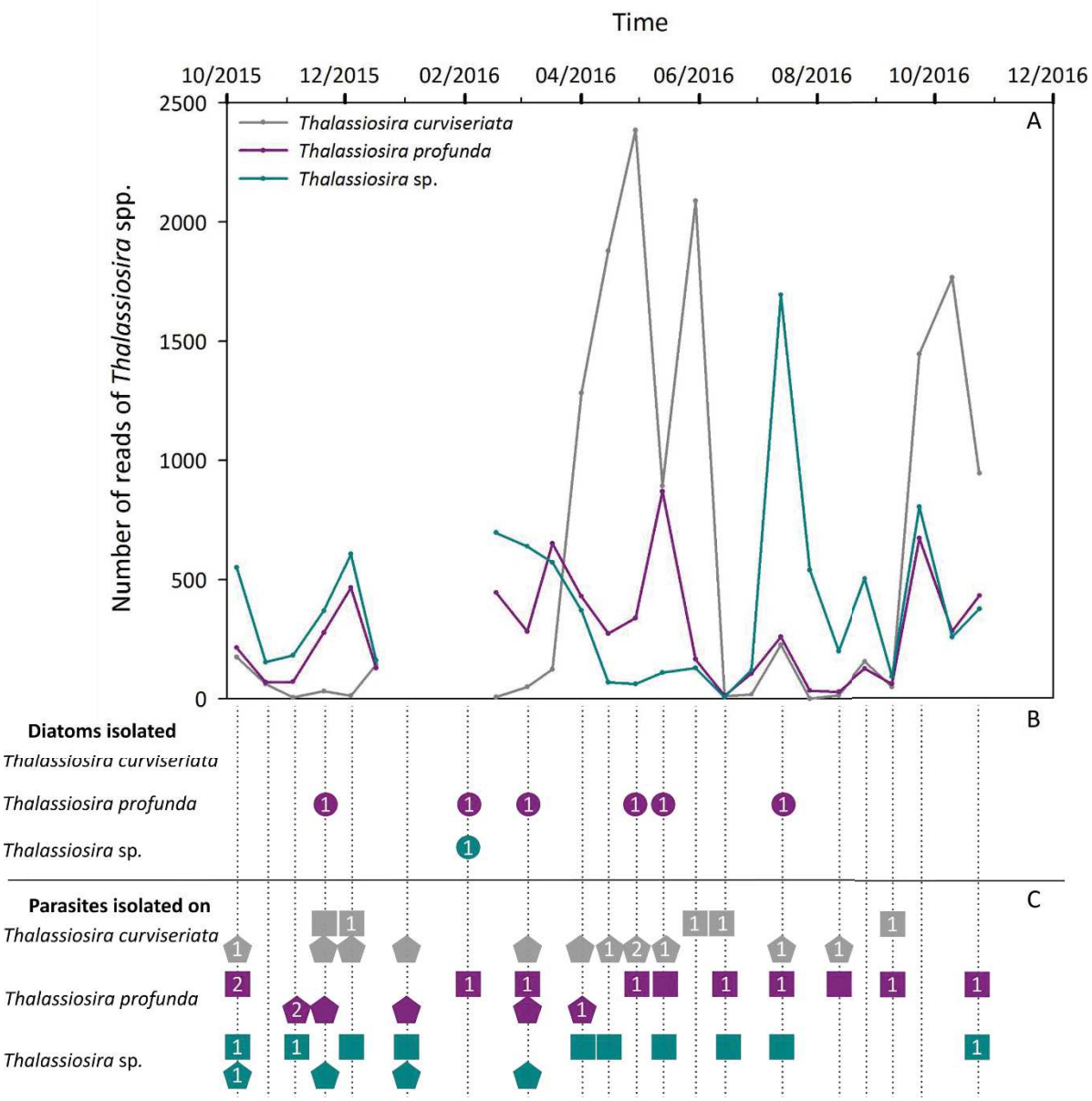

Figure III-9. ***A****. Temporal dynamics of the OTUs related to* Thalassiosira curviseriata *(grey line),* Thalassiosira profunda *(purple line) and* Thalassiosira *sp. (turquoise line) at the SOMLIT-Astan station during the 2015-2016 period. Ambiguous sequence abundances were removed from the dataset.* ***B****. Isolations of diatoms indicated by encircled numbers. Vertical dashed lines correspond to dates for which cell isolations were carried out.* ***C****. Isolations of parasites from* Thalassiosira *species represented by squares and by pentagons (originated from fractions > 0.2 µm and < 0.2 µm respectively). Numbers indicate the parasites still maintained in the laboratory while empty squares and pentagons represent the cultures lost during the project*

Parasite isolations along the seasonal cycle at the SOMLIT-Astan station

Minidiscus parasites were successfully isolated at each sampling date (except on August 12, 2016) (Figure III-8, C). Interestingly, isolations of parasites from the < 0.2 µm fraction (potential viruses) were successful only from October 2015 to May 2016, which roughly corresponded to the blooming periods of *M. comicus* and *M. spinulatus*. Parasites from the larger seawater fraction (> 0.2 µm) were isolated year round, regardless of the *Minidiscus* host species.

Thalassiosira parasites were also isolated throughout the year regardless of the prospected hosts (Figure III-9, C). Yet, the type of successfully isolated parasite varied depending on the host species and the time of the year. For *T. profunda* and *Thalassiosira* sp., the isolation patterns were strikingly similar to those of *Minidiscus* parasites. Parasites > 0.2 µm were isolated throughout the sampling period but putative viruses only between October 2015 and April 2016 (Figure III-9, C). Parasites associated to *T. curviseriata* showed a different isolation pattern as putative viruses were mostly isolated compared to > 0.2 µm parasites, and during the whole seasonal cycle. No clear relationship between the hosts blooming periods and the success of parasite isolations could be detected. Our analysis is however limited by missing data points.

Cryopreservation

A consequent diatom collection was generated in this study. In order to preserve it in a long-term, the strains RCC4661 (*M. comicus*), RCC4657 (*M. variabilis*), RCC5154 (*T. curviseriata*) and RCC4663 (*T. profunda*) were stored for one month at -150°C. After thawing out, strains RCC4661 and RCC4663 recovered in less than 2 weeks. Development of RCC4657 appeared later after 2-3 weeks of incubation and RCC5154 could not grow after being cryoconserved.

DISCUSSION

In this study, the results obtained using both environmental sequencing and culture approaches highlight that nanoplanktonic diatoms are key components of the phytoplankton community along the French coasts of the Western English Channel. We showed that these nanoplanktonic species developed seasonally at the SOMLIT-Astan times-series station. Since parasites (viruses and most probably bacteria) infecting these species were isolated either all year round or during bloom periods, we suspect that parasite-driven mortality is involved in their control.

Taxonomy and phylogeny of nanoplanktonic diatoms from the French coasts of the Western English Channel

Thalassiosirales are important components of phytoplankton populations in pelagic waters in the Western English Channel and North Sea (Guilloux *et al.*, 2013; Hoppenrath *et al.*, 2007; Widdicombe *et al.*, 2010) and nanoplanktonic species of this group have been recorded from these regions. This study revealed the presence of three species of *Minidiscus* (*M. comicus, M. spinulatus* and *M. variabilis*) as well as of three nanoplanktonic species of *Thalassiosira (T. curviseriata, T. profunda*, and a new undescribed *Thalassiosira* species).
Within the Thalassiosirales, the phylogenetic classification of genera is still under construction. Both new genera and emended descriptions of genera have been published over the last fifteen years (Alverson, 2008; Alverson *et al.*, 2006, 2011; Kaczmarska *et al.*, 2005; Park *et al.,*

2016a, 2017; Stachura-Suchoples and Williams, 2009). The genus *Minidiscus* is an example of taxon for which description has been recently emended (Park *et al.*, 2017). Originally described to include Thalassiosirales with central rimoportula and non-marginal fultoportulae, this taxon is now distinguished from other Thalassiosirales mainly by the size of its valve (< 10 µm) and both the position and structure of the rimoportula. However, this genus appears polyphyletic in phylogenies with two clades. *M. proschkinae*, *M. spinulatus* and *M. variabilis* form a monophyletic clade in multigene phylogenies (Park *et al.*, 2017 and this study), while *M. comicus* and *M. spinulosus* group together in a separate branch affiliated to species of the genus *Skeletonema* in phylogenies based on sequences of the partial 28S rDNA gene (Gu *et al.*, 2012 and this study).

In our study, a set of strains were assigned to species after examination of valves morphology using SEM. Comparisons of ribosomal sequences to published references served to confirm our conclusions. However, for *M. variabilis* it appeared that the main distinctive morphological character proposed by Kaczmarska *et al.* (2009), namely tangential-linear areolation for *M. trioculatus* and radial areolation for *M. variabilis*, was not adequate for a clear delineation of these species and a comparative analysis of ribosomal rRNA gene sequences was necessary.

Concerning *M. comicus* the morphological and genetic features of the isolated strains corroborated published records (Gu *et al.*, 2012; Jewson *et al.*, 2016; Takano, 1981). Our phylogenetic analyses, using both the 18S and 28S genes (only 28S gene sequences were available in public database prior to this study), confirms the position of *M. comicus* as sister species of *M. spinulosus* in a branch distant from the one that includes other species of *Minidiscus*. This suggests that *M. comicus* and *M. spinulosus* should be transferred to a novel genus in order to carry on in the construction of a phylogenetic classification of the order Thalassiosirales. But before this, careful examinations of morphological and genetic features of other *Minidiscus* species (*M. chilensis, M. decoratus, M. ocellatus* and *M. subtilis*) are needed in order to better understand the evolution and further clarify the taxonomy of this important genus. A more detailed analysis of the variations in genetic, morphological and ecological variability would also be needed for a proper delineation of species (Amato *et al.*, 2007).

A few species of the genus *Thalassiosira,* with sizes in the same range as those of the genus *Minidiscus* (< 10 µm), have been described (for example *T. mala* Takano, *T. profunda* (Hendey) Hasle and *T. exigua* Fryxell and Hasle). Assignation of the isolated strains to the species *T. curviseriata* and *T. profunda* was achieved based on the analysis of morphological features of the valve and confirmed by genetic characters. The morphological features of *Thalassiosira* sp. RCC4664 and RCC5887 did not fit with the description of any described species. We suspect that these strains correspond to a new species.

These results, and the fact that all nanoplanktonic diatoms identified in the frame of this study are new records for the Atlantic French coasts of the Western English Channel, point to an under sampling of nanophytoplankton in this region.

Given the global importance of nanoplanktonic diatoms (Leblanc *et al.*, 2018; Malviya *et al.*, 2016), these new data, and in particular the new sequences that we generated, will help to refine our understanding of the global nanodiatom distribution and to bridge the gap between laboratory identification and environmental studies.

Nanodiatoms dominate the diatom community at SOMLIT-ASTAN

The diversity and the seasonal variations of microphytoplanktonic diatoms have been well described in the Western English Channel and North Sea (Grall, 1972; Guilloux *et al.*, 2013; Jacques, 1963; Martin-Jezequel, 1983). At SOMLIT-Astan station, *Guinardia* (especially *G. delicatula*) and *Paralia sulcata* appear as key taxa, becoming dominant in spring/summer and winter, respectively (Guilloux *et al.*, 2013). Exploration of metabarcoding data provides a more thorough insight into species diversity including small sized organisms that are usually overlooked using traditional microscopy counts. One of the major findings of this study was that nanodiatoms, and more specifically *Minidiscus* species, largely dominate the diatom community. The analysis of the 8 year metabarcoding survey allowed the discrimination of *M. comicus*, *M. spinulatus*, *M. variabilis*, as well as *T. curviseriata*, *T. profunda* and *Thalassiosira* sp.. *M. variabilis* was the most abundant species, comprising 13.2% of the total diatom reads and exceeding *G. delicatula* read abundance by 2-fold. *M. variabilis* even ranked in the top 5 most abundant phytoplankton species. *M. comicus* was the third most abundant diatom at study site. Although the contribution of *M. spinulatus* and species of *Thalassiosira* were less important, they still ranked in the top 20 of the major diatom OTUs. The present results support the hypothesis that nano-sized diatoms are major contributors of the phytoplankton community in temperate coastal waters (Kaczmarska *et al.*, 2009; Leblanc *et al.*, 2018; Percopo *et al.*, 2011; Ribera d'Alcalà *et al.*, 2004) and emphasize the importance of better understanding their ecology and impacts in nature.

The 8 year monitoring of the 6 species indicated distinct periods of occurrence. *M. comicus*, *M. spinulatus* and *T. profunda* formed transient blooms during winter, *T. curviseriata* during springtime, and *Thalassiosira* sp. RCC4664 usually peaked twice a year in winter and in summer. Interestingly, *M. comicus* in the Western English Channel do not develop spring-summer blooms as observed in the Mediterranean Sea (Leblanc *et al.*, 2018; Ribera d'Alcalà *et al.*, 2004). While these previous species exhibited clear seasonal patterns, *M. variabilis* persisted year round, with important abundance fluctuations. Few number of *Thalassiosira* strains were isolated between 2015 and 2016 but their ITS analysis demonstrated an important intraspecific variability. Contrary to these latters, the isolation and genetic characterization of *Minidiscus* species between 2015 and 2016 suggest a relatively low intraspecific diversity during the occurrence periods of the studied species based on 18S and ITS sequencing. Genetic markers such as 5.8S + ITS-2 were proposed to be more appropriate to depict diatom diversity (Moniz and Kaczmarska, 2009, 2010), especially for species that belong to the Thalassiosirales (Guo *et al.*, 2015).

Drivers of nanodiatom dynamics: towards a biotic control?

The distinct patterns of nanodiatom occurrences (bloom forming vs. persistent) and the interannual variability in bloom amplitudes raised the question of whether nanodiatom species are regulated differently. The observed dynamics in read abundance most likely result from variable processes either affecting cell growth and cell losses through diverse mechanisms (for example, sedimentation, grazing, programmed cell death, internal clocks or infection by parasites). In the framework of the long-term monitoring program at SOMLIT-Astan, environmental parameters such as temperature, salinity, oxygen and macronutrients are collected every fortnight since 2000 (http://somlit.epoc.u-bordeaux1.fr/fr/). Although abiotic factors are known to affect diatom growth (*e.g.* Bidle, 2015; Bowler *et al.*, 2010; Litchman and Klausmeier, 2008; Sarthou *et al.*, 2005), they could not be explored for the present manuscript due to a lack of time. The dominance of *M. variabilis* over the other species year round however suggests a broad ability to respond to the natural environmental variability and thereby a weak influence of physico-chemical parameters. Conversely, the marked seasonal development of *M. comicus*, and of the other nanoplanktonic diatoms, may reflect adaptations to seasonal variations of the environmental factors. Jewson *et al.* (2016) have shown that, for *M. comicus*, the cycle of size decline and size restoration were used to time the life cycle. Size variations along time could be estimated at our time-series station using the collection of natural samples that we collected bimonthly during the period between October 2015 and October 2016 (see Part I). Using SEM we will be able to both depict the natural morphological variations in the morphology of nanodiatoms and study size variations.

Biotic control is also probably involved in the regulation of nanodiatoms. Grazing pressure on *Minidiscus* and small diatoms from *Thalassiosira* has been studied in culture conditions (Martin-Cereceda *et al.*, 2003). These authors have demonstrated the ability of the mixotrophic flagellate *Prymnesium parvum* to feed on this type of nanodiatoms when bacteria, their predilection prey, are limited or absent. This prey-switching possibility might have importance in food-webs functioning. However, diatoms are often considered as inedible phytoplankton due to their large size, their external processes and threads or also to their colonial form and aggregates (Hamm *et al.*, 2003; Kagami *et al.*, 2007; Raven and Waite, 2004). *Minidiscus* and *Thalassiosira* from our study displayed these last characteristics, that may entail less susceptibility to predation attacks in nature.

Pathogens have been described as important mortality agents that may control the dynamics of diatom populations (Gleason *et al.*, 2015; Gutiérrez *et al.*, 2016; Peacock *et al.*, 2014). Eukaryotic parasites infecting diatoms have been mostly described in association with microphytoplanktonic species (Scholz *et al.*, 2015), algicidal bacteria in association with *Skeletonema* species (Mitsutani *et al.*, 1992; Shi *et al.*, 2013; Wang *et al.*, 2016) and diatom viruses were mainly isolated from *Chaetoceros* species (Tomaru *et al.,* 2015b). For the first time, our study provides evidence of parasites that infect the genera *Minidiscus* and *Thalassiosira*. A collection of 82 clonal parasites was established and preliminary characterization indicates that they occur in two size fractions: < 0.2 µm, these are most likely viruses, and > 0.2 µm, these are, as yet, unaffiliated. Owing to the small size of *Minidiscus* and

Thalassiosira, we can suspect that parasites > 0.2 µm include algicidal bacteria rather than eukaryotes. The period of successful virus isolation (fall to spring) approximately corresponded to the blooming periods of the prospective hosts except for *T. curviseriata* for which viruses could be isolated year round. Isolation of larger parasites was possible all along the year 2015-2016 even when their isolation hosts were under detection limit. We suspect that these parasites may be generalists that switch host when the biomass is not sufficient to sustain their development. For example, the bacteria *Kordia* sp. RCC5776, isolated from *G. delicatula,* was also able to lyse the studied nanodiatom species (See Part II, Chapter III). More detailed functional and genetic analyses are of course needed to refine the parasite affiliation, their modes of action and their interplay with nanodiatom species in nature (Chapter II). Yet, the results suggest that different parasites have the ability to control nanodiatom species at the studied site. Considering our isolation (liquid enrichment) and purification methods, we probably selected the most abundant pathogens and thus we probably under-estimate the actual diversity of nanodiatom pathogens.

Concluding remarks

Recently, nanoplanktonic diatoms were proposed as major contributors to phytoplanktonic blooms in coastal as well as offshore regions. Their global ecological significance is however severely limited by the paucity of genetic references and isolates in culture. In this respect, establishing a nanodiatom reference collection was prerequisite for taking a census of this minute organisms and advancing our understanding of their ecology and impacts in nature. Using classical morphological and molecular approaches, our study provides a new insight in the diversity and dynamics of relevant nanoplanktonic diatoms in the Western English Channel. The genus *Minidiscus* numerically dominate the diatom community. Owing to their prominence in the French coastal waters of the Western English Channel, nanoplanktonic diatoms have undoubtedly important ecological and biogeochemical implications. Persistence and seasonality patterns of *Minidiscus* and *Thalassiosira* raise questions about the parameters which contribute in their proliferation and decline. Viruses and unassigned pathogens may exert a significant control on these tiny diatoms. Given the global significance of the nanodiatoms, the substantial collection of organism brought into culture should provide biological models of interest in ecological, biogeochemical and evolutionary studies.

ADDITIONAL EXPERIMENTS FOR MANUSCRIPT COMPLETION

Three main tasks need to be completed before the submission of this manuscript:

- To progress in the understanding of the seasonal variations of these important diatom taxa, environmental filters were prepared for examination by SEM to give an idea of the presence/absence and of the abundance of the genera *Minidiscus* and *Thalassiosira* (see Part

I for procedure). As cell isolation presents some methodological limits (growth in artificial structures, selective method, etc.), the environmental filters offer a good opportunity to visualize the silicifying phytoplanktonic diversity at each sampling time, its composition and abundance. A method for quantifying the diatom cells is still in discussion but these filters will allow us to have a link between the isolation and the metabarcoding dynamics, and to check if we accessed or not to a good representation of nanodiatom community with cell isolation.

- During the full seasonal cycle of sampling at the SOMLIT-Astan station, 17 other nanoplanktonic diatom strains were isolated along with *Minidiscus* and *Thalassiosira* strains. Preliminary analyses of these isolates indicated that they belong to the *Minutocellus polymorphus*/*Arcocellulus cornucervis* complex (order Cymatosirales). According to metabarcoding analyses, this complex seems to be an important contributor of the diatom community. OTU assigned to the *Minutocellus/Arcocellulus* complex was the fifth most abundant OTU among the Bacillariophyta and represented 6.2% of the total diatom reads abundance. However, compared to Thalassiosirales species, few reports are available in literature. Thus, morphological characterizations will be performed on cultures to better identify this ambiguous diatom complex and its environmental dynamics will be examined to determine its seasonal patterns at our coastal site.

- In addition to parasitism, abiotic factors will be considered in the control of *Minidiscus* and *Thalassiosira* dynamics using environmental parameters from the SOMLIT program. These data are collected bi-monthly since 2000 and they will be used to interpret nanodiatoms dynamics and determine ecological preferenda. In the study of Jewson *et al.* (2016), *M. comicus* grew in summer in the Mediterranean Sea under silica depletion. It would be interesting to examine if the same patterns occur in the WEC, and explore more largely the drivers controlling their development.

CHAPTER II- Viruses infecting the genera *Minidiscus* and *Thalassiosira*

The previous chapter exhibits the results of an intense parasite isolation work. Even if mainly isolates were lost during the project, we succeeded to maintained many representatives in culture. Concerning the viral isolates, a collection of 5 strains isolated from *M. comicus*, 1 from *M. spinulatus,* 8 from *M. variabilis*, 8 from *T. curviseriata,* 4 from *T. profunda*, and 1 viral strain from *Thalassiosira* sp. RCC4664 is well established and available in our laboratory (See Table I-4).

A partial characterization of some of these cultures was initiated with the morphological features. The morphology of the virions (i.e. free living viruses) was determined by TEM after negative staining using uranyl acetate (2% w/v) on a copper grid, exactly as described for GdelRNA viruses. Appropriate controls (uninfected hosts) have also been examined by TEM.

The viral strains P-RA151006 associated to *M. comicus* RCC4662, T-RA151006 on *M. spinulatus* RCC4659*,* X-RA150921 isolated on *T. profunda* RCC4663 and V-RA150921 on *T. curviseriata* RCC5154 shared common features with other viruses infecting diatoms (Figure III-10). The viral particles displayed a hexagonal morphology, lacked a tail and had diameters of 31.8 ± 1.5 nm (n=39), 30.5 ± 1 nm (n=51), 37.5 ± 2 nm (n=7), and 37.8 ± 2 nm (n=43) respectively (Figure III-10). No virus like particles were observed in the host controls.
Many other viral isolates associated from *Minidiscus* spp. and *Thalassiosira* spp. were successfully examined by TEM, unfortunately, those viral cultures were lost during the project.

More isolates are waiting for screening (Figure III-11, Table I-4). The full characterization of the viral cultures will contribute to determine the nature of the genomes (ssDNA or ssRNA viruses), their infection kinetics, their natural distributions, etc.. Also, sequencing their genomes is challenging but it will facilitate to design degenerated primers of specific genes such as RdRp or capsid genes, to study their intraspecific variability, to explore infection processes and to investigate their temporal dynamics to better understand their role and contribution in diatom regulations at the SOMLIT-Astan station.

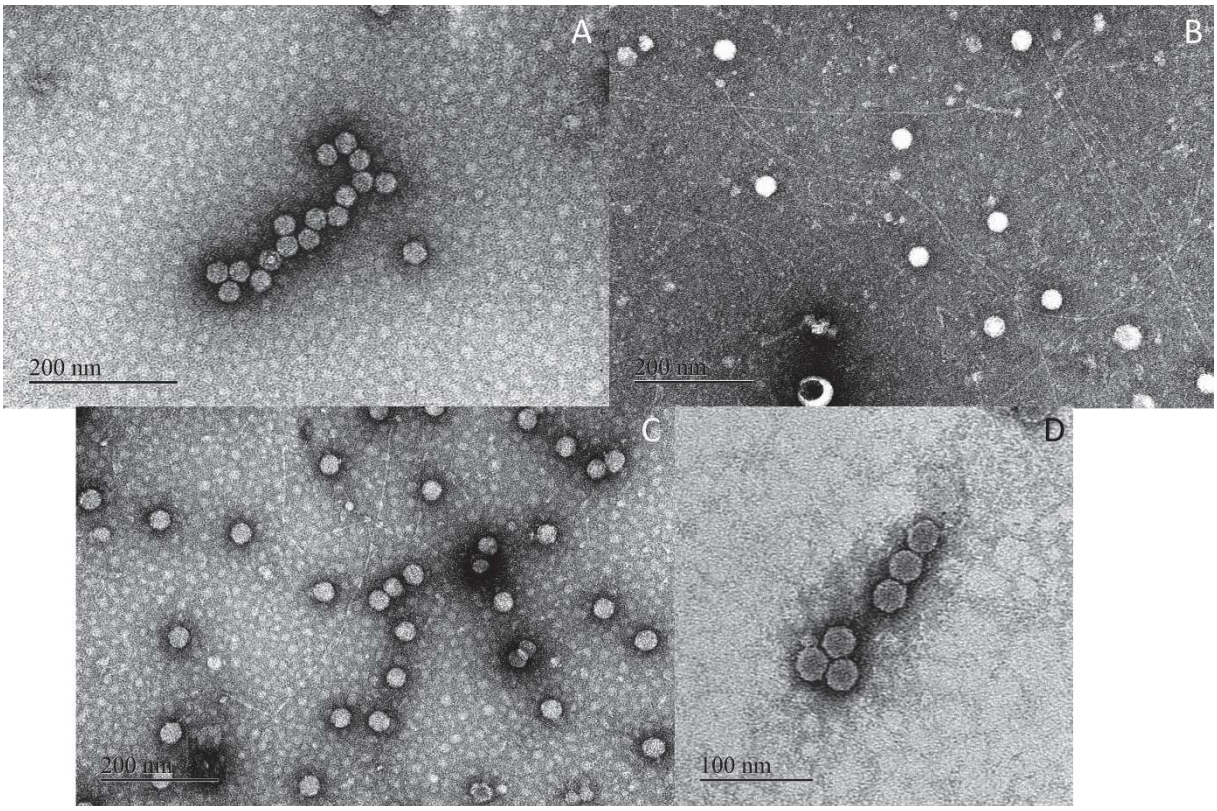

Figure III-10. Negatively stained viral particles. (A) Viral strain P-RA151006 isolated on Minidiscus comicus *RCC4662. (B) Viral strain X-RA150921 isolated on* Thalassiosira profunda *RCC4663. (C) Viral strain V-RA150921 isolated on* Thalassiosira curviseriata *RCC5154. (D) Viral strain T-RA151006 isolated on* Minidiscus spinulatus *RCC4659*

Figure III-11. Collection of parasites, including mainly viruses, isolated on Thalassiosira curviseriata *RCC5154*

CONCLUSIONS AND PERSPECTIVES

PARASITES OF DIATIOMS: TIME FOR A CLOSER LOOK

The overarching objective of this PhD research was to better understand the role of parasites in the regulation of marine diatoms. Therefore, intensive efforts of isolation and characterization were made in order to identify the network of parasites associated to the dominant diatoms in the coastal waters off Roscoff (Western English Channel, WEC). This demanding work has resulted in the establishment of a unique collection of 100 parasites and 70 diatoms. The characterization of a dozen of these isolates revealed an unsuspected parasite diversity. Considering the ecological significance of diatoms, this collection should provide relevant biological model systems to study multipartite biotic interactions, interpret the enormous sequence datasets generated by high-throughput approaches, and generate new fundamental knowledge on the regulation of diatoms. In this last part, the findings, shortcomings and contribution of my work to the field of microbial ecology will be discussed and perspectives will be proposed to improve our understanding of diatom-parasite interactions in the environment.

1. From seawater to the laboratory: Establishment of a parasite culture collection - Methodological insights

Although not shown in this thesis, different methods of parasite isolation were tested during this project. Besides the enrichment method, direct parasite isolations from visibly infected cells were conducted. The examination of plankton net samples (see Part I for isolation procedures) by light microscopy showed *Guinardia* sp. cells with suspicious organisms within the frustule, especially during blooms (Figure 0-1). We attempted to pick and transfer by micro pipetting the visibly infected cells to a fresh culture of diatom, in order to propagate the parasite. However, we never succeeded to maintain these putative parasites in culture.

Figure 0-1. Potential infected Guinardia *cells from the 20 µm pore-size plankton net, sampled at SOMLIT-Astan station. Arrows indicate organisms within the diatom cells. Pictures from Fabienne Rigaut-Jalabert*

The failures to isolate and maintain parasites from infected host cell may be explained by different reasons. First, the prospective host strains may be not permissive, or only partially, to pathogen infections. For example, the viruses GdelRNAV-01 to 04 displayed different host spectra (Part II, chapter 1). Using the most permissive hosts as possible is indeed critical to increase the probability of successful pathogen isolation (Carlson *et al.*, 2016). Second, the culture conditions used for the parasite isolation (18°C, 12:12 light regime, 100 µmol photons.m^{-2}.s^{-1}) were optimal for the prospective host growth, but they may not be appropriate for the parasite propagation. In particular, temperature appears to be a key factor in diatom host-parasite interactions (Mojica and Brussaard, 2014; Scholz *et al.*, 2015) and may result in host resistance (Demory *et al.*, 2017; Kendrick *et al.*, 2014). Third, culture conditions may facilitate escape strategies of hosts (Chambouvet *et al.*, 2011; Frada *et al.,* 2008). Indeed, during the isolation process, and then when maintaining our collection of parasites, we have occasionally observed auxospores in infected cultures while only vegetative cells were observed in control cultures. These observations suggest that parasites could induce sexual reproduction of diatom species. Sexual reproduction may generate genetic variability in the diatom population, and it may induce resistance to parasites (Theory of "sex against virulence" of the Red Queen Hypothesis (De Bruin *et al.,* 2004; Ebert and Hamilton, 1996)). Despite these personal observations, mechanisms involved in the life cycles of our species of *Guinardia*, *Minidiscus* and *Thalassiosira*, such as gametogenesis, fertilization, and auxospore formation, were not studied so far.

By comparison, isolations of algicidal strains using the enrichment and extinction-dilution methods provided more satisfactory results. However, this isolation work represented a demanding and time consuming process. The establishment of a clonal culture of parasite required at least three months of experiments, including the enrichment incubation, filtrations, lysis inspections, and extinction-dilution cycles. This process was repeated for the 22 samplings and isolates are now transferred every two weeks. Despite our efforts, losses of parasites occurred regularly (about more than 100 isolates lost in 3 years).

Viruses of diatoms are particularly troublesome to maintain. Tests for long-term preservation of diatoms and parasites are currently ongoing (collaboration with Roscoff Culture Collection) and preliminary results are promising. We are aware that the collection of parasites established during this project does not reflect the actual diversity of parasites that infect the targeted diatom species in nature. This isolation strategy indeed selects the most abundant parasites with rapid growth and life cycle. Also, we have probably neglected large parasites during the filtration process, since we first chose to use filters with small size porosity (0.2 µm filters and GF/F filters). Larger pore-size filtration (5 and 3 µm) were added during summer 2016 and led to the isolation of the aplanochytrid (Part II, chapter 2). These additional filtration steps could not be implemented year round as pico-organisms (Mamiellophyceae mainly) and pennate diatoms such as *Navicula* sp. were passing through the filters and contaminated the isolates.

Despite this methodological limitations, we succeeded to establish and maintain a collection of ca. 70 diatoms and ca. 100 pathogens. The *G. delicatula* parasites studied during this project represent only 3% of the whole collection but the characterizations of these isolates revealed an unsuspected diversity, with at least three types of parasites belonging to distinct lineages: viruses (Picornavirales, *Bacillarnavirus*), a eukaryotic parasite (Labyrinthulomycetes, *Aplanochytrium* sp.) and algicidal bacteria (Bacteroidetes, *Kordia* sp.). These pathogens have never been described in association with *Guinardia* and therefore add to the list of known parasites reported for this host species (Drebes *et al.*, 1996; Kühn, 1996; Kühn *et al.*, 1996; Peacock *et al.*, 2014; Schnepf *et al.*, 1990; Schnepf and Kühn, 2000).

These findings suggest that *G. delicatula* is a relevant biological model to study multiparasitism, a field of research that remains largely unexplored. The characterization of our collection of parasites should provide fundamental information for understanding the molecular mechanisms involved in diatom infection, the dynamics and succession of diatom blooms in natural environments, and it should contribute to the pool of reference sequences that are essential for the interpretation of the enormous datasets generated by high-throughput sequencing approaches. The diatoms and parasites described in this PhD thesis were deposited in the Roscoff Culture Collection and they are available for the scientific community.

2. Diatom-parasite interactions: Laboratory approaches

One major finding of this PhD project is that dominant diatom species are regulated by a complex assemblage of parasites in the WEC. The characterizations of these parasites indicate that they belong to different phylum and use different strategies to infect their host. Viruses of *G. delicatula* were specialists infecting a few strains within this species. GdelRNAV induced complete lysis of the host culture after 7 days of incubation. Our analysis also points out the host's variable viral susceptibilities during the early exponential growth phase. In

contrast, the pathogenic bacteria *Kordia* sp. and eukaryote *Aplanochytrium* sp. are generalist pathogens that killed *Guinardia* in a timely manner (< 3 days) using distinct modes of action. Based on our characterization, generalism was not associated with any apparent compensatory effect as could be expected according to past theories (trade-offs hypothesis, (Poulin, 1998)). During this project, the interactions between the parasite and *Guinardia* host were studied under the host culture conditions. It is however likely that the biological and physio-chemical environments of the parasites modulate their virulence (Mojica and Brussaard, 2014; Scholz *et al.*, 2015). For example, Peacock *et al.* (2014) have reported infections of *G. delicatula* by *Cryothecomonas aestivalis* at their marine coastal observatory from 2006 to 2013. During winter, infection stages were observed only when water temperature was above 4°C. Similarly, diatom-virus relationships were evaluated in an experimental study within a temperature range of 10 to 30°C (Tomaru *et al.*, 2014). These authors demonstrated that ssRNA and ssDNA viruses infecting *Chaetoceros tenuissimus* differed in their response to temperature changes, including also variations of susceptibilities of host strains. Temperature appears to be an important driver affecting host-parasite dynamics. Conducting experimentations on the effect of temperature on the viability of *Guinardia* parasites, on the one hand, and their interactions with their host, on the other hand, should be investigated to better figure out the natural interplays at SOMLIT-Astan.

So far, fundamental knowledge on host-parasite interactions is based on the study of a single host with a single parasite. The recurrent finding of complex assemblages of parasites that regulate a single host leads to question about the ecological role of multiparasitism. Our isolation work showed that multiple parasites of *Guinardia* could be isolated on the same sampling date, suggesting that different pathogens co-occurred in the environment. How parasites with so variable life strategies can share the same resource? Can a parasite outcompete another one? Does facilitation occur instead? For example, rapid attack of the aplanochytrid could weaken the host cells, which, in turn, may become more susceptible to viral infection? Can the proteases secreted by *Kordia* sp. alter the infectivity of GdelRNAV through the degradation of their capsid proteins for example? Antagonist effects were already reported between a bacteria and viruses (Kimura and Tomaru, 2014). Axenic culture of *C. tenuissimus* was totally lysed due to the viral infection by an RNA virus, while the presence of a bacterial community (nonpathogenic) in the culture led to the host survival (Kimura and Tomaru, 2014). These results showed that multipartite interactions are complex and that they deserve more attention. Our collection of *Guinardia* hosts and parasites, all isolated from the same location, provides a unique opportunity to tackle this important, yet largely unsolved, research question in the field of microbial ecology.

3. Diatom-parasite interactions: From the laboratory cultures to environmental approaches

This PhD research relied largely on the use of host-parasite model systems to begin to address the role of parasitism in the regulation of diatom dynamics. This work revealed that diatom are, at least partly, controlled by an assemblage of pathogens. The characterization of these parasites has resulted in elementary knowledge about their biology and hypotheses about their ecological implications. However, cultural approaches have limitations and it is evident that they do not provide an accurate estimation of the diversity of parasite community (see discussion in §1). In addition, parasites infecting a species under laboratory conditions may never meet this host in the natural environment, for example both entities may not occur at the same season. To overcome these limitations, high throughput environmental sequencing data are commonly used to provide a more thorough insights into the genetic diversity of microbial community, its spatio-temporal dynamics and to highlight significant species interactions.

By exploring the eukaryotic metabarcoding libraries collected at SOMLIT ASTAN since 2009, we can provide a more exhaustive inventory of potential diatom parasites and monitor their temporal dynamics.

Table 0-1. Search for best hits of sequences of parasites infecting Guinardia *species in the V4 SOMLIT-Astan database (8 788 OTUs). Host range of each parasite was obtained from the literature. The 5 first best hits from BLASTn are shown. [a]: Drebes* et al.*, (1996), [b]:Schnepf and Kühn,(2000), [c]: Kühn* et al.*, (1996), [d]: Schnepf* et al.*, (1990), [e]:Schweikert and Schnepf, (1997)*

parasite species -Accession number	Potential host species	5 first related OTU	Bit-Score	E-value	Identity	V4 length
Cryothecomonas aestivalis strain 1 - AF290539[a]	*Guinardia delicatula*	OTU_86 OTU_14252 OTU_1411 OTU_466 OTU_878	686.56 679.35 679.35 673.94 673.94	0 0 0 0 0	99.5% 99.2% 99.2% 99.0% 99.0%	385 385 384 385 385
Cryothecomonas aestivalis strain 2 - AF290541[a]	*Guinardia delicatula*	OTU_86 OTU_25487 OTU_1411 OTU_2097 OTU_4594	688.37 672.14 682.96 679.35 677.55	0 0 0 0 0	99.7% 99.7% 99.5% 99.2% 99.2%	386 377 385 386 386
Cryothecomonas longipes - AF290540[b]	*Cerataulina bergonii, Chaetoceros costatus, Chaetoceros debilis, Chaetoceros didymus, Coscinodiscus granii, Coscinodiscus radiates, Guinardia delicatula, Guinardia striata, Leptocylindrus danicus, Navicula* sp., *Pleurosigma* sp., *Rhizosolenia setigera, Thalassiosira rotula, Thalassiosira punctigera*	OTU_4321 OTU_443 OTU_556 OTU_6246 OTU_1332	702.797 688.37 688.37 688.37 688.37	0 0 0 0 0	100% 99.2% 99.2% 99.2% 99.2%	389 389 389 389 389
Pirsonia formosa strain 99-S isolate P846 - AJ561109[c]	*Eucampia zodiacus, Guinardia delicatula, Guinardia flaccida, Leptocylindrus danicus, Rhizosolenia imbricata, Rhizosolenia setigera*	OTU_231 OTU_3396 OTU_821 OTU_1322 OTU_4399	691.98 686.57 682.96 682.96 682.96	0 0 0 0 0	99.7% 99.5% 99.2% 99.2% 99.2%	388 387 388 388 388
Pirsonia formosa strain 99-2 isolate P842 - AJ561110[c]	*Eucampia zodiacus, Guinardia delicatula,*	OTU_231 OTU_3396	688.37 682.96	0 0	99.5% 99.2%	388 387

	Guinardia flaccida, Leptocylindrus danicus, Rhizosolenia imbricata, Rhizosolenia setigera	OTU_821 OTU_1322 OTU_4399	679.35 679.35 679.35	0 0 0	99.0% 99.0% 99.0%	388 388 388
Pirsonia formosa strain 99-1 isolate P841 - AJ561111[c]	*Eucampia zodiacus*, *Guinardia delicatula, Guinardia flaccida, Leptocylindrus danicus, Rhizosolenia imbricata, Rhizosolenia setigera*	OTU_231 OTU_3396 OTU_821 OTU_1322 OTU_4399	691.98 686.57 682.96 682.96 682.96	0 0 0 0 0	99.7% 99.5% 99.2% 99.2% 99.2%	388 387 388 388 388
Pirsonia guinardiae isolate P844 - AJ561112[d]	*Guinardia delicatula, Guinardia flaccida*	OTU_231 OTU_3396 OTU_821 OTU_1322 OTU_4399	700.99 693.78 691.98 691.98 691.98	0 0 0 0 0	100% 99.7% 99.5% 99.5% 99.5%	388 387 388 388 388
Pirsonia punctigera isolate P759 - AJ561115[e]	*Thalassiosira punctigera, Thalassiosira hendeyi*	OTU_3107 OTU_30528 OTU_231 OTU_1322	684.76 661.32 652.30 643.23 643.23	0 0 0 0 0	99.5% 98.2% 97.7% 97.2% 97.2%	388 388 388 388 388
Pirsonia verrucosa isolate P847 - AJ561113[c]	*Guinardia delicatula*	OTU_1322 OTU_231 OTU_17252 OTU_19847 OTU_17411	700.99 691.98 691.98 691.98 690.17	0 0 0 0 0	100% 99.5% 99.5% 99.5% 99.5%	388 388 388 388 387
Pseudopirsonia mucosa isolate P845 - AJ561116[c]	*Guinardia delicatula, Rhizosolenia imbricata, Rhizosolenia setigera*	OTU_1926 OTU_961 OTU_14401 OTU_1639 OTU_23731	693.78 664.93 646.89 572.95 576.56	0 0 0 6.11^{e}-163 5.02^{e}-164	99.7% 98.2% 97.2% 93.3% 93.2%	389 390 390 390 395

The recruitment of sequences corresponding to known *Guinardia* parasites, other than the aplanochytrid, from this 8 year survey indicated that many OTUs were highly related to the pathogenic species (Table 0-1). Especially OTUs with 100% of sequence identity with sequences of *Cryothecomonas longipes*, *Pirsonia guinardiae* and *Pirsonia verrucosa* were retrieved from this dataset. Automatic assignations using the PR2 reference database allowed to retrieve 21 OTUs related to *C. aestivalis*, 3 to *C. longipes*, 15 to the genus *Pirsonia* and 3 to *Pseudopirsonia mucosa.* These genera contributed to 0.33%, 0.07% and 0.01% of the total pool of planktonic reads, respectively. OTUs of the parasites *C. aestivalis* and *P. guinardiae* were the most abundant in terms of reads (Figure 0-2, A and B). According to these analyses, *P. guinardiae* mostly occurred in July 2010, where its relative abundance exceeded those of *G. delicatula* and *G. flaccida* (Figure 0-2, A and B). OTU related to *C. aestivalis* generally co-occurred with that of *G. delicatula* and formed two summer peaks of variable amplitude from year to year (Figure 0-2, A). A conspicuous peak was recorded in 2015 and corresponded to a *G. delicatula* bloom of low amplitude.

Besides parasites of *Guinardia*, we interrogated this database for known parasite (*Pirsonia punctigera*) that infects the diatom *Thalassiosira punctigera*, for which no parasite could be isolated during this project. The relative read abundance related to *P. punctigera* was extremely low during the monitoring period. Except for April 2012, this parasite seamed to thrive in winter, especially during *T. punctigera* blooms (Figure 0-2, C). According to Schweikert and Schnepf, (1997), this parasite can infect another species of *Thalassiosira*. Developments of this *Pirsonia* species outside *T. punctigera* blooms may be explained by the host spectrum reported by these authors.

At the SOMLIT-Astan station, the survey of prokaryote diversity is not yet implemented. Thus, following bacterial dynamics is not possible. To monitor the dynamics of pathogenic bacteria of the genus *Kordia* and to relate it to those of diatoms and other parasites, we proposed to design probes that specifically target *Kordia* genus (See Part II, chapter 3). Primers specificity will be evaluated and the most efficient one will be selected to quantify by qPCR the abundance of *Kordia* in 2015 and 2016 from archives of DNA extracts from the SOMLIT-Astan. This side project has been submitted recently (EC2CO project: “Les interactions entre les bactéries algicides du genre *Kordia* et les diatomées : leur importance écologique, spécificité et régulation (INTIMITE)”).

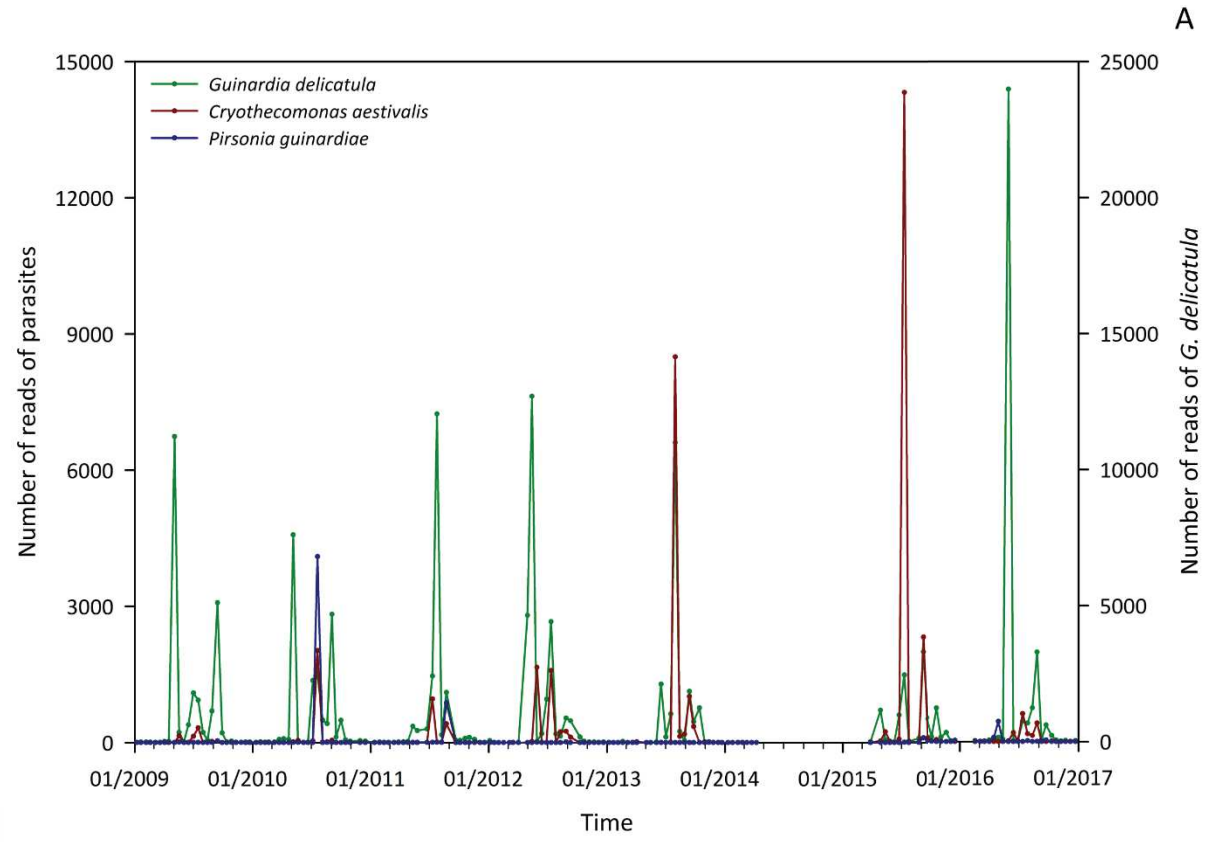
A
Guinardia delicatula
Cryothecomonas aestivalis
Pirsonia guinardiae
Number of reads of parasites
Number of reads of G. delicatula
15000
12000
9000
6000
3000
0
25000
20000
15000
10000
5000
0
01/2009
01/2010
01/2011
01/2012
01/2013
01/2014
01/2015
01/2016
01/2017
Time

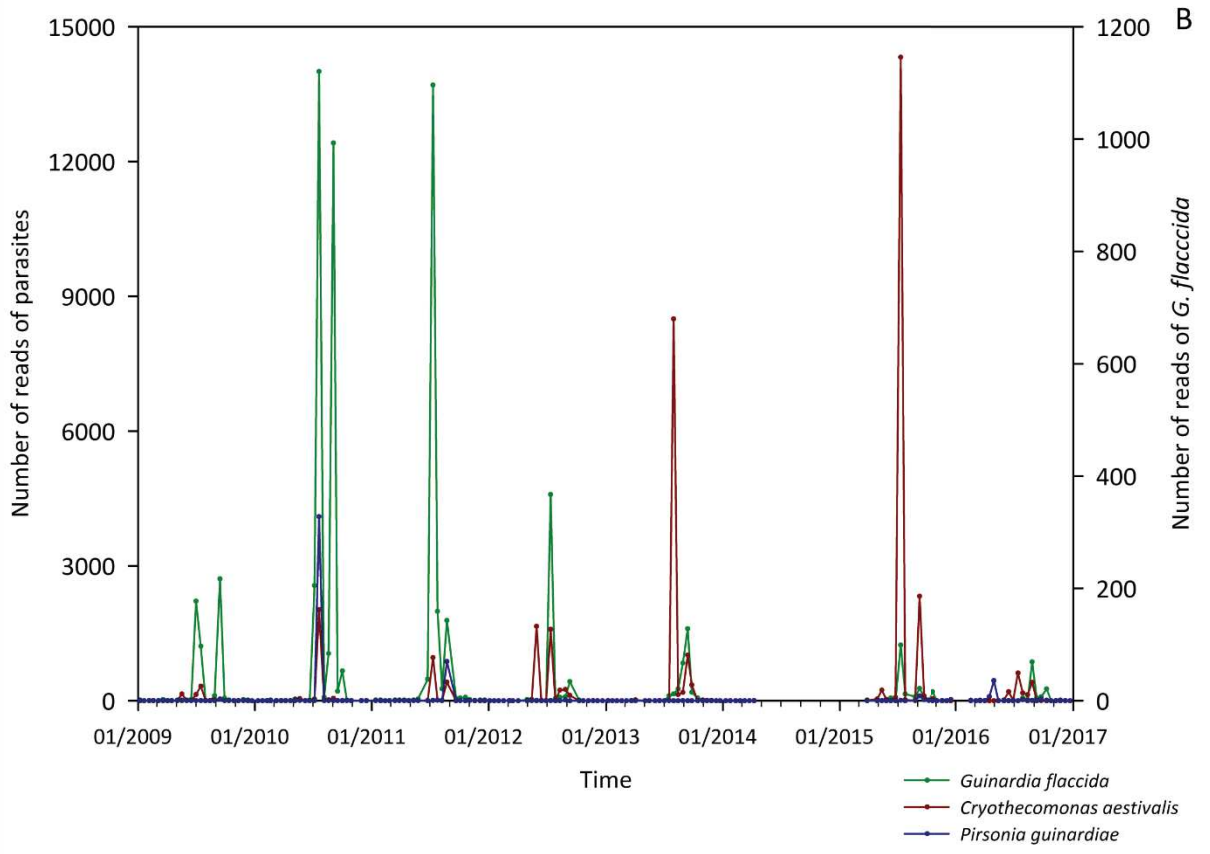
B
Number of reads of parasites
Number of reads of G. flaccida
15000
12000
9000
6000
3000
0
1200
1000
800
600
400
200
0
01/2009
01/2010
01/2011
01/2012
01/2013
01/2014
01/2015
01/2016
01/2017
Time
Guinardia flaccida
Cryothecomonas aestivalis
Pirsonia guinardiae

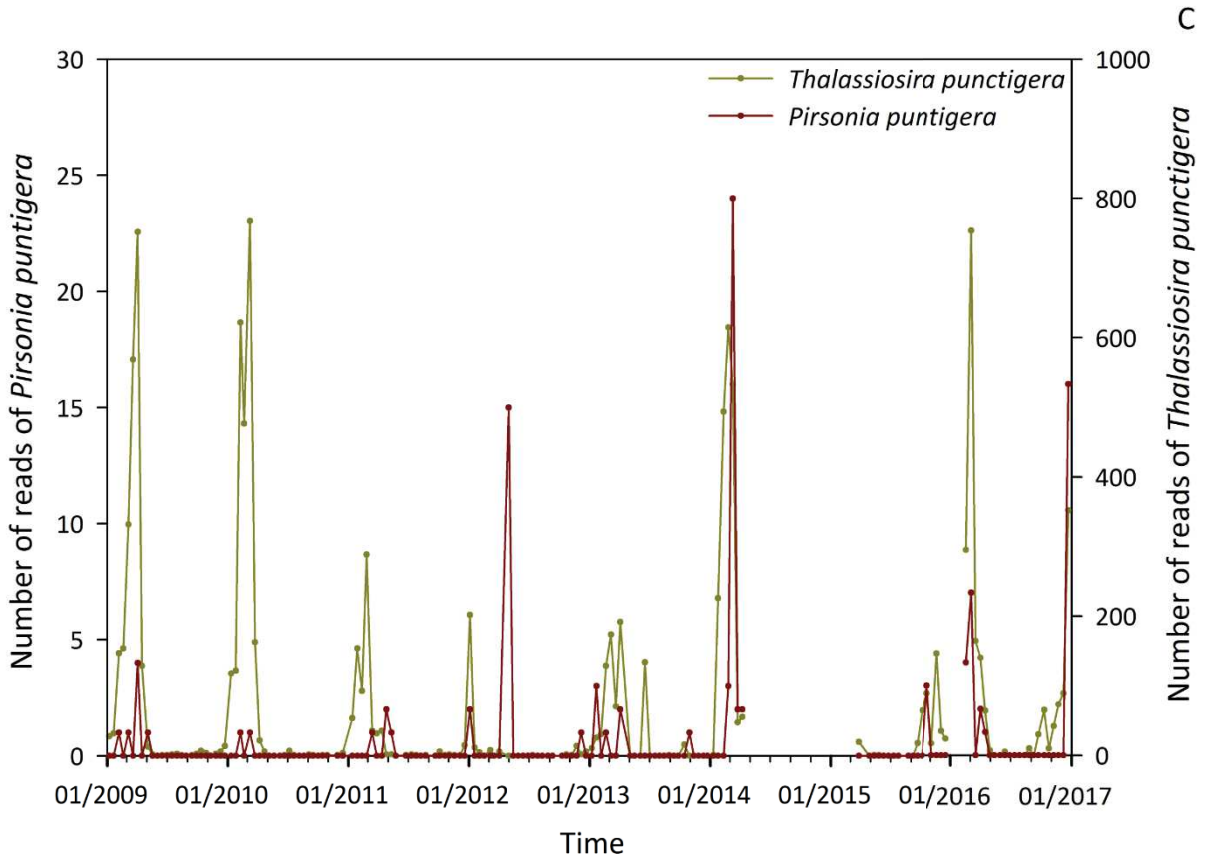

Figure 0-2.Relative abundances of G. delicatula ***(A)*** *and* G. flaccida ***(B)*** *with* C. aestivalis *and* P. guinardiae*, and of* T. punctigera *with* P. punctigera ***(C)*** *at the SOMLIT-Astan station*

In the future, similar approach should be developed to provide a more accurate assessment of the viral assemblage at SOMLIT-Astan. During this Ph.D. project, we only succeeded to isolate viruses associated to *G. delicatula* in summertime. We are aware that our isolation strategy has limitations, yet this isolation pattern suggests a marked temporal dynamics. To test this hypothesis, the design of molecular probes targeting core RNA virus genes, such as the RdRp, should be considered (Culley *et al.,* 2003, 2014; Culley and Steward, 2007; Gustavsen *et al.*, 2014). To study the intraspecific variability of GdelRNAV, three published couples of degenerated primers (reviewed in Culley *et al.*, (2010)) and newly designed primers based on the RdRp regions of GdelRNAV-01 and of Csp03RNAV were tested on *G. delicatula* viruses. In our case, only the new primers designed could successfully amplify GdelRNAV RdRp region. This molecular test illustrates the importance to have more viral representatives in culture, to better define and adapt tools to accurately assess virus diversity in nature. A viral metabarcoding and viral metagenomes (RNA and DNA viromes) time-series will be implemented in the laboratory in January 2019 and should enable to address questions about the composition, the relative abundance and the variations of the virioplankton and its interplay with microalgae in the WEC.

The combination of mathematical and molecular approaches provides invaluable analytical tools to describe complex ecological networks (that are interactions between

species) and evaluate the robustness of species interactions in a given ecosystem (Fuhrman and Steele, 2008; Ruan *et al.*, 2006; Weiss *et al.*, 2016). In the framework of a collaborative project (EC2CO project "CYCLOBS - Successions saisonnières cycliques du plancton en Manche Occidentale, interactions biotiques et résilience (preuve de concept pour la série temporelle SOMLIT-Astan)"), co-occurrence networks are being constructed (collab. S. Chaffron, University of Nantes), from the 8 years molecular survey to bring information about symbiotic, including parasitic, network associated to *Guinardia* species and to confirm the interactions detected in the laboratory. Integration of both biotic (OTUs) and abiotic (physico-chemical) variables to network analysis will also help describing and understanding how the environment influences biological interactions.

Although extremely powerful, metabarcoding and statistical tools do not provide actual rates of mortality due to parasitism. Quantifying the relative contribution of each parasite to the mortality of diatoms is challenging, yet, essential. The isolation and characterization of different parasites highlighted variable modes of action. It is likely that the chemical composition and the particle size distribution of the lysis products differ depending on the parasite. Diatoms such as *Guinardia* or *Minidiscus* rank amongst the most abundant species in the WEC, it is thus likely that the manner in which they die profoundly influences the functioning of the food-web. For example, microscopy analysis suggested that aplanochytrids (vegetative cells and sporangia) carry nutritive resources, which could be transferred to higher trophic levels via the predation as described for chytrids (Mycoloop pathway, (Kagami *et al.*, 2007)). By contrast, one of the known consequences of viral infection and subsequent lysis is to fuel the pool of DOM and to force the food-web towards a more regenerative pathway (viral loop, (Wilhelm and Suttle, 1999)). In this respect, methods that accurately assess the relative contribution of eukaryotes, bacteria, and viruses need to be developed in order to better understand the functioning of marine ecosystems.

We identified several potential tools that may be appropriate. The e-HCFM technique (for environmental high content fluorescence microscopy) is a high throughput method that enables the detection, visualization, and quantification of the coastal eukaryotic microbiodiversity but also their symbiotic associations, including parasitism (Colin *et al.*, 2017). Since this technique is not destructive (organisms are observed alive), their taxonomy can be defined after single cell isolation and sequencing. We could also use the different host-parasites model systems to identify discriminative biological markers that characterize the infection by the different parasites. For example, infected host transcriptome could be studied in order to identify specific genetic markers expressed during infection for each pathogen. Single cell mass spectrometry approach also emerges as powerful tool to explore cellular heterogeneity. It enables the detection of multiplexed molecules (protein, peptides, lipids and metabolites) in a single cell. An ongoing collaboration (M. Valley, Max Planck Institute for Chemical Ecology) aims at using our biological model systems to characterize the metabolite profile of infected *Guinardia* cells and discriminate diagnostic molecules of infection by each

parasite. Regardless of the approach, the identified diagnostic biomarkers could be traced back in the environment to determine who infects whom.

4. Concluding remarks

To sum up, this very exploratory Ph.D. research has highlighted a new and important diversity of pathogens of diatoms in the Western English Channel. The exploration of the collection of diatoms and parasites established in this project provides a unique opportunity to tackle the role of parasitism in the ocean. Multidisciplinary and multiscale approaches should provide new fundamental knowledge on the ecology and diversity of marine parasites and ultimately refine our understanding of ecological succession, evolution, and ocean biogeochemistry.

ANNEXES

1. Les interactions écologiques durables (Introduction)

Dans la nature, aucun être vivant ne peut vivre seul, sans interagir avec les organismes qui l'entourent. Les espèces forment entre elles des interactions biotiques complexes qui peuvent être de différentes natures. 5 types d'interactions écologiques, dites symbioses (en grec « vivre ensemble »), ont été recensés et sont présentées sur l'Annexe- 1 (Faust and Raes, 2012; Lewin, 1982; Lidicker, 1979).

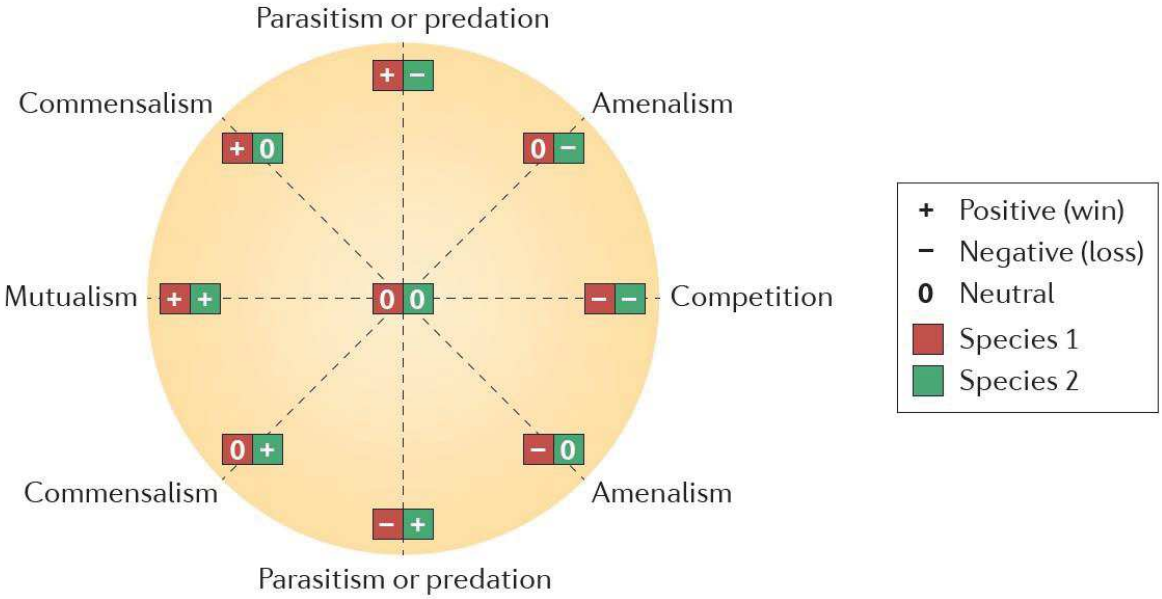

Annexe- 1. Schéma des interactions écologiques existant dans la nature (Faust and Raes, 2012). Dans chaque symbiose, l'effet pour chaque protagoniste est reporté en positif (+), négatif (-) ou neutre (0). Cette « roue » des associations a initialement été représentée par (Lidicker, 1979) pour introduire les notions d'intensité et de qualité des interactions entre les membres d'une même espèce ou d'espèces différentes

Il y a tout d'abord les interactions mutualistes qui sont bénéfiques pour chaque espèce. Par exemple, certaines diatomées ne possèdent pas le gène metE (pour « B12-independent methionine synthase ») impliqué dans la synthèse de la vitamine B12, nécessaire à leur survie, et dépendent donc d'un apport exogène. Des bactéries sont connues pour produire et fournir cette vitamine aux diatomées, profitant en retour de la matière organique dissoute produite par ces dernières. L'échange de ressources permet ainsi la croissance des deux organismes (Amin *et al.*, 2012). Face à ce mutualisme se trouve la compétition, où chaque protagoniste de l'interaction sera impacté négativement. Dans les écosystèmes marins, la compétition parmi les microorganismes pour les nutriments est un phénomène particulièrement commun (Litchman, 2007). Dans le commensalisme, une espèce va tirer profit de l'autre, qui ne sera en rien lésé. C'est le cas notamment dans les biodégradations, où l'organisme commensal se nourrit de composés libérés par d'autres organismes de la communauté (Faust and Raes, 2012; Lidicker, 1979). Ce type d'interaction s'oppose à l'amensalisme, où un organisme sera

défavorisé face à un effet neutre chez le partenaire. La production de métabolites secondaires par une espèce peut en effet inhiber le développement d'une autre, comme dans les processus d'allélopathie (Faust and Raes, 2012; Legrand *et al.*, 2003; Lidicker, 1979). Enfin, le parasitisme est défini comme une relation non-mutualiste entre deux espèces, où un partenaire, le parasite, va se développer aux dépends de l'autre, l'hôte. Contrairement au système proie-prédateur, les espèces protagonistes de cette association interagissent durablement et ne sont pas instantanées. Il n'y a pas simplement un transfert d'énergie mais des échanges complexes (comme par exemple de matériel génétique) qui s'établissent dans le temps (Combes, 2000).

2. Environmental parameters at the SOMLIT-Astan site (Part I)

Hydrological parameters collected and measured by the SOMLIT program between August 2015 and October 2016 are shown Annexe- 2. These seasonal variations are typical of those observed at SOMLIT-Astan for the 2009-2011 period (Simon *et al.*, in prep.).
Temperature varied between 15.8°C end of August-early September to 10.35°C in March. Salinity slightly varied, with optima in December 2015 and October 2016 (35.37 PSU) and minima (35.07 PSU) in February 2016. Oxygen increased during spring and showed minimum values during autumn. Nutrients also displayed a pronounced seasonality and never reached a total depletion. Ammonium had an important peak in June 2016. Nitrates + Nitrites had the highest values from January to early April 2016 and underwent an important decrease during the beginning of the summer time. Phosphates and Silicates exhibited the same trend, with peaks in January and February 2016 (0.43 µM and 0.43 µM for PO_4 and 3.8 and 3.9 µM for $SIOH_4$) and with lowest values from end of April to end of August 2016. Concentrations of chlorophyll *a* did not showed any seasonal trend during this period of time. However, its curve was similar to those shown in Simon *et al.*, (in prep.) over a 3 years period, with highest values during spring and summer.

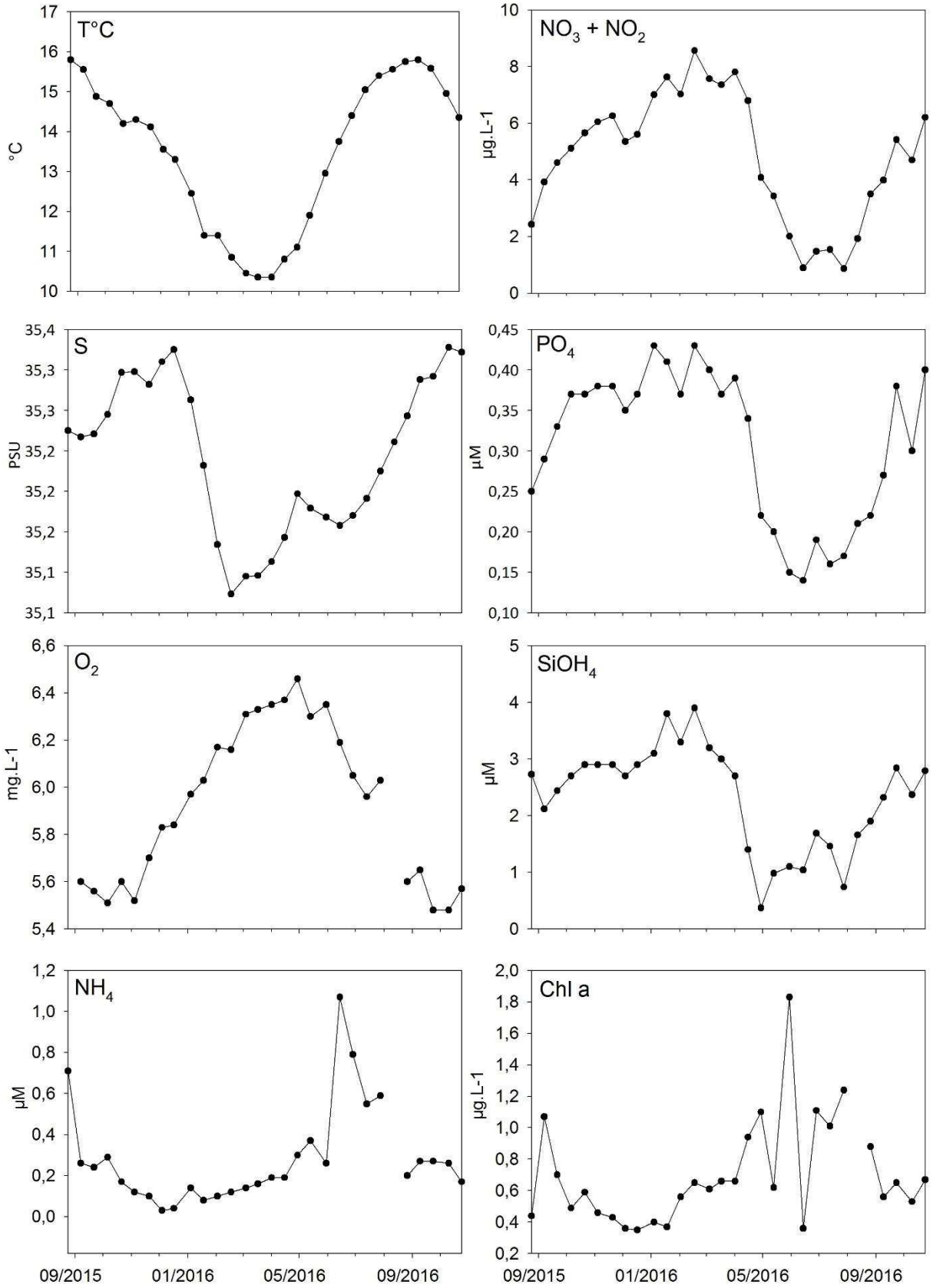

Annexe- 2. Temporal variations of the hydrological parameters (T°C: Temperature, S: Salinity, O2: Oxygen, NH4: Ammonium, NO3 + NO2: Nitrates + Nitrites, PO4: Phosphates, and SiOH4: Silicates) and Chlorophyll a at the SOMLIT-Astan station between August 2015 and October 2016

REFERENCES

A

Adl, S. M., Simpson, A. G. B., Lane, C. E., Lukeš, J., Bass, D., Bowser, S. S., et al. (2012). The revised classification of eukaryotes. *J. Eukaryot. Microbiol.* 59, 429–93. doi:10.1111/j.1550-7408.2012.00644.x.

Agha, R., Saebelfeld, M., Manthey, C., Rohrlack, T., and Wolinska, J. (2016). Chytrid parasitism facilitates trophic transfer between bloom-forming cyanobacteria and zooplankton (*Daphnia*). *Sci. Rep.* 6, 35039. doi:10.1038/srep35039.

Agusti, S., González-Gordillo, J. I., Vaqué, D., Estrada, M., Cerezo, M. I., Salazar, G., et al. (2015). Ubiquitous healthy diatoms in the deep sea confirm deep carbon injection by the biological pump. *Nat. Commun.* 6, 7608. doi:10.1038/ncomms8608.

Aké-Castillo, J. A., Hernandez-Becerril, D. U., Meave del Castillo, M. E., and Bravo-Sierra, E. (2001). Species of *Minidiscus* (Bacillariophyceae) in the Mexican Pacific Ocean. *Cryptogam. Algol.* 22, 101–107. doi:10.1016/S0181-1568(00)01051-5.

Altschul, S. F., Gish, W., Miller, W., Myers, E. W., and Lipman, D. J. (1990). Basic Local Alignment Search Tool. *J. Mol. Biol.* 215, 403–410.

Alverson, A. J. (2008). Molecular systematics and the diatom species. *Protist* 159, 339–353. doi:10.1016/j.protis.2008.04.001.

Alverson, A. J. (2014). Timing marine–freshwater transitions in the diatom order Thalassiosirales. *Paleobiology* 40, 91–101. doi:10.1666/12055.

Alverson, A. J., Beszteri, B., Julius, M. L., and Theriot, E. C. (2011). The model marine diatom *Thalassiosira pseudonana* likely descended from a freshwater ancestor in the genus *Cyclotella*. *BMC Evol. Biol.* 11, 125. doi:10.1186/1471-2148-11-125.

Alverson, A. J., Cannone, J. J., Gutell, R. R., and Theriot, E. C. (2006). The evolution of elongate shape in diatoms. *J. Phycol.* 42, 655–668. doi:10.1111/j.1529-8817.2006.00228.x.

Alverson, A. J., Jansen, R. K., and Theriot, E. C. (2007). Bridging the Rubicon: Phylogenetic analysis reveals repeated colonizations of marine and fresh waters by thalassiosiroid diatoms. *Mol. Phylogenet. Evol.* 45, 193–210. doi:10.1016/j.ympev.2007.03.024.

Alverson, A. J., and Kolnick, L. (2005). Intragenomic nucleotide polymorphism among small subunit (18S) rDNA paralogs in the diatom genus *Skeletonema* (Bacillariophyta). *J. Phycol.* 41, 1248–1257. doi:10.1111/j.1529-8817.2005.00136.x.

Amato, A., and Ferrante, M. I. (2018). Chitin synthases in diatoms. *Ann. Proteomics Bioinforma.* 1, 1001.

Amato, A., Kooistra, W. H. C. F., Levialdi Ghiron, J. H., Mann, D. G., Pröschold, T., and Montresor, M. (2007). Reproductive isolation among sympatric cryptic species in marine diatoms. *Protist* 158, 193–207. doi:10.1016/j.protis.2006.10.001.

Amin, S. A., Parker, M. S., and Armbrust, E. V. (2012). Interactions between diatoms and bacteria. *Microbiol. Mol. Biol. Rev.* 76, 667–684. doi:10.1128/MMBR.00007-12.

Andersen, J. B. O., Heydorn, A., Hentzer, M., Eberl, L. E. O., Geisenberger, O., Molin, R. E. N., et al. (2001). gfp-Based N-Acyl Homoserine-Lactone sensor systems for detection of bacterial communication. *Appl. Environ. Microbiol.* 67, 575–585. doi:10.1128/AEM.67.2.575.

Armbrust, E. V. (2009). The life of diatoms in the world's oceans. *Nature* 459, 185–192. doi:10.1038/nature08057.

Arsenieff, L. (2018). Parasitisme et contrôle des blooms de diatomées en Manche Occidentale.

Assmy, P., and Smetacek, V. (2009). "Algal Blooms," in *Encyclopedia of Microbiology*, ed. Moselio Schaechter (Oxford: Elsevier), 27–41.

Azam, F., Fenchel, T., Field, J., Gray, J., Meyer-Reil, L., and Thingstad, F. (1983). The ecological role of water-column microbes in the sea. *Mar. Ecol. Prog. Ser.* 10, 257–263. doi:10.3354/meps010257.

B

Baek, K., Choi, A., Kang, I., Lee, K., and Cho, J. C. (2013). *Kordia antarctica* sp. nov., isolated from Antarctic seawater. *Int. J. Syst. Evol. Microbiol.* 63, 3617–3622. doi:10.1099/ijs.0.052738-0.

Barak-Gavish, N., Frada, M. J., Lee, P. A., DiTullio, G. R., Ku, C., Malitsky, S., et al. (2018). Bacterial virulence against an oceanic bloom-forming phytoplankter is mediated by algal DMSP. *bioRxiv*, 1–38. doi:http://dx.doi.org/10.1101/321398.

Bassler, B. L. (1999). How bacteria talk to each other: Regulation of gene expression by quorum sensing. *Curr. Opin. Microbiol.* 2, 582–587. doi:10.1016/S1369-5274(99)00025-9.

Baudoux, A.-C., Lebredonchel, H., Dehmer, H., Latimier, M., Edern, R., Rigaut-Jalabert, F., et al. (2015). Interplay between the genetic clades of *Micromonas* and their viruses in the Western English Channel. *Environ. Microbiol. Rep.* 7, 765–773. doi:10.1111/1758-2229.12309.

Baudoux, A.-C., Veldhuis, M. J. W., Witte, H. J., and Brussaard, C. P. D. (2007). Viruses as mortality agents of picophytoplankton in the deep chlorophyll maximum layer during IRONAGES III. *Limnol. Oceanogr.* 52, 2519–2529. doi:10.4319/lo.2007.52.6.2519.

Baudoux, A. C., and Brussaard, C. P. D. (2005). Characterization of different viruses infecting the marine harmful algal bloom species *Phaeocystis globosa*. *Virology* 341, 80–90. doi:10.1016/j.virol.2005.07.002.

Baudoux, A. C., Noordeloos, A. A. M., Veldhuis, M. J. W., and Brussaard, C. P. D. (2006). Virally induced mortality of *Phaeocystis globosa* during two spring blooms in temperate coastal waters. *Aquat. Microb. Ecol.* 44, 207–217. doi:10.3354/ame044207.

Baudoux, A. C., Veldhuis, M. J. W., Noordeloos, A. A. M., Van Noort, G., and Brussaard, C. P. D. (2008). Estimates of virus- vs. grazing induced mortality of picophytoplankton in the North Sea during summer. *Aquat. Microb. Ecol.* 52, 69–82. doi:10.3354/ame01207.

Beakes, G. W., Canter, H. M., and Jaworski, G. H. M. (1992). Comparative ultrastructural ontogeny of zoosporangia of *Zygorhizidium affluens* and *Z. planktonicum*, chytrid parasites of the diatom *Asterionella formosa*. *Mycol. Res.* 96, 1047–1059. doi:10.1016/S0953-7562(09)80115-9.

Bennett, R. M., Honda, D., Beakes, G. W., and Thines, M. (2017). "Labyrinthulomycota," in *Handbook of the Protists*, eds. Archibald J., Simpson A., and Slamovits C. (Springer), 507–542. doi:10.1007/978-3-319-28149-0_25.

Bettarel, Y., Kan, J., Wang, K., Williamson, K. E., Cooney, S., Ribblett, S., et al. (2005a). Isolation and preliminary characterisation of a small nuclear inclusion virus infecting the diatom *Chaetoceros* cf. *gracilis*. *Aquat. Microb. Ecol.* 40, 103–114. doi:10.3354/ame040103.

Bettarel, Y., Sime-Ngando, T., Bouvy, M., Arfi, R., and Amblard, C. (2005b). Low consumption of virus-sized particles by heterotrophic nanoflagellates in two lakes of the French Massif Central. *Aquat. Microb. Ecol.* 39, 205–209. doi:10.3354/ame039205.

Bidle, K. D. (2015). The molecular ecophysiology of programmed cell death in marine phytoplankton. *Ann. Rev. Mar. Sci.*, 1–35. doi:10.1146/annurev-marine-010213-135014.

Biller, S. J., Berube, P. M., Dooley, K., Williams, M., Satinsky, B. M., Hackl, T., et al. (2018). Marine microbial metagenomes sampled across space and time. *Sci. Data* 5, 180176. doi:10.1038/sdata.2018.176.

Bochdansky, A. B., Clouse, M. A., and Herndl, G. J. (2016). Eukaryotic microbes, principally fungi and labyrinthulomycetes, dominate biomass on bathypelagic marine snow. *ISME J.*, 1–12. doi:10.1038/ismej.2016.113.

Bower, S. M. (1987a). *Labyrinthuloides haliotidis* n.sp. (Protozoa: Labyrinthomorpha), a pathogenic parasite of small juvenile abalone in a British Columbia mariculture facility. *Can. J. Zool.* 65, 1996–2007. doi:10.1139/z87-304.

Bower, S. M. (1987b). Pathogenicity and host specificity of *Labyrinthuloides haliotidis* (Protozoa: Labyrinthomorpha), a parasite of juvenile abalone. *Can. J. Zool.* 65, 2008–2012.

Bowler, C., Vardi, A., and Allen, A. E. (2010). Oceanographic and biogeochemical insights from diatom genomes. *Ann. Rev. Mar. Sci.* 2, 333–365. doi:10.1146/annurev-marine-120308-081051.

Bratbak, G., Egge, J. K., and Heldal, M. (1993). Viral mortality of the marine alga *Emiliania huxleyi* (Haptophyceae) and termination of algal blooms. *Mar. Ecol. Prog. Ser.* 93, 39–48. doi:10.3354/meps093039.

Brussaard, C. P. D. (2004). Viral Control of Phytoplankton Populations—a Review. *J. Eukaryot. Microbiol.* 51, 125–138. doi:10.1111/j.1550-7408.2005.000vol-cont.x.

Brussaard, C. P. D., Kempers, R. S., Kop, A. J., Riegman, R., and Heldal, M. (1996). Virus-like particles in a summer bloom of *Emiliania huxleyi* in the North Sea. *Aquat. Microb. Ecol.* 10, 105–113. doi:10.3354/ame010105.

Buaya, A. T., Ploch, S., Hanic, L., Nam, B., Nigrelli, L., Kraberg, A., et al. (2017). Phylogeny of *Miracula helgolandica* gen. et sp. nov. and *Olpidiopsis drebesii* sp. nov., two basal oomycete parasitoids of marine diatoms, with notes on the taxonomy of *Ectrogella*-like species. *Mycol. Prog.* 16, 1041–1050. doi:10.1007/s11557-017-1345-6.

Burki, F., Shalchian-Tabrizi, K., Minge, M., Skjæveland, Å., Nikolaev, S. I., Jakobsen, K. S., et al. (2007). Phylogenomics reshuffles the eukaryotic supergroups. *PLoS One* 2, 1–6. doi:10.1371/journal.pone.0000790.

C

Caamaño, E., Loperena, L., Hinzpeter, I., Pradel, P., Gordillo, F., Corsini, G., et al. (2017). Isolation and molecular characterization of *Thraustochytrium* strain isolated from Antarctic Peninsula and its biotechnological potential in the production of fatty acids. *Brazilian J. Microbiol.* 48, 671–679. doi:10.1016/j.bjm.2017.01.011.

Cai, G., Yang, X., Lai, Q., Yu, X., Zhang, H., Li, Y., et al. (2016). Lysing bloom-causing alga *Phaeocystis globosa* with microbial algicide: An efficient process that decreases the toxicity of algal exudates. *Sci. Rep.* 6, 1–11. doi:10.1038/srep20081.

Cariou, T., Macé, É., and Morin, P. (2002). La série océanographique littorale Estacade de l'Observatoire Océanologique de Roscoff : Résultats des observations 1985 – 2002.

Carlson, M. C. G., McCary, N. D., Leach, T. S., and Rocap, G. (2016). *Pseudo-nitzschia* Challenged with co-occurring viral communities display diverse infection phenotypes. *Front. Microbiol.* 7. doi:10.3389/fmicb.2016.00527.

Castberg, T., Larsen, A., Sandaa, R. A., Brussaard, C. P. D., Egge, J. K., Heldal, M., et al. (2001). Microbial population dynamics and diversity during a bloom of the marine coccolithophorid *Emiliania huxleyi* (Haptophyta). *Mar. Ecol. Prog. Ser.* 221, 39–46. doi:10.3354/meps221039.

Castberg, T., Thyrhaug, R., Larsen, A., Sandaa, R.-A., Heldal, M., Van Etten, J. L., et al. (2002). Isolation and characterization of a virus that infects *Emiliania huxleyi* (Haptophyta). *J. Phycol.* 38, 767–774.

Castresana, J. (2000). Selection of conserved blocks from multiple alignments for their use in phylogenetic analysis. *J.. Mol. Biol. Evol* 17, 540–552.

Chambouvet, A., Alves-de-Souza, C., Cueff, V., Marie, D., Karpov, S., and Guillou, L. (2011). Interplay between the parasite *Amoebophrya* sp. (Alveolata) and the cyst formation of the red tide dinoflagellate *Scrippsiella trochoidea*. *Protist* 162, 637–649. doi:10.1016/j.protis.2010.12.001.

Chambouvet, A., Morin, P., Marie, D., and Guillou, L. (2008). Control blooms of toxic marine by serial dinoflagellate parasitic killers. *Science (80-.).* 322, 1254–1257.

Chambouvet, A., Richards, T. A., Bass, D., and Neuhauser, S. (2015). "Revealing

microparasite diversity in aquatic environments using brute force molecular techniques and subtle microscopy," in *Parasite diversity and diversification - Evolutionary ecology meets phylogenetics*, eds. S. Morand, B. R. Krasnov, and T. J. Littlewood (Cambridge University Press), 93–116. doi:10.1017/CBO9781139794749.010.

Choi, A., Oh, H. M., Yang, S. J., and Cho, J. C. (2011). *Kordia periserrulae* sp. nov., isolated from a marine polychaete *Periserrula leucophryna*, and emended description of the genus *Kordia*. *Int. J. Syst. Evol. Microbiol.* 61, 864–869. doi:10.1099/ijs.0.022764-0.

Christaki, U., Genitsaris, S., Monchy, S., Li, L. L., Rachik, S., Breton, E., et al. (2017a). Parasitic eukaryotes in a meso-eutrophic coastal system with marked *Phaeocystis globosa* blooms. *Front. Mar. Sci.* 4, 416. doi:10.3389/fmars.2017.00416.

Christaki, U., Genitsaris, S., Monchy, S., Li, L. L., Rachik, S., Breton, E., et al. (2017b). Parasitic Eukaryotes in a Meso-Eutrophic Coastal System with Marked *Phaeocystis globosa* Blooms. *Front. Mar. Sci.* 4, 416. doi:10.3389/fmars.2017.00416.

Colin, S., Coelho, L. P., Sunagawa, S., Bowler, C., Karsenti, E., Bork, P., et al. (2017). Quantitative 3D-imaging for cell biology and ecology of environmental microbial eukaryotes. *Elife* 6, 1–15. doi:10.7554/eLife.26066.

Collado-Mercado, E., Radway, J. C., and Collier, J. L. (2010). Novel uncultivated labyrinthulomycetes revealed by 18S rDNA sequences from seawater and sediment samples. *Aquat. Microb. Ecol.* 58, 215–228. doi:10.3354/ame01361.

Combes, C. (2000). Parasitisme, écologie et évolution. *CNRS info* 385, 9–10.

Combes, C. (2001). *Les associations du vivant - L'art d'être parasite*. , ed. Flammarion Paris.

Coolen, M. J. L. (2011). 7000 years of *Emiliania huxleyi* viruses in the Black Sea. *Science (80-.).* 333, 451–452. doi:10.1126/science.1200072.

Coutinho, B. G., Mevers, E., Schaefer, A. L., Pelletier, D. A., Harwood, C. S., Clardy, J., et al. (2018). A plant-responsive bacterial-signaling system senses an ethanolamine derivative. *Proc. Natl. Acad. Sci.*, 201809611. doi:10.1073/pnas.1809611115.

Cox, B. A., and Mackin, J. G. (1974). Studies on a new species of *Labyrinthula* (Labyrinthulales) isolated from the marine gastropod *Thais haemastoma floridana*. *Trans. Am. Microsc. Soc.* 93, 62–70.

Crenn, K., Serpin, D., Lepleux, C., Overmann, J., and Jeanthon, C. (2016). *Silicimonas algicola* gen. nov., sp. nov., a member of the *Roseobacter* clade isolated from the cell surface of the marine diatom *Thalassiosira delicatula*. *Int. J. Syst. Evol. Microbiol.* 66, 4580–4588. doi:10.1099/ijsem.0.001394.

Culley, A. (2018). New insight into the RNA aquatic virosphere via viromics. *Virus Res.* 244, 84–89. doi:10.1016/j.virusres.2017.11.008.

Culley, A. I., Lang, A. S., and Suttle, C. A. (2003). High diversity of unknown picorna-like viruses in the sea. *Nature* 424, 1054–1057. doi:10.1038/nature01886.

Culley, A. I., Mueller, J. A., Belcaid, M., Wood-charlson, E. M., Poisson, G., and Steward, G. F. (2014). The characterization of RNA viruses in tropical seawater using targeted PCR and metagenomics. *MBio* 5, e01210-14. doi:10.1128/mBio.01210-14.

Culley, A. I., and Steward, G. F. (2007). New genera of RNA viruses in subtropical seawater, inferred from polymerase gene sequences. *Appl. Environ. Microbiol.* 73, 5937–5944. doi:10.1128/AEM.01065-07.

Culley, A. I., Suttle, C. A., and Steward, G. F. (2010). Characterization of the diversity of marine RNA viruses. *Man. Aquat. Viral Ecol.*, 193–201. doi:10.4319/mave.2010.978-0-9845591-0-7.193.

D

Damare, V., and Raghukumar, S. (2006). Morphology and physiology of the marine straminipilan fungi, the aplanochytrids isolated from the equatorial Indian

Ocean. *Indian J. Mar. Sci.* 35, 326–340.

Damare, V., and Raghukumar, S. (2010). Association of the stramenopilan protists, the aplanochytrids, with zooplankton of the equatorial Indian Ocean. *Mar. Ecol. Prog. Ser.* 399, 53–68. doi:10.3354/meps08277.

Daniels, C. J., Poulton, A. J., Esposito, M., Paulsen, M. L., Bellerby, R., St John, M., et al. (2015). Phytoplankton dynamics in contrasting early stage North Atlantic spring blooms: Composition, succession, and potential drivers. *Biogeosciences* 12, 2395–2409. doi:10.5194/bg-12-2395-2015.

Day, J. G., and Brand, J. J. (2005). "Cryopreservation methods for maintaining microalgal cultures," in *Algal culturing techniques*, ed. R. A. Andersen (New Yor: Elsevier Academic Press), 165–187.

De Bruin, A., Ibelings, B. W., Kagami, M., Mooij, W. M., and Van Donk, E. (2008). Adaptation of the fungal parasite *Zygorhizidium planktonicum* during 200 generations of growth on homogeneous and heterogeneous populations of its host, the diatom *Asterionella formosa*. *J. Eukaryot. Microbiol.* 55, 69–74. doi:10.1111/j.1550-7408.2008.00306.x.

De Bruin, A., Ibelings, B. W., Rijkeboer, M., Brehm, M., and Van Donk, E. (2004). Genetic variation in *Asterionella formosa* (Bacillariophyceae): Is it linked to frequent epidemics of host-specific parasitic fungi? *J. Phycol.* 40, 823–830. doi:10.1111/j.1529-8817.2004.04006.x.

de Vargas, C., Audic, S., Henry, N., Decelle, J., Mahé, F., Logares, R., et al. (2015). Eukaryotic plankton diversity in the sunlit ocean. *Science (80-.).* 348, 1261605–1/11. doi:10.1007/s13398-014-0173-7.2.

Dell'Anno, A., Corinaldesi, C., and Danovaro, R. (2015). Virus decomposition provides an important contribution to benthic deep-sea ecosystem functioning. *Proc. Natl. Acad. Sci.* 112, E2014–E2019. doi:10.1073/pnas.1422234112.

Demory, D., Arsenieff, L., Simon, N., Six, C., Rigaut-jalabert, F., Marie, D., et al. (2017). Temperature is a key factor in *Micromonas* – virus interactions. *ISME J.* 11, 601–612. doi:10.1038/ismej.2016.160.

Djikeng, A., Kuzmickas, R., Anderson, N. G., and Spiro, D. J. (2009). Metagenomic analysis of RNA viruses in a fresh water lake. *PLoS One* 4. doi:10.1371/journal.pone.0007264.

Doberva, M., Sanchez-Ferandin, S., Toulza, E., Lebaron, P., and Lami, R. (2015). Diversity of quorum sensing autoinducer synthases in the Global Ocean Sampling metagenomic database. *Aquat. Microb. Ecol.* 74, 107–119. doi:10.3354/ame01734.

Doi, K., and Honda, D. (2017). Proposal of *Monorhizochytrium globosum* gen. nov., comb. nov. (Stramenopiles, Labyrinthulomycetes) for former *Thraustochytrium globosum* based on morphological features and phylogenetic relationships. *Phycol. Res.* 65, 188–201. doi:10.1111/pre.12175.

Doucette, G. J., McGovern, E. R., and Babinchak, J. A. (1999). Algicidal bacteria active against *Gymnodinium breve* (Dinophyceae). I. Bacterial isolation and characterization of killing activity. *J. Phycol.* 35, 1447–1454. doi:10.1046/j.1529-8817.1999.3561447.x.

Drebes, G., Kühn, S. F., Gmelch, A., and Schnepf, E. (1996). *Cryothecomonas aestivalis* sp. nov., a colourless nanoflagellate feeding on the marine centric diatom *Guinardia delicatula* (Cleve) Hasle. *Helgoländer Meeresuntersuchungen* 50, 497–515.

Drebes, G., and Schnepf, E. (1982). Phagotrophy and development of *Paulsenella* cf. *chaetoceratis* (Dinophyta), an ectoparasite of the diatom *Streptotheca thamesis*. *Helgoländer Meeresuntersuchungen* 35, 501–515. doi:10.1007/BF01999138.

Drebes, G., and Schnepf, E. (1988). *Paulsenella Chatton* (Dinophyta), ectoparasites of marine diatoms: development and taxonomy. *Helgoländer Meeresuntersuchungen* 42, 563–581. doi:10.1007/BF02365627.

Drebes, G., and Schnepf, E. (1998). *Gyrodinium undulans* Hulburt, a marine dinoflagellate

feeding on the bloom-forming diatom *Odontella aurita*, and on copeod and rotifer eggs. *Helgoländer Meeresuntersuchungen* 52, 1–14. doi:10.1007/BF02908731.

Du, J., Liu, Y., Lai, Q., Dong, C., Xie, Y., and Shao, Z. (2015). *Kordia zhangzhouensis* sp. nov., isolated from surface freshwater. *Int. J. Syst. Evol. Microbiol.* 65, 3379–3383. doi:10.1099/ijsem.0.000424.

Durkin, C. a., Mock, T., and Armbrust, E. V. (2009). Chitin in diatoms and its association with the cell wall. *Eukaryot. Cell* 8, 1038–1050. doi:10.1128/EC.00079-09.

E

Ebert, D., and Hamilton, W. D. (1996). Sex against virulence: The coevolution of parasitic diseases. *Trends Ecol. Evol.* 11, 79–82. doi:10.1016/0169-5347(96)81047-0.

Eissler, Y., Wang, K., Chen, F., Wommack, K. E., and Coats, D. W. (2009). Ultrastructural characterization of the lytic cycle of an intranuclear virus infecting the diatom *Chaetoceros* cf. *wighamii* (bacillariophyceae) from Chesapeake Bay, USA. *J. Phycol.* 45, 787–797. doi:10.1111/j.1529-8817.2009.00705.x.

Evans, C., and Wilson, W. H. (2008). Preferential grazing of *Oxyrrhis marina* on virus-infected *Emiliania huxleyi*. *Limnol. Oceanogr.* 53, 2035–2040. doi:10.4319/lo.2008.53.5.2035.

F

Falkowski, P. G., Barber, R. T., and Smetacek, V. (1998). Biogeochemical controls and feedbacks on ocean primary production. *Sci. New Ser.* 281, 200–206. doi:10.1126/science.281.5374.200.

Faust, K., and Raes, J. (2012). Microbial interactions: From networks to models. *Nat. Rev. Microbiol.* 10, 538–550. doi:10.1038/nrmicro2832.

Field, C. B., Behrenfeld, M. J., Randerson, J. T., and Falkowski, P. (1998). Primary Production of the Biosphere: Integrating Terrestrial and Oceanic Components. *Science (80-.).* 281, 237–240. doi:10.1126/science.281.5374.237.

FioRito, R., Leander, C., and Leander, B. (2016). Characterization of three novel species of Labyrinthulomycota isolated from ochre sea stars (*Pisaster ochraceus*). *Mar. Biol.* 163. doi:10.1007/s00227-016-2944-5.

Frada, M. J., Schatz, D., Farstey, V., Ossolinski, J. E., Sabanay, H., Ben-Dor, S., et al. (2014). Zooplankton may serve as transmission vectors for viruses infecting algal blooms in the ocean. *Curr. Biol.* 24, 1–6. doi:10.1016/j.cub.2014.09.031.

Frada, M. J., and Vardi, A. (2015). Algal viruses hitchhiking on zooplankton across phytoplankton blooms. *Commun. Integr. Biol.* 8, e1029210. doi:10.1080/19420889.2015.1029210.

Frada, M., Probert, I., Allen, M. J., Wilson, W. H., and de Vargas, C. (2008). The “Cheshire Cat” escape strategy of the coccolithophore *Emiliania huxleyi* in response to viral infection. *Proc. Natl. Acad. Sci. U. S. A.* 105, 15944–15949.

Frenken, T., Alacid, E., Berger, S. A., Bourne, E. C., Gerphagnon, M., Grossart, H. P., et al. (2017). Integrating chytrid fungal parasites into plankton ecology: research gaps and needs. *Environ. Microbiol.* 19, 3802–3822. doi:10.1111/1462-2920.13827.

Friedman, J., and Alm, E. J. (2012). Inferring correlation networks from genomic survey data. *PLoS Comput. Biol.* 8, 1–11. doi:10.1371/journal.pcbi.1002687.

Fuhrman, J. A. (1999). Marine viruses and their biogeochemical and ecological effects. *Nature* 399, 541–548. doi:10.1038/21119.

Fuhrman, J. A., and Steele, J. A. (2008). Community structure of marine bacterioplankton: Patterns, networks, and relationships to function. *Aquat. Microb. Ecol.* 53, 69–81. doi:10.3354/ame01222.

Fuqua, C. (2006). The QscR Quorum-Sensing

regulon of *Pseudomonas aeruginosa*: an orphan claims its identity. *J. Bacteriol.* 188, 3169–3171. doi:10.1128/JB.188.9.3169.

Furusawa, G., Yoshikawa, T., Yasuda, A., and Sakata, T. (2003). Algicidal activity and gliding motility of *Saprospira* sp. SS98-5. *Can. J. Microbiol.* 49, 92–100. doi:10.1139/w03-017.

G

Gachon, C. M. M., Sime-Ngando, T., Strittmatter, M., Chambouvet, A., and Kim, G. H. (2010). Algal diseases: Spotlight on a black box. *Trends Plant Sci.* 15, 633–640. doi:10.1016/j.tplants.2010.08.005.

Gao, Y.-H., Zhao-Di, C., and Chin, T. G. (1992). *Minidiscus* a new recordded nanodiatom genus for China. *Acta Phytotaxon. Sin.* 30, 273–276.

Gerphagnon, M., Latour, D., Colombet, J., and Sime-Ngando, T. (2013). A double staining method using SYTOX green and calcofluor white for studying fungal parasites of phytoplankton. *Appl. Environ. Microbiol.* 79, 3943–3951. doi:10.1128/AEM.00696-13.

Gleason, F. H., Jephcott, T. G., Küpper, F. C., Gerphagnon, M., Sime-Ngando, T., Karpov, S. A., et al. (2015). Potential roles for recently discovered chytrid parasites in the dynamics of harmful algal blooms. *Fungal Biol. Rev.* 29, 20–33. doi:10.1016/j.fbr.2015.03.002.

Gleason, F. H., Kagami, M., Lefevre, E., and Sime-Ngando, T. (2008). The ecology of chytrids in aquatic ecosystems: roles in food web dynamics. *Fungal Biol. Rev.* 22, 17–25. doi:10.1016/j.fbr.2008.02.001.

Gleason, F. H., Küpper, F. C., Amon, J. P., Picard, K., Gachon, C. M. M., Marano, A. V., et al. (2011). Zoosporic true fungi in marine ecosystems: A review. *Mar. Freshw. Res.* 62, 383–393. doi:10.1071/MF10294.

Gómez, F., and Souissi, S. (2007). Unusual diatoms linked to climatic events in the northeastern English Channel. *J. Sea Res.* 58, 283–290. doi:10.1016/j.seares.2007.08.002.

González, J. F., and Venturi, V. (2013). A novel widespread interkingdom signaling circuit. *Trends Plant Sci.* 18, 167–174. doi:10.1016/j.tplants.2012.09.007.

Gowen, R. J., McCullough, G., Kleppel, G. S., Houchin, L., and Elliott, P. (1999). Are copepods important grazers of the spring phytoplankton bloom in the western Irish Sea? *J. Plankton Res.* 21, 465–483. doi:10.1093/plankt/21.3.465.

Graham, L. E., Wilcox, L. W., and Graham, J. E. (2009). *Algae - Second edition*. Pearson Benjamin Cummings.

Grahame, E. S. (1976). The occurrence of *Lagenisma coscinodisci* in *Palmeria hardmaniana* from Kingston harbour, Jamaica. *Br. Phycol. J.* 11, 57–61. doi:10.1080/00071617600650091.

Grall, J. R. (1972). Développement “printanier” de la diatomée *Rhizosolenia delicatula* près de Roscoff. *Mar. Biol.* 16, 41–48.

Gsell, A. S., de Senerpont Domis, L. N., Verhoeven, K. J., van Donk, E., and Ibelings, B. W. (2013). Chytrid epidemics may increase genetic diversity of a diatom spring-bloom. *ISME J.* 7, 2057–2059. doi:10.1038/ismej.2013.73.

Gu, H., Zhang, X., Sun, J., and Luo, Z. (2012). Diversity and seasonal occurrence of *Skeletonema* (Bacillariophyta) species in Xiamen Harbour and surrounding seas, China. *Cryptogam. Algol.* 33, 245–263. doi:10.7872/crya.v33.iss3.2012.245.

Guillard, R. R. L. (1975). “Culture of phytoplankton for feeding marine invertebrates,” in *Culture of marine invertebrate animals*, eds. W. Smith and M. Chanley (New-York: Plenum Press), 29–60.

Guillard, R. R. L., and Ryther, J. H. (1962). Studies of marine planktonic diatoms. I. *Cyclotella nana* Hustedt and *Detonula confervacea* (Cleve) Gran. *Can. J. Microbiol.* 8, 229–239. doi:10.1139/m62-029.

Guillou, L., Bachar, D., Audic, S., Bass, D., Berney, C., Bittner, L., et al. (2013). The Protist Ribosomal Reference database (PR2): a catalog of unicellular eukaryote Small Sub-Unit rRNA sequences with curated taxonomy. *Nucleic Acids Res.* 41, D597–D604. doi:10.1093/nar/gks1160.

Guillou, L., Eikrem, W., Chrétiennot-Dinet, M.-J., Le Gall, F., Massana, R., Romari, K., et al. (2004). Diversity of picoplanktonic prasinophytes assessed by direct nuclear SSU rDNA sequencing of environmental samples and novel isolates retrieved from oceanic and coastal marine ecosystems. *Protist* 155, 193–214. doi:10.1078/143446104774199592.

Guilloux, L., Rigaut-Jalabert, F., Jouenne, F., Ristori, S., Viprey, M., Not, F., et al. (2013). An annotated checklist of Marine Phytoplankton taxa at the SOMLIT-Astan time series off Roscoff (Western English Channel, France): Data collected from 2000 to 2010. *Cah. Biol. Mar.* 54, 247–256.

Guindon, S., Dufayard, J. F., Lefort, V., Anisimova, M., Hordijk, W., and Gascuel, O. (2010). New algorithms and methods to estimate maximum-likelihood phylogenies: Assessing the performance of PhyML 3.0. *Syst. Biol.* 59, 307–321. doi:10.1093/sysbio/syq010.

Guiry, M. D., and Guiry, G. M. (2018). AlgaeBase. *World-wide Electron. Publ. Natl. Univ. Ireland, Galw.* Available at: http://www.algaebase.org.

Guo, L., Sui, Z., Zhang, S., Ren, Y., and Liu, Y. (2015). Comparison of potential diatom 'barcode' genes (The 18S rRNA gene and ITS, COI, rbcL) and their effectiveness in discriminating and determining species taxonomy in the Bacillariophyta. *Int. J. Syst. Evol. Microbiol.* 65, 1369–1380. doi:10.1099/ijs.0.000076.

Gustavsen, J. A., Winget, D. M., Tian, X., and Suttle, C. A. (2014). High temporal and spatial diversity in marine RNA viruses implies that they have an important role in mortality and structuring plankton communities. *Front. Microbiol.* 5, 703. doi:10.3389/fmicb.2014.00703.

Gutiérrez, M. H., Jara, A. M., and Pantoja, S. (2016). Fungal parasites infect marine diatoms in the upwelling ecosystem of the Humboldt Current System off central Chile. *Environ. Microbiol.* 18, 1646–1653. doi:10.1111/1462-2920.13257.

H

Hallegraeff, G. M. (1984). Specied of the diatom genus *Thalassiosira* in Australian waters. *Bot. Mar.* 27, 495–513. Available at: Tassonomia Diatomee.

Hameed, A., Shahina, M., Lin, S. Y., Cho, J. C., Lai, W. A., and Young, C. C. (2013). *Kordia aquimaris* sp. nov., a zeaxanthin-producing member of the family *Flavobacteriaceae* isolated from surface seawater, and emended description of the genus *Kordia*. *Int. J. Syst. Evol. Microbiol.* 63, 4790–4796. doi:10.1099/ijs.0.056051-0.

Hamm, C. E., Merkel, R., Springer, O., Jurkojc, P., Maier, C., Prechtel, K., et al. (2003). Architecture and material properties of diatom shells provide effective mechanical protection. *Nature* 421, 841–843. doi:10.1038/nature01416.

Hanic, L. A., Sekimoto, S., and Bates, S. S. (2009). Oomycete and chytrid infections of the marine diatom Pseudo-nitzschia pungens (Bacillariophyceae) from Prince Edward Island, Canada. *Botany* 87, 1096–1105. doi:10.1139/B09-070.

Hasle, G. R. (1973). Thalassiosiraceae, a new diatom family. *Nor. J. Bot.* 20, 67–69.

Hasle, G. R. (1976). The biogeography of some marine planktonic diatoms. *Deep. Res. Oceanogr. Abstr.* 23, 319–338. doi:10.1016/0011-7471(76)90873-1.

Hasle, G. R. (1978). Some *Thalassiosira* species with one central process (Bacillariophyceae). *Nor. J. Bot.* 25, 77–110.

Hasle, G. R., and Syvertsen, E. E. (1997). "Marine Diatoms," in *Identifying Marine Phytoplankton*, ed. C. R. Tomas (San Diego: Academic Press), 5–386.

Hernández-Becerril, D. U. (1995). Planktonic diatoms from the gulf of california and coasts off baja california: The genera *Rhizosolenia*, *Proboscia*, *Pseudosolenia*, and former *Rhizosolenia* species. *Diatom Res.* 10, 251–267. doi:10.1080/0269249x.1995.9705348

Hernández-Becerril, D. U., Herrera-Hernández, P., Pérez-Mendoza, A., and Gerardo A Ceballos-Corona, J. (2010). Marine

planktonic diatoms of the order Rhizosoleniales (Bacillariophyta) From the tropical Mexican pacific. *Vie milieu - life Environ.* 60, 95–107.

Higgins, D. A., Pomianek, M. E., Kraml, C. M., Taylor, R. K., Semmelhack, M. F., and Bassler, B. L. (2007). The major *Vibrio cholerae* autoinducer and its role in virulence factor production. *Nature* 450, 883–886. doi:10.1038/nature06284.

Holligan, P. M., Viollier, M., Harbour, D. S., Camus, P., and Champagne-Philippe, M. (1983). Satellite and ship studies of coccolithophore production along a continental shelf edge. *Nature* 304, 339–342. doi:10.1038/304339a0.

Honda, D., Yokochi, T., Nakahara, T., Erata, M., and Higashihara, T. (1998). *Schizochytrium limacinum* sp. nov., a new thraustochytrid from a mangrove area in the west Pacific Ocean. *Mycol. Res.* 102, 439–448. doi:10.1017/S0953756297005170.

Honda, D., Yokochi, T., Nakahara, T., Raghukumar, S., Nakagiri, A., Schaumann, K., et al. (1999). Molecular phylogeny of labyrinthulids and thraustochytrids based on the sequencing of 18S ribosomal RNA gene. *J. Eukaryot. Microbiol.* 46, 637–647. doi:10.1111/j.1550-7408.1999.tb05141.x.

Hoppenrath, M., Beszteri, B., Drebes, G., Halliger, H., Van Beusekom, J. E. E., Janisch, S., et al. (2007). *Thalassiosira* species (Bacillariophyceae, Thalassiosirales) in the North Sea at Helgoland (German Bight) and Sylt (North Frisian Wadden Sea) – a first approach to assessing diversity. *Eur. J. Phycol.* 42, 271–288. doi:10.1080/09670260701352288.

I

Ianora, A., Miralto, A., Poulet, S. A., Carotenuto, Y., Buttino, I., Romano, G., et al. (2004). Aldehyde suppression of copepod recruitment in blooms of a ubiquitous planktonic diatom. *Nature* 429, 403–407. doi:10.1038/nature02526.

Ibelings, B. W., De Bruin, A., Kagami, M., Rijkeboer, M., Brehm, M., and Donk, E. Van (2004). Host parasite interactions between freshwater phytoplankton and chytrid fungi (*Chytridiomycota*). *J. Phycol.* 40, 437–453. doi:10.1111/j.1529-8817.2004.03117.x.

Imai, I., Sunahara, T., Nishikawa, T., Hori, Y., Kondo, R., and Hiroishi, S. (2001). Fluctuations of the red tide flagellates *Chattonella* spp. (Raphidophyceae) and the algicidal bacterium *Cytophaga* sp. in the Seto Inland Sea, Japan. *Mar. Biol.* 138, 1043–1049. doi:10.1007/s002270000513.

Iwata, I., Kimura, K., Tomaru, Y., Motomura, T., Koike, K., Koike, K., et al. (2017). Bothrosome Formation in *Schizochytrium aggregatum* (Labyrinthulomycetes, Stramenopiles) during Zoospore Settlement. *Protist* 168, 206–219. doi:10.1016/j.protis.2016.12.002.

J

Jacques, G. (1963). Variations saisonnières des populations phytoplanctoniques de la région de Roscoff (1962-1963).

Jacquet, S., Domaizon, I., Masquelier, S., Lepère, C., Guillou, L., Chambouvet, A., et al. (2011). Virus, bactéries et protistes pathogènes du phytoplancton le rôle insoupçonné des parasites dans le fonctionnement des écosystèmes aquatiques. *Courr. l'environnement l'INRA* 60, 37–50.

Jacquet, S., Heldal, M., Iglesias-Rodriguez, D., Larsen, A., Wilson, W., and Bratbak, G. (2002). Flow cytometric analysis of an *Emiliana huxleyi* bloom terminated by viral infection. *Aquat. Microb. Ecol.* 27, 111–124. doi:10.3354/ame027111.

Jephcott, T. G., Ogtrop, F. F. van, Gleason, F. H., Macarthur, D. J., and Scholz, B. (2017). "The ecology of chytrid and aphelid parasites of phytoplankton," in *The fungal community - its organization and role in the ecosystem - Fourth edition*, eds. J. Dighton and J. F. White (Boca Raton),

239–256. doi:10.1201/9781315119496-17.

Jewson, D., Kuwata, A., Cros, L., Fortuno, J. M., and Estrada, M. (2016). Morphological adaptations to small size in the marine diatom *Minidiscus comicus*. *Sci. Mar.* 80S1, in press. doi:10.3989/scimar.04331.06C.

Johnson, P. T. J., Dobson, A., Lafferty, K. D., Marcogliese, D. J., Memmott, J., Orlofske, S. A., et al. (2010). When parasites become prey: Ecological and epidemiological significance of eating parasites. *Trends Ecol. Evol.* 25, 362–371. doi:10.1016/j.tree.2010.01.005.

K

Kaczmarska, I., Beaton, M., Benoit, A. C., and Medlin, L. K. (2005). Molecular phylogeny of selected members of the order Thalassiosirales (Bacillariophyta) and evolution of the fultoportula. *J. Phycol.* 42, 121–138. doi:10.1016/j.ics.2005.09.099.

Kaczmarska, I., Lovejoy, C., Potvin, M., and Macgillivary, M. (2009). Morphological and molecular characteristics of selected species of *Minidiscus* (Bacillariophyta, Thalassiosiraceae). *Eur. J. Phycol.* 44, 461–475. doi:10.1080/09670260902855873.

Kagami, M., de Bruin, A., Ibelings, B. W., and Van Donk, E. (2007). Parasitic chytrids: their effects on phytoplankton communities and food-web dynamics. *Hydrobiologia* 578, 113–129. doi:10.1007/s10750-006-0438-z.

Kagami, M., Helmsing, N. R., and van Donk, E. (2011). Parasitic chytrids could promote copepod survival by mediating material transfer from inedible diatoms. *Hydrobiologia* 659, 49–54. doi:10.1007/s10750-010-0274-z.

Kagami, M., Ibelings, B. W., De Bruin, A., and Van Donk, E. (2005). Vulnerability of *Asterionella formosa* to *Daphnia* grazing: impact of a fungal parasite. *Verh. Internat. Verein. Limnol.* 29, 350–354.

Kang, I., Oh, H.-M., Kang, D., and Cho, J.-C. (2013). Genome of a SAR116 bacteriophage shows the prevalence of this phage type in the oceans. *Proc. Natl. Acad. Sci. U. S. A.* 110, 12343–8. doi:10.1073/pnas.1219930110.

Karpov, S. A., Mamkaeva, M. A., Aleoshin, V. V., Nassonova, E., Lilje, O., and Gleason, F. H. (2014). Morphology, phylogeny, and ecology of the aphelids (Aphelidea, Opisthokonta) and proposal for the new superphylum Opisthosporidia. *Front. Microbiol.* 5, 1–11. doi:10.3389/fmicb.2014.00112.

Kato, J., Amie, J., Murata, Y., Kuroda, A., Mitsutani, A., and Ohtake, H. (1998). Development of a genetic transformation system for an alga-lysing bacterium. *Appl. Environ. Microbiol.* 64, 2061–2064.

Katoh, K., Rozewicki, J., and Yamada, K. D. (2017). MAFFT online service: multiple sequence alignment, interactive sequence choice and visualization. *Brief. Bioinform.*, 1–7. doi:10.1093/bib/bbx108.

Kazlauskas, D., Dayaram, A., Kraberger, S., Goldstien, S., Varsani, A., and Krupovic, M. (2017). Evolutionary history of ssDNA bacilladnaviruses features horizontal acquisition of the capsid gene from ssRNA nodaviruses. *Virology* 504, 114–121. doi:10.1016/j.virol.2017.02.001.

Keller, M. D., Seluin, R. C., Claus, W., and Guillard, R. R. L. (1987). Media for the culture of oceanic ultraphytoplankton. *J. Phycol.* 23, 633–638. doi:10.1016/0198-0254(88)92621-0.

Kendrick, B. J., DiTullio, G. R., Cyronak, T. J., Fulton, J. M., Van Mooy, B. A. S., and Bidle, K. D. (2014). Temperature-induced viral resistance in *Emiliania huxleyi* (Prymnesiophyceae). *PLoS One* 9, e112134. doi:10.1371/journal.pone.0112134.

Kim, D. I., Lee, J. H., Kim, M. S., and Seong, C. N. (2017). *Kordia zosterae* sp. nov., isolated from the seaweed, *Zostera marina*. *Int. J. Syst. Evol. Microbiol.*, 2–7. doi:10.1099/ijsem.0.002379.

Kim, J. H., Park, J. H., Song, Y. H., and Chang, D. S. (1999). Isolation and characterization of the marine bacterium, *Alteromonas* sp. SR- 14 inhibiting the growth of diatom *Chaetoceros* species. *Korean J. Fish.*

Aquat. Sci. 32, 155–159ki.

Kim, J., Kim, C., Youn, S., and Choi, T. (2015a). Isolation and physiological characterization of a novel algicidal virus infecting the marine diatom *Skeletonema costatum*. *Plant Pathol. J.* 31, 186–191. doi:10.5423/PPJ.NT.03.2015.0029.

Kim, J., Yoon, S., and Choi, T. (2015b). Isolation and physiological characterization of a novel virus infecting *Stephanopyxis palmeriana* (Bacillariophyta). *Algae* 30, 81–87. doi:10.5423/PPJ.NT.03.2015.0029.

Kimura, K., and Tomaru, Y. (2013). Isolation and characterization of a single-stranded DNA virus infecting the marine diatom *Chaetoceros* sp. strain SS628-11 isolated from western Japan. *PLoS One* 8, e82013. doi:10.1371/journal.pone.0082013.

Kimura, K., and Tomaru, Y. (2014). Coculture with marine bacteria confers resistance to complete viral lysis of diatom cultures. *Aquat. Microb. Ecol.* 73, 69–80. doi:10.3354/ame01705.

Kimura, K., and Tomaru, Y. (2015). Discovery of two novel viruses expands the diversity of single-stranded DNA and single-stranded RNA viruses infecting a cosmopolitan marine diatom. *Appl. Environ. Microbiol.* 81, 1120–1131. doi:10.1128/AEM.02380-14.

King, A. M. Q., Lefkowitz, E. J., Mushegian, A. R., Adams, M. J., Dutilh, B. E., Gorbalenya, A. E., et al. (2018). Changes to taxonomy and the International Code of Virus Classification and Nomenclature ratified by the International Committee on Taxonomy of Viruses (2018). *Arch. Virol.*, 1–31. doi:10.1007/s00705-018-3847-1.

Koonin, E. V., Dolja, V. V., and Morris, T. J. (1993). Evolution and taxonomy of positive-strand RNA viruses: implications of comparative analysis of amino acid sequences. *Crit. Rev. Biochem. Mol. Biol.* 28, 375–430. doi:10.3109/10409239309078440.

Kraberg, A., Baumann, M., and Dürselen, C.-D. (2010). *Coastal phytoplankton: Photo guide for Northern European Seas*. Verlag Dr. Friedrich Pfeil, München.

Kröger, N., and Poulsen, N. (2008). Diatoms - From cell wall biogenesis to nanotechnology. *Annu. Rev. Genet.* 42, 83–107. doi:10.1146/annurev.genet.41.110306.130109.

Kühn, S. F. (1996). *Rhizamoeba schnepfii* sp. nov, a naked amoeba feeding on marine diatoms (North Sea, German Bight). *Arch. Fur Protistenkd.* 147, 277–282. doi:10.1016/S0003-9365(97)80054-1.

Kühn, S. F., Drebes, G., and Schnepf, E. (1996). Five new species of the nanoflagellate *Pirsonia* in the German Bight, North Sea, feeding on planktonic diatoms. *Helgoländer Meeresuntersuchungen* 50, 205–222.

Kühn, S., Lange, M., and Medlin, L. K. (2000). Phylogenetic position of *Cryothecomonas* inferred from nuclear-encoded small subunit ribosomal RNA. *Protist* 151, 337–45. doi:10.1078/S1434-4610(04)70032-2.

Kühn, S., Medlin, L., and Eller, G. (2004). Phylogenetic position of the parasitoid nanoflagellate Pirsonia inferred from nuclear-encoded small subunit ribosomal DNA and a description of *Pseudopirsonia* n. gen. and *Pseudopirsonia mucosa* (Drebes) comb. nov. *Protist* 155, 143–156. doi:10.1078/143446104774199556.

Kumar, S., Stecher, G., and Tamura, K. (2016). MEGA7: Molecular Evolutionary Genetics Analysis version 7.0 for bigger datasets. *Mol. Biol. Evol.* 33, 1870–1874. doi:10.1093/molbev/msw054.

Kurtz, Z. D., Müller, C. L., Miraldi, E. R., Littman, D. R., Blaser, M. J., and Bonneau, R. A. (2015). Sparse and compositionally robust inference of microbial ecological networks. *PLoS Comput. Biol.* 11, 1–25. doi:10.1371/journal.pcbi.1004226.

L

L'Helguen, S., Madec, C., and Le Corre, P. (1996). Nitrogen uptake in permanently well-mixed temperate coastal waters. *Estuar. Coast. Shelf Sci.* 42, 803–818. doi:10.1006/ecss.1996.0051.

Laber, C. P., Hunter, J. E., Carvalho, F., Collins, J. R., Hunter, E. J., Schieler, B. M., et al. (2018). *Coccolithovirus* facilitation of

carbon export in the North Atlantic. *Nat. Microbiol.* 3, 537–547. doi:10.1038/s41564-018-0128-4.

Lang, A. S., Rise, M. L., Culley, A. I., and Steward, G. F. (2009). RNA viruses in the sea. *FEMS Microbiol Rev* 33, 295–323. doi:10.1111/j.1574-6976.2008.00132.x.

Lawrence, J. E., and Suttle, C. A. (2004). Effect of viral infection on sinking rates of *Heterosigma akashiwo* and its implications for bloom termination. *Aquat. Microb. Ecol.* 37, 1–7.

Le Gall, O., Christian, P., Fauquet, C. M., King, A. M. Q., Knowles, N. J., Nakashima, N., et al. (2008). *Picornavirales*, a proposed order of positive-sense single-stranded RNA viruses with a pseudo-T = 3 virion architecture. *Arch. Virol.* 153, 715–27. doi:10.1007/s00705-008-0041-x.

Leander, C. A., and Porter, D. (2001). The Labyrinthulomycota is comprised of three distinct lineages. *Mycologia* 93, 459–464. doi:10.2307/3761732.

Leander, C. a., Porter, D., and Leander, B. S. (2004). Comparative morphology and molecular phylogeny of aplanochytrids (Labyrinthulomycota). *Eur. J. Protistol.* 40, 317–328. doi:10.1016/j.ejop.2004.07.003.

Leblanc, K., Arístegui, J., Armand, L., Assmy, P., Beker, B., Bode, A., et al. (2012). A global diatom database – abundance, biovolume and biomass in the world ocean. *Earth Syst. Sci. Data Discuss.* 5, 147–185. doi:10.5194/essdd-5-147-2012.

Leblanc, K., Quéguiner, B., Diaz, F., Cornet, V., Michel-Rodriguez, M., Durrieu de Madron, X., et al. (2018). Nanoplanktonic diatoms are globally overlooked but play a role in spring blooms and carbon export. *Nat. Commun.* 9, 953. doi:10.1038/s41467-018-03376-9.

Lee, S., Kato, J., Takiguchi, N., Kuroda, A., and Ikeda, T. (2000). Involvement of an extracellular protease in algicidal activity of the marine bacterium Pseudoalteromonas sp. strain A28. *Appl. Environ. Microbiol.* 66, 4334-. doi:10.1128/AEM.66.10.4334-4339.2000.

Lefort, V., Longueville, J. E., and Gascuel, O. (2017). SMS: Smart Model Selection in PhyML. *Mol. Biol. Evol.* 34, 2422–2424. doi:10.1093/molbev/msx149.

Legrand, C., Rengefors, K., Fistarol, G. O., and Granéli, E. (2003). Allelopathy in phytoplankton - biochemical, ecological and evolutionary aspects. *Phycologia* 42, 406–419. doi:10.2216/i0031-8884-42-4-406.1.

Lenaers, G., Maroteaux, L., Michot, B., and Herzog, M. (1989). Dinoflagellates in evolution. A molecular phylogenetic analysis of large subunit ribosomal RNA. *J Mol Evol* 29, 40–51.

Lepere, C., Demura, M., Kawachi, M., Romac, S., Probert, I., and Vaulot, D. (2011). Whole-genome amplification (WGA) of marine photosynthetic eukaryote populations. *FEMS Microbiol. Ecol.* 76, 513–523. doi:10.1111/j.1574-6941.2011.01072.x.

Letunic, I., Doerks, T., and Bork, P. (2015). SMART: Recent updates, new developments and status in 2015. *Nucleic Acids Res.* 43, D257–D260. doi:10.1093/nar/gku949.

Lewin, R. A. (1982). Symbiosis and parasitism: definitions and evaluations. *Bioscience* 32, 254–260. doi:10.2307/1308530.

Lewis, T. E., Nichols, P. D., and McMeekin, T. A. (1999). The biotechnological potential of thraustochytrids. *Mar. Biotechnol.* 1, 580–587. doi:10.1007/PL00011813.

Li, Y., Lei, X., Zhu, H., Zhang, H., Guan, C., Chen, Z., et al. (2016). Chitinase producing bacteria with direct algicidal activity on marine diatoms. *Sci. Rep.* 6, 1–13. doi:10.1038/srep21984.

Lidicker, W. Z. (1979). A clarification of interactions in ecological systems. *Bioscience* 29, 475–477. doi:10.2307/1307540.

Lindell, D., Jaffe, J. D., Johnson, Z. I., Church, G. M., and Chisholm, S. W. (2005). Photosynthesis genes in marine viruses yield proteins during host infection. *Nature* 438, 86–89. doi:10.1038/nature04111.

Litchman, E. (2007). Resource competition and the ecological success of phytoplankton. *Evol. Prim. Prod. Sea*, 351–375. doi:10.1016/B978-012370518-1/50017-5.

Litchman, E., and Klausmeier, C. a. (2008). Trait-based community ecology of phytoplankton. *Annu. Rev. Ecol. Evol. Syst.* 39, 615–639. doi:10.1146/annurev.ecolsys.39.110707.173549.

Loir, M. (2004). *Guide des diatomées : Plus de 200 micro-algues silicieuses photographiées*. , eds. Niestlé and Delachaux.

Lõpez-Bueno, A., Rastrojo, A., Peirõ, R., Arenas, M., and Alcamí, A. (2015). Ecological connectivity shapes quasispecies structure of RNA viruses in an Antarctic lake. *Mol. Ecol.* 24, 4812–4825. doi:10.1111/mec.13321.

Lovejoy, C., Bowman, J. P., and Hallegraeff, G. M. (1998). Algicidal effects of a novel marine *Pseudoalteromonas* isolate (class *Proteobacteria*, Gamma subdivision) on harmful algal bloom species of the genera *Chattonella*, *Gymnodinium*, and *Heterosigma*. *Appl. Environ. Microbiol.* 64, 2806–2813.

Luddington, I. A., Kaczmarska, I., and Lovejoy, C. (2012). Distance and character-based evaluation of the V4 region of the 18S rRNA gene for the identification of diatoms (Bacillariophyceae). *PLoS One* 7. doi:10.1371/journal.pone.0045664.

Ludwig, W., Strunk, O., Westram, R., Richter, L., Meier, H., Yadhukumar, A., et al. (2004). ARB: A software environment for sequence data. *Nucleic Acids Res.* 32, 1363–1371. doi:10.1093/nar/gkh293.

M

Mahé, F., Rognes, T., Quince, C., de Vargas, C., and Dunthorn, M. (2014). Swarm: robust and fast clustering method for amplicon-based studies. *PeerJ* 2, e593. doi:10.7717/peerj.593.

Malviya, S., Scalco, E., Audic, S., Vincent, F., Veluchamy, A., Poulain, J., et al. (2016). Insights into global diatom distribution and diversity in the world's ocean. *Proc. Natl. Acad. Sci.* 113, 1516–1525. doi:10.1073/pnas.1509523113.

Mann, D. G., and Droop, S. J. M. (1996). 3 . Biodiversity , biogeography and conservation of diatoms. *Hydrobiologia* 336, 19–32.

Mann, D. G., and Vanormelingen, P. (2013). An inordinate fondness? the number, distributions, and origins of diatom species. *J. Eukaryot. Microbiol.* 60, 414–420. doi:10.1111/jeu.12047.

Marchan, L. F., Lee Chang, K. J., Nichols, P. D., Mitchell, W. J., Polglase, J. L., and Gutierrez, T. (2017). Taxonomy, ecology and biotechnological applications of thraustochytrids: A review. *Biotechnol. Adv.* doi:10.1016/j.biotechadv.2017.09.003.

Margalef, R. (1978). Life-forms of phytoplankton as survival alternatives in an unstable environment. *Oceanol. Acta* 1, 493–509. doi:10.1007/BF00202661.

Marie, D., Le Gall, F., Edern, R., Gourvil, P., and Vaulot, D. (2017). Improvement of phytoplankton culture isolation using single cell sorting by flow cytometry. *J. Phycol.* 53, 271–282. doi:10.1111/jpy.12495.

Martin-Cereceda, M., Novarino, G., and Young, J. R. (2003). Grazing by *Prymnesium parvum* on small planktonic diatoms. *Aquat. Microb. Ecol.* 33, 191–199. doi:10.3354/ame033191.

Martin-Jezequel, V. (1983). Facteurs hydrologiques et phytoplancton en Baie de Morlaix (Manche Occidentale). *Hydrobiologia* 102, 131–143.

Martinez, J. M., Schroeder, D. C., Larsen, A., Bratbak, G., and Wilson, W. H. (2007). Molecular dynamics of *Emiliania huxleyi* and cooccurring viruses during two separate mesocosm studies. *Appl. Environ. Microbiol.* 73, 554–562. doi:10.1128/aem.00864-06.

Mayali, X., and Azam, F. (2004). Algicidal bacteria in the sea and their impact on algal blooms. *J. Eukaryot. Microbiol.* 51, 139–144. doi:10.1111/j.1550-7408.2004.tb00538.x.

Mayali, X., Franks, P. J. S., Tanaka, Y., and Azam, F. (2008). Bacteria-induced motility reduction in *Lingulodinium polyedrum* (Dinophyceae). *J. Phycol.* 44, 923–928. doi:10.1111/j.1529-8817.2008.00549.x.

Mcdaniel, L. D., Rosario, K., Breitbart, M., and

Paul, J. H. (2014). Comparative metagenomics: Natural populations of induced prophages demonstrate highly unique, lower diversity viral sequences. *Environ. Microbiol.* 16, 570–585. doi:10.1111/1462-2920.12184.

Médigue, C., Calteau, A., Cruveiller, S., Gachet, M., Gautreau, G., Josso, A., et al. (2017). MicroScope—an integrated resource for community expertise of gene functions and comparative analysis of microbial genomic and metabolic data. *Brief. Bioinform.*, 1–14. doi:10.1093/bib/bbx113.

Medlin, L. K. (2016). Evolution of the diatoms: major steps in their evolution and a review of the supporting molecular and morphological evidence. *Phycologia* 55, 79–103. doi:10.2216/15-105.1.

Medlin, L. K., and Kaczmarska, I. (2004). Evolution of the diatoms: V. Morphological and cytological support for the major clades and a taxonomic revision. *Phycologia* 43, 245–270.

Meyer, N., Bigalke, A., Kaulfuß, A., and Pohnert, G. (2017). Strategies and ecological roles of algicidal bacteria. *FEMS Microbiol. Rev.*, 1–20. doi:10.1093/femsre/fux029.

Miranda, J. A., Culley, A. I., Schvarcz, C. R., and Steward, G. F. (2016). RNA viruses as major contributors to Antarctic virioplankton. *Environ. Microbiol.* 00. doi:10.1111/1462-2920.13291.

Mitchell, A., Chang, H. Y., Daugherty, L., Fraser, M., Hunter, S., Lopez, R., et al. (2015). The InterPro protein families database: The classification resource after 15 years. *Nucleic Acids Res.* 43, D213–D221. doi:10.1093/nar/gku1243.

Mitsutani, A., Takesue, K., and Kirita, M. (1992). Lysis of *Skeletonema costatum* by *Cytophaga* sp. isolated from the Coastal Water of the Ariake Sea. *Water* 58, 2158–2167. doi:http://doi.org/10.2331/suisan.58.2159.

Mojica, K. D. A., and Brussaard, C. P. D. (2014). Factors affecting virus dynamics and microbial host-virus interactions in marine environments. *FEMS Microbiol. Ecol.* 89, 495–515. doi:10.1111/1574-6941.12343.

Mojica, K. D. A., Huisman, J., Wilhelm, S. W., and Brussaard, C. P. D. (2015). Latitudinal variation in virus-induced mortality of phytoplankton across the North Atlantic Ocean. *ISME J.* 10, 1–14. doi:10.1038/ismej.2015.130.

Monier, A., Pagarete, A., Vargas, C. De, Allen, M. J., Monier, A., Read, B., et al. (2009). Horizontal gene transfer of an entire metabolic pathway between a eukaryotic alga and its DNA virus. *Genome Res.* 19, 1441–1449. doi:10.1101/gr.091686.109.

Moniz, M. B. . J., and Kaczmarska, I. (2010). Barcoding of diatoms: nuclear encoded ITS revisited. *Protis* 161, 7–34. doi:10.1016/j.protis.2009.07.001.

Moniz, M. B. J., and Kaczmarska, I. (2009). Barcoding diatoms: Is there a good marker? *Mol. Ecol. Resour.* 9, 65–74. doi:10.1111/j.1755-0998.2009.02633.x.

Moro, I., Negrisolo, E., Callegaro, A., and Andreoli, C. (2003). *Aplanochytrium stocchinoi*: a new Labyrinthulomycota from the Southern Ocean (Ross Sea, Antarctica). *Protist* 154, 331–340.

Muehlstein, L. K., Porter, D., and Short, F. T. (1988). *Labyrinthula* sp., a marine slime mold producing the symptoms of wasting disease in eelgrass, *Zostera marina*. *Mar. Biol.* 99, 465–472.

Müller-Navarra, D. C., Brett, M. T., Liston, A. M., and Goldman, C. R. (2000). A highly unsaturated fatty acid predicts carbon transfer between primary producers and consumers. *Nature* 403, 74–77. doi:10.1038/47469.

Mystikou, A., Peters, A. F., Asensi, A. O., Fletcher, K. I., Brickle, P., van West, P., et al. (2014). Seaweed biodiversity in the south-western Antarctic Peninsula: surveying macroalgal community composition in the Adelaide Island/Marguerite Bay region over a 35-year time span. *Polar Biol.* 37, 1607–1619. doi:10.1007/s00300-014-1547-1.

N

Nagano, N., Matsui, S., Kuramura, T., Taoka, Y., Honda, D., and Hayashi, M. (2011). The distribution of extracellular cellulase activity in marine eukaryotes, thraustochytrids. *Mar. Biotechnol.* 13, 133–136. doi:10.1007/s10126-010-9297-8.

Nagasaki, K. (2008). Dinoflagellates, diatoms, and their viruses. *J. Microbiol.* 46, 235–243. doi:10.1007/s12275-008-0098-y.

Nagasaki, K., Ando, M., Itakura, S., Imai, I., and Ishida, Y. (1994). Viral mortality in the final stage of *Heterosigma akashiwo* (Raphidophyceae) red tide. *J. Plankton Res.* 16, 1595–1599.

Nagasaki, K., Tomaru, Y., Katanozaka, N., Shirai, Y., Nishida, K., Itakura, S., et al. (2004a). Isolation and characterization of a novel single-stranded RNA virus infecting the bloom-forming diatom *Rhizosolenia setigera*. *Appl. Environ. Microbiol.* 70, 704–711. doi:10.1128/AEM.70.2.704.

Nagasaki, K., Tomaru, Y., Nakanishi, K., Hata, N., Katanozaka, N., and Yamaguchi, M. (2004b). Dynamics of *Heterocapsa circularisquama* (Dinophyceae) and its viruses in Ago Bay, Japan. *Aquat. Microb. Ecol.* 34, 219–226. doi:10.3354/ame035219.

Nagasaki, K., Tomaru, Y., Takao, Y., Nishida, K., Shirai, Y., Suzuki, H., et al. (2005). Previously unknown virus infects marine diatom. *Appl. Environ. Microbiol.* 71, 3528–3535. doi:10.1128/AEM.71.7.3528-3535.2005.

Nagasaki, K., and Yamaguchi, M. (1998). Effect of temperature on the algicidal activity and the stability of HaV (*Heterosigma akashiwo* virus). *Aquat. Microb. Ecol.* 15, 211–216.

Nelson, D. M., Tréguer, P., Brzezinski, M. A., Leynaert, A., and Quéguiner, B. (1995). Production and dissolution of biogenic silica in the ocean: Revised global estimates, comparison with regional data and relationship to biogenic sedimentation. *Global Biogeochem. Cycles* 9, 359–372. doi:10.1029/95GB01070.

NF EN 15024 ed. (2006). Qualité de l'eau - Norme guide pour le dénombrement du phytoplancton par microscopie inversée (méthode Utermöhl). AFNOR.

O

Ohno, H., Endo, Y., Sato-Okoshi, W., and Nishitani, G. (2013). Feeding and growth characteristics of a Diatom-feeding flagellate isolated from the bottom sediment of Onagawa Bay, Northeastern Japan. *Open J. Mar. Sci.* 03, 9–14. doi:10.4236/ojms.2013.32A002.

Orsini, L., Sarno, D., Procaccini, G., Poletti, R., Dahlmann, J., and Montresor, M. (2002). Toxic *Pseudo-nitzschia multistriata* (Bacillariophyceae) from the Gulf of Naples: morphology, toxin analysis and phylogenetic relationships with other *Pseudo-nitzschia* species. *Eur. J. Phycol.* 37, 247–257. doi:10.1017/S0967026202003608.

P

Pagarete, A., Kusonmano, K., Petersen, K., Kimmance, S. A., Martínez Martínez, J., Wilson, W. H., et al. (2014). Dip in the gene pool: Metagenomic survey of natural coccolithovirus communities. *Virology* 466–467, 129–137. doi:10.1016/j.virol.2014.05.020.

Pan, J., del Campo, J., and Keeling, P. J. (2017). Reference tree and environmental sequence diversity of Labyrinthulomycetes. *J. Eukaryot. Microbiol.* 64, 88–96. doi:10.1111/jeu.12342.

Park, J. S., Alverson, A. J., and Lee, J. H. (2016a). A phylogenetic re-definition of the diatom genus *Bacterosira* (Thalassiosirales, Bacillariophyta), with the transfer of *Thalassiosira constricta* based on morphological and molecular characters. *Phytotaxa* 245, 1–16. doi:10.11646/phytotaxa.245.1.1.

Park, J. S., Jung, S. W., Ki, J. S., Guo, R., Kim, H.

J., Lee, K. W., et al. (2017). Transfer of the small diatoms *Thalassiosira proschkinae* and *T. spinulata* to the genus *Minidiscus* and their taxonomic re-description. *PLoS One* 12, 1–20. doi:10.1371/journal.pone.0181980.

Park, J. S., Jung, S. W., Lee, S. D., Yun, S. M., and Lee, J. H. (2016b). Species diversity of the genus *Thalassiosira* (Thalassiosirales, Bacillariophyta) in South Korea and its biogeographical distribution in the world. *Phycologia* 55, 403–423. doi:10.2216/15-66.1.

Park, M. G., Yih, W., and Coats, D. W. (2004). Parasites and phytoplankton, with special emphasis on dinoflagellate infections. *J. Eukaryot. Microbiol.* 51, 145–155. doi:10.1111/j.1550-7408.2004.tb00539.x.

Park, S., Jung, Y.-T., and Yoon, J.-H. (2014). *Kordia jejudonensis* sp. nov., isolated from the junction between the ocean and a freshwater spring, and emended description of the genus *Kordia*. *Int. J. Syst. Evol. Microbiol.* 64, 657–662. doi:10.1099/ijs.0.058776-0.

Paul, C., and Pohnert, G. (2011). Interactions of the algicidal bacterium *Kordia algicida* with diatoms: Regulated protease excretion for specific algal lysis. *PLoS One* 6. doi:10.1371/journal.pone.0021032.

Paul, C., and Pohnert, G. (2013). Induction of protease release of the resistant diatom *Chaetoceros didymus* in response to lytic enzymes from an algicidal bacterium. *PLoS One* 8, e57577. doi:10.1371/journal.pone.0057577.

Peacock, E. E., Olson, R. J., and Sosik, H. M. (2014). Parasitic infection of the diatom *Guinardia delicatula*, a recurrent and ecologically important phenomenon on the New England Shelf. *Mar. Ecol. Prog. Ser.* 503, 1–10. doi:10.3354/meps10784.

Percopo, I., Siano, R., Cerino, F., Sarno, D., and Zingone, A. (2011). Phytoplankton diversity during the spring bloom in the northwestern Mediterranean Sea. *Bot. Mar.* 54, 243–267. doi:10.1515/BOT.2011.033.

Perkins, F. O. (1973). Observations of thraustochytriaceous (Phycomycetes) and labyrinthulid (Rhizopodea) ectoplasmic nets on natural and artificial substrates-an electron microscope study. *Can. J. Bot.* 51, 485–491. doi:10.1139/b73-057.

Poulin, R. (1998). Large-scale patterns of host use by parasites of freshwater fishes. *Ecol. Lett.* 1, 118–128. doi:10.1046/j.1461-0248.1998.00022.x.

Q

Qi, F., Huang, Z., Lai, Q., Li, D., and Shao, Z. (2016). *Kordia ulvae* sp. nov., a bacterium isolated from the surface of green marine algae *Ulva* sp. *Int. J. Syst. Evol. Microbiol.* 66, 2623–2628. doi:10.1099/ijsem.0.001098.

Quick, J. A. (1974). Labyrinthuloides schizochytrops n . sp ., a new marine labyrinthula with spheroid. *Trans. Am. Microsc. Soc.* 93, 344–365.

Quiroga, I., and Chretiennot Dinet, M. J. (2004). A new species of *Minidiscus* (Diatomophyceae, Thalassiosiraceae) from the eastern English Channel, France. *Bot. Mar.* 47, 341–348. doi:10.1515/BOT.2004.040.

R

Raghukumar, C. (1986). Thraustochytrid fungi associated with marine algae. *Indian J. Mar. Sci.* 15, 121–122.

Raghukumar, C. (2006). Algal-fungal interactions in the marine ecosystem: symbiosis to parasitism. *Recent Adv. Appl. Asp. Indian Mar. Algae with Ref. to Glob. Scenar.* 1. Available at: http://drs.nio.org/drs/handle/2264/819.

Raghukumar, S. (2002). Ecology of the marine protists, the Labyrinthulomycetes (thraustochytrids and labyrinthulids). *Eur. J. Protistol.* 38, 127–145. doi:10.1078/0932-4739-00832.

Raghukumar, S., and Damare, V. S. (2011). Increasing evidence for the important role of Labyrinthulomycetes in marine ecosystems. *Bot. Mar.* 54, 3–11.

doi:10.1515/BOT.2011.008.

Ramanan, R., Kim, B. H., Cho, D. H., Oh, H. M., and Kim, H. S. (2016). Algae-bacteria interactions: Evolution, ecology and emerging applications. *Biotechnol. Adv.* 34, 14–29. doi:10.1016/j.biotechadv.2015.12.003

Rasconi, S., Jobard, M., Jouve, L., and Sime-Ngando, T. (2009). Use of calcofluor white for detection, identification, and quantification of phytoplanktonic fungal parasites. *Appl. Environ. Microbiol.* 75, 2545–2553. doi:10.1128/AEM.02211-08.

Rasconi, S., Niquil, N., and Sime-Ngando, T. (2012). Phytoplankton chytridiomycosis: community structure and infectivity of fungal parasites in aquatic ecosystems. *Environ. Microbiol.* 14, 2151–2170. doi:10.1111/j.1462-2920.2011.02690.x.

Raven, J. A., and Waite, A. M. (2004). The evolution of silicification in diatoms: Inescapable sinking and sinking as escape? *New Phytol.* 162, 45–61. doi:10.1111/j.1469-8137.2004.01022.x.

Ribera d'Alcalà, M., Conversano, F., Corato, F., Licandro, P., Mangoni, O., Marino, D., et al. (2004). Seasonal patterns in plankton communities in a pluriannual time series at a coastal Mediterranean site (Gulf of Naples): an attempt to discern recurrences and trends. *Sci. Mar.* 68, 65–83. doi:10.3989/scimar.2004.68s165.

Riedel, K., Hentzer, M., Geisenberger, O., Huber, B., Steidle, A., Wu, H., et al. (2001). Communication between *Pseudomonas aeruginosa* and *Burkholderia cepacia* in mixed biofilms. *Microbiology*, 3249–3262. doi:10.1099/00221287-147-12-3249.

Riemann, F., and Schaumann, K. (1993). Short note Thraustochytrid protists in Antarctic fast ice? *Antarct. Sci.* 5, 279–280. doi:10.1017/S0954102093000379.

Rolland, J. L., Stien, D., Sanchez-Ferandin, S., and Lami, R. (2016). Quorum sensing and quorum quenching in the phycosphere of phytoplankton: a case of chemical interactions in ecology. *J. Chem. Ecol.* 42, 1201–1211. doi:10.1007/s10886-016-0791-y.

Rosario, K., Nilsson, C., Lim, Y. W., Ruan, Y., and Breitbart, M. (2009). Metagenomic analysis of viruses in reclaimed water. *Environ. Microbiol.* 11, 2806–2820. doi:10.1111/j.1462-2920.2009.01964.x.

Round, F. E., Crawford, R. M., and Mann, D. G. (1990). *The diatoms, biology and morphology of the genera*. Cambridge University Press.

Rousseau, V., Leynaert, A., Daoud, N., and Lancelot, C. (2002). Diatom succession, silicification and silicic acid availability in Belgian coastal waters (Southern North Sea). *Mar. Ecol. Prog. Ser.* 236, 61–73. doi:10.3354/meps236061.

Ruan, Q., Dutta, D., Schwalbach, M. S., Steele, J. A., Fuhrman, J. A., and Sun, F. (2006). Local similarity analysis reveals unique associations among marine bacterioplankton species and environmental factors. *Bioinformatics* 22, 2532–2538. doi:10.1093/bioinformatics/btl417.

S

Sabater, S. (2009). The diatom cell and its taxonomical entity. *Encycl. Inl. Waters* 1, 149–156.

Salomon, P. S., and Imai, I. (2006). Pathogens of harmful microalgae. *Ecol. Harmful Algae* 189.

Sarno, D., Kooistra, W. H. C. F., Balzano, S., Hargraves, P. E., and Zingone, A. (2007). Diversity in the genus *Skeletonema* (Bacillariophyceae): III. Phylogenetic position and morphological variability of *Skeletonema costatum* and *Skeletonema grevillea*, with the description of *skeletonema ardens* sp. nov. *J. Phycol.* 43, 156–170. doi:10.1111/j.1529-8817.2006.00305.x.

Sarthou, G., Timmermans, K. R., Blain, S., and Tréguer, P. (2005). Growth physiology and fate of diatoms in the ocean: A review. *J. Sea Res.* 53, 25–42. doi:10.1016/j.seares.2004.01.007.

Schlüter, M. H., Kraberg, A., and Wiltshire, K. H. (2012). Long-term changes in the seasonality of selected diatoms related to grazers and environmental conditions. *J. Sea Res.* 67, 91–97.

doi:10.1016/j.seares.2011.11.001.

Schnepf, E., Deichgraber, G., and Drebes, G. (1978a). Development and ultrastructure of the marine, parasitic oomycete, *Lagenisma coscinodisci* (Lagenidiales). Thallus, Zoosporangium, Mitosis and Meiosis. *Arch. Microbiol.* 116, 141–150. doi:10.1007/BF00406029.

Schnepf, E., Deichgraber, G., and Drebes, G. (1978b). Development and Ultrastructure of the Marine, Parasitic Oomycete, *Lagenisma coscinodisci* Drebes (Lagenidiales). The infection. *Arch. Microbiol.* 116, 133–139.

Schnepf, E., Drebes, G., and Elbrächter, M. (1990). *Pirsonia guinardiae*, gen. et spec. nov.: A parasitic flagellate on the marine diatom *Guinardia flaccida* with an unusual mode of food uptake. *Helgoländer Meeresunters* 44, 275–293.

Schnepf, E., and Kühn, S. F. (2000). Food uptake and fine structure of *Cryothecomonas longipes* sp. nov., a marine nanoflagellate incertae sedis feeding phagotrophically on large diatoms. *Helgol. Mar. Res.* 54, 18–32. doi:10.1007/s101520050032.

Scholz, B., Guillou, L., Marano, A. V., Neuhauser, S., Sullivan, B. K., Karsten, U., et al. (2015). Zoosporic parasites infecting marine diatoms – A black box that needs to be opened. *Fungal Ecol.* 19, 59–76. doi:10.1016/j.funeco.2015.09.002.

Scholz, B., Küpper, F. C., Vyverman, W., and Karsten, U. (2014). Eukaryotic pathogens (Chytridiomycota and Oomycota) infecting marine microphytobenthic diatoms - a methodological comparison. *J. Phycol.* 50, 1009–1019. doi:10.1111/jpy.12230.

Schroeder, D. C., Oke, J., Hall, M., Malin, G., and Wilson, W. H. (2003). Virus succession observed during an *Emiliania huxleyi* bloom. *Appl Env. Microbiol* 69, 2484–2490. doi:10.1128/AEM.69.5.2484–2490.2003.

Schweikert, M. (2015). "Biology of parasitic heterotrophic nanoflagellates: parasitoids of diatoms," in *Marine Protists*, eds. S. Ohtsuka, T. Suzaki, T. Horiguchi, N. Suzuki, and F. Not (Springer Japan), 519–530. doi:10.1007/978-4-431-55130-0_21 519.

Schweikert, M., and Schnepf, E. (1996). *Pseudaphelidium drebesii*, gen. et spec. nov. (incerta sedis), a parasite of the marine centric diatom *Thalassiosira punctigera*. *Arch. für Protistenkd.* 147, 11–17. doi:10.1016/S0003-9365(96)80004-2.

Schweikert, M., and Schnepf, E. (1997a). Electron microscopical observations on *Pseudaphelidium drebesii* Schweikert and Schnepf, a parasite of the centric diatom *Thalassiosira punctigera*. *Protoplasma* 199, 113–123.

Schweikert, M., and Schnepf, E. (1997b). Light and electron microscopical observations on *Pirsonia punctigerae* spec., nov., a nanoflagellate feeding on the marine centric diatom *Thalassiosira punctigera*. *Eur. J. Protistol.* 33, 168–177. doi:10.1016/S0932-4739(97)80033-8.

Segev, E., Wyche, T. P., Kim, K. H., Petersen, J., Ellebrandt, C., Vlamakis, H., et al. (2016). Dynamic metabolic exchange governs a marine algal-bacterial interaction. *Elife* 5, e17473. doi:10.7554/eLife.17473.

Sharon, I., Tzahor, S., Williamson, S., Shmoish, M., Man-Aharonovich, D., Rusch, D. B., et al. (2007). Viral photosynthetic reaction center genes and transcripts in the marine environment. *ISME J.* 1, 492–501. doi:10.1038/ismej.2007.67.

Shi, R., Huang, H., Qi, Z., Hu, W., Tian, Z., and Dai, M. (2013). Algicidal activity against Skeletonema costatum by marine bacteria isolated from a high frequency harmful algal blooms area in southern Chinese coast. *World J. Microbiol. Biotechnol.* 29, 153–62. doi:10.1007/s11274-012-1168-1.

Shirai, Y., Takao, Y., Mizumoto, H., Tomaru, Y., Honda, D., and Nagasaki, K. (2006). Genomic and phylogenetic analysis of a single-stranded RNA virus infecting *Rhizosolenia setigera* (Stramenopiles: Bacillariophyceae). *J. Mar. Biol. Assoc. UK* 86, 475–483. doi:10.1017/S0025315406013373.

Shirai, Y., Tomaru, Y., Takao, Y., Suzuki, H., Nagumo, T., and Nagasaki, K. (2008). Isolation and characterization of a single-stranded RNA virus infecting the marine planktonic diatom *Chaetoceros*

tenuissimus Meunier. *Appl. Environ. Microbiol.* 74, 4022–4027. doi:10.1128/AEM.00509-08.

Sime-Ngando, T., Lefèvre, E., and Gleason, F. H. (2011). Hidden diversity among aquatic heterotrophic flagellates: Ecological potentials of zoosporic fungi. *Hydrobiologia* 661, 5–22. doi:10.1007/s10750-010-0358-9.

Simon, N., Manno, M., Rigaut-Jalabert, F., Romac, S., Audic, S., Hernandez-Farinas, T., et al. Annual patterns of plankton diversity revealed using molecular metabarcoding. *In prep.*

Sims, P. A., Mann, D. G., and Medlin, L. K. (2006). Evolution of the diatoms: insights from fossil, biological and molecular data. *Phycologia* 45, 361–402. doi:10.2216/05-22.1.

Skerratt, J. H., Bowman, J. P., Hallegraeff, G., James, S., and Nichols, P. D. (2002). Algicidal bacteria associated with blooms of a toxic dinoflagellate in a temperate Australian estuary. *Mar. Ecol. Prog. Ser.* 244, 1–15. doi:10.3354/meps244001.

Smetacek, V. (1999). Diatoms and the ocean carbon cycle. *Protist* 150, 25–32. doi:10.1016/S1434-4610(99)70006-4.

Smetacek, V. (2001). A watery arms race. *Nature* 411, 745.

Sohn, J. H., Lee, J. H., Yi, H., Chun, J., Bae, K. S., Ahn, T. Y., et al. (2004). *Kordia algicida* gen. nov., sp. nov., an algicidal bacterium isolated from red tide. *Int. J. Syst. Evol. Microbiol.* 54, 675–680. doi:10.1099/ijs.0.02689-0.

Sorensen, G., Baker, A. C., Hall, M. J., Munn, C. B., and Schroeder, D. C. (2009). Novel virus dynamics in an *Emiliania huxleyi* bloom. *J. Plankton Res.* 31, 787–791. doi:10.1093/plankt/fbp027.

Sournia, A., Birrien, J. L., Douvillé, J. L., Klein, B., and Viollier, M. (1987). A daily study of the diatom spring bloom at Roscoff (France) in 1985. I. The spring bloom within the annual cycle. *Estuar. Coast. Shelf Sci.* 25, 355–367. doi:10.1093/plankt/14.3.409.

Stachura-Suchoples, K., and Williams, D. M. (2009). Description of *Conticribra tricircularis*, a new genus and species of Thalassiosirales, with a discussion on its relationship to other continuous cribra species of *Thalassiosira* Cleve (Bacillariophyta) and its freshwater origin. *Eur. J. Phycol.* 44, 477–486. doi:10.1080/09670260903225431.

Steward, G. F., Culley, A. I., Mueller, J. a, Wood-Charlson, E. M., Belcaid, M., and Poisson, G. (2013). Are we missing half of the viruses in the ocean? *ISME J.* 7, 672–679. doi:10.1038/ismej.2012.121.

Stoeck, T., Bass, D., Nebel, M., Christen, R., Jones, M. D. M., Breiner, H.-W., et al. (2010). Multiple marker parallel tag environmental DNA sequencing reveals a highly complex eukaryotic community in marine anoxic water. *Mol. Ecol.* 19, 21–31. doi:10.1111/j.1365-294X.2009.04480.x.

Subramoni, S., and Venturi, V. (2009). LuxR-family "solos": Bachelor sensors/regulators of signalling molecules. *Microbiology* 155, 1377–1385. doi:10.1099/mic.0.026849-0.

Sullivan, M. B., Lindell, D., Lee, J. A., Thompson, L. R., Bielawski, J. P., and Chisholm, S. W. (2006). Prevalence and evolution of core photosystem II genes in marine cyanobacterial viruses and their hosts. *Plos Biol.* 4, e234. doi:e234 10.1371/journal.pbio.0040234.

Sunagawa, S., Coelho, L. P., Chaffron, S., Kultima, J. R., Labadie, K., Salazar, G., et al. (2015). Structure and function of the global ocean microbiome. *Science (80-.).* 348, 1261359–1261359. doi:10.1126/science.1261359.

Suttle, C. A. (1993). "Enumeration and Isolation of Viruses," in *Handbook of Methods in Aquatic Microbial Ecology*, eds. P. F. Kemp, B. F. Sherr, E. B. Sherr, and J. J. Cole (Boca Raton: Lewis Publisher), 121–137.

T

Tai, V., Lawrence, J. E., Lang, A. S., Chan, A. M., Culley, A. I., and Suttle, C. A. (2003). Characterization of HaRNAV, a single-stranded RNA virus causing lysis of *Heterosigma akashiwo* (Raphidophyceae). *J. Phycol.* 39, 343–352.

Takahashi, Y., Yoshida, M., Inouye, I., and Watanabe, M. M. (2014). *Diplophrys mutabilis* sp. nov., a new member of Labyrinthulomycetes from freshwater habitats. *Protist* 165, 50–65. doi:10.1016/j.protis.2013.10.001.

Takano, H. (1981). New and rare diatoms from Japanese marine waters – VI. Three new species in Thalassiosiraceae. *Bull. Tokai Reg. Fish. Res. Lab.* 105, 31–43.

Takao, Y., Nagasaki, K., and Honda, D. (2007). Squashed ball-like dsDNA virus infecting a marine fungoid protist *Sicyoidochytrium minutum* (Thraustochytriaceae, Labyrinthulomycetes). *Aquat. Microb. Ecol.* 49, 101–108. doi:10.3354/ame01141.

Takao, Y., Nagasaki, K., and Mise, K. (2005). Isolation and characterization of a novel single-stranded RNA virus infectious to a marine fungoid protist, *Schizochytrium* sp. (Thraustochytriaceae, Labyrinthulea). *Appl. Environmantal Microbiol.* 71, 4516–22. doi:10.1128/AEM.71.8.4516-4522.2005.

Takao, Y., Tomaru, Y., Nagasaki, K., and Honda, D. (2015). Ecological dynamics of two distinct viruses infecting marine eukaryotic decomposer thraustochytrids (Labyrinthulomycetes, Stramenopiles). *PLoS One* 10, e0133395. doi:10.1371/journal.pone.0133395.

Thingstad, T. F. (2000). Elements of a theory for the mechanisms controlling abundance, diversity, and biogeochemical role of lytic bacterial viruses in aquatic systems. *Limnol. Oceanogr.* 45, 1320–1328. doi:10.4319/lo.2000.45.6.1320.

Thomas, R., Grimsley, N., Escande, M., Subirana, L., Derelle, E., and Moreau, H. (2011). Acquisition and maintenance of resistance to viruses in eukaryotic phytoplankton populations. *Environ. Microbiol.* 13, 1412–1420. doi:10.1111/j.1462-2920.2011.02441.x.

Thomsen, H. a., Buck, K. R., Bolt, P. a., and Garrison, D. L. (1991). Fine structure and biology of *Cryothecomonas* gen. nov. (Protista Incertae Sedis) from the Ice Biota. *Can. J. Zool.* 69, 1048–1070. doi:10.1139/z91-150.

Throndsen, J., Hasle, G. R., and Tangen, K. (2007). *Phytoplankton of Norwegian Coastal Waters*. Almatter Forlag AS, Oslo.

Tillmann, U., Hesse, K. J., and Tillmann, A. (1999). Large-scale parasitic infection of diatoms in the Northfrisian Wadden Sea. *J. Sea Res.* 42, 255–261. doi:10.1016/S1385-1101(99)00029-5.

Tomaru, Y., Fujii, N., Oda, S., Toyoda, K., and Nagasaki, K. (2011a). Dynamics of diatom viruses on the western coast of Japan. *Aquat. Microb. Ecol.* 63, 223–230. doi:10.3354/ame01496.

Tomaru, Y., Kimura, K., and Nagasaki, K. (2015a). "Marine Protist Viruses," in *Marine Protists*, eds. S. Ohtsuka, T. Suzaki, T. Horiguchi, N. Suzuki, and F. Not (Springer Japan), 501–517. doi:10.1007/978-4-431-55130-0_20.

Tomaru, Y., Kimura, K., and Yamaguchi, H. (2014). Temperature alters algicidal activity of DNA and RNA viruses infecting *Chaetoceros tenuissimus*. *Aquat. Microb. Ecol.* 73, 171–183. doi:10.3354/ame01713.

Tomaru, Y., Shirai, Y., Suzuki, H., Nagumo, T., and Nagasaki, K. (2008). Isolation and characterization of a single-stranded DNA virus infecting the marine planktonic diatom *Chaetoceros debilis*. *Aquat. Microb. Ecol.* 50, 103–112. doi:doi: 10.3354/ame01170.

Tomaru, Y., Shirai, Y., Toyoda, K., and Nagasaki, K. (2011b). Isolation and characterisation of a single-stranded DNA virus infecting the marine planktonic diatom *Chaetoceros tenuissimus*. *Aquat. Microb. Ecol.* 64, 175–184. doi:10.3354/ame01517.

Tomaru, Y., Takao, Y., Suzuki, H., Nagumo, T., Koike, K., and Nagasaki, K. (2011c). Isolation and characterization of a single-stranded DNA virus infecting *Chaetoceros lorenzianus* Grunow. *Appl. Environ. Microbiol.* 77, 5285–5293. doi:10.1128/AEM.00202-11.

Tomaru, Y., Takao, Y., Suzuki, H., Nagumo, T., and Nagasaki, K. (2009). Isolation and characterization of a single-stranded RNA virus infecting the bloom-forming diatom *Chaetoceros socialis*. *Appl. Environ. Microbiol.* 75, 2375–2381. doi:10.1128/AEM.02580-08.

Tomaru, Y., Toyoda, K., and Kimura, K. (2015b). Marine diatom viruses and their hosts: Resistance mechanisms and population dynamics. *Perspect. Phycol.* 2, 69–81. doi:10.1127/pip/2015/0023.

Tomaru, Y., Toyoda, K., and Kimura, K. (2018). Occurrence of the planktonic bloom-forming marine diatom *Chaetoceros tenuissimus* Meunier and its infectious viruses in western Japan. *Hydrobiologia* 805, 221–230. doi:10.1007/s10750-017-3306-0.

Tomaru, Y., Toyoda, K., Kimura, K., Hata, N., Yoshida, M., and Nagasaki, K. (2012). First evidence for the existence of pennate diatom viruses. *ISME J.* 6, 1445–1448. doi:10.1038/ismej.2011.207.

Tomaru, Y., Toyoda, K., Kimura, K., Takao, Y., Sakurada, K., Nakayama, N., et al. (2013a). Isolation and characterization of a single-stranded RNA virus that infects the marine planktonic diatom *Chaetoceros* sp. (SS08-C03). *Phycol. Res.* 61, 27–36. doi:10.1111/j.1440-1835.2012.00670.x.

Tomaru, Y., Toyoda, K., Suzuki, H., Nagumo, T., Kimura, K., and Takao, Y. (2013b). New single-stranded DNA virus with a unique genomic structure that infects marine diatom *Chaetoceros setoensis*. *Sci. Rep.* 3, 3337. doi:10.1038/srep03337.

Toyoda, K., Kimura, K., Hata, N., Nakayama, N., Nagasaki, K., and Tomaru, Y. (2012). Isolation and characterization of a single-stranded DNA virus infecting the marine planktonic diatom *Chaetoceros* sp. (strain TG07-C28). *Plankt. Benthos Res.* 7, 20–28. doi:10.3800/pbr.7.20.

Tréguer, P., Bowler, C., Moriceau, B., Dutkiewicz, S., Gehlen, M., Aumont, O., et al. (2018). Influence of diatom diversity on the ocean biological carbon pump. *Nat. Geosci.* 11, 27–37. doi:10.1038/s41561-017-0028-x.

Tréguer, P., Nelson, D. M., Van Bennekom, A. J., DeMaster, D. J., Leynaert, A., and Queguiner, B. (1995). The silica balance in the world ocean: A reestimate. *Science (80-.).* 268, 375–379. doi:10.1126/science.268.5209.375.

U

Ueda, M., Nomura, Y., Doi, K., Nakajima, M., and Honda, D. (2015). Seasonal dynamics of culturable thraustochytrids (Labyrinthulomycetes, Stramenopiles) in estuarine and coastal waters. *Aquat. Microb. Ecol.* 74, 187–204. doi:10.3354/ame01736.

V

Van Donk, E., and Ringelberg, J. (1983). The effect of fungal parasitism on the succession of diatoms in Lake Maarsseveen I (The Netherlands). *Freshw. Biol.* 13, 241–251. doi:10.1111/j.1365-2427.1983.tb00674.x.

Van Valen, L. (1973). A new evolutationary law. *Evol. Theory* 1, 1–30.

Venturi, V., and Fuqua, C. (2013). Chemical signaling between plants and plant-pathogenic bacteria. *Annu. Rev. Phytopathol.* 51, 17–37. doi:10.1146/annurev-phyto-082712-102239.

Venturi, V., Subramoni, S., Sabag-daigle, A., and Ahmer, B. M. M. (2018). "Methods to study solo/orphan quorum-sensing receptors," in *Quorum Sensing: Methods and Protocols*, eds. L. Leoni and G. Rampioni (New Yor: Humana Press), 145–159.

Villarino, E., Watson, J. R., Jönsson, B., Gasol, J. M., Salazar, G., Acinas, S. G., et al. (2018). Large-scale ocean connectivity and planktonic body size. *Nat. Commun.* 9. doi:10.1038/s41467-017-02535-8.

W

Wafar, M. V. M., Le Corre, P., and Birrien, J. L. (1983). Nutrients and primary production in permanently well-mixed temperate coastal waters. *Estuar. Coast. Shelf Sci.* 17, 431–446. doi:10.1016/0272-

7714(83)90128-2.

Wang, H., Butt, L., Rooks, P., Khan, F., Allen, M. J., and Ali, S. T. (2016). Characterisation of algicidal bacterial exometabolites against the lipid-accumulating diatom *Skeletonema* sp. *Algal Res.* 13, 1–6. doi:10.1016/j.algal.2015.11.012.

Weiss, S., Van Treuren, W., Lozupone, C., Faust, K., Friedman, J., Deng, Y., et al. (2016). Correlation detection strategies in microbial data sets vary widely in sensitivity and precision. *ISME J.* 10, 1669–1681. doi:10.1038/ismej.2015.235.

Widdicombe, C. E., Eloire, D., Harbour, D., Harris, R. P., and Somerfield, P. J. (2010). Long-term phytoplankton community dynamics in the Western English Channel. *J. Plankton Res.* 32, 643–655. doi:10.1093/plankt/fbp127.

Wilhelm, S. W., and Suttle, C. A. (1999). Viruses and nutrient cycles in the sea. *Bioscience* 49, 781–788.

Wilson, W. H., Francis, I., Ryan, K., and Davy, S. K. (2001). Temperature induction of viruses in symbiotic dinoflagellates. *Aquat. Microb. Ecol.* 25, 99–102. doi:10.3354/ame025099.

Wilson, W. H., Schroeder, D. C., Allen, M. J., Holden, M. T. G., Parkhill, J., Barrell, B. G., et al. (2005). Complete genome sequence and lytic phase transcription profile of a *Coccolithovirus*. *Science (80-.).* 309, 1090–1092. doi:10.1126/science.1113109.

Wiltshire, K. H., Kraberg, A., Bartsch, I., Boersma, M., Franke, H.-D., Freund, J., et al. (2010). Helgoland Roads, North Sea: 45 Years of Change. *Estuaries and Coasts* 33, 295–310. doi:10.1007/s12237-009-9228-y.

Worden, A. Z., Follows, M. J., Giovannoni, S. J., Wilken, S., Zimmerman, A. E., and Keeling, P. J. (2015). Rethinking the marine carbon cycle: Factoring in the multifarious lifestyles of microbes. *Science (80-.).* 347, 1257594. doi:10.1126/science.1257594.

Wu, Q., Peng, Z., Zhang, Y., and Yang, J. (2018). COACH-D: Improved protein-ligand binding sites prediction with refined ligand-binding poses through molecular docking. *Nucleic Acids Res.* 46, W438–W442. doi:10.1093/nar/gky439.

Y

Yau, S., Hemon, C., Derelle, E., Moreau, H., Piganeau, G., and Grimsley, N. (2016). A viral immunity chromosome in the marine picoeukaryote, *Ostreococcus tauri*. *PLoS Pathog.* 12, e1005965. doi:10.1371/journal.ppat.1005965.

Yun, S. M., and Lee, J. H. (2011). Morphology and distribution of some marine diatoms, family Rhizosoleniaceae, genus *Proboscia, Neocalyptrella, Pseudosolenia, Guinardia,* and *Dacyliosolen* in Korean coastal waters. *Algae* 26, 299–315. doi:10.4490/algae.2011.26.2.141.

Z

Zingone, A., Sarno, D., Siano, R., and Marino, D. (2011). The importance and distinctiveness of small-sized phytoplankton in the Magellan Straits. *Polar Biol.* 34, 1269–1284. doi:10.1007/s00300-010-0937-2.

Parasitisme et contrôle des blooms de diatomées en Manche Occidentale

Résumé

Les diatomées constituent un groupe majeur du phytoplancton marin. Ces microalgues peuvent former des blooms saisonniers considérables ayant des implications biogéochimiques importantes notamment sur l'export de carbone. A ce jour, la manière dont le parasitisme structure leur développement reste élusive. L'objectif de cette thèse était d'identifier le(s) parasite(s) associé(s) aux diatomées prédominantes en Manche Occidentale afin de mieux comprendre comment le parasitisme contrôle les blooms de ces microalgues. La première partie de cette thèse visait à décrire le réseau de parasites qui régule les diatomées du genre *Guinardia,* taxon-clef du microphytoplancton en Nord-Atlantique. Pour cela un travail d'isolement intensif des espèces de *Guinardia* et des parasites associés a été réalisé entre Août 2015 et Octobre 2016 à la station d'échantillonnage à long terme SOMLIT-Astan. La caractérisation des isolats a permis de mettre en évidence une diversité insoupçonnée de parasites régulant *Guinardia delicatula*, avec au minimum trois types de parasites appartenant à des lignées distinctes : des virus (Picornavirales, *Bacillarnavirus*), un parasite eucaryote (Labyrinthulomycetes, *Aplanochytrium* sp.) et des bactéries algicides (Bacteroidetes, *Kordia* sp.). Ces nouveaux parasites n'ont jamais été décrits en association avec *Guinardia* et s'ajoutent donc aux autres parasites connus pour cet hôte. Les parasites isolés à SOMLIT-Astan présentent des stratégies d'infections différentes, suggérant des interactions complexes dans la nature. Dans un second temps, nous avons étendu notre étude à des nanodiatomées appartenant aux genres *Minidiscus* et *Thalassiosira*, largement distribuées dans l'océan global mais dont les dynamiques saisonnières et leur contrôle sont quasi-inexplorées. La combinaison d'outils microscopiques et moléculaires a mis en évidence que ces nanodiatomées dominent numériquement la communauté phytoplanctonique à SOMLIT-Astan et qu'elles présentent des patrons saisonniers très marqués. La collection importante de 82 parasites, dont 27 virus, isolés tout au long de l'année à partir de ces deux genres indique pour la première fois un rôle-clé des interactions biotiques dans la régulation des dynamiques des nanodiatomées. Ce projet de thèse révèle une diversité nouvelle et importante de parasites associés aux diatomées au Manche Occidentale. La contribution relative de ces parasites dans la régulation des diatomées, leurs implications biogéochimiques, et évolutives reste à mettre en lumière.

Control of diatom blooms by parasites in the Western English Channel

Abstract

Diatoms are one of the most successful phytoplankton groups. They can form considerable seasonal blooms with important biogeochemical implications, especially with respect to carbon export. To date, the role of parasites in the regulation of diatom blooms remains elusive. The main objective of this thesis was to identify the parasites associated to dominant diatom species in the Western English Channel to better understand how parasitism regulates diatom blooms. The first part of the project aimed to identify parasitic network that controls the diatom *Guinardia*, a major component of microphytoplankton communities in coastal systems of the North Atlantic. Intensive isolation of *Guinardia* species and associated parasites into laboratory culture was carried out between August 2015 and October 2016 from the SOMLIT-Astan long-term monitoring station. Characterization of these isolates revealed an unsuspected diversity of parasites that infect *Guinardia delicatula*, with at least three types of parasites belonging to distinct lineages: viruses (Picornavirales, *Bacillarnavirus*), a eukaryotic parasite (Labyrinthulomycetes, *Aplanochytrium* sp.) and algicidal bacteria (Bacteroidetes, *Kordia* sp.). These pathogens have never previously been described in association with *Guinardia* and therefore add to the list of known parasites reported for this host species. The parasites isolated from SOMLIT-Astan displayed different infection strategies, suggesting complex interplays in nature. In the second part of this thesis, the study was extended to nanoplanktonic diatoms that belong to the genera *Minidiscus* and *Thalassiosira*. These minute microalgae are widespread in the global ocean, but their seasonal dynamics are quasi-unexplored. Using a combination of microscope observations and molecular tools, we showed that these nanodiatoms numerically dominated the phytoplankton community at the SOMLIT-Astan station and that they have contrasted seasonal patterns. The large set of 82 parasites, including 27 viruses, isolated from these two genera throughout the sampling period highlights, for the first time, the key role of biotic interactions in the regulation of nanodiatom dynamics. This Ph.D. project has revealed significant novel diversity of pathogens of diatoms in the Western English Channel. The relative contribution of these parasites to regulation of diatom populations and their resulting biogeochemical and evolutionary implications remain to be investigated.